Universität Rostock Traditio et Innovatio

Phosphorus speciation in soil and sediment indicating transformation processes from terrestrial to aquatic ecosystems

Kumulative Dissertation

zur Erlangung des akademischen Grades

doctor agriculturae (Dr. agr.)

an der Professur für Bodenkunde

der Agrar- und Umweltwissenschaftlichen Fakultät

der Universität Rostock

vorgelegt von

M.Sc. Pflanzenproduktion und Umwelt, Julia Prüter

aus Rostock

Rostock, 25.01.2023

https://doi.org/10.18453/rosdok_id00004187

Gutachter

Prof. Dr. Peter Leinweber
Universität Rostock, Agrar- und Umweltwissenschaftliche Fakutät, Bodenkunde

Prof. Dr. Jörg Rinklebe
Bergische Universität Wuppertal, Institut für Grundbau, Abfall- und Wasserwesen, Boden- und Grundwassermanagement

Prof. Dr. Yvonne Oelmann
Universität Tübingen, Fachbereich Geowissenschaften, Geoökologie

Datum der Einreichung: 28.09.2022

Datum der Verteidigung: 25.01.2023

„Nur wer nicht sucht, ist vor Irrtum sicher.“

- Albert Einstein

Table of Contents

List of Figures

List of Tables

List of Abbreviations

Al	aluminium
AMP	adenosine 5‘ monophosphate
BL8	beamline 8
C	carbon
Ca	calcium
CLS	Canadian Light Source
DNA	deoxyribonucleic acid
EDTA	ethylenediaminetetraacetic acid
EDX	energy-dispersive X-ray microanalyses
ESM	electronic supplementary material
Fe	iron
FT	fish tank
HELCOM	Helsinki Convention
HSD	honest significant difference
ICP-AES	inductively coupled plasma-atomic emission spectroscopy
ICP-OES	inductively coupled plasma-optical emission spectrometer
IG	inverse gated decoupled
IHP	inositol hexakisphosphate
IOW	Leibniz Institute for Baltic Research Warnemünde
IR	infrared
K	potassium
LCF	linear combination fitting
MAP	Mediterranean Action Plan
MDPA	methylenediphosphonic acid sodium salt
MED POL	Mediterranean Sea pollution
Mg	magnesium
MS	mass spectrometry
myo-IHP	myo-inositol hexa(kis)phosphate
N	nitrogen
Na	sodium
NanoSIMS	nano-scale secondary ion mass spectrometry

NMDS	nonmetric multidimensional scaling
NMR	nuclear magnetic resonance
OM	organic matter
ortho-P	orthophosphate
OSPAR	Oslo-Paris Convention
P	phosphorus
P_i	inorganic phosphorus
P_o	organic phosphorus
P_t	total phosphorus
PCA	principal component analysis
Pyro-P	pyrophosphate
Py-FIMS	pyrolysis-field ionization mass spectrometry
RAS	recirculation aquaculture system
redox	oxidation-reduction
S	sulphur
SDD	silicon drift detector
SDF	spectral deconvolution fitting
SEM	scanning electron microscopy
SLRI	Synchrotron Light Research Institute
SOM	soil organic matter
SPM	suspended particulate matter
SXRMB	soft X-ray micro-characterization beamline
TII	total ion intensity
UNEP	United Nations Environment Programme
VM	volatile matter
XAS	X-ray absorption spectroscopy
XANES	*K*-edge X-ray absorption near edge structure
XPS	X-ray photoelectron spectroscopy
XRF	X-ray fluorescence
Zn	zinc
α-glycerol	*α*-glycerophosphate
β-glycerol	*β*-glycerophosphate

Summary

Phosphorus (P) is an indispensable nutrient element for all organisms but at the same time contributes significantly to excessive eutrophication in aquatic ecosystems. Knowledge about the chemical P speciation is essential to assess possible risks of P transport towards vulnerable aquatic ecosystems. To date, this knowledge, especially for transects including soil and sediment samples from terrestrial to aquatic ecosystems, is still insufficient. Thus, the general objective of the present work was to characterize the P speciation and to detect transformation processes along transport pathways at the fluent boundaries between land and sea including terrestrial soils, semiterrestrial wetlands and aquatic sediments. Besides analyses of elemental concentrations and water contents, terrestrial/semiterrestrial soils and aquatic sediments from micro-, meso- and macroscale ecosystems were analyzed by a multi-method approach including sequential P fractionation, P *K*-edge X-ray absoprtion near edge structure (XANES) spectroscopy and ^{31}P nuclear magnetic resonance (NMR) spectroscopy. The detection of specific organic P species with terrestrial origin in arable soils as well as in adjacent sediments supported the assumption of P transport processes from terrestrial towards aquatic ecosystems. The complementary results confirmed a transition from labile and moderately labile Fe- and Al-associated P and great variety of organic P species in terrestrial soils towards more stable Ca- and Mg-P and less differrent organic P species in aquatic sediments. Kettle hole sediments, coastal wetland soils and Baltic Sea lagoon sediments acted as sinks for accumulations of especially stable P and complex organically bound P species. Some of the stable P species in aquatic sediments at the bottom of lake or sea waters can originate from Ca-P dominated fish fecal matter. To protect vulnerable aquatic ecosystems from further P inputs, kettle holes, coastal wetland buffer strips and deeper areas in shallow Baltic Sea lagoons have to be preserved and maintained or created in areas where they have not been available so far. Forthcoming studies have to focus on possible P recycling from terrestrial as well as aquatic sinks to contribute to closing P cycles in agricultural fertilization and adjacent ecosystems.

Zusammenfassung

Phosphor (P) ist ein unverzichtbares Nährelement für die Landwirtschaft, aber trägt gleichzeitig erheblich zur Eutrophierung aquatischer Ökosysteme bei. Das Wissen über die P-Speziierung ist unerlässlich, um ein mögliches Risiko des P-Transports in gefährdete aquatische Ökosysteme abzuschätzen. Vorkommen chemischer P-Verbindungen in Böden und Sedimenten entlang von Feuchtigkeitsgradienten von terrestrischen zu aquatischen Ökosystemen sind bisher unzulänglich bekannt. Um eine Charakterisierung der P-Speziierung zu ermöglichen, wurden terrestrische/semiterrestrische Böden und aquatische Sedimente aus Ökosystemen verschiedener Größen mithilfe eines multimethodischen Ansatzes untersucht. Dieser Ansatz umfasste unter anderem die Methoden sequentielle P-Fraktionierung, P-*K*-Kanten-Röntgenabsorptionsspektroskopie (XANES) und ^{31}P Kernmagnetresonanz (NMR) Spektroskopie. Der Nachweis spezifischer organischer P-Spezies terrestrischen Ursprungs in Ackerböden sowie in angrenzenden aquatischen Sedimenten bekräftigte die Annahme vom P-Transport von terrestrischen zu aquatischen Ökosystemen. Die Ergebnisse der komplementären Methoden bestätigten eine Transformation von labilen und moderat labilen Fe- und Al-P-Verbindungen und einer großen Vielfalt organischer P-Spezies in terrestrischen Böden zu stabileren Ca- und Mg-P-Verbindungen und weniger verschiedenen organischen P-Spezies in aquatischen Sedimenten. Anreicherungen von stabilen P-Verbindungen und komplexen organisch gebundenen P-Spezies in Sollsedimenten, Böden in Küstenfeuchtgebieten und Boddensedimenten deuten auf Senkenfunktionen hin. Stabile P-Verbindungen in Sedimenten am Grund von Seen oder Meeren können aus Fischfäkalien stammen, in welchen Ca-P als Hauptbindungsform von P auftrat. Um gefährdete aquatische Ökosysteme vor weiteren P-Einträgen schützen zu können, müssen besonders Sölle, Küstenfeuchtgebiete und tiefere Boddenbereiche erhalten und gepflegt oder neu angelegt werden. Weitere Studien sollten in Zukunft Möglichkeiten zum P-Recycling aus terrestrischen und aquatischen Senken untersuchen, um P-Kreisläufe in der Landwirtschaft und angrenzenden Ökosystemen zu schließen.

1 Introduction

1.1. Justification of the research

Phosphorus (P) is essential to all living organisms and in the form of fertilizer an integral part of the current intensive agriculture. Rock phosphate is the basis for the production of mineral P fertilizers, which are used in agriculture next to organic amendments such as manure or slurry. Rock phosphate is a non-renewable resource requiring a responsible economic use. Once applied to arable fields, translocation and leaching of P from the soils is possible. However, inputs of P to aquatic environments can cause severe problems all over the world. Next to nitrogen (N), P has long been identified as main contributor to eutrophication of aquatic ecosystems and even small quantities can cause serious consequences such as excessive algae blooming, release of toxins, reduced water transparency, oxygen depletion, and a general deterioration of the water quality (Bonsdorff et al., 1997).

The need for comprehensive regulation of nutrient inputs to aquatic ecosystems was already established in the 1970s and progress has been reported in the reduction of discharges from major point sources such as wastewater treatment plants since then (Lewis et al., 2011; Withers et al., 2014). Especially in Europe, there were made many political efforts for the protection and management of marine environments resulting in marine conventions such as the Helsinki Convention (HELCOM) for the protection of the Baltic Sea area, the Oslo-Paris Convention (OSPAR) to protect the marine environment of the North-East Atlantic, the United Nations Environment Programme Mediterranean Action Plan (UNEP/MAP) to protect the marine environment and coastal region of the Mediterranean or the Mediterranean Sea pollution (MED POL) to monitor the Mediterranean Sea region. Nonetheless, non-point nutrient sources such as diffuse inputs especially from P fertilizers applied to arable crops, remain a serious threat to many surface waters, which are still in poor ecological condition (Withers et al., 2014).

Phosphorus can be present in many inorganic (P_i) and organic (P_o) chemical forms in different ecosystems (Cade-Menun et al., 2019). Soil P_i can appear as orthophosphate anions in

solution, orthophosphate minerals or orthophosphate sorbed to minerals surfaces and organic matter (OM), while P_o occurs in forms where P atoms are bonded to carbon (C), such as phosphomonoesters or phosphodiesters. Furthermore, there are condensed forms of P, such as pyrophosphate or polyphosphates with origins in living organisms (McLaren et al., 2020). The chemical form of P is one of the major factors influencing the risk of P mobilization and transportation from arable soil to aquatic environments (Kerr et al., 2011). The P speciation in terrestrial soils and aquatic sediments depends on various biological and chemical transformation processes such as sorption, reduction/oxidation, precipitation and mineralization. Thus, many current studies addressed the research topic of chemical P speciation in agricultural soils (e.g. Koch et al., 2018; Turner et al., 2008; Schmieder et al., 2020), sediments (e.g. Frankowski et al., 2002; Łukawska-Matuszewska and Bolałek, 2008; Kraal and Slomp, 2014) and biogenic materials such as organic fertilizers or biological soil crusts (Ajiboye et al., 2007; Baumann et al., 2017). The presence of Fe and Al (oxyhydr)oxides has been identified as important controlling factor among solid phases for P solubility in soils by having high affinities for oxyanions like phosphate (Gypser et al., 2021). Humic substances can also strongly affect P adsorptions by binding with metal hydroxides and blocking the adsorption site for P and inhibiting the crystallization of Fe and Al hydroxides (Chen and Arai, 2020). Among organic P species in soils, myo-inositol hexaphosphate (myo-IHP) was determined to be the most abundant as a result of preferential adsoprtion to soil colloids (Chen and Arai, 2020). Furthermore, changes of the oxidation-reduction (redox) status greatly affect sorption and desorption processes of P in soils and sediments (Patrick and Khalid, 1974). Anaerobic conditions, present in deeper sediments or caused by flooding of soils induce a lower redox potential because of decreased oxygen concentrations, can increase pH in acidic soils and decrease it in alkaline soils. Higher soil pH can enhance hydrolysis of Al and Fe phosphates and processes of P desorption by anion exchange. A decreased pH in calcareous soils can lead to a higher dissolution of Ca-P minerals. Reducing conditions slowly dissolve Fe^{3+}-P minerals, releasing Fe^{2+} and phosphate into solution and can alter the surface activity of Fe oxides for P, resulting in decreased P sorption capacities and bonding strength for P (Sims and Pierzynski, 2005).

However, it is not only important to investigate the P speciation in individual samples such as soil, water or sediment, but also to reveal functional relations between P from different

environmental compartments to derive knowledge about transformation processes along transport pathways of P in terrestrial and aquatic ecosystems. Investigations about the P speciation and their transformation processes along transects for example from arable soil to aquatic sediments are scarce, not least because of methodological limitations within P research. Concentrations of P in the environment are much lower than those of carbon (C) and N, and P has no significant gaseous forms on earth and only one stable isotope (^{31}P) (Cade-Menun et al., 2019). Nonetheless, Audette et al. (2018) analyzed transects from polder agricultural muck soils to river and lake sediments in Ontario, Canada with regard to characterization of P in sediments affected by agricultural land use. Along these transects of muck soils to river and lake sediments Audette et al. (2018) reported that recalcitrant P_o tends to accumulate in the terrestrial soils whereas the sediments were dominated by fractions of redox-sensitive P_i, extracted by borate dithionite. Another investigation of soils and sediments along a continuum from arable fields to nearshore lake sediments in the area of New York, USA revealed a significant shift from Al-P and OM associated P to Ca-P compounds dominating lake sediments (Noll et al., 2009). Significant amounts of P were lost from field soils, transported to the adjacent lake system and either became available to biota or were deposited in deeper portions of the lake (Noll et al. 2009). The export of P along its transport pathway into the aquatic environment and the changes in P composition had also great impacts on the macrophyte biomass in the stream water entering the lake (Noll et al., 2009).

Thus, it is necessary to ascertain if similar mechanisms and transport processes such as P_o accumulations in distinct areas, shifts from Al-P to Ca associated P forms and general links between soil and sediment P speciation are universal in different environmental compartments. Therefore, we selected three investigation areas with various sizes including soil and sediment samples along sequences from terrestrial to aquatic conditions (Figure 1-1). The first investigation area, rather small in size, is represented by samples along a transect from arable soil to sediments from a kettle hole with a maximum distance of about 70 m between all samples. The second sampling set of soils and sediments along a sequence starting at arable soils leading to sediments from a small lagoon of the Baltic Sea, called ‘Bodden’, within about 700 m illustrates a mesoscale ecosystem. Finally, the largest investigated area representing a macroscale transect, includes soils and sediments from coastal areas up to the central Baltic Sea with distances up to 600,000 m between the samples.

1.2. Methodological approach

Methods to determine total P (P_t) and operationally defined P pools in soils and sediments have a long and well-established history. Nowadays, advances have been made in soil and sediment P research because the need for methods providing structural information across spatial and temporal scales had been recognised. Thus, over recent years, numerous innovative and advanced methods for soil and sediment P research were developed. There are bulk and spatially resolved spectroscopic and spectrometric P speciation methods such as 1 and 2D nuclear magnetic resonance (NMR) spectroscopy, Raman spectroscopy, infrared (IR) spectrometry, high resolution-mass spectrometry (MS), nano-scale secondary ion mass spectrometry (NanoSIMS) or X-ray fluorescence (XRF) spectroscopy, X-ray absorption spectroscopy (XAS), and X-ray photoelectron spectroscopy (XPS) as well as methods focussing on P reactions such as sorption isotherms, quantum-chemical modeling, microbial biomass P, enzyme activity or ^{33}P isotopic exchange (Kruse et al., 2015).

To gain a comprehensive picture of the P speciation in soil and sediment samples from different environments, a combination of traditional methods in P research, such as chemical fractionations with advanced state-of-the-art methods, such as X-ray absoprtion near edge structure (XANES) spectroscopy and ^{31}P NMR spectroscopy is reasonable. These methods detect P pools and single P compounds based on different physical and chemical principles enabling complementary results and a profound evaluation of P speciation. In the following, fundamental principles, advantages and disadvantages of these three methods in P research are explained.

The sequential P fractionation established by Hedley et al. (1982), modified by Tiessen and Moir (1993), is one of the most widely used wet chemical methods to characterize pools of P in different environmental samples (Condron and Newman, 2011; Kruse et al., 2010; Negassa and Leinweber, 2009). In this fractionation scheme, a series of reagents with increasing extraction strengths is used to successively extract P pools on the basis of interactions between P moieties and other components of the soil matrix (Condron and Newman, 2011). The sequential fractionation method by Hedley et al. (1982) was originally developed for soils, but it was also used to investigate the P speciation of sediments, aeolian dust and biological soil crusts (Baumann et al., 2017; Eger et al., 2013; Li et al., 2015; Zhang et al., 2018). To separate the

occurring P compounds, the differently extracted P forms are assigned to operationally defined P pools. We distinguished the following P fractions: 1) resin-P, representing soil solution P and very readily desorbable P; 2) inorganic ($NaHCO_3$-P_i) and organic ($NaHCO_3$-P_o) bicarbonate P, representing labile P_i and P_o, including readily desorbable P and very labile pools of Ca phosphates, microbial P, and an unknown portion of the soil P_o; 3) inorganic (NaOH-P_i) and organic (NaOH-P_o) hydroxide P, representing moderately labile P_i, including moderately desorbable P, and Al- and Fe-phosphates and P_o associated with the soil OM and IPs, and; 4) the H_2SO_4-P fraction, which represents pools of more stable Ca-phosphates (e.g., hydroxylapatite). Recently, Barrow et al. (2020) criticized the accuracy of fractionation procedures designed to measure chemically specified phosphate fractions in soil extracts. They falsely detected Fe-P, Al-P and Ca-P in sequential extraction solutions of synthesized P-bearing minerals (Barrow et al., 2020). Although there is a certain risk of false detection in the common interpretation of extractable P fractions, many studies demonstrated the value of P fractionations especially in combination with other analytical P characterization techniques such as isotope analyses or XANES spectroscopy (Bromfield, 1967; Gu et al., 2020; Gu and Margenot, 2021; Guppy, 2021; Prüter et al., 2022; Williams and Walker, 1969).

The P *K*-edge XANES spectroscopy is an element-specific method to describe the P speciation in terrestrial soils as well as aquatic sediments (e.g. Acksel et al., 2016; Koch et al., 2018; Li et al., 2015; Prietzel et al., 2013). In contrast to sequential fractionation procedures, XANES spectroscopy has the advantage of direct sample usage without further extraction or destruction (Kruse et al., 2010; Prüter et al., 2020). Within the linear combination fitting (LCF) of P XANES spectroscopy, distinct reference P compounds are used to estimate proportions of atomic P that has similar local coordination environment as in the environmental samples (Gu and Margenot, 2021). However, XANES spectroscopy is not able to differentiate reliably between P_o and P_i species under certain soil conditions (Prietzel et al., 2016), but results of P_o concentrations from sequential fractionation or ^{31}P NMR spectroscopy can be used to complement the XANES spectroscopy (Gu and Margenot, 2021).

^{31}P NMR spectroscopy can be used to detect P species in both solid and liquid samples. Even if solid-state ^{31}P NMR spectroscopy has the advantage of direct measurements of unaltered samples such as soil without extraction or complex pretreatments, it is not widley used in soil science to date because of insufficient spectral resolutions caused by paramagnetic metal

cations such as Mn and Fe in soil (Kruse et al., 2015). Solution ^{31}P NMR spectroscopy on soil extracts has been used for over 40 years to detect simultaneously all forms of P_o that could be brought into solution (McLaren et al., 2021). The biggest advantage of solution- over solid-state ^{31}P NMR spectroscopy is the much higher spectral resolution. Prior to analysis with solution ^{31}P NMR spectrsocopy, P needs to be extracted from soil or other environmental samples such as sediments or organic amendments, with NaOH-EDTA by shaking the sample together with the extractant for several hours (Kruse et al., 2015). Most signals in NMR spectra of soil extracts were found in the orthophosphate and phosphomonoester region but there were also signals detected in the regions of phosphodiesters, pyrophosphates, polyphosphates and phosphonates (Turner et al., 2002; Cade-Menun, 2005; McLaren et al., 2020). An addition of known P species to extracted samples, called “spiking”, enables an assignment of unknown peaks especially within the phosphomonoester region of NMR spectra. Another possibility to identify unknown peaks is a comparison of chemical shifts of known P_o forms from different chemical matrices with the observable NMR signal in the sample extract (McLaren et al., 2020). Due to many overlapping singals in the phosphomonoester region of NMR spectra, spectral deconvolution fitting (SDF) is needed to obtain a partition of the NMR signal and enable a quantification of distinct P_o compounds (Reusser et al., 2020). Peak areas within the NMR spectrum can be calculated by expressing them as a proportion of the total net peak area of the NMR spectrum and multiplying them by the P_t concentration of the samples extract (McLaren et al., 2020). Nonetheless, the method of solution ^{31}P NMR spectroscopy has also some limitations such as the risk of sample alteration by alkaline extraction or the presence of P compounds that are not extractable by NaOH-EDTA and thus cannot be determined using ^{31}P NMR spectroscopy (Kruse et al., 2015; McLaren et al., 2020).

As many analytical methods for the characterization of P in soils and sediments carry advantages and disadvantages, comprehensive studies should never be based on one single method for P characterization. Thus, we decided on the application of the complementary techniques sequential P fractionation, XANES spectroscopy and ^{31}P NMR spectroscopy to gain a profound picture of P speciation and to ensure the quality of results.

1.3. General and specific objectives

The general objective of the present work was to uncover the P speciation and to detect functional interactions between single chemical P compounds and transformation processes of P along transport pathways from terrestrial to aquatic environments including terrestrial, arable soils, semiterrestrial wetlands and aquatic sediments along sequences in different sized ecosystems.

In this context, the specific objectives were:

- to determine the influence of common sample pretreatment on P speciation and to confirm the applicability of P fractionation procedures to detect and quantify P pools in soil and sediment samples from the investigated environments
- to characterize the P speciation in terrestrial and semiterrestrial soils and aquatic sediments and to reveal major differences between them by a multi-method approach
- to detect transformations within the P composition along transport pathways from terrestrial soils towards aquatic sediments in three ecosystems of different size
- to uncover possible sinks in the environment where P can be trapped and conserved
- to identify alternative origins of P in aquatic sediments by investigating the possible contribution of P from solid fish waste to the P speciation of aquatic sediments

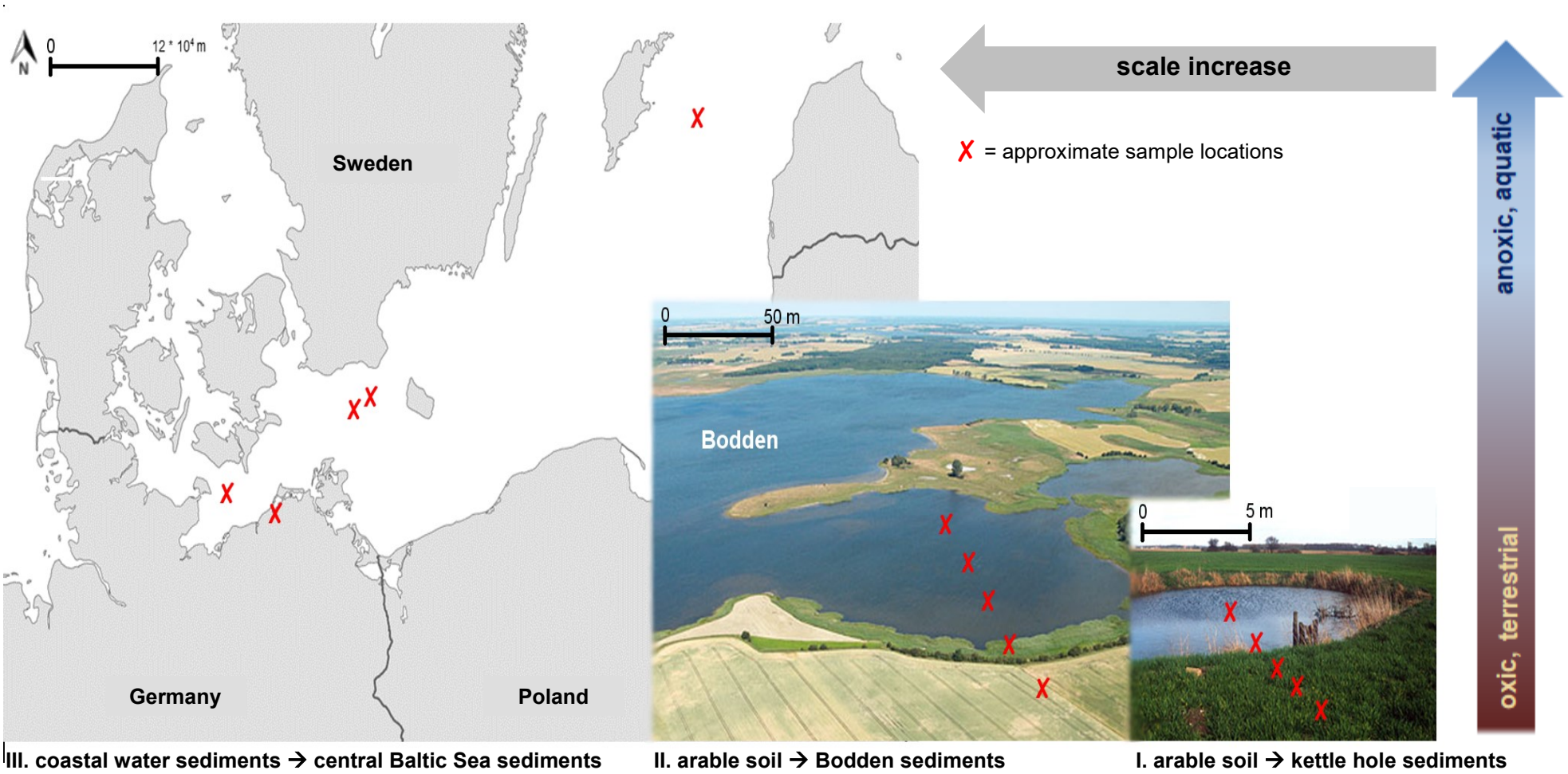

Figure 1-1 Sampling strategy in three different environments: I. soil and sediment samples from an arable field to a kettle hole (microscale) II. soil and sediment samples along a transect from arable soil to Bodden sediments (mesoscale), III. soil and sediment samples from coastal areas up to the central Baltic Sea (macroscale).

2 Influence of sample pretreatment on P speciation in sediments evaluated with sequential fractionation and P *K*-edge XANES spectroscopy

Julia Prüter[1], Yongfeng Hu[2], Peter Leinweber[1]

[1]*University of Rostock, Soil Science, Justus-von-Liebig Weg 6, 18051 Rostock, Germany*

[2]*Canadian Light Source, Inc., University of Saskatchewan, 44 Innovation Boulevard, Saskatoon, Saskatchewan S7N 2V3, Canada*

Published in

Communications in Soil Science and Plant Analysis (2022) 53(14), 1712-1230

2.1. Abstract

Sequential phosphorus (P) fractionation procedures are one of the most widely used wet chemical methods for characterizing P pools in soils and sediments, but have also been criticized repeatedly for their lack of accuracy to measure chemically specified phosphate fractions. In the recent investigation, sediments from two different sample locations with the same pretreatments were analyzed with sequential P fractionation. To verify traditional assignments of P fractionation results, P *K*-edge X-ray absorption near edge structure (XANES) spectroscopy was applied on the sediments and especially on the residues after the sequential extraction steps. Results of both methods indicated that the influence of sample pretreatment on the distribution of P pools was much lower compared to the effects of different sample origins. Kettle hole sediments were dominated by moderately labile iron (Fe) and aluminum (Al) associated P species, whereas Bodden sediments contained more stable calcium (Ca)-P species. Sample pretreatment of sediments can be similar to traditional soil sample pretreatment without causing fundamental changes in P speciation. The P *K*-edge XANES spectroscopy confirmed most assumptions of sequential P fractionation.

Keywords: Phosphorus • P fractionation • pretreatment • P XANES • sediment

2.2. Introduction

Phosphorus (P), as an indispensable element for all organisms and a limiting key factor in various ecosystems, has been intensively studied in past and present (e.g. Addiscott et al. 2000; Baumann et al. 2020; Condron and Newman 2011; Cordell and White 2011; Elser et al. 2007; Kruse et al. 2015). In unchanged and modified terrestrial as well as aquatic environments, P plays an essential role for, inter alia, ecosystem productivity and the general environmental constitution (Bonsdorff et al. 1997; Condron and Newman 2011). There is an enormous variety of different P species in matrices such as soils, sediments, manures and other wastes. A combination of proven and innovative reliable P research methods is required in order to characterize the P pools, reveal the transfer of P compounds from terrestrial to aquatic environments and to gain an overall better insight into the complexity of interactions between inorganic, organic and microbial P (Condron and Newman 2011; Kruse et al. 2010; 2015).

Until today, the sequential P fractionation established by Hedley, Stewart, and Chauhan (1982), eventually with modifications by Tiessen and Moir (1993), is one of the most widely used wet chemical methods to characterize forms of P in different biological and geological materials (Condron and Newman 2011; Kruse et al. 2010; Negassa and Leinweber 2009). This fractionation scheme uses a series of reagents with different extraction strengths to successively extract various forms of P on the basis of interactions between P moieties and other components of the soil matrix (Condron and Newman 2011). The sequential fractionation method by Hedley, Stewart, and Chauhan (1982) was originally developed for soils, but was also applied on sediments, aeolian dust and biological soil crusts (Baumann et al. 2017; Eger, Almond, and Condron 2013; Li et al. 2015; Zhang et al. 2018). The necessary separation of

different P forms is achieved by assignment to operationally defined P pools but not inevitably chemically defined P species in the sequential fractionation (Cross and Schlesinger 1995). Heavy criticism was drawn about the accuracy of fractionation procedures designed to measure chemically specified phosphate fractions in soil in a recent investigation by Barrow et al. (2020). They showed a false assignment of iron (Fe)-P, aluminum (Al)-P and calcium (Ca)-P in extracts from two types of synthesized P-bearing goethite and Al oxide extracted with the fractionation method of Chang and Jackson (1957). Although there is no doubt about a certain risk of false assignment of specific P forms to distinct fractions confirmed by several investigations (Bromfield 1967; Gu et al. 2020; Williams and Walker 1969), very recently Gu and Margenot (2021) and Guppy (2021) demonstrated the value of fractionations under certain conditions. Results of existing fractionation procedures should be interpreted with caution and comprehensive studies should never be based on one single analytical soil P characterization technique as many of them have advantages and disadvantages (Gu and Margenot 2021). The necessity of a combination of fractionation measurements with P *K*-edge X-ray absorption near edge structure (XANES) spectroscopy to constrain uncertainties and increase the accuracy of fractionation procedures has been emphasized by both Gu and Margenot (2021) and Guppy (2021).

Generally, P *K*-edge XANES spectroscopy is a promising method to describe P speciation of soils and sediments (e.g. Acksel et al. 2016; Hesterberg et al. 1999; Koch et al. 2018; Kraal et al. 2015; Li et al. 2015; Morshedizad et al. 2018; Prietzel et al. 2013). Although P XANES spectroscopy is an expensive and time consuming method in P research and can be applied only to a limited number of samples, its element-specific approach and chemical sensitivity to P-species can help to validate and improve interpretation of results from P fractionation (Kruse et al. 2010). Furthermore, and contrasting to the fractionation method by Hedley, Stewart, and Chauhan (1982), it has the advantage of direct sample usage without further extraction or destruction (Kruse et al. 2010; Prüter et al. 2020). Condron and Newman (2011) suggested the use of XANES spectroscopy to evaluate the structural attributes of P compounds in sediment and soil. Baumann et al. (2017) revealed the suitability of P *K*-edge XANES spectroscopy for at least a rough classification of P species into organic (P_o) and inorganic (P_i) P compounds in soil. Investigations of sequentially extracted fen peat soils and agro-industrial by-products with P XANES spectroscopy could confirm the stepwise removal of single P pools during sequential fractionation by peak intensity of XANES spectra (Kruse and Leinweber 2008; Kruse et al. 2010). Especially the interpretation of sulfuric acid (H_2SO_4)-extracted P fraction was validated by P *K*-edge XANES in post-extraction solid residues from sugarcane and niger seed filter cakes (Kruse et al. 2010). Kar et al. (2011) also ascertained a correlation of the quantity of P removed by extraction steps from soils amended with different fertilizers with results from XANES spectroscopy, although they emphasize that some assumptions in sequential chemical extractions may be incorrect and strongly depend on fertilizer type and soil characteristics. Gu et al. (2020) evaluated the accuracy of sequential P extraction of soils with different chemical properties with XANES spectroscopy and found an overestimation of Ca-bound P of sequential extraction. Thus, they suggest ongoing research on sequential extraction schemes of other

types of soils and aquatic sediments to reduce uncertainties in quantifying P pools. To the best of our knowledge, verification of P fractionation by P *K*-edge XANES spectroscopy has been done for soils, organic amendments or synthesized samples (Ajiboye at al. 2007; Barrow et al. 2020; Gu et al. 2020; Kar et al. 2011; Kruse and Leinweber 2008, Kruse et al. 2010), but never for sediments to date.

To further facilitate research of P transformation processes especially at the fluent boundaries of terrestrial/semiterrestrial soils towards sediments in aquatic environments, it is beneficial to treat samples of the various different origins the same way prior to analyses in order to exclude the factor “sample pretreatments” and enable disclosing the real environmental influences on the P species. However, several investigations revealed a considerable influence of drying, grinding and storage on the extractability of P from soil (Schlichting and Leinweber 2002; Turner and Haygarth 2001; Turner et al. 2005). To date, there are only a few publications examining especially the effects of sediment handling and pretreatment on the determination and interpretation of P fractionation results (Condron and Newman 2011; Psenner, Pucsko, and Sager 1984). Condron and Newman (2011) suggested different extraction schemes and sample handlings to evaluate the P speciation of distinct groups of sediments and soils like organic samples, inorganic sediments, calcareous sediments or samples from highly reduced environments. Freeze-drying has been discovered to transform labile P compounds (Martin, Nirel, and Thomas 1987) as well as reduce the total extractability of P compared to non-freeze-dried sediments (Goedkoop and Pettersson 2000). Until now, it is not clear to what extent the traditional sample pretreatments in soil sciences such as drying, sieving and grinding affect the results of P fractionation of sediments.

Thus, the objectives of this study were (1) to characterize differences in P speciation of sediments induced by sample pretreatment with the help of sequential P fractionation and (2) to validate the interpretation and assignment of the single P fractionation extraction steps by P *K*-edge XANES spectroscopy.

2.3. Material and methods

2.3.1. Sampling area and sediment collection

Sampling was conducted in January 2020 from two different ecosystems. The first sample set was collected from a kettle hole surrounded by an arable field near the village Huckstorf, about 10 km south of the city of Rostock in Mecklenburg-Western Pomerania in northeast Germany. This kettle hole has been water-filled for many years but became dry for the past three years due to summer draughts. The sampling area is located in an arable field situated in Weichselian Pleistocene lowland. Kettle hole sediments were taken by a soil corer from depths of 0-10 cm (samples K1) and 10-20 cm (samples K2) in five replicates from one square meter. These five subsamples were each merged to one mixed sample per depth to minimize effects of small-scale heterogeneity.

The sampling location of the second sample set was near Dabitz on the Darss-Zingst Bodden Chain, a shallow lagoon system connected to the Baltic Sea in Mecklenburg-Western Pomerania in northeast Germany (further site description in Karstens, Buczko, and Glatzel 2015). Triplicate samples of Bodden sediment were collected 300 m from shore in a water depth of 80 cm using a 10-cm-plastic tube. The three replicates were merged to one sample to obtain a representative mixed sample.

To study the influence of sample pretreatment, subsamples of the mixed kettle hole and Bodden sediments were treated in four different ways before P analyses. Samples K-f and B-f were kept completely **f**resh, wet and untreated; K-s and B-s were dried at 40°C and **s**ieved < 2 mm; samples K-m and B-m were dried at 40°C, sieved (< 2 mm) and finely ground in a mortar **m**ill and samples named K-l and B-l were **l**yophilized directly from fresh condition.

2.3.2. Particle size distribution and elemental concentrations

Sediment particle size distribution was determined after chemical and physical disaggregation of 20 g sample with 50 mL of 0.1 M sodium diphosphate ($Na_4P_2O_7$) solution and ultrasonic treatment (Vibra-Cell™, Sonics & Materials, Inc., Newtown) for 9 minutes by wet sieving of the sand fraction (2 mm to 0.063 mm) and automated sedimentation analysis (Sedimat 4-12, UGT GmbH, Müncheberg, Germany) of the silt (< 63 µm to 2 µm) and clay fraction (< 2 µm).

Elemental concentrations of P, Ca, magnesium (Mg), Al, Fe and zinc (Zn) were determined with an inductively coupled plasma-optical emission spectrometer (ICP-OES) after microwave-assisted digestion (Mars Xpress CEM GmbH Kamp-Linfort, Germany) of about 50 mg sediment with aqua regia consisting of 2 mL nitric acid (HNO_3) and 6 mL hydrochloric acid (HCl) (ISO standard 11466) in duplicates. Elemental concentrations in mg kg^{-1} were calculated referring to the dry matter content of every sample.

2.3.3. Sequential P frationation

A sequential fractionation method according to Hedley, Stewart, and Chauhan (1982), modified by Tiessen and Moir (1993) was used to extract different P fractions from sediment. About 0.42 g dry sediment was weighed into 50 mL centrifuge tubes in duplicates. For the fresh sediments, weights were adjusted for the water content in order to also obtain about 0.42 g dry matter in the centrifuge tubes. This resulted in about 0.70 g sample for the fresh kettle hole sediment K2-f, and 0.55 g for the fresh Bodden sediment B-f. Calculations of P in mg kg^{-1} in the different fractions were referred to individual dry matter contents of the samples. In each fractionation step, samples were shaken for 18 h followed by centrifugation at 4000 g for 20 min, and decanted. The chemical P fractionation included the following extraction steps: (1) anion exchange resin strips (6 × 2 cm resin membrane, 551642S, BDH Laboratory Supplies, Poole, England), (2) 0.5 M sodium hydrogen carbonate ($NaHCO_3$), (3) 0.1 M sodium hydroxide (NaOH) and (4) 1 M H_2SO_4, which were all conducted under ambient air temperature. In the fraction of anion exchange resin, P was removed from the resin using 1 M hydrochloric acid (HCl). H_2SO_4

was used instead of HCl because Tiessen, Stewart, and Moir (1983) reported P_o losses by the use of hot HCl. Solid residues after the last fractionation step were digested in microwave (Mars Xpress CEM GmbH Kamp-Linfort, Germany) with aqua regia solution (3:1 hydrochloric acid – nitric acid; ISO standard 11466) and concentrations of residual-P were measured in these extracts.

The P concentrations in different extracts were determined in the supernatants using an ICP-OES while the remaining sediment pellet was used for the next extraction step. Concentrations of P_i in the extracts were determined colorimetrically with the molybdate-blue method as described by Murphy and Riley (1962). The concentration of P_o was estimated by subtracting P_i from P determined with ICP-OES. To enable an additional analysis of P speciation with XANES spectroscopy after the single extraction steps, replicate sediment pellets of the extraction steps with $NaHCO_3$, NaOH and H_2SO_4 were removed and dried at 40°C.

2.3.4. P K-*edge X-ray absorption near edge structure (XANES) spectroscopy*

The P *K*-edge XANES spectra for characterizing P species in the samples were recorded at the Canadian Light Source (CLS) in Saskatoon, Saskatchewan, Canada on the soft X-ray micro-characterization beamline (SXRMB) (Hu et al. 2010) covering an energy range of 1.7 to 10 keV. The XANES data were collected from dry sediment samples with different pretreatments thinly spread on P-free carbon tape. Sample spectra were collected in fluorescence yield mode by using a 7-element silicon drift detector (SDD) and reference standards in total electron yield mode at photon energies between 2130 and 2200 eV for the P *K*-edge. The step size was 1 eV in the pre-edge region (2130 to 2140 eV), 0.15 eV at the edge step (2140 to 2180 eV), and 0.5 eV in the post-edge region (2180 to 2200 eV) with a dwell time of 4 s for the samples and 1 s for reference standards. Two to three scans were collected and averaged for each sample. The position of the sample holder was changed after each scan.

All P *K*-edge XANES spectra were background corrected, normalized, and the replicates were merged. Linear combination fitting (LCF) was performed using the ATHENA software package (Ravel and Newville 2005) in the energy range between -20 eV and +30 eV of E_0. The same ranges were used for the reference P *K*-edge XANES spectra. To achieve the best compatible set of references with each specified sample spectrum, LCF analysis was performed using the combinatorics function of ATHENA software to attain all possible binary to quaternary combinations between all P reference spectra in which the share of each compound was ≥ 10%. The following set of 15 reference P *K*-edge XANES spectra was used for fitting and calculations: phytic acid sodium salt hydrate ($C_6H_{18}O_{24}P_6 \cdot xNa^+ \cdot yH_2O$), calcium hydrogenphosphate dihydrate ($CaHPO_4 \cdot 2H_2O$), hydroxyapatite ($Ca_{10}(PO_4)_6(OH)_2$), iron(III)-phosphate dihydrate ($FePO_4 \cdot 2H_2O$), iron(III)-phosphate tetrahydrate ($FePO_4 \cdot 4H_2O$), vivianite ($Fe^{3+}(PO_4)_2 \cdot 8H_2O$), P adsorbed on goethite (P-FeOOH), P adsorbed on ferrihydrite (P-Fe_2O_3), aluminium phosphate hydrate ($AlPO_4 \cdot xH2O$), aluminum metaphosphate ($Al(PO_3)_3$), P adsorbed on gibbsite (P-($Al(OH)_3$)), P adsorbed on boehmite (P-AlOOH), magnesium

hydrogenphosphate trihydrate ($MgHPO_4 \cdot 3H_2O$), struvite ($(NH_4)MgPO_4 \cdot 6H_2O$), and zinc phosphate ($Zn_3(PO_4)_2$). The *R*-factor values were used as goodness-of-fit criteria and significant differences between fits were evaluated using the Hamilton test ($p < 0.05$) (Calvin, 2013) with the number of independent data points calculated by ATHENA, estimated as data range divided by core-hole lifetime broadening. Best fits were chosen according to the lowest *R* factor of P reference compound combinations and considered as the most probable P species in the material. If *R* factors of fits with the same number of reference compounds were not significantly different from each other according to the Hamilton test, fit proportions were averaged. *R* factors were smaller than 0.009 for most unfractionated kettle hole and Bodden samples, smaller than 0.01 for most kettle hole residues and smaller than 0.07 for most Bodden residues of sequential fractionation, indicating good fits.

2.3.5. Statistical analyses

Data analysis was performed using the open-source statistical software R (version 3.6.3). R package agricolae was used for Tukey's honest significant difference (HSD) test, which enables multiple comparisons. The significance level was 0.05 (https://cran.r-project.org/web/packages/agricolae/index.html). The Tukey's HSD test was used to find differences in the elemental concentrations and the results of P fractionation between the sediments with different pretreatments and origins.

2.4. Results and discussion

2.4.1. Basic physical and chemical properties

Analyses of grain size distribution showed much higher proportions of silt and clay in the kettle hole sediments from both depths compared to the Bodden sediment, clearly dominated by coarser sand particles (Table 1).

On average K1 contained about 2064 mg kg^{-1} P almost without significant differences among the pretreatments (Table 1). There were slight, but insignificant differences in Ca, Mg, Al, and Zn concentrations according to the pretreatments of K1. Exclusively the Fe concentration was significantly higher in the fresh K1 sediment, followed by the lyophilized subsample and even lower amounts in the sieved and milled kettle hole sediment. Among the pretreatments of K2, the average P concentration was 1917 mg kg^{-1}. The amount of P in the fresh sediment of K2 was considerably lower than in the sieved, milled and lyophilized subsamples. Concentrations of Ca, Mg, Al, and Zn were not significantly different among the pretreatments of K2. Again, there were significant differences of Fe concentrations. The lyophilized, the sieved and the milled K2 sediments contained significantly more Fe than the fresh sample variant. The average P concentration of Bodden sediment samples was 172 mg kg^{-1} with no significant differences among the pretreatments. Elemental concentrations of Ca, Mg, Al, Fe and Zn in the pretreatments of Bodden sediment were also not significantly different from each other. Coefficients of variation (data not shown for reasons of clarity) appear in a range from 0.0004 to

0.0510 for all determined elements in the kettle hole sediments and from 0.0023 to 0.2149 in the Bodden sediments.

There were considerably higher concentrations of all analyzed elements in the kettle hole sediments compared to the Bodden sediments as displayed in Table 1. The P concentrations in the kettle hole samples were about 12 times higher compared to the Bodden sediments.

Calculated ratios of P to the other possible P binding partner elements (Table 1) showed similar results as the elemental concentrations. There were slight differences in one sample set of kettle hole and Bodden sediments between the distinct pretreatments but there was no clear, directed influence of a certain sample treatment on an element concentration and P-to-element ratio. Overall, the elemental ratios of P/Mg, P/Al, P/Fe and P/Zn were much lower in the kettle hole compared to the Bodden sediment. The P/Ca ratio was about three times higher in the kettle hole samples than in the Bodden sediments, which indicated lower relative Ca contents in the kettle hole samples compared to Bodden sediments.

Table 2-1 Grain size distribution of kettle hole (K1, K2) and Bodden (B) sediments, mean elemental concentrations of phosphorus (P), calcium (Ca), magnesium (Mg), aluminum (Al), iron (Fe) and zinc (Zn) in mg kg^{-1} determined by ICP-OES (n = 2), and ratios of P to the other elements in K1, K2, and B with different pretreatments (f = fresh, s = sieved, m = milled, l = lyophilized). Significant differences at 5% probability level between samples are designated by different letters (a, b, c, d, e, f).

Sample	Sand	Silt	Clay	P	Ca	P/Ca	Mg	P/Mg	Al	P/Al	Fe	P/Fe	Zn	P/Zn
	%			mg kg^{-1}	mg kg^{-1}		mg kg^{-1}		mg kg^{-1}		mg kg^{-1}		mg kg^{-1}	
K1-f	1	50	49	2079^{a}	2798^{a}	0.74	5901^{a}	0.35	30143^{a}	0.07	32834^{a}	0.06	141^{ab}	14.79
K1-s				2040^{a}	2631^{a}	0.78	5467^{ab}	0.37	28603^{a}	0.07	29802^{cde}	0.07	135^{b}	15.15
K1-m				2080^{a}	2533^{a}	0.82	5404^{ab}	0.38	28082^{a}	0.07	29470de	0.07	133^{b}	15.59
K1-l				2056^{a}	2591^{a}	0.79	5698^{ab}	0.36	29805^{a}	0.07	30944^{bc}	0.07	143^{a}	14.42
K2-f	1	54	45	1742^{b}	2545^{a}	0.68	5322^{b}	0.33	25814^{a}	0.07	29221^{e}	0.06	133^{b}	13.08
K2-s				1970^{a}	2739^{a}	0.72	5740^{ab}	0.34	29289^{a}	0.07	31320^{b}	0.06	140^{ab}	14.08
K2-m				1999^{a}	2981^{a}	0.67	5624^{ab}	0.36	27735^{a}	0.07	30600^{bcd}	0.07	138^{ab}	14.44
K2-l				1959^{a}	2748^{a}	0.71	5774^{ab}	0.34	28868^{a}	0.07	31888^{ab}	0.06	141^{ab}	13.94
B-f	93	2	5	175^{c}	894^{b}	0.20	408^{c}	0.43	738^{b}	0.24	1231^{f}	0.14	8^{c}	20.69
B-s				186^{c}	743^{b}	0.25	376^{c}	0.49	607^{b}	0.31	1076^{f}	0.17	5^{c}	40.62
B-m				164^{c}	920^{b}	0.18	403^{c}	0.41	879^{b}	0.19	1203^{f}	0.14	5^{c}	30.89
B-l				162^{c}	800^{b}	0.20	424^{c}	0.38	1049^{b}	0.15	1527^{f}	0.11	5^{c}	30.60

The P contents in the kettle hole sediments of both depths agree with an investigation of two different kettle holes in Northeast Germany, where a maximum of 2000 mg kg^{-1} P was determined at the sediment surface (Kleeberg et al. 2016). The much lower P concentration of Bodden sediment coincides with P contents of about 118 - 435 mg kg^{-1} measured in 0-2 cm and 2-10 cm depth of sediment from the fringe zone of Darss-Zingst Bodden Chain (Karstens et al. 2016).

The significantly higher amounts of all examined elements at both depths in the kettle hole compared to the Bodden sediments can be due to several reasons. Main factors influencing elemental contents of sediments were sample position and surrounding environment. Plausibly, much more nutritional elements for plants such as P, Ca and Mg likely have been introduced from the surrounding highly fertilized arable fields into the kettle hole sediments as compared to Bodden sediments, which is 300 m off the coast. These sites received freshwater and matter inputs most likely from the rivers Recknitz and Barthe but not from the Baltic Sea due to the small opening (Karstens, Buczko, and Glatzel 2015; Selig et al. 2007). Furthermore, erosion can introduce soil particles together with elements from mineral weathering such as Al, Fe and Zn especially into kettle holes. For example, Frielinghaus and Vahrson (1998) and Nitzsche et al. (2017) reported significant amounts of soil and nutrient translocation from agricultural cropland into different kettle holes in Northern Germany. Another influencing factor concerning elemental contents is the sediment texture. Generally, fine sediments are able to keep more P than coarser ones (Łukawska-Matuszewska and Bolałek 2008). As grain sizes of kettle hole sediments were much lower compared to the Bodden sediments in this investigation, this is an additional explanation for the higher concentrations of P and other elements in the kettle hole sediments.

The slight, insignificant differences in elemental concentrations among the pretreatments of one sample position can be explained by small-scale heterogeneity at the sampling positions in combination with a possibly better homogenization of the sieved, milled and lyophilized compared to the fresh samples. The lower P/Ca ratio and thus higher relative amount of Ca in the Bodden sediments compared to the kettle hole sediments agreed with a previous study, where even more Ca-bound P compounds were determined in sediments with an increasing aquatic influence compared to more terrestrially influenced sediments near the coast of Northern Germany (Prüter et al. 2020). The up to four times lower P/Al and P/Fe ratios and thereby higher relative Al and Fe contents of the kettle hole compared to the Bodden sediments also accord with a previous investigation, where coastal sediments of the northeastern Baltic Sea, influenced by high inputs from clayey soils rich in poorly crystallized Fe and Al oxides, had the biggest Fe and Al contents (Lukkari et al. 2009).

Generally, differences in elemental concentrations among sample pretreatments were small in this study whereas the sample position and environmental conditions had greater impact on the available amount of nutritional elements.

2.4.2. Sequential P fractionation

The kettle hole sediments were dominated by the P pools of NaOH-P_i (28%), NaOH-P_o (20 – 23%) and $NaHCO_3$-P_i (14 – 16%). There was a rather similar distribution of P pools within the different pretreatments of kettle hole and Bodden sediments, respectively. As displayed in Table 2, significant differences of P concentrations between the pretreatments of kettle hole sediment only appeared in the fractions of resin-P and NaOH-P. The fresh kettle hole sediment contained significantly less resin-P_i, resin-P_o and NaOH-P_i compared to the sieved and milled samples. The concentration of NaOH-P_o was significantly higher in the fresh kettle hole sample than in the milled and sieved variants. Proportions of P_o were highest in NaOH fraction (20 – 23%), but at least small proportions of P_o were determined in all fractions of kettle hole sediments. Equally as determined with aqua regia (Table 1), the sum of the single P fractions was significantly lower in the fresh kettle hole sample compared to the sieved and milled sediments.

The largest P pools in all Bodden pretreatment samples were H_2SO_4-P_i (42 - 55%) and $NaHCO_3$-P_i (25 - 36%). There were some differences in P concentrations among the pretreatments of Bodden sediment, but they were insignificant in most cases. The milled Bodden sediment contained significantly more $NaHCO_3$-P_i than the fresh and sieved samples. P_o could be determined exclusively in the H_2SO_4 fraction in small proportions of 4 – 5%. The sum of all P fractions in the fresh Bodden sediment was slightly lower than in the sieved and milled samples but this difference was not significant. Overall, the P-extractability of kettle hole and Bodden sediments was high because proportions of not extractable, residual P were very low (1 – 6%).

A comparison of the sequential P fractionation results of kettle hole and Bodden sediments showed considerably higher P concentrations in all fractions of kettle hole sediment. Furthermore, proportions of P_o were higher in most sequential fractions in the kettle hole sediments compared to the Bodden sediments. Percentages of resin-P were similar in kettle hole and Bodden samples, whereas the average proportion of $NaHCO_3$-P_i was nearly two times lower in kettle hole sediments compared to Bodden sediments. Percentages of residual-P are low in both kettle hole and Bodden sediments, but the concentration of P in mg kg^{-1} is many times higher in the kettle hole sediment (122 - 132 mg P kg^{-1}) compared to the Bodden sediment (2 - 9 mg P kg^{-1}). Sum of P extracted with sequential fractions was slightly higher compared to the amount of P determined with aqua regia (Table 1) in both the kettle hole and Bodden sediments with different pretreatments.

Table 2-2 Mean concentrations (mg kg^{-1}) (*n* = 2) and percentages (%) of the sequentially extracted inorganic (P_i) and organic (P_o) P fractions resin-P, $NaHCO_3$-P, NaOH-P, H_2SO_4-P, and residual-P from the sum of all fractions determined in the fresh (K2-f), sieved (K2-s) and milled (K2-m) kettle hole sediment (depth: 10-20 cm) and in the fresh (B-f), sieved (B-s) and milled (B-m) Bodden sediment. Significant differences at 5% probability level between samples are designated by different letters (a, b, c).

Sample	Resin-P_i		Resin-P_o		$NaHCO_3$-P_i		$NaHCO_3$-P_o		NaOH-P_i		NaOH-P_o	
	mg kg^{-1}	(%)	mg kg^{-1}	(%)	mg kg^{-1}	(%)	mg kg^{-1}	(%)	mg kg^{-1}	(%)	mg kg^{-1}	(%)
K2-f	102^{b}	(5)	22^{b}	(1)	323^{a}	(16)	165^{a}	(8)	567^{b}	(28)	469^{a}	(23)
K2-s	222^{a}	(10)	42^{a}	(2)	343^{a}	(15)	149^{a}	(7)	632^{a}	(28)	443^{b}	(20)
K2-m	241^{a}	(11)	33^{ab}	(2)	322^{a}	(14)	159^{a}	(7)	635^{a}	(28)	442^{b}	(20)
B-f	21^{c}	(10)	1^{c}	(0)	56^{c}	(27)	0^{b}	(0)	23^{c}	(11)	0^{c}	(0)
B-s	16^{c}	(6)	0^{c}	(0)	63^{c}	(25)	0^{b}	(0)	18^{c}	(7)	0^{c}	(0)
B-m	20^{c}	(7)	0^{c}	(0)	99^{b}	(36)	0^{b}	(0)	28^{c}	(10)	0^{c}	(0)

Sample	H_2SO_4-P_i		H_2SO_4-P_o		Residual-P		Sum
	mg kg^{-1}	(%)	mg kg^{-1}	(%)	mg kg^{-1}	(%)	mg kg^{-1}
K2-f	203^{a}	(10)	57^{a}	(3)	132^{a}	(6)	2040^{b}
K2-s	218^{a}	(10)	59^{a}	(3)	131^{a}	(6)	2239^{a}
K2-m	215^{a}	(10)	60^{a}	(3)	122^{a}	(5)	2229^{a}
B-f	90^{b}	(44)	11^{b}	(5)	2^{b}	(1)	204^{c}
B-s	140^{b}	(55)	11^{b}	(4)	9^{b}	(3)	257^{c}
B-m	117^{b}	(42)	10^{b}	(4)	5^{b}	(2)	279^{c}

The significantly lower and slightly lower concentrations of resin-P_i and $NaHCO_3$-P_i concentrations in the fresh compared to the dried and sieved kettle hole samples, respectively, agreed with an investigation of a constructed wetland, where air-drying resulted in an increase of bioavailable inorganic P at the expense of labile organic P (Olila, Reddy, and Stites 1997). Although some proportions of labile organic P, especially resin-P_o were even higher in the dry kettle hole samples, slight reductions of $NaHCO_3$-P_o and NaOH-P_o were determined after drying in the sieved and milled kettle hole sediments in the recent study. Decreases in $NaHCO_3$-P_o and NaOH-P_o caused by drying were also reported for peat soils (Schlichting and Leinweber 2002). This shift in labile P fractions from P_o to P_i caused by drying can be explained by microbial activity. Sparling, Whale, and Ramsay (1985) reported high contributions of microbial P from killed soil organisms to $NaHCO_3$-P in air-dried soils. Cell material of soil microorganisms can be destroyed by drying or freezing (Shields et al. 1973) and, therefore, can release P (Olila, Reddy, and Stites 1997). An enhanced P turnover of dry peat soils during re-wetting and extraction was

also confirmed by Brake, Höper, and Joergensen (1999). Effects of drying on P_o in the $NaHCO_3$ and NaOH fractions did not occur in the Bodden sediments, because nearly no P_o was determined in the first three extracted fractions. The only significant difference among the pretreatments of Bodden sediment was the higher amount of $NaHCO_3$-P_i in the milled sample compared to the fresh and sieved one (Table 2). Although grinding is known to increase the surface area of soil samples and thereby makes more P available for adsorption by resin (Potter et al. 1991), as detected in the kettle hole sediment, this is not visible in the Bodden sediment (Table 2). On the one hand, the generally very low P concentrations in all fractions of Bodden sediment could be responsible for the disappearance of this effect in the resin fraction. On the other hand, the same effect could explain the higher amount of $NaHCO_3$-P_i in the milled Bodden sediment compared to the fresh and sieved samples. The high proportions of 42-55% H_2SO_4-P_i in the Bodden sediment coincide with the results of a sequential P extraction of sediments from the shallow coastal zone of the Gulf of Gdańsk (Poland), where up to 43% Ca-bound P was extracted with HCl (Łukawska-Matuszewska and Bolałek 2008). Although residual-P of the Hedley fractionation can constitute a significant proportion of total P (P_t) in soils (Condron and Newman 2011), percentages were small in the kettle hole and Bodden sediments. This indicates a good applicability and efficacy of this fractionation method for the present sediments. Contrarily to Schlichting and Leinweber (2002), who detected a greater P extractability from moist than dry peat soils, extractability of P_t was slightly lower in the fresh Bodden sediments and significantly lower in the fresh kettle hole sediments compared to the respective dry samples determined with both aqua regia digestion and the sequential fractionation (Tables 1 and 2). Turner et al. (2007) also detected significant changes in P fractions following pretreatment, especially drying, in wetland soils from the Florida Everglades, but there was no consistent influence of sample pretreatment on chemical characteristics.

Summarizing the recent findings so far, sample alterations by drying were present but caused inconsistent changes of P concentrations in the two different sediment types from the kettle hole and Bodden environment.

2.4.3. P K-*edge XANES spectra of unfractionated samples and residues of sequential fractionation*

In Figure 1 stacked XANES spectra of milled unfractionated Bodden and kettle hole sediment and respective solid residues after extraction steps of P fractionation are displayed (spectra of fresh and sieved Bodden and kettle hole sediment and respective solid residues are available in Figures S1 and S2 of supplementary material). All spectra were characterized by an intense white line peak at around 2152 eV and a second broader peak at around 2170 eV. Due to much greater P concentrations in the unfractionated kettle hole sediment (2229 mg kg^{-1}), the signal-to-noise ratio is better for kettle hole sample compared to the unfractionated Bodden sediment (279 mg kg^{-1}). Removal of NaOH-P especially increased the noise in the spectrum of kettle hole sediment. The final extraction step with H_2SO_4 had considerably effects on both, the kettle hole and Bodden sediments. Intensities of noise increased in the spectra of kettle hole and Bodden sample due to the very low P concentrations after H_2SO_4 extraction especially in the Bodden

sediment (5 mg kg^{-1}). Furthermore, the small "bump" on the lower energy side of the broad peak, prominently appearing in the first three spectra of Bodden sediment, disappeared after H_2SO_4 extraction of the Bodden sediment. The same "bump" became weakly visible in the kettle hole residue after H_2SO_4 extraction. It is remarkable that although the concentration of 5 mg kg^{-1} P of the final Bodden sediment residue is extremely low, the new detector at the SXRMB was able to generate reasonable P XANES spectra. This higher sensibility now allows comparisons of P *K*-edge XANES measurements to extraction data of many different types of samples even if they have with very low P concentrations.

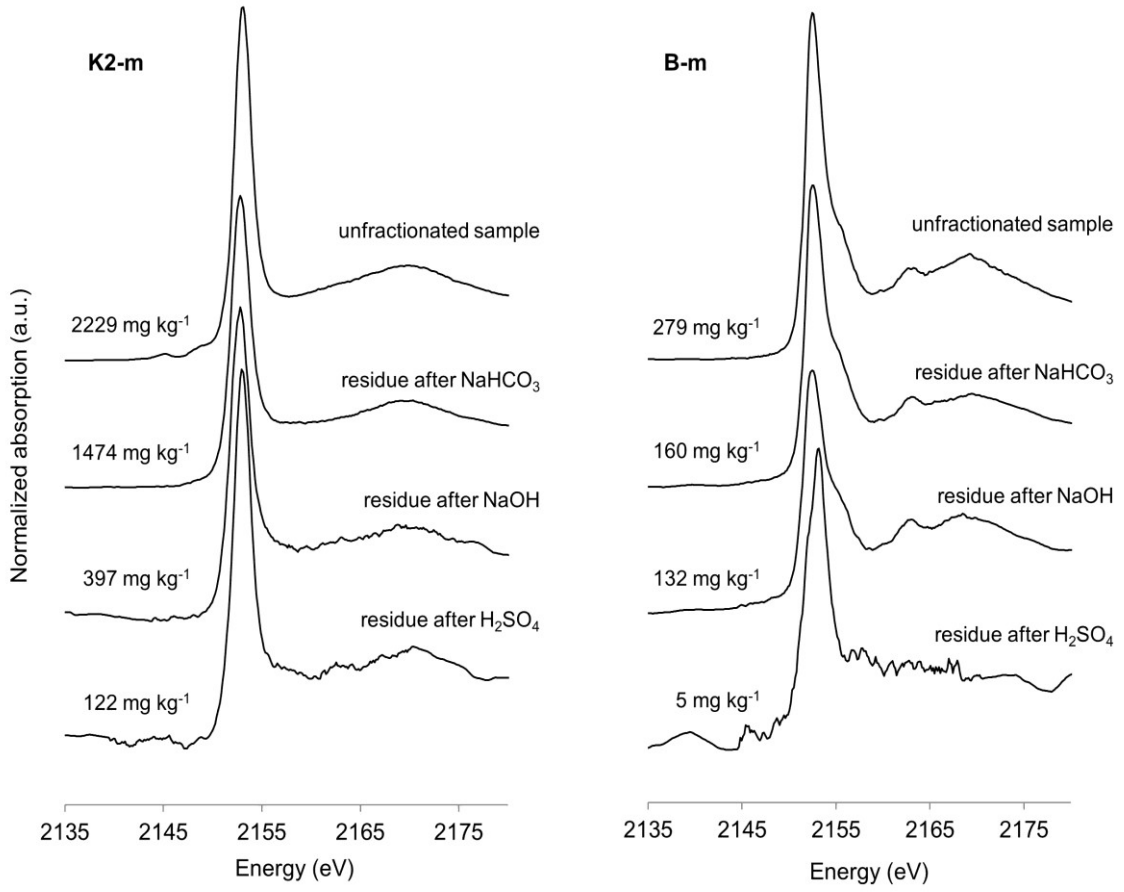

Figure 2-1 Stacked P *K*-edge XANES spectra of unfractionated, milled kettle hole and Bodden sediment and the respective solid extraction residues after the extractions steps with resin and $NaHCO_3$, NaOH, and H_2SO_4. Concentrations of P (mg kg^{-1}) were calculated as the sum of concentrations of all sequentially extracted fractions minus concentrations of fractions that resulted in the respective residue.

The good spectral quality of kettle hole extraction residues is due to the higher P concentrations compared to the Bodden sediment extraction residues with poorer spectra and low P concentrations, especially in the Bodden sediment residue after H_2SO_4 extraction (Figure 1). The spectrum of unfractionated kettle hole sample shows the unique pre-edge peak for spectra of Fe phosphate reference standards at around 2148 eV (Kruse and Leinweber 2008). This

feature disappears during the following extraction steps of the kettle hole sediment and recurs weakly after the final H_2SO_4 extraction. This is in accordance with the common assumption of sequential P fractionation where Fe- and Al-P species are extracted predominantly with NaOH (Hedley, Stewart, and Chauhan 1982) and with Schlichting et al. (2002) who characterized P in the residual fraction as very stable complexes with metal ions or pedogenic oxides. Since no good quality P *K*-edge spectra have been reported for extracted samples to date, it was not possible to compare the recent spectra to other extraction data.

Spectra of the unfractionated Bodden sediment and corresponding residues after $NaHCO_3$ and NaOH extraction show a shoulder at the high-energy side of the white line peak as well as a feature on the left of the broad peak at around 2162.75 eV in Figure 1, which are characteristic for Ca associated P compounds (Kruse and Leinweber 2008). The disappearance of the small "bump" on the left of the broad peak, characteristic for Ca associated P species and especially apatite-group minerals (Ingall et al. 2010), in the residual fraction of Bodden sediment suggests that Ca-P species were especially extracted with H_2SO_4. This result agrees with the common assignment of P fractionation that acid extractable P is mainly associated with Ca- and Mg-P species (Hedley, Stewart, and Chauhan 1982). The slight appearance of this "bump" of Ca associated P species in the kettle hole residue after H_2SO_4 extraction could indicate the occurrence of non-extractable Ca- or sodium (Na)-P compounds. However, these P species could not be assigned by LCF of this sample (Figure 3).

Generally, visual assessment of P *K*-edge XANES spectra confirmed the outcomes of sequential extraction to some extent. Kettle hole samples were basically dominated by P extracted with NaOH, commonly interpreted as moderately labile P adsorbed to Al and Fe oxide minerals, whereas Bodden sediments contained more P extracted with H_2SO_4, interpreted as relatively stable P associated with Ca and Mg minerals and apatite (Cross and Schlesinger 1995; Sims and Pierzynski 2005; Tiessen and Moir 1993). This difference determined by P fractionation (Table 2) is clearly reflected by the overview of the XANES spectra of both sample sets (Figure 1).

2.4.4. Linear combination fitting of XANES spectra of unfractionated samples

The results of LCF of spectra obtained by P *K*-edge XANES of the unfractionated kettle hole and Bodden sediments with different pretreatments are displayed in Figure 2 (corresponding P *K*-edge XANES spectra are available in the Figures S3, S4, and S5 of supplementary material). Proportions of Fe-P species ranged between 84 and 100% in the kettle hole and between 39 and 57% in the Bodden sediments. In the upper 10 cm of kettle hole sediment (K1), exclusively Fe-bound P was assigned irrespective of the pretreatment. The same was true for the milled version of kettle hole samples from a depth of 10-20 cm (K2) whereas in the sieved and lyophilized subsamples additionally 6 and 16% Al-bound P species, respectively, were assigned. In contrast to the kettle hole samples, Ca-P species were present in all Bodden sediments and represented 28 to 48% of P_t. The sieved Bodden sediment consisted of 39% Fe-P, 26% Al-P and 36% Ca-P compounds and the milled version contained 52% Fe-P and 48%

Ca-P. The lyophilized Bodden sediment consisted of 57% Fe-P and 28% Ca-P and it was the only sample among all unfractionated sediments in which the LCF assigned a considerable amount of P_o species (15%).

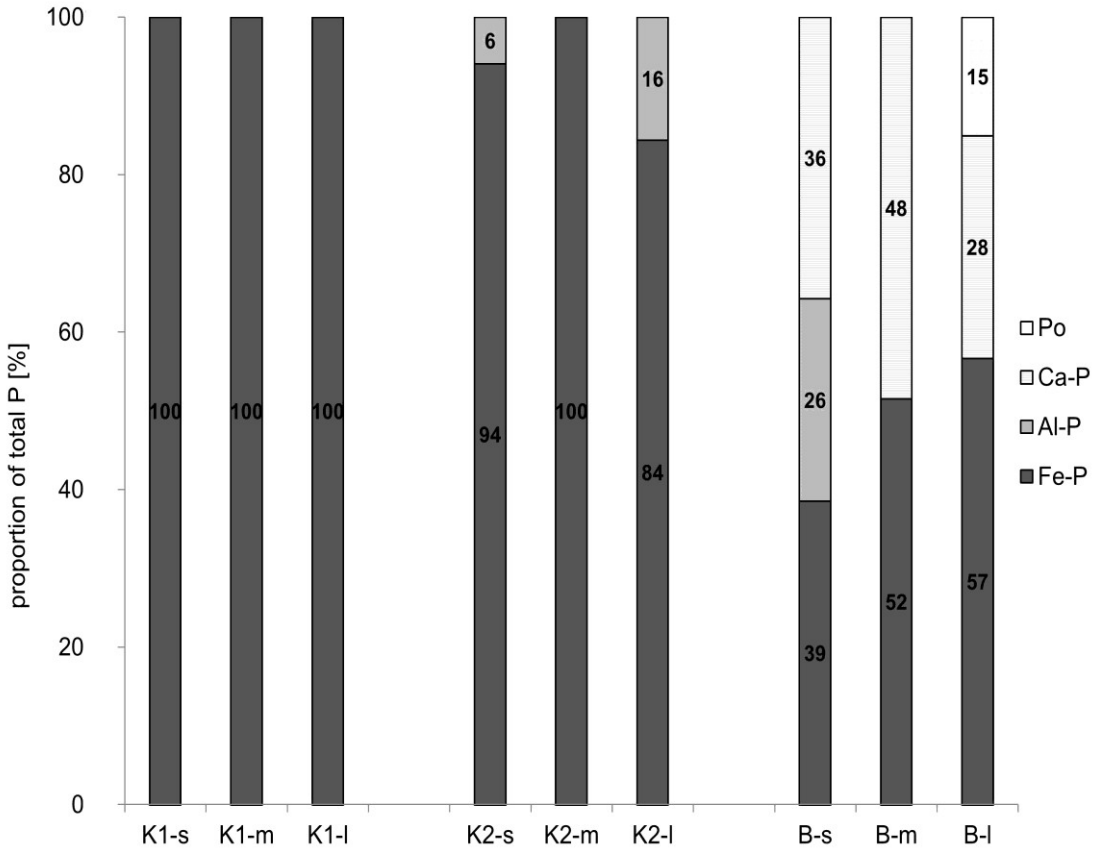

Figure 2-2 Proportions of P (% of total P determined with aqua regia digestion) as obtained by linear combination fitting (LCF) on P *K*-edge XANES spectra of three different pretreatments (s = sieved, m = milled, l = lyophilized) of kettle hole (K1 = 0-10 cm depth, K2 = 10–20 cm depth) and Bodden (B) sediments. Standards and spectra were recorded at the CLS-SXRMB beamline, Canada.

Clear differences in the P speciation were visible between the kettle hole and Bodden sediments, whereas the differences among the pretreatment variants of the individual sampling position are rather small. Furthermore, the results of LCF confirm the visual inspection of XANES spectra of unfractionated kettle hole and Bodden sediment (Figure 1), where kettle hole sediments were dominated by Fe-P species and Bodden sediments additionally contained prominent proportions of Ca associated P species. The fact that XANES spectroscopy determined exclusively Fe associated P in the upper 10 cm of kettle hole sediment coincides with the results of other studies using P XANES spectroscopy to investigate different soils and sediments. For example, Prüter et al. (2020) found much higher amounts of Fe associated P in sediments near the coast of Northern Germany compared to sediments more distant from the shoreline. Li et al. (2015) identified Fe-bound P as the dominant P form in sediments from the

Chesapeake Bay in the United States. A possible explanation for this can be the fact that Fe oxides have excellent binding capacities for P (Ganta et al. 2021). In soil, several studies detected P associated with Fe also as dominating P component. Koch et al. (2018) reported the predominance of Fe-P compounds in Stagnic Cambisol profiles of an experiment with different P fertilizer applications. The kettle hole sediments likely originated largely from the surrounding arable topsoils with P already attached to Fe oxides, so the similarity of this sediment to soil samples is not surprising.

The small proportions of Al-bound P next to the dominating amounts of Fe associated P compounds in the sieved and lyophilized kettle hole sediments from a depth of 10-20 cm may partly also be assigned to P_o compounds. The spectral features of the selected Al-P XANES standards are not sufficiently different from the phytic acid reference standard, and XANES spectroscopy is in some cases apparently unable to differentiate whether P_i or P_o is sorbed on Al and Fe (Kruse et al. 2015).

The occurrence of considerable amounts of Ca associated P in all three pretreatment variants of the Bodden sediment can be associated to the generally higher relative amounts of Ca in the Bodden than in the kettle hole samples (Table 1). Furthermore, high proportions of Ca-P can be related to the sediment texture, where primary Ca minerals are usually present in the silt to sand fraction (Saunders 1959). The proportion of sand in the Bodden sediments is distinctly higher compared to the kettle hole sediments (Table 1), so this can explain the higher relative amounts of Ca and Ca-P species in the Bodden sediments. Furthermore, the high amount of sand could contribute to some pre-edge features in the spectra of Bodden sediment leading to an overestimation of Fe associated P compounds by LCF. The silicon *K*-edge, e.g. prominent in quartz sand, is around 1840 eV (Gilbert et al. 2003), which could appear as background in P *K*-edge spectra, especially in the near edge region. Larger percentages of Ca associated P in the Bodden sediments compared to the kettle hole sediments agree with a study of sediments near the coast of Northern Germany where more Ca-bound P was detected in marine sediments compared to sediments under stronger terrestrial influence (Prüter et al. 2020). The highest percentage of Ca-P in the milled sample variant of Bodden sediment is visually reflected by the XANES spectrum (Figure S5, supplementary material) and might be initiated due to a release of Ca from the crush of small Ca-rich particles as for example seashells.

Although results of XANES spectroscopy concerning P_o concentrations should be considered with caution (Gu et al. 2020), the lyophilized Bodden sediment was the only sample where P_o compounds were assigned. A possible explanation is that lyophilization could be more gentle for P_o compounds compared to drying, sieving and milling for this sample type. Other studies also found inconsistent variations of organic P in stream sediments and wetland soils due to lyophilization, indicating that pretreatment effects may be sample specific (Simpson, McDowell, and Condron 2018; Turner et al. 2007).

Overall, the XANES analysis of the unfractionated kettle hole and Bodden sediments confirmed the results of P fractionation. The identification of mainly Fe associated P species in the kettle hole sediments by LCF of XANES spectra agrees with the high proportions of NaOH-P determined by sequential P fractionation and its common assignment to P adsorbed by Al- and

Fe oxide minerals. Considerable proportions of Ca associated P species in the unfractionated Bodden sediments assigned by LCF of XANES spectra also reflected the high proportions of P extracted with H_2SO_4 from the Bodden sediments in the sequential P fractionation and its interpretation as stable P associated with Ca and Mg minerals and apatite.

2.4.5. Linear combination fitting of XANES spectra of residues of sequential fractionation

Figure 3 shows the LCF results of P XANES spectra from the kettle hole and Bodden solid residues after the extraction steps of sequential P fractionation. After the first two extraction steps with resin and $NaHCO_3$, proportions of Fe associated P species declined distinctly in all pretreatment variants of kettle hole sediment compared to the unfractionated samples (Figure 2). Different from the unfractionated samples, Al associated P (29 – 55%) and P_o species (8 – 31%) were assigned in the fresh, sieved and milled solid kettle hole residues after resin and $NaHCO_3$ extraction. The next extraction step with NaOH further reduced proportions of Al-P species in the kettle hole residues. Proportions of P_o species declined after NaOH extraction in the fresh and milled residues and remained roughly the same in the sieved sample. In the milled residue, no Fe-P compounds or P_o species has been assigned in the LCF after NaOH extraction. Furthermore, the extraction step with NaOH revealed 18 – 20% Ca associated P species in the fresh, sieved and milled kettle hole residues. Extraction with H_2SO_4 clearly changed the P speciation results of LCF in the solid kettle hole sediment residues. In all three sample pretreatments, Al-, Ca-, and P_o associated compounds from the previous residues disappeared and exclusively Fe associated P species remained in the samples (Figure 3).
The solid sequential P fractionation residues of Bodden sediments show a different distribution of P species compared to those of the kettle hole sediments. The residues of Bodden sediments after the first two extraction steps with resin and $NaHCO_3$ were dominated by Mg and Ca associated P species (Figure 3). Compared to the LCF of unfractionated Bodden sediments as displayed in Figure 2, proportions of Fe associated P decreased clearly, proportions of Ca associated P declined slightly after resin and $NaHCO_3$ extraction but remained predominant. Percentages of Mg-P increased in the fresh and sieved Bodden sediment residues and the proportion of Al-P compounds increased in the milled residue compared to the unfractionated Bodden sediments. After the subsequent extraction with NaOH, proportions of Mg associated P species declined in the fresh and sieved residues and the percentage of Ca-P species remained roughly at the same level in all three pretreatment variants. Furthermore, proportions of Fe and Al associated P species (13 - 35%) were determined in the samples after the NaOH extraction, which were not detected before in the fresh and sieved residues. After the last extraction with H_2SO_4, Ca- and Mg-associated P species disappeared almost completely in the Bodden sediment residues, and Fe- and Al associated P species remained in the samples. Exclusively in the residue of milled Bodden sediment small proportions of Ca-P (11%) and P_o (4%) were detected additionally.

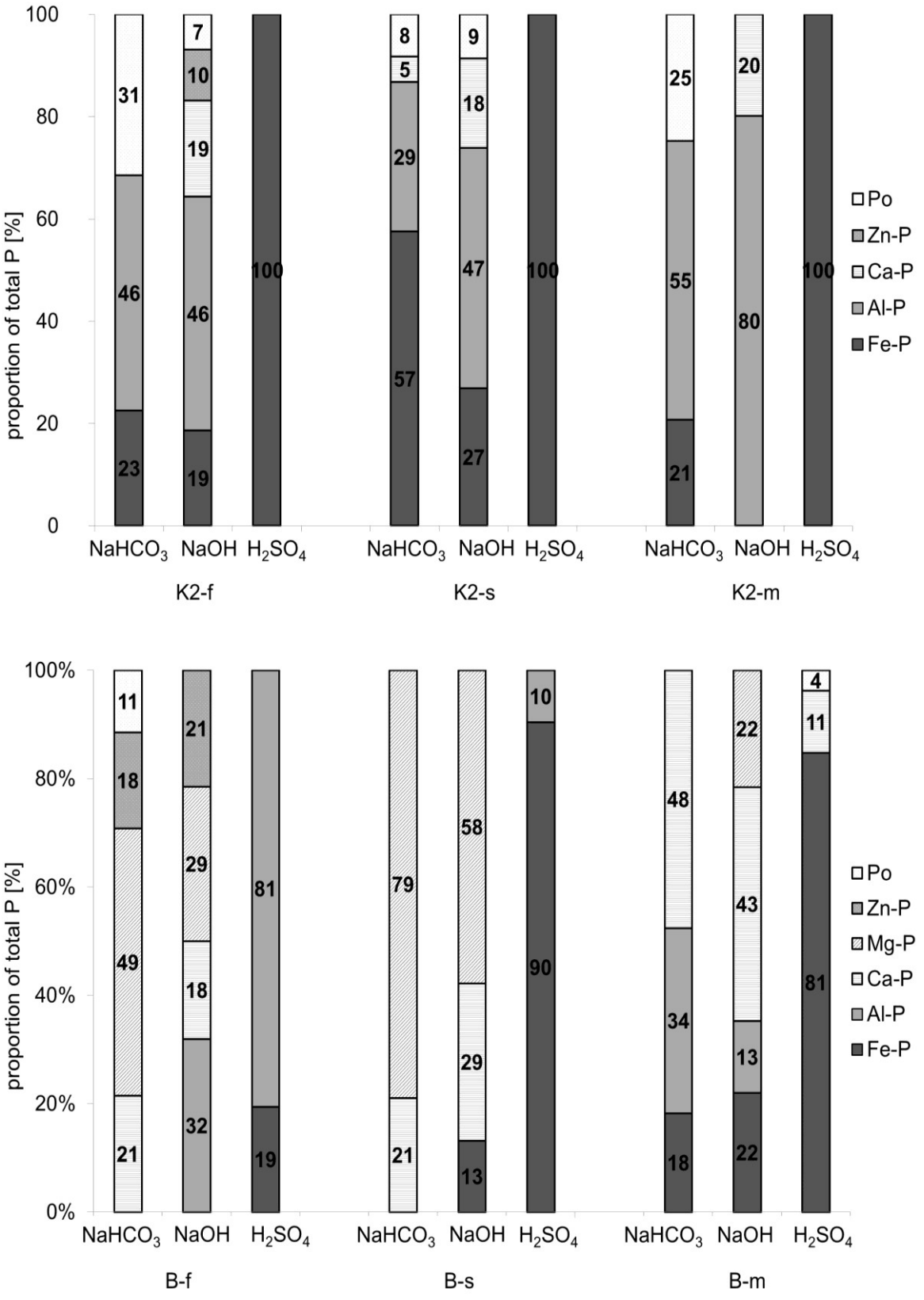

Figure 2-3 Proportions of P (% of total P determined with aqua regia digestion) as obtained by linear combination fitting (LCF) on P *K*-edge XANES spectra of solid residues of kettle hole (K2) and Bodden (B) sediments with three different pretreatments (f = fresh, s = sieved, m = milled) after the extraction steps with resin and $NaHCO_3$ ($NaHCO_3$), NaOH and H_2SO_4 of sequential P fractionation. Standards and spectra were recorded at the CLS-SXRMB beamline, Canada.

The fresh and the milled kettle hole sediments after the first two extraction steps with resin and $NaHCO_3$ showed a very similar P speciation (Figure 3), indicating a small influence of pretreatment in this case. This is also reflected in the results of the P fractionation, where no significant differences according to sample pretreatment were determined in the fraction of $NaHCO_3$-P of kettle hole sediment (Table 2). The higher amounts of Fe- and Al-bound P in the sieved compared to the fresh and milled kettle hole sediments can be related to the separation of grain sizes by pretreatment. While in the fresh and milled sediment all particle size fractions were present originally, the sieved sample contains exclusively particles < 2 mm. Lukkari et al. (2009) reported that the fine particulate fraction of sediments is enriched with poorly crystalline Fe and Al oxides. In accordance with that, more Fe and Al associated P species were assigned by LCF in the sieved than in the fresh and milled kettle hole samples in the present investigation. After the next fractionation step with NaOH, results of XANES spectroscopy again were basically similar for the three different pretreatments of kettle hole sediment. Proportions of Fe-P species and labile P_o compounds decreased and some Ca-P compounds became visible compared to the previous residues, confirming the assumption that the P fractionation adsorbed to Al and Fe oxide minerals and P in humic and fulvic acids is predominantly extracted by NaOH (Tiessen and Moir 1993). However, the significantly lower amount of NaOH-P_i in the fresh compared to the sieved and milled kettle hole sediments determined with P fractionation (Table 2) is not reflected by the results of XANES spectroscopy. Since P_o is still present in the fresh and sieved sample in small proportions, its absence in the milled kettle hole sediment can be correlated to the difficulty in distinguishing Al-bound P and the phytic acid standard by this method (Kruse et al. 2015). Among all kettle hole and Bodden sediments, Zn associated P has been assigned exclusively in the fresh samples after the extractions with $NaHCO_3$ and NaOH. Koopmans and Groenenberg (2011) found evidence for small decreases of Zn due to oven-drying of soil solution extracts of sandy soils, so Zn-P compounds could be sensitive to drying pretreatment and thus, they only appeared in fresh and wet sediments. The abundance of exclusively Fe associated P in all three pretreatment variants of the kettle hole sediment after the last extraction step with H_2SO_4 agrees with the common interpretation of P fractionation, where Ca and Mg minerals and apatite are considered to be extracted with H_2SO_4. Schlichting et al. (2002) also ascertained the residual fraction after the last step of sequential fractionation of peat-derived soils to contain mainly very stable complexes of organic matter with multivalent metal ions or pedogenic oxides.

Contrasting to the kettle hole samples that were dominated by Fe-P and Al-P, LCF of the XANES spectra of the Bodden sediment residues indicated mostly Ca and Mg associated P (Figure 3). Lower proportions of Fe associated P compounds in favor of more Ca-P were already found by LCF of the spectra of unfractionated Bodden sediment samples. Unlike the kettle hole samples, milled residue of Bodden sediment after the first two extraction steps with resin and $NaHCO_3$, was the sample with highest amounts of Fe-P and Al-P. The amount of Fe- and Al-P could be so low in the Bodden sediments that grinding is needed to detect considerable proportions of Fe- and Al associated P compounds with XANES spectroscopy. Fe and Al particles could have been destroyed and finely spread during the grinding process by

contrast to the fresh and sieved sample. After extraction with NaOH, the proportions of P_o compounds and Mg-P species decreased (Figure 3). A decrease in P_o proportions agrees with the assumption of P fractionation that considerable amounts of humic substances and P_o are extracted by NaOH, whereas proportions of Ca- and Mg-P are predominantly assigned to the H_2SO_4-extracted fraction (Hedley, Stewart, and Chauhan 1982) and, thus, should not be decreased until the last extraction step. All three Bodden sediment residues were dominated by Fe- and Al-associated P and proportions of Ca- and Mg-P compounds were clearly reduced after H_2SO_4 extraction compared to the previous extraction step. As this was disclosed similarly for the kettle hole samples by LCF of XANES spectroscopy, the common assignment of H_2SO_4 extracts of P fractionation to stable P associated with Ca and Mg minerals and apatite is confirmed. Since the fraction of residual P contained very low P contents of 2 - 9 mg kg^{-1} in the Bodden sediments (Table 2), sequential P fractionation was more effective in extracting P from the Bodden sediments compared to the kettle hole samples. Even if previous studies assigned mainly P_o as residual P in soil and sediment (Dobermann, George, and Thevs 2002; Koch, Benz, and Rudnick 2001), this assignment largely depends on the distinct sample type. The low proportions of P_o in the residual fraction of the recent sediments (Figure 3) strongly agree with a study about Bermuda carbonate sediments, where P_o in the residual fraction accounted for < 2% of P_t (Jensen et al. 1998) and with Schlichting et al. (2002) who described the P in the residual fraction as very stable complexes of organic matter with metal ions or pedogenic oxides. However, it remains unclear to some extent if small amounts of occluded P can be re-adsorbed by crystalline iron oxides or if these are natural residual P species (Kar et al. 2011).
It can be emphasized that most differences in results of XANES LCF appeared between sample origin instead of pretreatments, indicating a stronger influence of the sediment origin and surrounding environment on the sediment P composition than due to the sample pretreatments such as drying, sieving and grinding. However, there were differences in one sample set of kettle hole and Bodden sediments between the pretreatments but there was no clear, directed effect of a certain sample treatment. Furthermore, the general assignments of sequential P fractionation of resin-P to easily exchangeable and mobile P, bicarbonate P ($NaHCO_3$-P) to labile P weakly adsorbed by mineral surfaces, NaOH-P to moderately labile P adsorbed to Al- and Fe oxide minerals and P in humic and fulvic acids, H_2SO_4-P to relatively stable P associated with Ca and Mg minerals and apatite and residual-P to not extractable P, occluded P or stable forms of organic P compounds can be confirmed for most fractions by XANES analyses of the kettle hole and Bodden sediment residues after different extraction steps.

2.5. Conclusions

The methodological approach of using sequential P fractionation and P XANES spectroscopy to determine the P speciation of sediments with different pretreatments was appropriate for the selected samples in this study. Both methods provided compliant results and revealed that the kettle hole sediments were dominated by moderately labile, Fe- and Al-associated P species

and contained more P_o compared to the Bodden sediments, in which stable Ca-P species were most abundant.

Thanks to the extremely sensitive 7-element SDD, the P *K*-edge XANES at the SXRMB was able to detect very low P concentrations in extraction residues of sequential P fractionation. Consequently, the P *K*-edge XANES spectra of single sequential P fractionation steps confirmed the common assignment of different P forms to operationally defined P pools in the fractionation scheme for both investigated sediment types, confirming the value of these methods, especially if applied in conjunction.

Any effect of the sediment sample pretreatment on the distribution of P pools and occurrence of distinct P species was much lower than the influence of the sample origins from kettle hole and Bodden. Significant differences in the P composition of one sediment type appeared exclusively in the fractions of easily exchangeable, mobile P and moderately labile P of sequential fractionation due to sample drying in the present investigation. Therefore, it is possible to apply traditional soil sample pretreatments such as drying, sieving and grinding on sediments without fundamentally changing the composition of P speciation. This similar pretreatment can facilitate research of P transformation processes especially at the fluent boundaries of terrestrial/semiterrestrial soils and sediments in aquatic environments.

Furthermore, various samples with great differences in genesis such as terrestrial and wetland soils, peat and sediments seem to show different sensitivities to sample pretreatments concerning P extractability and results of sequential extractions. If research is directed to disclose the differences in P species between such widely different samples, systematic tests for pretreatment effects or application of different pretreatments are recommended. Furthermore, additional complementary analyses, such as liquid-state or solid-state ^{31}P nuclear magnetic resonance (NMR) spectroscopy could be done prior to extraction steps with NaOH in order to identify the P_o compounds in greater detail.

2.6. Acknowledgments

The authors thank Elena Heilmann and Britta Balz (Soil Science, University of Rostock) for analytical help concerning P fractionation and ICP measurement. The XANES research referred to in this paper was performed at the Canadian Light Source, which is supported by the Canada Foundation for Innovation, Natural Sciences and Engineering Research Council of Canada, the University of Saskatchewan, the Government of Saskatchewan, Western Economic Diversification Canada, the National Research Council Canada, and the Canadian Institutes of Health Research.

2.7. Funding

This research was funded by the Leibniz Association within the scope of the Leibniz ScienceCampus “Phosphorus Research Rostock”. No potential competing interest was reported by the authors.

2.8. References

Acksel, A., W. Amelung, P. Kühn, E. Gehrt, T. Regier, and P. Leinweber. 2016. Soil organic matter characteristics as indicator of Chernozem genesis in the Baltic Sea region. *Geoderma Regional* 7:187-200.

Addiscott, T. M., D. Brockie, J. A. Catt, D. G. Christian, G. L. Harris, K. R. Howse, N. A. Mirza, and T. J. Pepper. 2000. Phosphate losses through field drains in a heavy cultivated soil. *Journal of Environmental Quality* 29:522-532.

Ajiboye, B., O. O. Akinremi, Y Hu, and D. N. Flaten. 2007. Phosphorus speciation of sequential extracts of organic amendments using nuclear magnetic resonance and X-ray absorption near-edge structure spectroscopies. *Journal of Environmental Quality* 36:1563-1576.

Barrow, N. J., A. Sen, N. Roy, and A. Debnath. 2020. The soil phosphate fallacy. *Plant Soil* 459:1-11. doi: 10.1007/s11104-020-04476-6.

Baumann, K., K. Glaser, J.-E. Mutz, U. Karsten, A. MacLennan, Y. Hu, D. Michalik, J. Kruse, K.-U. Eckhardt, P. Schall, and P. Leinweber. 2017. Biological soil crusts of temperate forests: Their role in P cycling. *Soil Biology & Biochemistry* 109:156-166.

Baumann, K., S. M. Shaheen, Y. Hu, P. Gros, E. Heilmann, M. Morshedizad, J. Wang, S.-L. Wang, J. Rinklebe, and P. Leinweber. 2020. Speciation and sorption of phosphorus in agricultural soil profiles of redoximorphic character. *Environ Geochemistry and Health* 42:3231-3246. https://doi.org/10.1007/s10653-020-00561-y.

Bonsdorff, E., E. M. Blomqvist, J. Mattila, and A. Norkko. 1997. Coastal eutrophication: Causes, consequences and perspectives in the archipelago areas of the Northern Baltic Sea. *Estuarine, Coastal and Shelf Science* 44:63-72.

Brake, M., H. Höper, and R. G. Joergensen. 1999. Land use-induced changes in activity and biomass of microorganisms in raised bog peats at different depths. *Soil Biology and Biochemistry* 31:1489-1497.

Bromfield, S. 1967. An examination of the use of ammonium fluoride as a selective extractant for aluminium-bound phosphate in partially phosphated systems. *Soil Research* 5:225-234.

Calvin, S. 2013. *XAFS for Everyone*. 1st ed. Boca Raton, USA: CRC Press.

Chang, S., and M. L. Jackson. 1957. Fractionation of soil phosphorus. *Soil Science* 84:133-144.

Condron, L. M., and S. Newman. 2011. Revisiting the fundamentals of phosphorus fractionation of sediments and soils. *Journal of Soils and Sediments* 11:830-840.

Cordell, D., and S. White. 2011. Peak phosphorus: clarifying the key issues of a vigorous debate about long-term phosphorus security. *Sustainability* 3:2027-2049.

Cross, A. F., and W. H. Schlesinger. 1995. A literature review and evaluation of the Hedley fractionation: Applications to the biogeochemical cycle of soil phosphporus in natural ecosystems. *Geoderma* 64:197-214.

Dobermann, A., A. T. George, and N. Thevs. 2002. Phosphorus fertilizer effects on soil phosphorus pools in acid upland soils. *Soil Science Society of America Journal* 66:652-660.

Eger, A., P. C. Almond, and L. M. Condron. 2013. Phosphorus fertilization by active dust deposition in a super-humid, temperate environment – Soil phosphorus fractionation and accession processes. *Global Biogeochemical Cycles* 27:108-118.

Elser, J. J., M. E. S. Bracken, E. E. Cleland, D. S. Gruner, W. S. Harpole, H. Hillebrand, J. T. Ngai, E. W. Seabloom, J. B. Shurin, and J. E. Smith. 2007. Global analysis of nitrogen and phosphorus limitation of primary producers in freshwater, marine and terrestrial ecosystems. *Ecology Letters* 10:1135-1142. doi: 10.1111/j.1461-0248.2007.01113x.

Frielinghaus, M., and W.-G. Vahrson. 1998. Soil translocation by water erosion from agricultural cropland into wet depressions (morainic kettle holes). *Soil & Tillage Research* 46:23-30.

Ganta, P. B., M. Morshedizad, O. Kühn, P. Leinweber, and A.A. Ahmed. 2021. The binding of phosphorus species at goethite: a joint experimental and theoretical study. *Minerals* 11:323.

Gilbert, B., B. H. Frazer, F. Naab, J. Fournelle, J. W. Valley, and G. De Stasio. 2003. X-ray absorption spectroscopy of silicates for in situ, sub-micrometer mineral identification. *American Mineralogist* 88:763-769.

Goedkoop, W., and K. Pettersson. 2000. Seasonal changes in sediment phosphorus forms in relation to sedimentation and benthic bacterial biomass in Lake Erken. *Hydrobiologia* 431:41-50.

Gu, C., A. J. Margenot. 2021. Navigating limitaions and opportunities of soil phosphorus fractionation. *Plant Soil* 459:13-17.

Gu, C., T. Dam, S. C. Hart, B. L. Tuner, O. A. Chadwick, A. A. Berhe, Y. Hu, and M. Zhu. 2020. Quantifying uncertainties in sequential chemical extraction of soil phosphorus using XANES spectroscopy. *Environmental Science & Technology* 54:2257-2267. doi: 10.1021/acs.est.9b05278.

Guppy, C. 2021. Is soil phosphorus fractionation as valuable as we think? *Plant Soil* 459:19-21. doi: 10.1007/s11104-020-04817-5.

Hedley, M. J., J. W. B. Stewart, and B. S. Chauhan. 1982. Changes in inorganic and organic soil phosphorus fractions induced by cultivation practices and by laboratory incubations. *Soil Science Society of America Journal* 46:970-976.

Hesterberg, D., W. Zhou, J. Hutchison, S. Beauchemin, and D. E. Sayers. 1999. XAFS study of adsorbed and mineral forms of phosphate. *Jorunal of Synchrotron Radiation* 6:636-638.

Hu, Y. F., I. Coulthard, D. Chevrier, G. Wright, R. Igarashi, A. Sitnikov, E. L. Yates, E. L. Hallin, T. K. Sham, and R. Reiniger. 2010. Preliminary commissioning and performance of the soft X-ray micro-characterization beamline at the Canadian Light Source. *AIP Conference Proceedings* 1234:343–346.

Ingall, E. D., J. A. Brandes, J. M. Diaz, M. D. de Jonge, D. Paterson, I. McNulty, W. C. Elliott, and P. Northrup. 2010. Phosphorus *K*-edge XANES spectroscopy of mineral standards. *Journal of Synchrotron Radiation* 18:189-197.

Jensen, H. S., K. J. McGlathery, R. Marino, and R. W. Howarth. 1998. Forms and availability of sediment phosphorus in carbonate sand of Bermuda seagrass beds. *Limnology and Oceanography* 43:799-810.

Kar, G., L. S. Hundal, J. J. Schoenau, and D. Peak. 2011. Direct chemical speciation of P in sequential chemical extraction residues using P *K*-edge X-ray absorption near-edge structure spectroscopy. *Soil Science* 176:589-595.

Karstens, S., U. Buczko, and S. Glatzel. 2015. Phosphorus storage and mobilization in coastal *Phragmites* wetlands: influence of local-scale hydrodynamics. *Estuarine, Coastal and Shelf Science* 164:124-133.

Karstens, S., U. Buczko, G. Jurasinski, R. Peticzka, and S. Glatzel. 2016. Impact of adjacent land use on coastal wetland sediments. *Science of the Total Environment* 550:337-348.

Kleeberg, A., M. Neyen, U.-K. Schkade, T. Kalettka, and G. Lischeid. 2016. Sediment cores from kettle holes in NE Germany relveal recent impacts of agriculture. *Environmental Science and Pollution Research*. 23:7409-7424.

Koch, M. S., R. E. Benz, and D. T. Rudnick. 2001. Solid-phase phosphorus pools in highly organic carbonate sediments of Northeastern Florida bay. *Estuarine, Coastal and Shelf Science* 52:279-291.

Koch, M., J. Kruse, B. Eichler-Löbermann, D. Zimmer, S. Willbold, P. Leinweber, and N. Siebers. 2018. Phosphorus stocks and speciation in soil profiles of a long-term fertilizer experiment: Evidence from sequential fractionation, P *K*-edge XANES, and ^{31}P NMR spectroscopy. *Geoderma* 316:115–126. doi: 10.1016/j.geoderma.2017.12.003.

Koopmans, G. F., and J. E. Groenenberg. 2011. Effects of soil oven-drying on concnetrations and speciation of trace metals and dissolved organic matter in soil solution extracts of sandy soils. *Geoderma* 161:147-158.

Kraal, P., B. C. Bostick, T. Behrends, G.-J. Reichart, and C. Slomp. 2015. Characterization of phosphorus species in sediments from the Arabian Sea oxygen minimum zone: combining sequential extractions and X-ray spectroscopy. *Marine Chemistry* 168:1-8.

Kruse, J., and P. Leinweber. 2008. Phosphorus in sequentially extracted fen peat soils: A *K*-edge X-ray absorption near edge structure (XANES) spectroscopy study. *Journal of Plant Nutrition and Soil Science* 171:613-620.

Kruse, J., W. Negassa, N. Appathurai, L. Zuin, and P. Leinweber. 2010. Phosphorus speciation in sequentially extracted agro-industrial by-products: evidence from X-ray absorption near edge structure spectroscopy. *Journal of Environmental Quality* 39(6):2179-2184.

Kruse, J., M. Abraham, W. Amelung, C. Baum, R. Bol, O. Kühn, H. Lewandowski, J. Niederberger, Y. Oelmann, C. Rüger, et al. 2015. Innovative methods in soil phosphorus research: A review. *Journal of Plant Nutrition and Soil Science* 178:43-88.

Li, W., S. R. Joshi, G. Hou, D. J. Burdige, D. L. Sparks, and D. P. Jaisi. 2015. Characterizing phosphorus speciation of Chesapeake Bay sediments using chemical extraction, ^{31}P NMR, and X-ray absorption fine structure spectroscopy. *Environmental Science & Technology* 49:203-211.

Lukkari, K., Leivuori, M., Vallius, H., and A. Kotilainen. 2009. The chemical character and burial of phosphorus in shallow coastal sediments in the Northeastern Baltic Sea. *Biogeochemistry* 94:141-162.

Łukawska-Matuszewska, K., and J. Bolałek. 2008. Spatial distribution of phosphorus forms in sediments in th Gulf of Gdańsk (southern Baltic Sea). *Continental Shelf Research* 28:977-990.

Martin, J. M., P. Nirel, and A. J. Thomas. 1987. Sequential extraction techniques: promises and problems. *Marine Chemistry* 22:313-341.

Morshedizad, M., K. Panten, W. Klysubun, and P. Leinweber. 2018. Bone char effects on soil: sequential fractionations and XANES spectroscopy. *Soil* 4:23–35. doi: 10.5194/soil-4-23-2018.

Murphy, J., and J.P. Riley. 1962. A modified single solution method for the determination of phosphate in natural waters. *Analytical Chemistry ACTA* 27:31-36.

Negassa, W., P. Leinweber. 2009. How does Hedley sequential phosphorus fractionation reflect impacts of land use and management on soil phosphorus: a review. *Journal of Soil Science and Plant Nutrition* 172:305-325.

Nitzsche, K. N., M. Kaiser, K. Premke, A. Gessler, R. H. Ellerbrock, C. Hoffmann, A. Kleeberg, and Z. E. Kayler. 2017. Organic matter distribution and retention along transects from hilltop to kettle hole within an agricultural landscape. *Biogeochemistry* 136:47-70. doi: 10.1007/s10533-017-0380-3.

Olila, O. G., K. R. Reddy, and D. L. Stites. 1997. Influence of draining on soil phosphorus forms and distribution an a constructed wetland. *Ecological Engineering* 9:157-169.

Potter, R. L., C. F. Jordan, R. M. Guedes, G. J. Batmanian, and X.G. Han. 1991. Assessment of a phosphorus fractionation method for soils: problems for further investigation. *Agriculture, Ecosystems and Environment* 34:453-463.

Prietzel, J., A. Dümig, Y. Wu, J. Zhou, and W. Klysubun. 2013. Synchrotron-based P *K*-edge XANES spectroscopy reveals rapid changes of phosphorus speciation in the topsoil of two glacier foreland chronosequences. *Geochimica et Cosmochimica Acta* 108:154–171. doi: 10.1016/j.gca.2013.01.029.

Prüter, J., T. Leipe, D. Michalik, W. Klysubun, and P. Leinweber. 2020. Phosphorus speciation in sediments from the Baltic Sea, evaluated by a multi-method approach. *Journal of Soils and Sediments* 20:1676-1691.

Psenner, R, R. Pucsko, and M. Sager. 1984. Fractionation of organic and inorganic phosphorus compounds in lake sediments. *Archiv für Hydrobiologie* 70:111-155.

Ravel, B., and M. Newville. 2005. ATHENA, ARTEMIS, HEPHAESTUS: Data analysis for X-ray absorption spectroscopy using IFEFFIT. *Journal of Synchrotron Radiation* 12:537–541. doi: 10.1107/S0909049505012719.

Saunders, W. M. H. 1959. Effect of phosphate topdressing on a soil from andesitic volcanic ash. *New Zealand Journal of Agricultural Research* 2:427-444.

Schlichting, A., and P. Leinweber. 2002. Effects of pretreatment on sequentially-extracted phosphorus fractions from peat soils. Communications in Soil Science and Plant Analysis 33:1617-1627.

Schlichting, A., P. Leinweber, R. Meissner, and M. Alterman. 2002. Sequentially extracted phosphorus fractions in peat-derived soils. *Journal of Plant Nutrition and Soil Science* 165:290-298.

Selig, U., M. Schubert, A. Eggert, T. Steinhardt, S. Sagert, and H. Schubert. 2007. The influence of sediments of soft bottom vegetation in inner coastal waster of Mecklenburg-Vorpommern (Germany). *Estuarine, Coastal and Shelf Science* 71:241-249.

Shields, J. A., E. A. Paul, W. E. Loewe, and D. Parkinson. 1973. Turnover of micorbial tissue in soil under field conditions. *Soil Biology and Biochemistry* 5:753-764.

Simpson, Z. P., R. W. McDowell, and L. M. Condron. 2018. The error in stream sediment phosphorus fractionation and sorption properties effected by drying pretreatments. *Journal of Soil and Sediments* 19:1587-1597.

Sims, J. T., and G. M. Pierzynski. 2005. Chemistry of phosphorus in soils. In *Chemical Processes in Soils*, ed. M. A. Tabatabai and D. L. Sparks, 151-192. 8th ed. Madison: SSSA Book Series.

Sparling, G. P., K. N. Whale, and R. J. Ramsay. 1985. Quantifying the contribution from the soil microbial biomass to the extractable level of fresh and air-dried soils. *Australian Journal of Soil Research* 23:613-621.

Tiessen, H., J. W. B. Stewart, and J. Moir. 1983. Changes in organic and inorganic phosphorus composition of two grassland soils and their particle-size fractions during 60-90 years of cultivation. *Journal of Soil Science* 34:815-823.

Tiessen, H., and J. Moir. 1993. Characterization of available P by sequential extraction. *Soil Sampling and Methods of Analysis* 7:5-229.

Turner, L., and P. M. Haygarth. 2001. Phosphorus solubilisation in rewetted soils. *Nature* 411:258.

Turner, L., B. J. Cade-Menun, L.M. Condron, and S. Newman. 2005. Extraction of soil organic phosphorus. *Talanta* 66:294-306.

Turner, B. L., S. Newman, W. Cheesman, and K.R. Reddy. 2007. Sample pretreatment and phosphorus speciation in wetland soils. *Soil Science of America Journal* 71:1538-1546.

Williams, J., and T. Walker. 1969. Fractionation of phosphate in a maturity sequence of New Zealand basaltic soil profiles: 2. *Soil Science* 107:213-219.

Zhang, Z., H. L. Goldstein, R. L. Reynolds, Y. Hu, X. Wang, and M. Zhu, 2018. Phosphorus speciation and solubility in aeolian dust deposited in the interior American West. *Environmental Science & Technology* 52:2658-2667.

3 Phosphorus speciation along a soil to kettle hole transect: sequential P fractionation, P XANES, and ^{31}P NMR spectroscopy

Julia Prüter[1], Timothy I. McLaren[2], Marlene Pätzig[3], Yongfeng Hu[4], Peter Leinweber[1]

[1]*University of Rostock, Soil Science, Justus-von-Liebig Weg 6, 18051 Rostock, Germany*

[2]*University of Queensland, School of Agriculture and Food Sciences, St Lucia, Queensland 4072, Australia*

[3]*Leibniz Centre for Agricultural Landscape Research, Eberswalder Straße 84, 15373 Müncheberg, Germany*

[4]*Canadian Light Source, Inc., University of Saskatchewan, 44 Innovation Boulevard, Saskatoon, Saskatchewan S7N 2V3, Canada*

Published in

Geoderma 429 (2023), 116215

3.1. Abstract

Phosphorus (P) is an essential element for all living organisms but can also be an important factor in the eutrophication of aquatic/marine ecosystems. Kettle holes are often situated in regions under intense agricultural land use where there is a high risk of nutrient transfer to larger waterbodies. The chemical speciation of soil P influences its rate of transfer from arable fields to aquatic environments. However, there is a paucity of information on the P speciation in kettle holes and their effect on the P cycle. Thus, we investigated the P composition of arable soils and kettle hole sediments in surface and subsurface layers along a transect of an agricultural field. Multiple P analyses were carried out including modified sequential Hedley P fractionation, P *K*-edge X-ray absorption near edge structure (XANES) spectroscopy, and ^{31}P nuclear magnetic resonance (NMR) spectroscopy. The total P (P_t) concentrations ranged from 680 to 1123 mg kg^{-1} in the soils and 797 to 2591 mg kg^{-1} in the sediments. A predominance of the residual-P fraction, characterized as not extractable P, occluded P or stable forms of organic P (P_o) was determined by sequential fractionation, ranging from 37 to 67% followed by 3 to 38% H_2SO_4-P_i and 3 to 16% NaOH-P_o of P_t in the soils and sediments. Analyses with P *K*-edge XANES spectroscopy assigned 61 to 100% Fe- and Al-P, 0 to 14% Ca-P, and 0 to 39% P_o in the arable soils and 46 to 74% Fe- and Al-P, 14 to 43% Ca-P, and 0 to 38% P_o in the adjoining kettle hole sediments. Solution ^{31}P NMR spectra on alkaline extracts revealed a broad signal in the phosphomonoester region which was the most abundant form of organic P across all samples. Besides, the proportion of ‘complex’ phosphomonesters (broad signal) to that of total extractable P was about 2-fold greater in the kettle hole sediments than in soils. Complex forms of organic P are known to be strongly associated with organic matter (OM) and appear to accumulate on a decadel timeframe. Therefore, it is desirable that kettle hole sediments are conserving P (and carbon), which will help reduce the transfer of P from agricultural fields to other, more vulnerable aquatic/marine ecosystems.

Keywords: arable soil, sediment, kettle hole, sequential fractionation, XANES, ^{31}P NMR

3.2. Introduction

Inland aquatic systems play an important role in biogeochemical cycles (Downing, 2010; Raymond et al. 2013). Worldwide, small lentic waterbodies (with an area <0.1 km^2) account for up to 20% of the global lake surface area (Holgerson & Raymond, 2016). An important waterbody type is that of ‘kettle holes’ (also called ‘praire potholes’ in North America), which are defined as glacially created ponds less than 1 ha in size (Lischeid and Kalettka, 2012). In Mecklenburg-Western Pomerania in northern Germany, there are around 40,000 kettle holes (Klafs & Lippert, 2000). Kettle holes originated glacially by delayed melting of ice blocks creating depressions in the moraine landscape about 10,000 to 12,000 years ago and often become obvious via anthropogenic clearing of forests and tillage practices (Kalettka et al., 2001). Consequently, kettle holes are now generally located in intensively used arable fields of late Pleistocene landscapes. Kettle holes contribute to several ecosystem functions, including

species richness and diversity (Oertli et al., 2002; Williams et al., 2003; Vasić et al., 2020), they provide habitats (Frielinghaus and Vahrson, 1998), and play an important role in nutrient cycling and water retention (Fiener et al., 2005). Ecologically relevant processes, such as carbon (C), nitrogen (N) and phosphorus (P) turnover, occur simultaneously in the sediments of kettle holes (Reverey et al., 2016). The availability of P is known to greatly affect the primary production of lakes and enhance OM sedimentation and mineralization (Gudasz et al., 2012; Serrano et al., 2017). Furthermore, P has been identified as one of the major factors contributing to eutrophication and a general deterioration of the quality of aquatic ecosystems (Correll 1998; Reddy et al. 1999). Besides the environmental importance in aquatic ecosystems, in agriculture the P is an essential macronutrient fertilizer element for field crops, often limiting the crop/pasture productivity. The chemical composition of P plays a crucial role in its availability in soil for crops (e.g. Richardson et al., 2009) and the potential to be mobilized and/or transported from arable soil to aquatic environments (e.g. Favaretto et al., 2012).

However, knowledge is limited on the nutrient cycling and the chemical composition of P in kettle hole sediments, especially in agricultural landscapes, where there is a high risk of nutrient transfer to larger waterbodies and eutrophication as a possible consequence (Reddy et al., 1999; Søndergaard et al., 2001; Zak et al., 2004; Hupfer and Lewandowski, 2008; Schönbrunner et al., 2012).

Several studies have investigated the chemical composition of P in agricultural soils (e.g. Koch et al., 2018; Turner et al., 2008; Schmieder et al., 2020) and sediments (e.g. Frankowski et al., 2002; Łukawska-Matuszewska and Bolałek, 2008; Kraal and Slomp, 2014). Little information is available on the P speciation and transformation of P along transects covering soils and sediments, i.e. along terrestrial to aquatic gradients. There is a study of arable soils in northern Germany towards sediments in the central Baltic Sea where increasing proportions of stable P fractions (i.e., H_2SO_4-P and residual-P) compared to iron-associated P were detected with increasing distance from the coastline (Prüter et al., 2020). Furthermore, an accumulation of organic P (P_o) in soils compared to sediments dominated by fractions of inorganic P (P_i) has been ascertained in polder agricultural muck soils and river/lake sediments in Ontario, Canada (Audette et al., 2018), similarly to the above Baltic Sea transect. A limitation of the aforementioned studies is that there was no direct comparison of soils and sediments along a transect in agricultural fields, especially at a small scale area around a kettle hole.

Solution ^{31}P nuclear magnetic resonance (NMR) spectroscopy has been widley used to identify the chemical compostion of P_o in environmental samples, including soils (Turner et al., 2008), manures (Giles et al., 2011), organic amendments (Ajiboye et al., 2008), biological soil crusts (Baumann et al., 2017), agro-industrial byproducts (Negassa et al., 2010), and constructed wetlands (Alewell et al., 2020). Several studies have investigated the chemical composition of P_o using NMR in marine sediments (Ingall et al., 1990; Carman et al., 2000), sediments from estuaries (Li et al., 2015; Watson et al., 2018), river sediments (Zhang et al., 2013; Watson et al., 2019) and lake sediments (e.g. Hupfer et al., 2004; Ahlgren et al., 2005; Reitzel et al., 2007; Zhang et al., 2017). In summary, these studies reported that orthophosphate, phosphomonoesters, and pyrophosphates were the most abundant P species in sediments.

The methods of sequential P fractionation and P *K*-edge X-ray absorption near edge structure (XANES) spectroscopy often have been used in conjuction with ^{31}P NMR spectroscopy to provide a comprehensive assessment of P speciation in environmental samples (e.g. Ajiboye et al., 2008; Negassa et al., 2010; Li et al., 2015; Baumann et al., 2017; Koch et al., 2018; Prüter et al., 2020). In response to Barrow et al. (2020), who critized the accuracy of fractionation procedures to measure chemically specified phosphate fractions in soil, Gu and Margenot (2021) and Guppy (2021) emphasized the value of fractionations. If results are interpreted with caution and comprehensive studies are based on a combination of fractionation measurements with XANES spectroscopy, uncertainties in data interpretation can be overcome and the value of sequential fractionation results can be increased (Gu and Margenot, 2021; Guppy, 2021). Thus, in our view sequential P fractionation has its value as a simple method to provide an overview of the occurring P pools and the distribution of P contents in individual fractions of complex environmental samples (e.g. Kruse et al., 2010).

Phosphorus chemistry can be affected by sample pretreatment, as for example He et al. (2007) determined an increase of orthophosphate up to 8.4% of P_t in dairy manure through P mineralization. Although Turner et al. (2007) also identified differences in P extraction efficiency of different wetland soils and sediments caused by sample pretreatment (fresh, air dried, frozen and lyophilized), changes were inconsistent and mostly within the range of error associated with replicate analyses. Pezzolesi et al. (2000) revealed a significant influence of freezing and air-drying on EDTA-extractable P_i in seasonally flooded wetland soil from Texas for subsurface samples only. Extractable P showed statistical significance with respect to the sample treatment but there is no ‘one true answer’ for the best treatment of wetland soils (Pezzolesi et al., 2000). Furthermore, a previous study about the influence of sample pretreatment on the P speciation of different sediments from a kettle hole and the ‘Bodden’ lagoon system at the Baltic Sea concluded that soil sample pretreatments such as drying, sieving and grinding can be applied to sediments without fundamentally changing the composition of P speciation (Prüter et al., 2022). Although those results may have some site-specifity, the investigation of kettle hole sediments makes the outcomes applicable for the current study of kettle hole sediments and adjacent soil samples.

The main objective of the present study was to identify the chemical composition of P in soils and sediments along a transect from an arable field to a kettle hole for the first time. To the best of our knowledge such soil-to-kettle hole transect study has not yet been undertaken by a multi methods-approach using ^{31}P NMR and P XANES spectroscopy and sequential P fractionation. We hypothesize that the inorganic (e.g., Fe-P and Ca-P proportions) and organic P speciation (e.g. mono- and diester P proportions) differs between arable soil samples and kettle hole sediments. The expected new insight on the P composition of arable soils and kettle hole sediments along a transect can contribute to improve the risk assessment of possible drivers causing eutrophication and P translocation towards aquatic ecosystems.

3.3. Material and methods

3.3.1. *Sampling area, soil and sediment collection*

Soil samples and sediment cores were collected along a transect from an arable site towards the kettle hole 'Rittgarten', both situated in the Uckermark region in the federal state of Brandenburg in Northeastern Germany. The arable land around the kettle hole is dominated by calcareous sandy soils (Kleeberg et al., 2016). Mineral fertilizers were used since the second half of the 19th century and manure applications intensified since 1970 (Nitzsche et al. 2017). Overall, the P supply in this part of Germany has been above plant uptake and removal from fields in the time period between the 1970ies and 1990ies (Harenz 1991) so that considerable enrichment of legacy P in soil can be assumed. The general setup of experimental region, a kettle hole basin with a total size of 1459 m^2 and maximum depth of 2.34 m, surrounded by sandy to loamy Cambisols and Luvisols, is typical for large agricultural areas in the Late Pleistocene landscape in Northeastern Germany (Kleeberg et al., 2016). Two to three single subsamples were merged to one mixed sample for each soil and sediment sample location and depth to minimize effects of small-scale heterogeneity.

Sediment sampling was carried out in October 2015 at two depths: 0 - 5 cm and 5 - 10 cm, as described in Reverey et al. (2018). Sediment samples included: (1) a location 7 m southwest of the deepest point of the kettle hole, frequently exposed to drying-wetting cycles and exposed to atmosphere for 5 months prior to sampling (Reverey et al. 2018), which is a direct extension of the transect of soil samples (W1); (2) the deepest point of the kettle hole, permanently submerged for at least the last five years, exposed to the atmosphere for one month before sampling (Reverey et al., 2018) (W2), and; (3) at the opposite position of W1, 12 m northeast of the deepest point of the kettle hole, constituting the end of the transect, also frequently exposed to drying-wetting cycles and exposed to the atmosphere for 5 months prior to sampling (W3). Subsamples of sediment were deeply frozen and stored until provided for the present study.

Soil sampling was carried out in October 2018 at two depths: 0 – 30 cm and 30 – 50 cm using a soil corer. Soil samples include an arable field (IIS1 and S1), a marginal grassland strip (S2) and a reed belt (S3) around the kettle hole (Table 1). The samples IIS1 are not located on the transect, but about 70 m apart (see Table 1). They were taken to have additional samples from a temporarily flooded agricultural area. The remaining samples S1, S2, S3 and S4 are situated on a straight transect with decreasing distances towards the kettle hole. The last soil sample on the transect was taken directly from the edge of the reed belt near the water surface of the kettle hole (S4). This sample was available only from a depth of 0 – 30 cm, because samples from greater depths were saturated with water that prevented further sampling. Coordinates of precise sample positions are compiled in Table 1.

The above stored sediment and recently taken soil samples were dried at 40°C, sieved with a 2 mm mesh and finely ground to a particle size of < 0.1 mm using a mortar mill (Laboratory Mortar Grinder Pulverisette 2, FRITSCH GmbH, Idar-Oberstein, Germany) prior to further analyses.

Table 3-1 Label, sample type, origin, depth, distance and compass direction from the center of the kettle hole, and coordinates of all collected samples. Subscript letter „a“ declares the surface sample and „b“ the subsurface sample of one sample spot, respectively.

Label	Sample type	Origin	Depth in cm	Distance and direction from center of kettle hole	Coordinates
$IIS1_a$	soil	arable field	0 - 30	68 m SE	N 53° 23' 2.34613" E 13° 42' 28.85194"
$IIS1_b$	soil		30 - 50		
$S1_a$	soil	arable field	0 - 30	24 m SW	N 53° 23' 2.283746" E 13° 42' 24.09032"
$S1_b$	soil		30 - 50		
$S2_a$	soil	marginal grassland strip	0 - 30	21 m SW	N 53° 23' 2.329288" E 13° 42' 24.20221"
$S2_b$	soil		30 - 50		
$S3_a$	soil	reed belt	0 - 30	16 m SW	N 53° 23' 2.432927" E 13° 42' 24.47010"
$S3_b$	soil		30 - 50		
$S4_a$	soil	edge soil - water	0 - 30	9 m SW	N 53° 23' 2.456321" E 13° 42' 24.90761"
$W1_a$	sediment	marginal kettle hole	0 - 5	7 m SW	N 53° 23' 2.693559" E 13° 42' 25.16554"
$W1_b$	sediment		5 - 10		
$W2_a$	sediment	deepest point of kettle hole	0 - 5	no distance	N 53° 23' 2.713872" E 13° 42' 25.19336"
$W2_b$	sediment		5 - 10		
$W3_a$	sediment	marginal kettle hole, opposite of W1	0 - 5	12 m NE	N 53° 23' 2.739634" E 13° 42' 25.22107"
$W3_b$	sediment		5 - 10		

3.3.2. *Determination of total C, N, S, P, Ca, Mg, Al, Fe and Zn*

Concentrations of total C, N and sulfur (S) were obtained by dry combustion on ground soil and sediment material using an elemental analyzer (VARIO EL, Elementar Analysensysteme GmbH, Hanau, Germany). Concentrations of total P (P_t), calcium (Ca), magnesium (Mg), aluminium (Al), iron (Fe) and zinc (Zn) were determined on ground soil and sediment using microwave-assisted (Mars Xpress CEM GmbH Kamp-Linfort, Germany) *aqua regia* digestion (ISO standard 11466) followed by inductively coupled plasma-optical emission spectrometry (ICP-OES) at 214.941 nm wavelength using a Perkin-Elmer Optima 8300 DV instrument.

3.3.3. *Sequential P fractionation*

A slightly modified sequential fractionation method according to Hedley et al. (1982) and Tiessen and Moir (1993) was used to extract different P fractions from soil and sediment. About 0.42 g finely-ground sediment was weighed into 50 mL centrifuge tubes. Tubes with extractant-sample-suspensions were generally shaken for 18 h followed by centrifugation at 4000 *g* for 20 min, and decanted after each extraction step. Chemical P fractionation included the following extraction steps: 1) anion-exchange resin strips; 2) 0.5 M $NaHCO_3$; 3) 0.1 M NaOH, and; 4) 1 M H_2SO_4. In the fraction of anion exchange resin, P was removed from the resin using 1 M HCl.

The P fractions were interpreted as: 1) resin P (Resin-P) representing soil solution P and very readily desorbable P; 2) inorganic ($NaHCO_3$-P_i) and organic ($NaHCO_3$-P_o) bicarbonate P. The former represents readily labile P_i, including readily desorbable P and very labile pools of Ca phosphates. The latter represents P_o that is readily desorbable, microbial P, and an unknown portion of the soil P_o; 3) inorganic (NaOH-P_i) and organic (NaOH-P_o) hydroxide P. The former represents moderately labile P_i, including moderately desorbable P, and Al- and Fe-phosphates. The latter represents P_o associated with the soil OM and IPs, and; 4) the H_2SO_4-P fraction, which represents pools of more stable Ca-phosphates (e.g., hydroxylapatite) (Walker and Syers, 1976; Hedley et al., 1982; Tiessen and Moir, 1993; Guo et al., 2000; Wu et al., 2014; Koch et al., 2018; Morshedizad et al., 2018). Concentrations of P_t in the supernatants were determined by ICP-OES. Concentrations of molybdate reactive P, which is largely considered to be P_i, were determined in the supernatents using the molybdate blue method of Murphy and Riley (1962). Concentrations of molybdate unreactive P, which is largely considered to be P_o, were calculated as the difference between P_t and P_i. The concentration of non-extractable P (termed 'residual-P') was calculated as the difference of cumulative extractable P and the concentration of P_t in soil using *aqua regia* digestion and ICP-OES.

3.3.4. *P* K-*edge XANES analysis*

Bulk P *K*-edge XANES spectra were acquired on soils and sediments at the Canadian Light Source (CLS) in Saskatoon, Saskatchewan, Canada, at the Soft X-Ray Microcharacterization Beamline (SXRMB, Hu et al., 2010). Photon energy from 2 to 10 KeV was covered with a Si(111) double-crystal monochromator with a 7-element Si(Li) drift detector for flourescence measurements (Baumann et al., 2017). Energy calibration was done with Al phosphate ($AlPO_4$) and the main peak position was around 2152.9 eV. XANES data were collected from dry and finely-ground samples, thinly spread on P-free double adhesive C tape attached to a Cu sample holder. Every spectrum was based on at least two replicate samples with 2 to 5 scans per sample. Sample spectra were recorded in fluorescence yield mode and reference standards in total electron yield mode at photon energies between 2130 and 2200 eV for the P *K*-edge. The step size was 1 eV in the pre-edge region (2130 to 2140 eV), 0.15 eV at the edge step (2140 to 2180 eV), and 0.5 eV in the post-edge region (2180 to 2200 eV) with a dwell time of 1 s for the samples and reference standards.

All P *K*-edge XANES spectra were background corrected, normalized, and replicates were merged to obtain better spectral quality. Linear combination fitting (LCF) was performed using the ATHENA software package (Ravel and Newville 2005) in the energy range between -10 eV and +30 eV of E_0. LCF analysis was performed using the combinatorics function of ATHENA software to attain all possible binary to quaternary combinations among all 18 P reference spectra in which the share of each compound was ≥ 10%. The following set of reference P *K*-edge XANES spectra were used for fitting and calculations: ammonium-P: $(NH_4)H_2PO_4$, Zn-P: $Zn_3(PO_4)_2$, K-P: KH_2PO_4, $K_2HPO_4 \cdot 3H_2O$, $K_4P_2O_7$, Al-P: $AlPO_4 \cdot xH_2O$, $Al(PO_3)_3$, P-($Al(OH)_3$) (P adsorbed on gibbsite), P adsorbed on boehmite (P-AlOOH), Ca-P: $Ca(H_2PO_4)_2 \cdot 2H_2O$,

$Ca_{10}(PO_4)_6(OH)_2$ (hydroxylapatite), Mg-P: $MgHPO_4 \cdot 3H_2O$, Fe-P: vivianite ($Fe^{2+}{}_3[PO_4]_2 \cdot 8H_2O$), $FePO_4 \cdot 4H_2O$, $FePO_4 \cdot 2H_2O$, P-FeOOH (P adsorbed on goethite), P-Fe_2O_3 (P adsorbed on ferrihydrite) and phytic acid sodium salt hydrate ($C_6H_{18}O_{24}P_6 \cdot xNa^+ \cdot yH_2O$). The *R*-factor values were used as goodness-of-fit criteria and significant differences between fits were evaluated using the Hamilton test ($p < 0.05$) (Calvin, 2013) with the number of independent data points calculated by ATHENA, estimated as data range divided by core-hole lifetime broadening. Best fits were chosen according to the lowest *R* factor of P reference compound combinations and considered as the most probable P species in the material. If *R* factors of fits with the same number of reference compounds were not significantly different from each other according to the Hamilton test, fit proportions were averaged. For this reason, averaged proportions of some reference compounds can be ≤ 10%.

To facilitate the presentation of the LCF results of P *K*-edge XANES analyses, proportions of individual Fe-, Al- and Ca-P compounds were summed so that the soil samples contained the compound groups of Fe-P, Al-P, Ca-P, and P_o and the sediments Fe-P, Al-P, Ca-P, P_o, and NH_4-P (Figure 1).

3.3.5. *Extraction and solution preparation for solution ^{31}P NMR spectroscopy*

Extraction of P_o from soil and sediment samples was carried out based on the method of Cade-Menun et al. (2002). Briefly, 2 g of dry sample was extracted with 20 mL of 0.25 M NaOH + 0.05 M Na_2EDTA. Extracts were shaken on a horizontal shaker for 16 h, centrifuged for 20 min at 5000 rpm, and the supernatant passed through a Whatman no. 42 filter paper. A 10 mL aliquot of the filtrate was then frozen and lyophilized. This resulted in 272 to 539 mg of lyophilized material across all samples. Concentrations of P_t, P_i and P_o in the remaining filtrate were measured as described above. The NaOH-EDTA filtrates were diluted considerably before measurement by ICP-OES and the molybdate blue method of Murphy and Riley (1962), which are routinely used to measure concentrations of P_t and P_i in NaOH-EDTA filtrates, respectively (Turner et al., 2005). Furthermore, studies have shown that concentrations of 'inorganic' P as measured by the molybdate blue method of Murphy and Riley (1962) in NaOH-EDTA filtrates are similar to that of orthophosphate as determined by solution ^{31}P NMR spectroscopy (Doolette et al., 2011; McLaren et al., 2014).

Lyophilized material was prepared for solution ^{31}P NMR spectroscopy based on a modification of the methods described in Vincent et al. (2013) and Spain et al. (2018). Briefly, 120 mg of lyophilized material was weighed into 1.5 mL microcentrifuge tubes and 600 µL aliquot of 0.25 M NaOH + 0.05 M Na_2EDTA solution was added. However, spectral quality for the sediment samples was poor due to high sample viscosity and these were repeated using a wider ratio (30 mg of lyophilized material and 600 µL of 0.25 M NaOH + 0.05 M Na_2EDTA), which solved the issue. The solution was vortexed for 2 min and then left to stand several hours to allow for complete hydrolysis of RNA and phospholipids (Makarov et al., 2002; Turner et al., 2003a; Doolette et al., 2009; Vestergren et al., 2012). The microcentrifuge tubes were then centrifuged at 10,000 rpm for 20 min, and a 500 µL aliquot of the supernatant was transferred to another

1.5 mL microcentrifuge tube, which then received 25 µL of a 0.03 M methylenediphosphonic acid (MDP) standard in D_2O (Sigma-Aldrich, product no. M9508) and 25 µL of sodium deuteroxide (NaOD) at 40% (*w/w*) in D_2O (Sigma-Aldrich, product no. 372072). The solution was vortexed and then transferred into a 5 mm NMR tubes for analysis.

3.3.6. Characterisation of organic P using solution ^{31}P NMR spectroscopy

All NMR analyses were carried out with a Bruker Avance IIIHD 500 MHz NMR spectrometer equipped with a 5 mm liquid-state Prodigy™ CryoProbe (Bruker Corporation; Billerica, MA) at the NMR facility of the Laboratory of Inorganic Chemistry (Hönggerberg, ETH Zürich). Solution ^{31}P NMR spectra were acquired using a ^{31}P frequency of 202.5 MHz, with inverse gated broadband proton decoupling and 90° pulses (duration of 12 µs) for excitation. Shimming of the samples resulted in a spectral resolution of <0.1 Hz. The recycle delay of each sample was based on preliminary inversion recovery experiments (Vold et al., 1968), as described in McLaren et al. (2021). The recycle delay for each sample was calculated by multiplying the longest T_1 value from the inversion recovery experiment by five, which ranged from 3.6 s to 32.4 s across all samples. The number of scans per sample ranged from 3607 to 4096.

Spectra were processed with TopSpin® software (Bruker Corporation, Billerica, MA). Spectral processing involved Fourier transformation, phase and baseline correction. The known concentration of added MDP standard enabled quantification of all P species in the NMR spectra. As the net peak area of MDP is directly proportional to the other NMR signals, quantification was based on integral ranges according to the presence of ^{31}P NMR signals (Turner, 2008; Doolette et al., 2011). Integration of ^{31}P NMR signals was carried out for the soil samples in the regions of phosphonates (δ 19.8 to 17.4 ppm), the added MDP (δ 17.1 to 16.3 ppm) including its two ^{13}C satellite peaks, combined orthophosphate and phosphomonoesters (δ ~ 6.0 to 3.0 ppm), phosphodiesters (δ -0.8 to -1.5 ppm), and polyphosphates (δ -4.9 to -5.0 ppm). For the sediment samples, integral regions included phosphonates (δ 19.8 to 17.4 ppm), the added MDP (δ 17.3 to 15.8 ppm) including its two ^{13}C satellite peaks, unknown P species (δ ~ 9.0 ppm), combined orthophosphate and phosphomonoesters (δ ~ 6.0 to 3.0 ppm), unknown phosphoesters (δ 2.7 to 1.3 ppm), phosphodiesters (δ 1.2 to -1.6 ppm) and polyphosphates (δ -4.9 to -5.5 ppm). Due to the occurrence of several overlapping NMR signals in the combined orthophosphate and phosphomonoester region, spectral deconvolution fitting was carried out using Matlab (The MathWorks Inc., Natick, MA), as described in Reusser et al. (2020a).

Peak assignments were largely based on comparing previously spiked soil extracts which were overlayed with NMR spectra of the current study (Reusser et al., 2020b; Neal et al., 2021). Differences in chemical shifts were minor, but the presence of *myo*-inositol pentakisphosphate (IP_5) of the (1,2,4,5,6) enantiomer in a soil extract was confirmed via spiking with an authentic standard: 10 µl of 2 mg/L of *myo*-IP_5 standard in D_2O (Cayman Chemical, product no. CAY-10008452-1) was added to one soil extract (Figure S2 of supplementary material).

Some studies report a ‘corrected’ value for phosphodiesters based on the known alkaline hydrolysis of phospholipids and RNA to that of phosphomonoesters under alkaline conditions,

i.e., α- and β-glycerophosphate and mononucleotides (e.g., see Cade-Menun et al. (2021)). These corrections often assume that 100% of the NMR signals assigned to α- and β-glycerophosphate and RNA mononucleotides are exclusively due to the alkaline hydrolysis of phospholipids and RNA (i.e., phosphodiesters). In the present study, no corrections have been made to the concentration of phosphodiesters because it is unknown how much of the α- and β-glycerophosphate and RNA mononucleotides were originally present in the soil, and how much were derived from the alkaline hydrolysis of phospholipids and RNA by the NaOH-EDTA extractant. There is some evidence to suggest this varies widely among soils (e.g., 6% to 84%), and that the relative importance of alkaline hydrolysis of phospholipids and RNA appears to be low in mineral soils (Wang et al., 2021).

There are several reasons why the approach as described above was taken. The decision on no corrections of the concentration of phosphodiesters during spectra processing was made because the alkaline hydrolysis of phospholipids and RNA to glycerophosphates and RNA mononucleotides, respectively, is a known pathway with clearly identified end products in the phosphomonoester region (Turner et al., 2003a; Doolette et al., 2009). The reason for standing times of several hours of the soil and sediment extracts before further analysis was enabling all NMR spectra to be processed in a consistent manner whereby differences in analysis duration will not artificially affect the resultant NMR spectra of some soil samples compared to that of others for quantitative purposes (Doolette et al., 2009). Differences in recycles delays among soil samples vary widely (e.g., < 5 s to > 60 s), which can result in short (e.g., < 6 hours) to long (e.g., > 24 hours) analysis times (Jarosch et al., 2015; McLaren et al., 2015a; Reusser et al., 2020a).

3.3.7. Statistical analysis

Data analysis was performend using open-source statisical software R (version 3.6.3). Calculation of correlations and regression functions for P_o contents of the NaOH-EDTA extracts and C proportions was conducted with the help of linear models from the R package vegan. Significances were tested by the Student *t* test (**P* <0.05, ***P* < 0.01, ****P* < 0.001).

3.4. Results

3.4.1. Sediment characteristics

Concentrations of total C ranged from 6.3 to 68.5 g kg^{-1} in the soils and from 18.1 to 213.9 g kg^{-1} in the sediment samples, among which the latter were on average 6.3 times higher than the former (Table 2). Generally, concentrations of C and N were greater in the surface horizons than in subsurface horizons. Furthermore, concentrations of N (ranging between 0.49 and 20.81 g kg^{-1}) and S (ranging between 0.25 and 20.41 g kg^{-1}) were also greater in the sediments than in the soil samples. The average C/N ratio of the surface soils and sediments was 11.4 and of the subsurface samples 11.5. The C and N concentrations increased along the soil transect towards the kettle hole starting from soil S1 in the surface and in the subsurface horizons.

Within the transect of kettle hole sediments from W1 over W2 in the middle to W3 the conentrations of C, N and S and all other elements were comparably low at the marginal zone, clearly increased towards the middle of the kettle hole and decreased towards the end of the transect but not to such a great extent as in the first marginal zone. In general, concentrations of total P, Ca, Mg, Al, Fe and Zn were higher in the sediments compared to the soil samples (Table 2). Most notably, concentrations of P_t ranged from 680 to 1123 mg kg^{-1} in the surface soils and from 797 to 2591 mg kg^{-1} in the surface sediments. The average concentration of Ca and Zn was about 3.2 times higher in the sediments than in the soils. The mean P/Ca ratio in the sediments (0.11) was about half of it in the soils (0.23).

Table 3-2 verage proportions of carbon (C), nitrogen (N) and sulphur (S) determined by an elemental analyzer and elemental concentrations of phosphorus (P), calcium (Ca), magnesium (Mg), aluminum (Al), iron (Fe), and zinc (Zn) in mg kg^{-1} and their ratios (P/Ca, P/Mg, P/Al, P/Fe, P/Zn) determined by ICP-OES in the surface and subsurface soil and sediment samples.

Depth	Sample type	Label	C	N	S	P	Ca	P/Ca	Mg	P/Mg	Al	P/Al	Fe	P/Fe	Zn	P/Zn
cm			mg kg^{-1}	mg kg^{-1}	mg kg^{-1}	mg kg^{-1}	mg kg^{-1}		mg kg^{-1}		mg kg^{-1}		mg kg^{-1}		mg kg^{-1}	
0 - 30	soil	$IIS1_a$	15933	1407	417	844	3358	0.25	2519	0.34	14405	0.06	12103	0.07	61	13.76
		$S1_a$	8900	770	350	964	3330	0.29	2299	0.42	8994	0.11	10122	0.10	53	18.28
		$S2_a$	12233	1047	307	949	4591	0.21	2805	0.34	8854	0.11	10930	0.09	57	16.60
		$S3_a$	15700	1403	353	680	3208	0.21	1707	0.40	9899	0.07	8916	0.08	56	12.09
		$S4_a$	68500	5753	2153	1123	10660	0.11	2847	0.39	18523	0.06	13248	0.08	93	12.12
0 - 5	sediment	$W1_a$	95133	8243	2930	797	8497	0.09	1435	0.56	7277	0.11	8468	0.09	79	10.05
		$W2_a$	213900	20807	20413	2591	26378	0.10	4770	0.54	23231	0.11	46554	0.06	284	9.12
		$W3_a$	130700	11133	3883	1555	12196	0.13	2953	0.53	15839	0.10	17291	0.09	184	8.46
30 - 50	soil	$IIS1_b$	14367	1250	437	817	3487	0.23	2372	0.34	15095	0.05	11822	0.07	57	14.37
		$S1_b$	6333	490	257	686	2558	0.27	1881	0.36	8888	0.08	8644	0.08	48	14.31
		$S2_b$	9667	850	253	983	2913	0.34	1968	0.50	9939	0.10	11604	0.08	54	18.28
		$S3_b$	10900	933	260	625	3119	0.20	1806	0.35	11321	0.06	9460	0.07	46	13.55
5 - 10	sediment	$W1_b$	18100	1500	667	225	3254	0.07	955	0.24	4555	0.05	4045	0.06	26	8.65
		$W2_b$	173200	16643	12920	2211	18655	0.12	4998	0.44	30212	0.07	37668	0.06	426	5.19
		$W3_b$	53067	4660	1553	1043	8277	0.13	3049	0.34	16720	0.06	13811	0.08	123	8.46

3.4.2. Sequentially extracted P fractions

Sequential chemical fractionation extracted on average 47% of P_t from microwave digestion across all samples (Table 3). Pools of residual-P were generally the largest fraction ranging from 45% to 61% of P_t in the soils and from 37% to 67% in the sediments. Pools of P_i were the predominant form of P in most fractions except that of the NaOH fraction (all samples) and the $NaHCO_3$ fraction (W2), which contained 3% to 16% of P_t as P_o. Pools of resin-P were generally large for most samples, particularly in $W3_b$ (25% of P_t). Pools of 'plant-available' P (i.e., resin-P + $NaHCO_3$-P) were very high in most samples ranging from 10% to 35% of P_t. Concentrations of P were also quantitatively important in the fractions of NaOH-P_o (3% to 16% of P_t) and H_2SO_4-P_i (3% to 38% of P_t). Especially along the transect within the kettle hole, concentrations of $NaHCO_3$-P_o, NaOH-P_o and H_2SO_4-P_o in the sediments of the surface and subsurface layers clearly increased towards the middle of the kettle hole and decreased towards the end of the transect but not to such a great extent as in the frist marginal zone. Along the transect of soils towards the kettle hole there was no clear change in P concentrations. Generally, pools of extractable P in surface layers were higher than in the subsurface layers.

Table 3-3 Concentrations (mg kg^{-1}) and percentages (%) of total P (P_t) and the sequentially extracted inorganic (P_i) and organic (P_o) P fractions resin-P, $NaHCO_3$-P, NaOH-P, H_2SO_4-P, and residual-P determined in the surface and subsurface soil and sediment samples.

Depth	Sample type	Label	P_t	Resin-P_i		Resin-P_o		$NaHCO_3$-P_i		$NaHCO_3$-P_o		NaOH-P_i		NaOH-P_o		H_2SO_4-P_i		H_2SO_4-P_o		Residual-P	
cm			mg kg^{-1}	mg kg^{-1}	(%)	mg kg^{-1}	(%)	mg kg^{-1}	(%)	mg kg^{-1}	(%)	mg kg^{-1}	(%)	mg kg^{-1}	(%)	mg kg^{-1}	(%)	mg kg^{-1}	(%)	mg kg^{-1}	(%)
0 - 30	soil	$IIS1_a$	844	53	(6)	12	(1)	91	(11)	46	(5)	65	(8)	96	(11)	58	(7)	15	(2)	409	(48)
		$S1_a$	964	83	(9)	2	(0)	108	(11)	58	(6)	67	(7)	25	(3)	111	(11)	0	(0)	510	(53)
		$S2_a$	949	79	(8)	7	(1)	114	(12)	43	(5)	13	(1)	127	(13)	111	(12)	9	(1)	446	(47)
		$S3_a$	680	46	(7)	0	(0)	94	(14)	33	(5)	2	(0)	103	(15)	47	(7)	12	(2)	344	(51)
		$S4_a$	1123	36	(3)	20	(2)	32	(3)	78	(7)	35	(3)	139	(12)	99	(9)	41	(4)	641	(57)
0 - 5	sediment	$W1_a$	797	23	(3)	11	(1)	106	(13)	12	(2)	29	(4)	96	(12)	52	(7)	0	(0)	467	(59)
		$W2_a$	2591	8	(0)	0	(0)	23	(1)	225	(9)	46	(2)	353	(14)	98	(4)	108	(4)	1729	(67)
		$W3_a$	1555	99	(6)	3	(0)	2	(0)	175	(11)	19	(1)	202	(13)	89	(6)	51	(3)	915	(59)
30 - 50	soil	$IIS1_b$	817	68	(8)	9	(1)	51	(6)	61	(7)	68	(8)	127	(16)	52	(6)	15	(2)	365	(45)
		$S1_b$	686	46	(7)	1	(0)	57	(8)	40	(6)	2	(0)	78	(11)	105	(15)	0	(0)	357	(52)
		$S2_b$	983	69	(7)	2	(0)	103	(10)	48	(5)	18	(2)	117	(12)	86	(9)	15	(2)	524	(53)
		$S3_b$	625	40	(6)	1	(0)	41	(7)	0	(0)	32	(5)	51	(8)	68	(11)	8	(1)	383	(61)
5 - 10	sediment	$W1_b$	225	2	(1)	8	(4)	11	(5)	1	(0)	12	(5)	22	(10)	84	(38)	0	(0)	86	(38)
		$W2_b$	2211	29	(1)	9	(0)	50	(2)	220	(10)	48	(2)	318	(14)	71	(3)	79	(4)	1385	(63)
		$W3_b$	1043	263	(25)	0	(0)	2	(0)	102	(10)	37	(4)	97	(9)	123	(12)	37	(4)	382	(37)

3.4.3. Bulk P K-*edge XANES spectra*

All XANES spectra were characterized by an intense white line peak at around 2152 eV and varying pre- and post-edge features. The *R* factors from LCF were 0.0012 to 0.0030 for the soil samples and 0.0019 to 0.0324 for the sediment samples but sample $W3_b$ had an *R* factor of 0.1101 (Table S1 of supplementary material). The P speciations of all samples based on XANES spectra and LCF are diplayed in Figure 1 (corresponding XANES spectra can be found in Figure S1 of supplementary material).

The average proportion of Fe-P compounds was higher in the soil samples (53%) than in the sediments (46%) although the spectra of W1b, W2a show an intense pre-edge feature. The average proportion of Ca-P compounds was lower in the soils (7%) compared to the sediments (25%). Proportions of P_o compounds ranged from 0% to 39% of P_t in the surface layers and from 0% to 23% in the subsurface layers. Al-P compounds were present in all soil samples with proportions of 16% to 46%, whereas they were assigned in only two of the subsurface sediments (49% and 24%). Along the transect towards the kettle hole, the surface soils S1a, S2a and S3a showed a decrease of proportions of Al-P in favor of more Fe-P compounds. This increase of Fe-P compounds continues along the transect within the kettle hole in the surface sediments, with the difference being that in these sediments no Al-P species were assigned but more Ca-P compounds.

In the P-XANES, proportions of P_o were assigned in the soils IIS1b, S1a, S3a and S4a and sediments W1a, W1b and W3a, ranging from 12% to 39% of P_t, whereas P fractionation yielded summed proportions of 9% to 28% P_o in the other samples. Nonetheless, there is a very good agreement of 23% XANES P_o and 25% P_o from fractionation in the sample S4a and an equal proportion of 28% P_o determined by both methods in the sample W3a. In the soils IIS1b and S3a proportions of P_o from XANES were about 10% lower than P_o from fractionation and in the samples S1a, W1a and W1b XANES assigned clearly higher percentages of P_o compared to P fractionation.

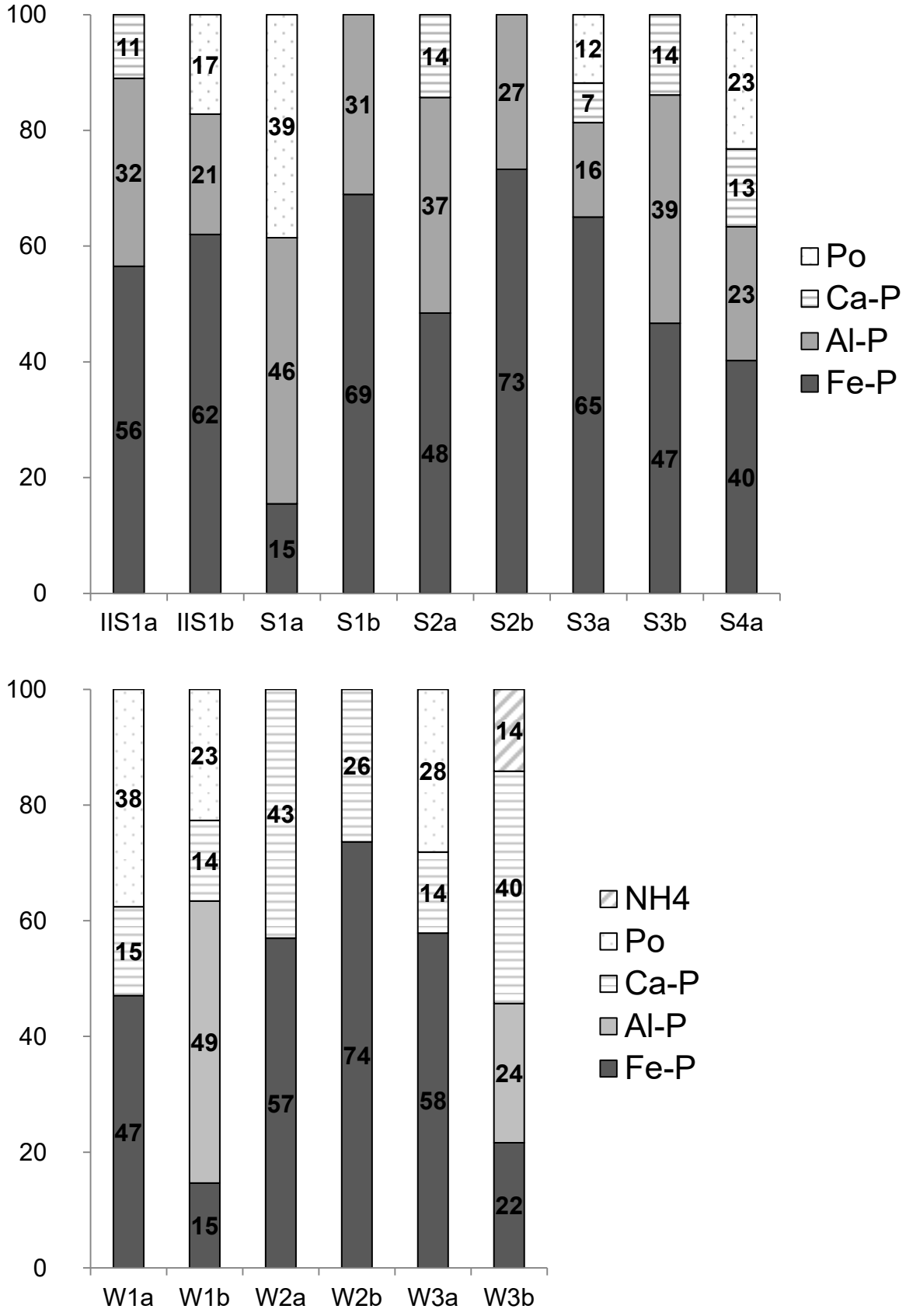

Figure 3-1 Proportions of P (% of total P determined with aqua regia digestion) as obtained by linear combination fitting (LCF) on P *K*-edge XANES spectra of soil (S) and sediment (W) samples in different depths. Standards and spectra were recorded at the CLS-SXRMB beamline, Canada.

3.4.4. NaOH-EDTA extracts

Pools of NaOH-EDTA extractable P_t were on average 40% of the P_t as determined by *aqua regia* digestion across all samples (Table 4). Pools of NaOH-EDTA extractable P_o ranged from 133 – 313 mg P kg^{-1} in the soils and 277 – 971 mg P kg^{-1} in the sediments, which comprised on average 48% and 86% of NaOH-EDTA extractable P, respectively. Pools of NaOH-EDTA extractable P_o were strongly correlated with that of the cumulative pool of alkali soluble P_o (i.e. resin-P_o, $NaHCO_3$-P_o, and NaOH-P_o) as part of the sequential chemical fractionation across all samples (y = 1.3x – 6.7, r^2=83, P<0.05). The recovery of the NaOH-EDTA extractable P_o compared to the summed pool of alkali soluble P_o from the sequential fractionation was on average 109% and 163% for the surface soils and sediments, respectively. Furthermore, pools of NaOH-EDTA extractable P_o were also strongly correlated with that of total C across all samples (Table 2) (EDTA-P_o = 33.06 C + 82.17; r^2 = 0.88***). Along the transect of soils towards the kettle hole starting with S1 in the surface as well as subsurface soils, P_o concentrations increased, although this trend was not reflected by $P_{tNaOH\text{-}EDTA}$.

Table 3-4 Concentrations (mg kg^{-1}) of total P ($P_{tNaOH\text{-}EDTA}$), inorganic P (P_i), and organic P (P_o) in the surface and subsurface soil and sediment samples extracted with NaOH-EDTA.

Depth	Sample type	Label	$P_{tNaOH\text{-}EDTA}$	P_i	P_o
cm				mg/kg	
0 - 30	soil	$IIS1_a$	362	205	157
		$S1_a$	399	267	133
		$S2_a$	406	261	145
		$S3_a$	292	133	159
		$S4_a$	426	113	313
0 - 5	sediment	$W1_a$	310	33	277
		$W2_a$	1112	141	971
		$W3_a$	609	112	497
30 - 50	soil	$IIS1_b$	358	174	184
		$S1_b$	282	168	114
		$S2_b$	406	266	140
		$S3_b$	254	118	136
5 - 10	sediment	$W1_b$	74	22	52
		$W2_b$	927	421	505
		$W3_b$	365	118	248

3.4.5. Solution ^{31}P NMR spectroscopy

Solution ^{31}P NMR spectra of the soil and sediment extracts were highly resolved and included a large number of different P_o species (Figures 2 and 3). The analyses showed a predominance of orthophosphate in all investigated soil and sediment spectra, which comprised 56 - 78% of P_t in the NaOH-EDTA extracts of all soil and 46 - 82% of P_t in the NaOH-EDTA extracts of the

sediment samples. Phosphomonoesters were the most abundant form of P_o and comprised 21 – 40% of P_t (75 – 150 mg P kg^{-1}) in the soil extracts and of 16 – 45% of P_t (10 – 297 mg P kg^{-1}) in the sediments.

In general, the most abundant forms of phosphomonoesters were indicated by a broad signal, followed by IPs, glycerophosphate and RNA mononucleotides. The *myo* stereoisomer of IP_6 was most dominant, which comprised 60% of total IP_6 in the soils and 53% of total IP_6 in the sediments. Furthermore, two enantiomers of *myo*-, and the stereoisomer of *scyllo*-inositol pentakisphosphate (IP_5) could be identified in the soil extracts at low concentrations, but these were absent in the sediments.

Phosphonates, phosphodiesters and polyphosphates were also detected but comprised a minor fraction of NaOH-EDTA extractable P (generally less than 4% of P_t), whereas phosphodiesters were relatively more abundant (up to 7% of P_t) in the sediment extracts. The variety of P species was lower in the sediments extracts compared to the soils (Figures 2 and 3), particularly in the phosphomonoester region which the former contained about half the number of compounds than the latter. Pyrophosphate was detected across all samples, but at low concentrations (Table 5).

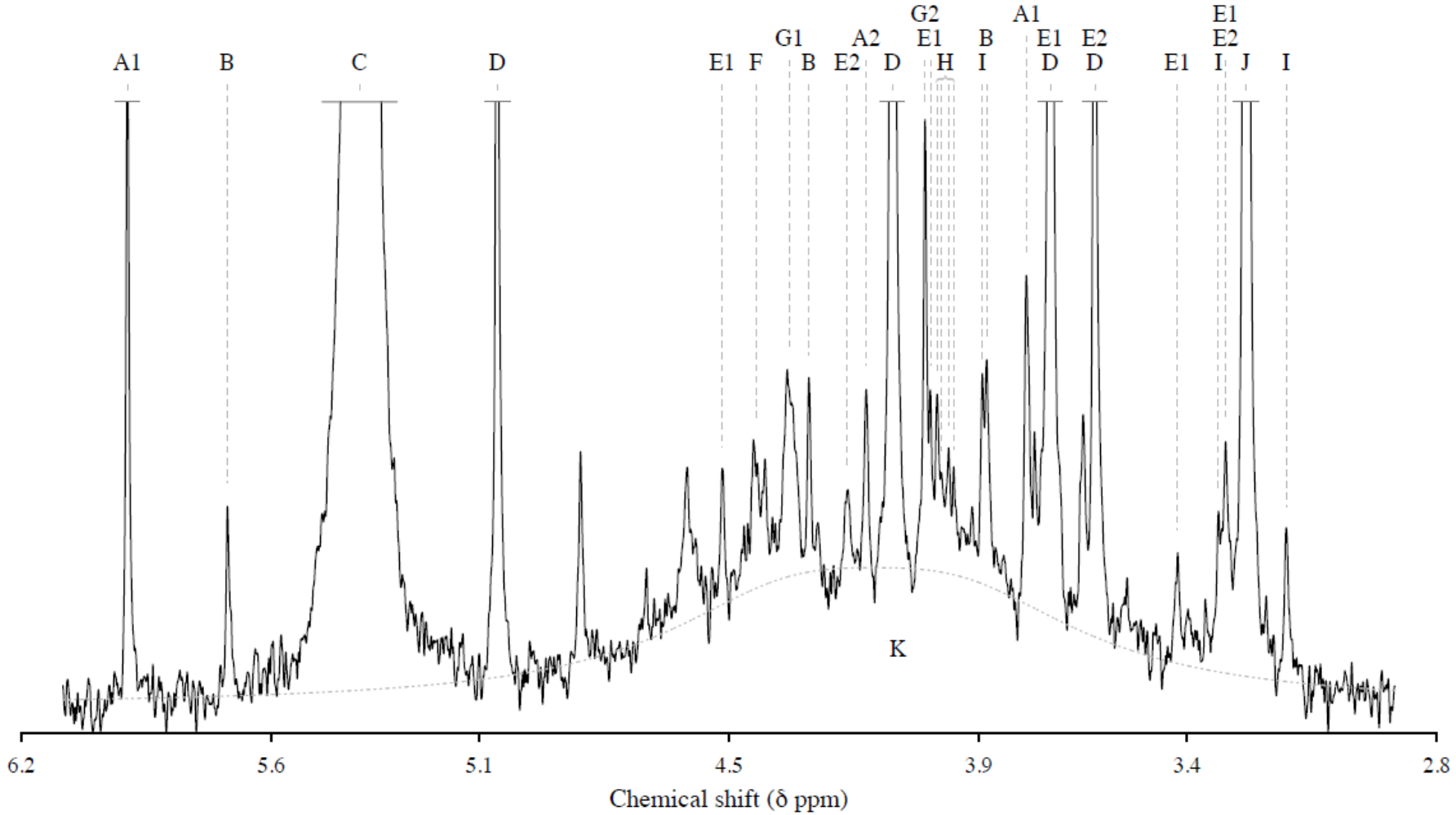

Figure 3-2 Orthophosphate and phosphomonoester regions (δ 6.2 to 2.8 ppm) of the solution ^{31}P NMR spectrum from the extract of soil sample $S2_a$. Identified P species in these regions include: A1 – *neo*-IP6 in the 4-equatorial/2-axial conformation (δ 5.94 and 3.78 ppm), A2 - *neo*-IP_6 in the 2-equatorial/4-axial conformation (δ 4.17 ppm), B – *chiro*-IP_6 in the 2-equatorial/4-axial conformation (δ 5.71, 4.31 and 3.88 ppm), C – Orthophosphate (δ 5.39 ppm), D – *myo*-IP_6 (δ 5.01, 4.11, 3.73 and 3.62 ppm), E1- *myo*-IP_5 of the (1,2,4,5,6) enantiomers (δ 4.52, 4.02, 3.73, 3.42 and 3.31 ppm), E2 – *myo*-IP_5 of the (1,3,4,5,6) enantiomers (δ 4.22, 3.62 and 3.31 ppm), F – other sharp signal of high molecular weight (δ 4.44 ppm), G1 – alpha-Glycerophosphate (δ 4.35 ppm), G2 – beta-Glycerophosphate (δ 4.03 ppm), H – RNA mononucleotides (δ 4.00, 3.99, 3.97 and 3.96 ppm), I – *scyllo*-IP_5 (δ 3.89, 3.32 and 3.16 ppm), J – *scyllo*-IP_6 (δ 3.26 ppm) and K – a broad signal (centered around δ 4.09 ppm).

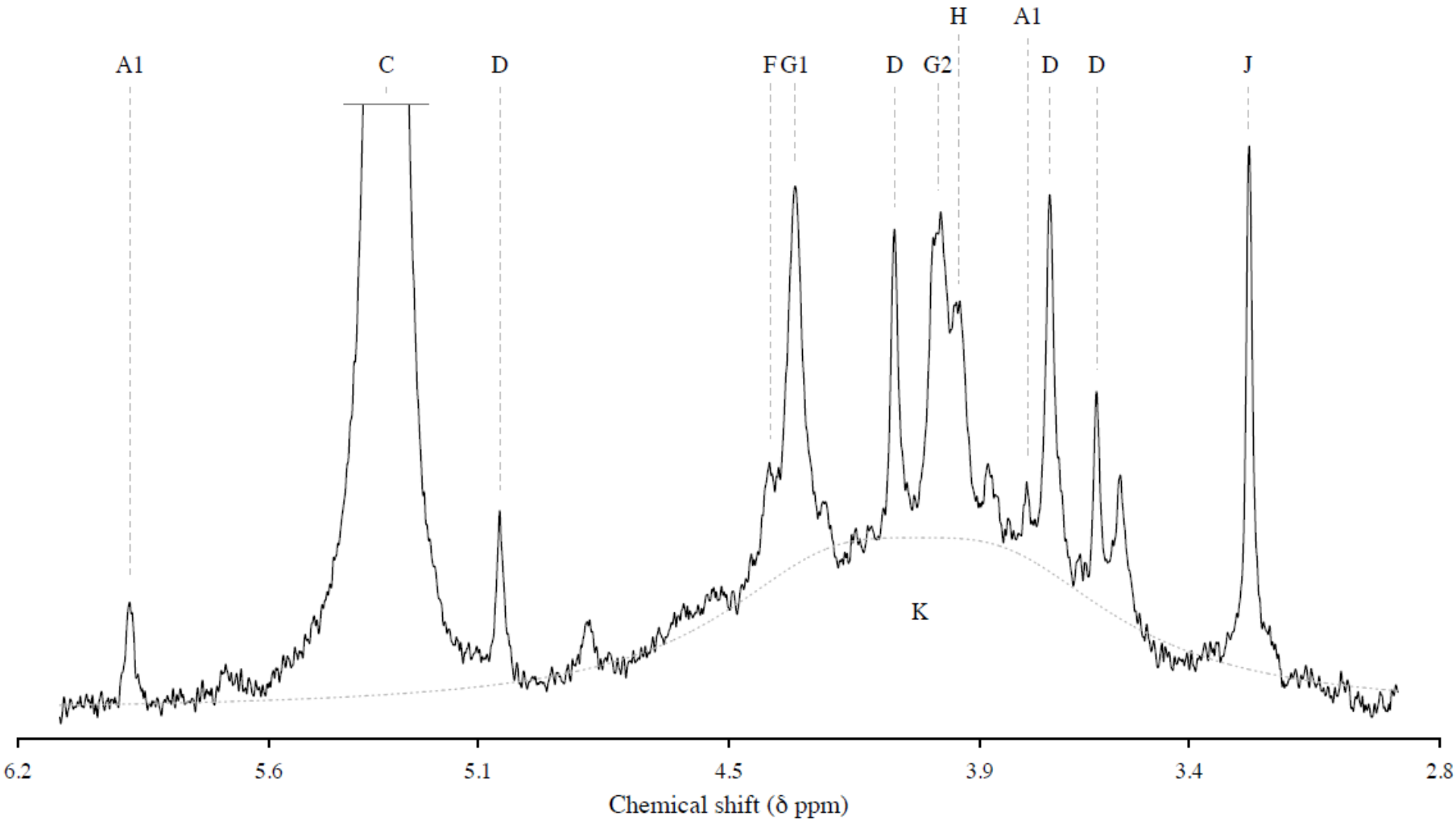

Figure 3-3 Orthophosphate and phosphomonoester regions (δ 6.2 to 2.8 ppm) of the solution ^{31}P NMR spectrum from the extract of sediment sample $W3_a$. Identified P species in these regions include: A1 – *neo*-IP6 in the 4-equatorial/2-axial conformation (δ 5.93 and 3.78 ppm), C – Orthophosphate (δ 5.32 ppm), D – *myo*-IP_6 (δ 5.05, 4.10, 3.73 and 3.62 ppm), F – other sharp signal of high molecular weight (δ 4.40 ppm), G1 – alpha-Glycerophosphate (δ 4.34 ppm), G2 – beta-Glycerophosphate (δ 4.00 ppm), H – RNA mononucleotide (δ 3.95 ppm), J – *scyllo*-IP_6 (δ 3.26 ppm) and K – a broad signal (centered around δ 4.04 ppm).

Table 3-5 Concentrations (mg kg^{-1}) of P species in NaOH-EDTA extracts of the surface and subsurface soil and sediment samples as determined from solution ^{31}P NMR spectroscopy.

	Soil				Sediment				Soil				Sediment		
P species	$IIS1_a$	$S1_a$	$S2_a$	$S3_a$	S_4	$W1_a$	$W2_a$	$W3_a$	$IIS1_b$	$S1_b$	$S2_b$	$S3_b$	$W1_b$	$W2_b$	$W3_b$
Phosphonates															
2-AEP	0.7	0.5	0.7	0.9	1.3	0.0	0.0	2.7	1.6	0.8	0.5	0.9	0.0	2.5	2.0
Other[1]	0.0	0.0	0.0	0.0	0.0	0.0	0.0	0.0	0.7	0.3	0.2	0.4	0.0	0.0	1.0
Orthophosphate	245.5	301.6	289.7	164.8	209.7	112.7	433.2	246.2	213.1	191.9	293.0	146.8	51.9	431.5	185.1
Phosphomonoesters															
Broad signal	34.7	27.4	29.4	44.5	96.7	79.9	184.1	142.4	50.4	31.5	30.2	47.2	0.0	160.2	75.4
scyllo-IP_6	7.2	10.8	13.2	10.1	5.4	1.9	0.0	10.3	10.1	8.9	11.4	7.9	1.5	0.0	8.2
myo-IP_6	22.0	27.9	23.5	18.0	22.6	0.0	59.7	18.4	30.6	19.4	23.8	16.8	0.0	21.7	13.7
chiro-IP_6	1.8	1.7	1.6	1.8	1.5	0.0	0.0	0.0	2.8	1.5	1.4	1.4	0.0	0.0	0.0
neo-IP_6	4.0	3.3	3.1	3.3	4.4	0.0	0.0	1.6	5.3	3.0	3.5	2.9	0.0	0.0	2.1
myo-IP_5[2]	2.5	2.6	2.5	2.1	0.0	0.0	0.0	0.0	3.9	2.7	2.6	2.2	0.0	0.0	0.0
scyllo-IP_5	1.3	1.3	1.3	1.4	0.0	0.0	0.0	0.0	1.7	1.5	1.6	1.3	0.0	0.0	0.0
RNA mononucleotides	2.2	1.0	1.1	1.7	4.3	6.5	10.3	10.1	1.5	0.4	1.2	0.5	0.0	3.2	3.7
Glycerophosphate	3.4	1.6	2.7	1.1	7.4	10.9	36.5	20.8	1.5	0.6	0.7	0.7	0.0	30.1	4.7
HMW sharp	2.0	1.2	1.1	3.0	3.7	0.0	0.0	2.6	4.2	3.0	3.0	2.1	0.0	0.0	2.2
Other[1]	5.1	2.8	3.6	3.9	3.9	9.8	6.3	9.0	5.1	2.7	5.0	3.1	8.5	3.4	5.3
Phosphodiesters															
DNA	1.9	1.8	1.9	2.7	12.8	14.3	55.3	29.7	1.4	0.0	1.0	0.9	0.0	35.7	5.7
Other[1]	0.0	0.0	0.0	0.0	0.0	0.0	48.8	0.0	0.0	0.0	0.0	0.0	0.0	16.1	0.0
Polyphosphates															
Pyrophosphate	1.9	1.2	1.7	1.6	2.6	7.5	8.2	10.6	0.6	0.3	1.3	0.7	1.1	4.3	3.3
Inorganic P	247.4	302.8	291.3	166.5	212.3	120.2	441.4	256.8	213.8	192.2	294.3	147.5	53.0	435.8	188.4
Organic P	88.8	83.9	85.7	94.7	164.1	123.4	401.0	247.7	120.6	76.3	86.1	88.3	10.0	273.0	124.0
Total P	336.2	386.6	377.1	261.2	376.3	243.5	842.4	504.5	334.4	268.6	380.3	235.7	62.9	708.8	312.4

[1]Sum of all unknown sharp signals within phosphonates, phosphomonoesters, and phosphodiesters.
[2]Sum of *myo*-IP_5 (1,2,3,5,6) and (1,3,4,5,6) enantiomers

3.5. Discussion

3.5.1. Phosphorus speciation

Concentrations of most elements were higher in the kettle hole sediments compared to the adjacent arable soils (Table 2) because kettle holes are known to often act as sinks for nutrients and metals from eroded soils around them and are affected by agricultural pollution (Bilotta et al., 2007; Kleeberg et al., 2016). Most detected elements are typical components of common mineral fertilizers, thus, it is likely that the elevated elemental concentrations in the kettle hole sediments were a result of emissions from agriculture. This explanation is supported by the fact that the soils around the kettle hole are intensively used for arable cropping at large fields up to 200 ha in size, without erosion-inhibiting structures making soils in this area especially susceptible to erosion by water and wind (Kleeberg et al., 2016). The about two times higher concentrations of C and N in IIS1a compared to S1a from the same arable field could be caused by the sloping terrain and previous flooding at the sampling position of IIS1. In Late Pleistocene ground moraines, the soils in depressions are closer to groundwater that restricts the aerobic decomposition of litter and enriches soil organic matter in the topsoil. From other landscapes, it has been reported that temporarily flooded soils, often located in lowlands are receiving eroded fine particles, leading to accumulation of clay, OM and nutrients (Berhongaray et al., 2013). Concentrations of P_t in the arable soils were similar to that of unfertilized soils (Stagnic Cambisol) from a long-term field experiment under cultivation (Koch et al., 2018). At the current arable field and that of Koch et al. (2018), soils were developed on similar parent material and experienced similar weather conditions (Kleeberg et al., 2016). An approximately two-fold higher P concentration of kettle hole sediments compared to soils is likely due to their position in the agricultural field. Concentrations of P_t in the kettle hole sediments of a previous investigation were in a similar range (~ 2000 mg kg^{-1} P) as in sediments from a kettle hole surrounded by an arable field near Rostock/Mecklenburg-Western Pomerania in northeast Germany. The occasional exposure to air can be one factor explaining the by far highest P_t concentrations (Table 2) especially in the surface sediment W2. Whereas W1 and W3 from drier zones of the kettle hole may have been enriched with oxygen even in deeper layers, sediment W2 from the moister centre of the kettle hole was only exposed to the atmosphere one month prior sampling (Reverey et al., 2018). Consequently, the redox potential was increased only at sediment surfaces in the moist centre of the kettle hole (Reverey et al., 2018). As sorption processes of P are known to be redox-sensitive and a low redox potential can promote remobilization of bound P (Braskerud et al., 2005), P could be conserved especially in the surface sediments W2 with a higher redox potential. Furthermore, silt, clay and fine OM particles accumulated in the center of the kettle hole (W2) compared to the outer zones due to transport processes during heavy rain events (Reverey et al., 2018). It is already known for soils that greatest amounts of P_t are closely associated to the clay fraction (Bates and Baker, 1960; Hanley and Murphy, 1966; Lekwa and Whiteside, 1986). Thus, the lower sand and higher silt, clay and OM content at the position of W2 compared to W1 and W3 results in highest P_t concentrations in the surface sediment W2.

The slightly lower elemental concentrations in the subsoil and subsurface sediments compared to the surface samples (Table 2) agreed with an earlier study of kettle hole sediments, where concentrations of P, Ca, Mg, Al and Fe were lower in a depth of 10-20 cm compared to surface sediments (Prüter et al., 2022). This can be explained by fewer inputs of nutrients and OM to the deeper soil and sediment layers (e.g. Schrumpf et al., 2013; Heinze et al., 2018; Koch et al., 2018; Liang et al., 2018). Similarly as in the present soils and sediments (Table 2), Koch et al. (2018) reported significantly smaller stocks of C and N in deeper soil samples compared to topsoils from an agricultural site with different fertilization treatments. Furthermore, Kleeberg et al. (2016) reported less OM and N with increasing sediment depth in sediments from the kettle hole Rittgarten. The very high proportion of 25% resin-P_i in the 5-10 cm layer at W3 (Table 3) compared to the other sediments could be related to the clear differences in biogeochemistry between the hydrological zones of the kettle hole caused by varying patterns of previous dry-wet cycles as revealed by Revery et al. (2018). The inner, moister zone of the kettle hole differs from outer, drier zones in physicochemical parameters such as water content, sediment texture and organic matter (OM) contents (Revery et al., 2018). For example, fine sediment particles can accumulate in the kettle hole center, whereas wind can deposit fine sediment particles from dry areas, reflected by higher sand and lower silt, clay and OM contents in the outer, drier kettle hole zones (Reverey et al. 2018). Furthermore, in contrast to sediments from drier zones, sediments from the deepest point of the kettle hole (W2) were water-saturated, even when they were exposed to the atmosphere accompanied by an increase of the redox potential Revery et al. (2018).

The extractability of P from sediments and soils with sequential fractionation in the present study was similar to that reported in the reviewed literature (Negassa and Leinweber, 2009). Residual-P in soils and sediments is often a large fraction of P_t (Condron and Newman 2011). A similar proportion of residual-P to P_t between soil samples and kettle hole sediments in the present study indicates that there were no fundamental differences in the general distribution of P fractions between the soils and sediments.

The clear dominance of Fe- and Al-P species especially in the soil samples derived from XANES spectroscopy (Figure 1) agreed with, e.g., Luo et al. (2017), Koch et al. (2018) and Schmieder et al. (2018) who also identified Fe-P and Al-P as predominant P species in different soils. Proportions of P_o determined by XANES spectroscopy roughly agreed with P_o results from P fractionation (Figure 1 and Table 3). The fact that P fractionation detected small percentages of P_o in samples where there was no P_o from the XANES analyses can be attributed to the use of phytic acid sodium salt hydrate as P_o reference compound in the P-XANES. An underestimation of P_o compounds by XANES spectroscopy is likely because some P_o can be associated with Fe and Al oxides (Prietzel et al. 2015) and XANES spectra of phytic acid are known to be lack of strong and distinguishing features (Ajiboye et al 2008). Furthermore, a recent investigation revealed that phytates can also be described with a combination of Fe- and Al-associated P to some extend due to a change of the white-line energy and intensity (Gustafsson et al., 2020). In the light of these limitations, the contribution of P_o to soil P derived from LCF of XANES spectra is reliable. Higher proportions of Ca-P compounds were

determined by XANES analyses in the soils IIS1a, S2a, S3b, S4a and most sediments compared to percentages of H_2SO_4-P fraction of sequential fractionation, representing P associated with Ca and Mg minerals and apatite (Walker and Syers, 1976; Hedely et al., 1982; Tiessen and Moir, 1993) in most soil and sediment samples.

In the ^{31}P NMR spectra, a broad signal in the phosphomonoester region was most abundant (Figures 2 and 3). Average concentrations of assigned P compounds within the broad signal were more than two times higher in the sediments compared to the soil samples (Table 5). Compounds forming this broad signal were previously assigned to complex forms of P_o in apparent high molecular weight material especially present in macro-molecular structures and associated with the soil OM (McLaren et al., 2015b; McLaren et al., 2019; Reusser et al., 2020a; Alewell et al., 2021). The predominance of phosphomonoesters in the soil as well as sediment extracts (Table 5) coincides with several investigations of soils, where phosphomonoesters also made up major proportions of P_o in NaOH-EDTA extracts (e.g. Turner et al., 2003b; Alewell et al., 2020; McLaren et al., 2020). The predominance of *myo*-IP_6 among the different stereoisomers of IP_6 in the soils and sediments (Table 5) with ^{31}P NMR spectroscopy agreed with findings from four contrasting soils (Irving and Cosgrove, 1982) and extracts of constructed wetlands (Alewell et al., 2020), where it comprised about 64% of total IP_6. There were higher concentrations of RNA mononucleotides and glycerophopshates in the sediments compared to soils. These compounds are known to be formed by the alkaline hydrolysis of RNA and phospholipids (Makarov et al., 2002), but it is unclear what portions of them are naturally present in soil (Wang et al., 2021). Based on potentially higher amounts of microbial mass in the sediments, more RNA, DNA and their degradation products are present and can be detected via ^{31}P NMR spectroscopy in the sediments compared to the soils. The very small amounts of phosphonates in the soil as well as in the sediments agreed with other studies, where also low concentrations of these compounds were detected in mineral soils with ^{31}P NMR spectroscopy (Jarosch et al., 2015; McLaren et al., 2015b).

3.5.2. Implications to environmental processes and the P cycle

Bioavailable (labile) P is represented by the sum of resin-P and $NaHCO_3$-P in sequential fractionation procedures (Cross and Schlesinger, 1995). The high concentrations of this bioavailable P pool, especially in the kettle hole sediments (Table 3), can be explained by several reasons. The decomposition of submerged macrophytes supported the release of easily bioavailable P followed by an increase of phytoplankton biomass (Onandia et al., 2018). The generally high sediment surface to water volume ratio in kettle holes can enhance water-sediment interactions and nutrient turnover (Meerhoff and Jeppesen, 2009). Furthermore, the higher concentrations of bioavailable P in the kettle hole sediments compared to the soils can be related to the higher C concentrations in the sediments than in the soils (Table 2). In this line, an earlier investigation of the Rittgarten kettle hole sediments reported a peak in OM at a distinct depth together with high P concentrations at the same depth (Kleeberg et al., 2016). Additionally, one of the main nutrient sources in the kettle hole sediments can be plant material

which is transferred into the kettle hole from neighbouring areas. In particular, kettle holes are a sink of high nutrient inputs (e.g., fertilizer) and soil translocation from surrounding arable fields (Frielinghaus and Vahrson, 1998; Lischeid and Kalettka, 2012; Kleeberg et al., 2016). These nutrients cannot be as highly consumed by natural vegetation in the kettle hole as from crop plants at the agricultural field and are also not removed via the harvested products, often leading to high trophic states of kettle holes (Lischeid and Kalettka, 2012). This has also been supported by earlier studies at this site that show a large transfer of plant debris and crop plants on the soil surface from adjacent areas to kettle hole soil in the catchment (Onandia et al., 2018). Plant material contains largely orthophosphate that can be leached out into the soil and/or sediment and be adsorbed onto sediment surfaces or remains in solution (Noack et al., 2014). Kerr et al. (2011) also detected differences in P sorption between soils and sediments of a subtropical river catchment. There were hints for more reactive surfaces (clay, soil OM, Al- and Fe-oxyhydroxides) to be present for orthophosphate to adsorb onto in sediments rather than soils (Kerr et al., 2011).

Sequential P fractionation determined nearly two times higher average concentrations of NaOH-P (sum of NaOH-P_i and NaOH-P_o) in the surface kettle hole sediments compared to the surface soils (Table 3). Proportions of NaOH-P_o were clearly higher than NaOH-P_i proportions in all soils and sediments with the exception of S1a. Pools of extractable NaOH-P, considered as moderately labile Fe- and Al-P species and P adsorbed to reactive surfaces (e.g., Al- and Fe-oxyhydroxides, clay and soil OM) (Hedley et al., 1982), contain great amounts of P_o, which will be largely associated with the soil OM or complex forms of phosphomonoesters (McLaren et al., 2016). On the one hand, the particularly high NaOH-P_o concentrations in the kettle hole sediments compared to the soils were related to the greater P_t concentrations in the sediments than in the soils and, on the other hand, this can be associated with the differing hydrological conditions between the sediments and adjacent soils explained by the enrichment of OM under mostly anaerobic conditions in the kettle hole sediments. Under reducing conditions, the pH of sediments can decrease, leading to an increased dissolution of P from occluded P within aggregates (Baumann et al., 2020). Especially during longer periods of inundation there is a certain risk for the development of reducing conditions in kettle hole sediments. This promotes the release of P from the sediment into the overlying water column by a reduction of Fe-oxides that bind P (Onandia et al., 2018). As the proportions of Fe-P in the kettle hole sediments were gernerally high (Figure 1) compared to other sediments from environments such as the Baltic Sea (Prüter et al., 2020), this mobilization of P and its subsequent upward transport has been described as one of the major P release pathways in an approximate equilibrium between P sources and sinks over a year within the sediments of this kettle hole (Onandia et al., 2018). Thus, this kettle hole contributes importantly to a retention of nutrients and contaminants in the landscape with intense agricultural land use, due to accumulation processes within the kettle hole sediment.

In the soil samples $IIS1_a$ and $S1_a$, more distant from the kettle hole, proportions of the NaOH-P_i fraction were even higher compared to the surface kettle hole sediments (Table 3). The XANES spectroscopy confirmed this result of sequential fractionation by an assignment of 61 - 88% Fe-

and Al-bound P species in these soils and 47 – 58% in the surface kettle hole sediments (Figure 1). Analyses with P *K*-edge XANES spectroscopy assigned generally higher proportions of Fe bound P species and lower percentages of Ca-P compounds in the arable soil compared to the kettle hole sediments (Figure 1) and thereby agreed with the determined elemental concentrations and with sequential fractionation results of these samples (Table 2). The H_2SO_4-P fraction of sequential fractionation is known to represent insoluble P associated with Ca and Mg minerals and apatite (Walker and Syers, 1976; Hedely et al., 1982; Tiessen and Moir, 1993). Maximum H_2SO_4-P (H_2SO_4-P_i + H_2SO_4-P_o) concentrations of 140 mg kg^{-1} were determined in the surface soils and up to 206 mg kg^{-1} in the surface kettle hole sediments (Table 3). In accordance with that, XANES spectroscopy assigned proportions of 0 – 14% Ca-associated P compounds in the surface soils and up to 43% in the surface sediments (Figure 1). Even if it can be difficult to distinguish different P species, especially P_o with XANES, results of LCF are more accurate for Ca phosphates due to their richness in unique spectral features (Gustafsson et al., 2020). As the pH of the inundated kettle hole sediments was 6.1 at W1 and W3, the starting and ending point of the transect of kettle hole sediments, and 6.4 at W2, the deepest point in the middle of the kettle hole (Reverey et al., 2018), these were conditions supporting the formation of Ca-phosphates (e.g. Agbenin 1996). Frankowski et al. (2002) detected Ca bound P to be the most dominant form of P species in sediments from the Baltic Sea and Kraal et al. (2015) even found a transition with depth of Fe-associated P to Ca-P in sediments from the Arabian Sea. However, such a decline of Fe-P in favour of Ca-P with depth occurred in the current investigation in the kettle hole sediment pair of W3 (Figure 1). A possible explanation for the transition with depth of Fe-associated P to Ca-P in the kettle hole sediment pair of W3 could be a change of the availability of oxygen in this area. Iron-associated P compounds are likely to be dissolved under anoxic conditions, typically occurring at greater depths in sediments, as a result of reductive dissolution-precipitation reactions in contrast to Ca-P compounds (Kraal et al., 2015).

Pools of NaOH-EDTA extractable P_o were overall consistent with that of chemical fractionation (Tables 3 and 4), confirming the connection of total P_o with soil OM and thus with total (organic) C in soil as suggested by Kirkby et al. (2011). The higher amounts of P extracted with NaOH-EDTA compared to the results of sequential P fractionation until the extraction step with NaOH (Tables 3 and 4) can be explained by the effect of EDTA, which is known to improve the extraction efficiency of P_o in NaOH for soils and aquatic sediments (Harrap, 1963; Turner, 2008). Even if EDTA is able to increase phosphate solution due to metal chelation and thus can improve also the extraction efficiency of P_i (Bowman and Moir, 1993), in most of the current samples the greater extraction efficiency of NaOH-EDTA compared to the results of sequential P fractionation can be attributed to higher concentrations of P_i.

Accumulations of phosphomonoesters contributing to the broad ^{31}P NMR signal were associated with the degradation of plant and microbial material and a following stabilization with metals and other C-containing molecules (Alewell et al., 2021). Due to higher C concentrations measured in the kettle hole sediments compared to the soil samples (Table 2), this relationship could explain the higher spectral proportions of the broad signal in the sediments than soils.

These differences in the spectral proportions of the broad signal between the soil and kettle hole sediment extracts can be related on the one hand to the additional crop plant and soil translocation inputs into the kettle hole (Frielinghaus and Vahrson, 1998; Lischeid and Kalettka, 2012) and on the other hand to the higher amounts of phytoplankton biomass and greater activities of microbial communities in the kettle hole sediments compared to soils (Reverey et al., 2018). The slightly higher percentages of *myo*-IP_6 in the soil extracts compared to the sediments (Table 5) could represent higher direct inputs of plant tissue from field crops to the soils than to the sediments, because *myo*-IP_6 is known to act as P storage in plants for developing seeds (Negassa et al., 2010; Noack et al., 2014; Alewell et al., 2020).

While it is known that most P in arable and primarily mineral soils occurs as P_i associated with Al, Fe and Ca (Sims and Pierzynski, 2005), the current results suggest that kettle hole sediments appear to contain higher concentrations and a greater diversity of P_o compounds. Especially the determination of greater spectral proportions of the broad signal with ^{31}P NMR spectroscopy must be emphasized. This finding can be linked to the previously reported nature of kettle hole sediments which have a high potential to act as C sink and thereby also contain high amounts of OM (Reverey et al., 2016). Complex forms of P_o, strongly associated with the soil (or sediment) OM, are more resilient than other forms of P_o, such as diesters, to microbial degradation (Reusser et al., 2022).

This investigation discovered different risks of mobilization or transformation processes of P to aquatic/marine ecosystems from kettle hole sediments and adjacent arable soil samples. The P XANES spectroscopy detected Fe-P compounds in the soil samples to be dominant and simultaneously higher average proportions of Ca-P compounds in the sediments compared to the soils (Figure 1). As the probability of P leaching in subsurface flow can be decreased by Ca (Favaretto et al., 2012), high concentrations of Ca and Ca-associated P in soils or sediments potentially contribute to avoiding water pollution by P entries. Reflecting this, the kettle hole sediments may pose a lower risk of leaching P to aquatic ecosystems compared to the investigated arable soil samples. Similar to an investigation of sediments from a transect in the Baltic Sea (Prüter et al., 2020), XANES spectroscopy revealed an increase of Ca-associated P compounds compared to Fe-P species with an increasing aquatic influence. Furthermore, we determined significantly higher spectral proportions of the broad signal in ^{31}P NMR spectra in the kettle hole sediments compared to the soil samples. These more complex forms of P_o in apparent high molecular weight material have not been quantified in the transect of Baltic Sea sediments, where ^{31}P NMR spectroscopy detected less variety of mono- and diester P compounds with increasing distance from the coast (Prüter et al., 2020).

We conclude that the combination of the complementary methods of sequential P fractionation, P XANES spectroscopy and ^{31}P NMR spectroscopy was well-suited for tracing the fate of P along the terrestrial-to-aquatic transect and, for the first time, described a combined C- and P sink function of kettle holes. That sink function for C and P is derived from enrichments in H_2SO_4-P, Ca-P compounds and complex organically bound P compared to surrounding soils, therefore kettle holes need to be preserved and protected from undesired inputs of soil material, contaminants or even waste. Since kettle holes in northeastern Germany are hydrologically

connected with pipe drainages and drainage ditches, trapping P in sediments by complex organic substances and Ca phosphates may prevent larger regional freshwater resources such as rivers, lakes and the Baltic Sea from further eutrophication.

3.6. Acknowledgments

The authors would like to thank Elena Heilmann and Britta Balz (Soil Science, University of Rostock) for analytical help concerning elemental analyses and P fractionation. We thank Dr. René Verel of the Laboratory of Inorganic Chemistry (Hönggerberg, ETH Zürich) for technical assistance and the whole team of the Group of Plant Nutrition (Eschikon, ETH Zürich) for their support during NMR analyses. The XANES research referred to in this paper was performed at the Canadian Light Source, which is supported by the Canada Foundation for Innovation, Natural Sciences and Engineering Research Council of Canada, the University of Saskatchewan, the Government of Saskatchewan, Western Economic Diversification Canada, the National Research Council Canada, and the Canadian Institutes of Health Research. Furthermore, we are thankful to Daniel Rasche (GeoForschungsZentrum, Potsdam) who provided the coordinates of sampling positions for this study.

3.7. Funding

This research was funded by the Leibniz Association within the scope of the Leibniz ScienceCampus “Phosphorus Research Rostock”. No potential competing interest was reported by the authors.

3.8. References

Agbenin, J.O., 1996. Phosphorus sorption by three cultivated savanna Alfisols as influences by pH. Fertil. Res. 44, 107-112.

Ahlgren, J., Tranvik, L., Gogoll, A., Waldemack, M., Markides, K., Rydin, E., 2005. Sediment depth attenuation of biogenic phosphorus compounds measured by ^{31}P NMR. Environ. Sci. Technol. 39, 867-872.

Ajiboye, B., Akinremi, O.O., Hu, Y., Jürgensen, A., 2008. XANES speciation of phosphorus in organically amended and fertilized vertisol and mollisol. Soil Sci. Soc. Am. J. 72, 1256.

Alewell, C., Huang, J.-W., McLaren, T.I., Huber, L., Bünemann, E.K., 2020. Phosphorus retention in constructed wetlands enhanced by zeolite- and clinopyroxene-dominated lava sand. Hydrol. Process. 35, e14040.

Audette, Y., O'Halloran, I.P., Nowell, P.M., Dyer, R., Kelly, R., Voroney, R.P., 2018. Speciation of phosphorus from agricultural muck soils to stream and lake sediments. J. Environ. Qual. 47, 884-892.

Barrow, N. J., A. Sen, N. Roy, and A. Debnath. 2020. The soil phosphate fallacy. Plant Soil 459, 1-11. doi: 10.1007/s11104-020-04476-6.

Bates, J.A.R., Baker, T.C.N., 1960. Studies on a Nigerian forest soil. II. The distribution of phosphorus in the profile and various soil fractions. J. Soil Sci. 2, 257-265.

Baumann, K., Glaser, K., Mutz, J.E., Karsten, U., MacLennan, A., Hu, Y., Michalik, D., Kruse, J., Eckhardt, K.-U., Schall, P., Leinweber, P., 2017. Biological soil crusts of temperate forests: their role in P cycling. Soil Biol. Biochem. 109, 156–166. https://doi.org/10.1016/j.soilbio.2017.02.011.

Baumann, K., Shaheen, S.M., Hu, Y., Gros, P., Heilmann, E., Morshedizad, M., Wang, J., Wang, S.-L., Rinklebe, J., Leinweber, P., 2020. Speciation and sorption of phosphorus in agricultural soil profiles of redoximorphic character. Environ. Geochem. Health 42, 3231-3246.

Berhongaray, G., Alvarez, R., De Paepe, J., Caride, C., Cantet, R. 2013. Land use effects on soil carbon in the Argentine Pampas. Geoderma 192, 97-110.

Bilotta, G.S., Brazier, R.E., Haygarth, P.M., 2007. Processes affecting transfer of sediments and colloids, with associated phosphorus, from intensively farmed grasslands: erosion. Hydrol. Process. 21, 135-139.

Bowman, R.A., Moir, J.O. 1993. Basic EDTA as an extractant for soil organic phosphorus. Soil Sci. Soc. Am. J. 57, 1516-1518.

Braskerud, B.C., Hartnik, T., Løvstad, Ø. 2005. The effect of the redox-potential on the retention of phosphorus in a small contructed wetland. Water Science & Technology 51, 127-134.

Cade-Menun, B.J., Liu, C.W., Nunlist, R., McColl, J.G., 2002. Soil and litter phosphorus-31 nuclear magnetic resonance spectroscopy. J. Environ. Qual. 31, 457-465.

Cade-Menun, B., Chen, S., Bainard, L.D., St. Luce, M., Hu, Y., Chen, Q., 2021. The influence of long-term N and P fertilization on soil P forms and cycling in a wheat/fallow cropping system. Geoderma 404, 115274.

Calvin, S., 2013. XAFS for everyone. CRC Press p. 427.

Carman, R., Edlund, G., Damberg, C., 2000. Distribution of organic and inorganic phosphorus compounds in marine and lacrustrine sediments: a ^{31}P NMR study. Chem. Geol. 163, 101-114.

Condron, L.M., Newman, S., 2011. Revisiting the fundamentals of phosphorus fractionation of sediments and soils. J. Soils Sediments 11, 830-840.

Correll DL, (1998) Role of phosphorus in the eutrophication of receiving waters: a review. J Environ Qual 27, 261-267.

Cross, A.F., Schlesinger, W.H., 1995. A literature review and evaluation of the Hedley fractionation: applications to the biogeochemical cycle of soil phosphorus in natural ecosystems. Geoderma 64, 197-214.

Doolette, A.L., Smernik, R.J., Dougherty, W.J., 2009. Spiking improved solution phosphorus-31 nuclear magnetic resonance identification of soil phosphorus compounds. Soil Sci. Soc. Am. J. 73, 919–927.

Doolette, A.L., Smernik, R.J., Dougherty, W.J., 2011. Overestimation of the importance of phytate in NaOH-EDTA soil extracts as assessed by ^{31}P NMR analyses. Org. Geochem. 42, 955-964.

Downing, J.A., 2010. Emerging global role of small lakes and ponds: little things mean a lot. Limnetica 29, 9–24.

Favaretto, N., Norton, L.D., Johnston, C.T., Bigham, J., Sperrin, M., 2012. Nitrogen and phosphorus leaching as affected by gypsum amendment and exchangeable calcium and magnesium. Soil Sci. Soc. Am. J. 76, 575-585.

Fiener, P., Auerswald, K., Weigand, S., 2005. Managing erosion and water quality in agricultural watersheds by small detention ponds. Agric. Ecosyst Environ 110, 132–142. https://doi.org/10.1016/j.agee.2005.03.012.

Frankowski, L., Bolałek, J., Szostek, A., 2002. Phosphorus in bottom sediments of Pomeranian Bay (Southern Baltic - Poland). Estuar. Coast. Shelf Sci. 54, 1027-1038.

Frielinghaus, M., Vahrson, W.G., 1998. Soil translocation by water erosion from agricultural cropland into wet depressions (morainic kettle holes). Soil Tillage. Res. 46, 23–30. https://doi.org/10.1016/S0167-1987(98)80104-9.

Giles, C.D., Cade-Menun, B.J., Hill, J.E., 2011. The inositol phosphates in soils and manures: abundance, cycling, and measurement. Can. J. Soil Sci. 91, 397-416.

Gu, C., A. J. Margenot. 2021. Navigating limitaions and opportunities of soil phosphorus fractionation. Plant Soil 459, 13-17.

Gudasz, C., Bastviken, D., Premke, K., Steger, K., Tranvik, L.J., 2012. Constrained microbial pocessing of allochthonous organic carbon in boreal lake sediments. Limnol. Oceanogr. 57, 163-175.

Guo, F., Yost, R.S., Hue, N.V., Evensen, C.I., Silva, J.A., 2000. Changes in phosphorus fractions in soils under intensive plant growth. Soil Sci. Soc. Am. J. 64, 1681. https://doi.org/10.2136/sssaj2000.6451681x.

Guppy, C., 2021. Is soil phosphorus fractionation as valuable as we think? Plant Soil 459, 19-21. doi: 10.1007/s11104-020-04817-5.

Gustafsson, J.P., Braun, S., Tuyishime, J.R.M., Adediran, G.A., Warrinnier, R., Hesterberg, D., 2020. A probabilistic approach to phosphorus speciation of soils using P *K*-edge XANES spectroscopy with linear combination fitting. Soil Syst. 4(2), 26.

Hanley, P.K., Murphy, M., 1966. Phosphorus forms in particle-size separates. Agron. Abstr. American Society of Agronomy, Madison, WI, p. 57.

Harenz, H., 1991. Ursachen der permanenten Überdüngung. Kritische Anmerkungen zu den Düngeempfehlungen für Phosphor. Feldwirtschaft 32, 372-376.

Harrap, F.E.G., 1963. Use of sodium EDTA in the determination of soil organic phosphorus. J. Soil Sci. 14, 82-87.

He, Z., Cade-Menun, B.J., Toor, G.S., Fortuna, A.M., Honeycutt, C.W., Sims, J.T. 2007. Comparison of phosphorus forms in wet and dried animal manures by solution phosphorus-31 nuclear magnetic resonance spectroscopy and enzymatic hydrolysis. J. Environ. Qual. 36, 1086-1095.

Hedley, M.J., Stewart, J.W.B., Chauhan, B.S., 1982. Changes in inorganic and organic soil phosphorus fractions induced by cultivation practices and by laboratory incubations 1. Soil Sci. Soc. Am. J. 46, 970. https://doi.org/10.2136/sssaj1982.03615995004600050017x.

Heinze, S., Ludwig, B., Piepo, H.P., Mikutta, R., Don, A., Wordell-Dietrich, P., Helfrich, M., Hertel, D., Leuschner, C., Kirfel, K., 2018. Factors controlling the variability of organic matter in the top-and subsoil of a sandy Dystic Cambisol under beech forest. Geoderma 311, 37-44.

Holgerson, M.A., Raymond, P.A., 2016. Large contribution to inland water CO_2 and CH_4 emissions from very small ponds. Nat. Geosci. 9, 222-226.

Hu, Y.F., Coulthard, I., Chevrier, D., Wright, G., Igarashi, R., Sitnikov, A., Yates, E.L., Hallin, E.L., Sham, T.K., Reiniger, R., 2010. Preliminary commissioning and performance of the soft X-ray micro-characterization beamline at the Canadian Light Source. AIP Conference Proceedings 1234, 343–346.

Hupfer, M., Rübe, B., Schmieder, P., 2004. Origin and diagenesis of polyphosphate in lake sediments: a ^{31}P NMR study. Limnol. Oceanogr. 49(1), 1-10.

Hupfer, M., Lewandowski, J., 2008. Oxygen controls the phosphorus release from lake sediments - a long-lasting paradigm in limnology. Int. Rev. Hydrobiol. 93, 415–432. https://doi.org/10.1002/iroh.200711054.

Ingall, E.D., Schroeder, P.A., Berner, R.A., 1990. The nature of organic phosphorus in marine sediments: new insights from ^{31}P NMR. Geochim. Cosmochim. Acta 54, 2617-2620.

Irving, G.C.J, Cosgrove, D.J., 1982. The use of gas-liquid chromatography to determine the proportions of inositol isomers present as pentakis- and hexakisphosphates in alkaline extracts of soils. Commun. Soil Sci. Plant Anal. 13 (11), 957-967.

Jarosch, K.A., Doolette, A.L., Smernik, R.J., Tamburini, F., Frossard, E., Bunemann, E.K., 2015. Characterisation of soil organic phosphorus on NaOH-EDTA extracts: a comparison of P-31 NMR spectroscopy and enzyme addition assays. Soil Biol. Biochem. 91, 298-309.

Kalettka, T., Rudat, C., Quast, L., 2001. „Potholes“ in Northeast German agro-landscapes: functions, land use impacts, and protection strategies, in: Tenhunen, J.D., Lenz, R., Hantschel, R. (Eds.), Ecosystem Approaches to Landscape Management in Central Europe. Ecological Studies, Vol. 147. Springer, Berlin, Heidelberg, pp. 291-298.

Kazanjian, G., Flury, S., Attermeyer, K., Kalettka, T., Kleeberg, A., Premke, K., Köhler, J., Hilt, S., 2018. Primary production in nutrient-rich kettle holes and consequences for nutrient and carbon cycling. Hydrobiologia 806, 77–93. https://doi.org/10.1007/s10750-017-3337-6.

Kerr, J.G., Burford, M., Olley, J., Udy, J., 2011. Phosphorus sorption in soils and sediments: implications for phosphate supply to a subtropical river in southeast Queensland, Australia. Biogeochemistry 102, 73-85.

Kirkby, C.A., Kirkegaard, J.A., Richardson, A.E., Wade, L.J., Blanchard, C., Batten, G., 2011 Stable soil organic matter: a comparison of C:N:P:S ratios in Australian and other world soils. Geoderma 163, 197-208.

Klafs, G., Lippert, K., 2000. Landschaftselemente Mecklenburg-Vorpommerns im hundertjährigen Vergleich. –Naturschutzarbeit in Mecklenburg-Vorpommern 43, Güstrow 2, 58-65.

Kleeberg, A., Neyen, M., Schkade, U.K., Kalettka, T., Lischeid, G., 2016. Sediment cores from kettle holes in NE Germany reveal recent impacts of agriculture. Environ. Sci. Pollut. Res. 23, 7409–7424. https://doi.org/10.1007/s11356-015-5989-y.

Koch, M., Kruse, J., Eichler-Löbermann, B., Zimmer, D., Wilbold, S., Leinweber, P., Siebers, N., 2018. Phosphorus stocks and speciation in soil profiles of a long-term fertilizer experiment: evidence from sequential fractionation, P *K*-edge XANES, and 31P NMR spectroscopy. Geoderma 316, 115–126. https://doi.org/10.1016/j.geoderma.2017.12.003.

Kraal, P., Bostick, B.C., Behrends, T., Reichart, G.-J., 2015. Characterization of phosphorus species in sediments from the Arabian Sea oxygen minimum zone: combining sequential extractions and X-ray spectroscopy. Mar. Chem. 168, 1-8.

Kraal, P., Slomp, C.P., 2014. Rapid and extensive alteration of phosphorus speciation during oxic storage of wet sediment samples. PLoS One 9, 1-6.

Kruse, J., Negassa, W., Appathurai, N., Zuin, L., Leinweber, P., 2010. Phosphorus speciation in sequentially extracted agro-industrial by-products: evidence from X-ray absorption near edge structure spectroscopy. J. Environ. Qual. 39, 2179.

Kruse, J., Abraham, M., Amelung, W., Baum, C., Bol, R., Kühn, O., Lewandowski, H., Niederberger, J., Oelmann, Y., Rüger, C., Santner, J., Siebers, M., Siebers, N., Spohn, M., Vestergren, J., Vogts, A., Leinweber, P., 2015. Innovative methods in soil phosphorus research: a review. J. Plant Nutr. Soil Sci. 178, 43-88.

Lekwa, G., Whiteside, E.P., 1986. Coastal plain soils of southern Nigeria: II. Forms of extractable iron, aluminum, and phosphorus. Soil Sci. Soc. Am. J. 50, 160-166.

Li, W., Joshi, S.R., Hou, G., Burdige, D.J., Sparks, D.L., Jaisi, D.P., 2015. Characterizing phosphorus speciation of chesapeake cay sediments using chemical extraction, ^{31}P NMR, and X-ray absorption fine structure spectroscopy. Environ. Sci. Technol. 49, 203-211.

Liang, Z., Elsgaard, L., Haubjerg Nicolaisen, M., Lyhne-Kjærbye, A., Eivind Olesen, J., 2018. Carbon mineralization and microbial activity in agricultural topsoil and subsoil as regulated by root nitrogen and recalcitrant carbon concentrations. Plant Soil 433, 65-82.

Lischeid, G., Kalettka, T., 2012. Grasping the heterogeneity of kettle hole water quality in Northeast Germany. Hydrobiologia 689, 63–77. https://doi.org/10.1007/s10750-011-0764-7.

Łukawska-Matuszewska, K., Bolałek, J., 2008. Spatial distribution of phosphorus forms in seduments in the Gulf of Gdańsk (southern Baltic Sea). Cont. Shelf REs. 28, 977-990.

Luo, L., Ma, Y., Sanders, R.L., Xu, C., Li, J., Myneni, S.C.B., 2017. Phosphorus speciation and transformation in long-term fertilized soil: evidence from chemical fractionation and P *K*-edge XANES spectroscopy. Nutr. Cycl. Agroecosyst. 107, 215-226.

Makarov, M.I., Haumaier, L., Zech, W., 2002. Nature of soil organic phosphorus: an assessment of peak assignments in the diester region of ^{31}P NMR spectra. Soil Biol. Biochem. 34, 1467–1477.

McLaren, T.I., Smernik, R.J., Guppy, C.N., Bell, M.J., Tighe, M.K., 2014. The organic P composition of vertisols as determined by ^{31}P NMR spectroscopy. Soil Sci. Soc. Am. J. 78, 1893-1902.

McLaren, T.I., Guppy, C.N., Tighe, M.K., Schefe, C.R., Flavel, R.J., Cowie, C.C., Tadich, A., 2015a. Validation of soil phosphate removal by alkaline and acidic reagents in a Vertosol soil using XANES spectroscopy. Commun. Soil Sci. Plant Anal. 46, 1998-2017.

McLaren, T.I., Smernik, R.J., McLaughlin, M.J., McBeath, T.M., Kirby, J.K., Simpson, R.J., Guppy, C.N., Doolette, A.L., Richardson, A.E., 2015b. Complex forms of soil organic phosphorus - a major component of soil phosphorus. Environ. Sci. Technol. 49(22), 13238-13245.

McLaren, T.I., Smernik, R.J., Simpson, R.J., McLaughlin, M.J., McBeath, T.M., Guppy, C.N., Richardson, A.E., 2016. The chemical nature of organic phosphorus that accumulated in fertilized soils of a temperate pasture as determined by solution ^{31}P NMR spectroscopy. J. Plant Nutr. Soil Sci. 180(1), 1-12.

McLaren, T.I., Verel, R., Frossard, E., 2019. The structural composition of soil phosphomonoesters as determined by solution 31P NMR spectroscopy and transverse relaxation (T2) experiments. Geoderma 345, 31-37.

McLaren, T.I., Smernik, R.J., McLaughlin, M.J., Doolette, A.L., Richardson, A.E., Frossard, E., 2020. The chemical nature of soil organic phosphorus: a critical review and global compilation of quantitative data. Adv. Agron. 160(1), 51-124.

McLaren, T.I., Verel, R., Frossard, E., 2021. Soil phosphomonoesters in large molecular weight material comprise of multiple components. Soil Sci. Soc. Am. J. 2022, 1-13. https://doi.org/10.1002/saj2.20347.

Meerhoff, M., Jeppesen, E., 2009. Shallow lakes and ponds, in: Likens, G.E. (Ed.), Encyclopedia of inland waters. Elsevier, Amsterdam, pp. 645-655.

Murphy, J, Riley, J.P., 1962. A modified single solution method for the determination of phosphate in natural waters. Anal. Chem. ACTA 27, 31–36. https://doi.org/10.1016/S0003-2670(00)88444-5.

Morshedizad, M., Panten, K., Klysubun, W., Leinweber, P., 2018. Bone char effects on soil:

sequential fractionations and XANES spectroscopy. Soil 4, 23–35. https://doi.org/10.5194/soil-4-23-2018.

Neal, A.L., McLaren, T., Campolino, M.L., Hughes, D., Coelho, A.M., de Paula Lana, U.G., Aparecida Gomes, E., Morais de Sousa, S., 2021. Crop type exerts greater influence upon rhizosphere phosphohydrolase gene abundance and phylogenetic diverstity than phosphorus fertilization. FEMS Microbiology Ecology 97(4), fiab033.

Negassa, W., Leinweber, P., 2009. How does the Hedley sequential phosphorus fractionation reflect impacts of land use and management on soil phosphorus: a review. J. Plant Nutr. Soil Sci. 172, 305-325.

Negassa, W., Kruse, J., Michalik, D., Appathurai, N., Zuin, L., Leinweber, P., 2010. Phosphorus speciation in agro-industrial byproducts: sequential fractionation, solution ^{31}P NMR, and P *K*- and $L_{2,3}$-edge XANES spectroscopy. Einviron. Sci. Technol. 44, 2092-2097.

Nitzsche, K.N., Kalettka, T., Premke, K., Lischeid, G., Gessler, A., Kayler, Z.E. (2017) Land-use and hydroperiod affect kettle hole sediment carbon and nitrogen biogeochemistry. Science of the total environment 574:46-56

Noack, S.R., McLaughlin, M.J., Smernik, R.J., McBeath, T.M., Armstrong, R.D., 2014. Phosphorus speciation in mature wheat and canola plants as affected by phosphorus supply. Plant Soil 378, 125-137.

Oertli, B., Auderset, J.D., Castella, E., Juge, R., Cambin, D., Lachavanne, J.B., 2002. Does size matter? The relationship between pond area and biodiversity. Bio. Conserv. 104, 59-70.

Onandia, G., Lischeid, G., Kalettka, T., Kleeberg, A., Omari, M., Premke, K., Arhonditsis, G.B., 2018. Biogeochemistry of natural ponds in agricultural landscape: lessons learned from modeling a kettle hole in Northeast Germany. Sci. Total Environ. 634, 1615-1630.

Pezzolesi, T.P., Zartman, R.E., Hickey, M.G., 2000. Effects of storage methods on chemical values of waterlogged soils. Wetlands 20, 189-193.

Prietzel, J., Harrington, G., Häusler, W., Heister, K., Werner, F., Klysubun, W. (2015) Reference spectra of important adsorbed organic and inorganic phosphate binding forms for soil P speciation using synchrotron-based *K*-edge XANES spectroscopy. J. Synchrotron Rad. 23, 532-544

Prüter, J., Leipe, T., Michalik, D., Klysubun, W., Leinweber, P., 2020. Phosphorus speciation in sediments from the Baltic Sea, evaluated by a multi-method approach. J. Soils Sediments 20, 1676-1691.

Prüter, J., Hu, Y., Leinweber, P. 2022. Influence of sample pretreatment on P speciation in sediments evaluated with sequential fractionation and P *K*-edge XANES spectroscopy. Commun. in Soil Sci. Plant Anal. 53, 1712-1730.

Ravel, B., Newville, M., 2005. ATHENA, ARTEMIS, HEPHAESTUS: data analysis for X-ray absorption spectroscopy using IFEFFIT. J. Synchrotron Radiat. 12, 537–541. https://doi.org/10.1107/S0909049505012719.

Raymond, P.A., Hartmann, J., Lauerwald, R., Sobek, S., McDonald, C., Hoover, M., Butman, D., Striegl, R., Mayorga, E., Humborg, C., Kortelainen, P., Dürr, H., Meybeck, M., Ciais, P., Guth, P., 2013. Global carbon dioxide emissions from inland waters. Nature 503, 355–359. https://doi.org/10.1038/nature12760.

Reddy, K.R., Kadlec, R.H., Flaig, E., Gale, P.M., 1999. Phosphorus retention in streams and wetlands: a review. Crit. Rev. Environ. Sci. Technol. 29, 83-146.

Reitzel, K., Ahlgren, J., DeBrabandere, H., Waldebäck, M., Gogoll, A., Tranvik, L., Rydin, E., 2007. Degradation rates of organic phosphorus in lake sediments. Biogeochemistry 82, 15-28.

Reusser, J.E., Verel, R., Frossard, E., McLaren, T.I., 2020a. Quantitative measures of myo-IP6 in soil using solution 31P NMR spectroscopy and spectral deconvolution fitting including a broad signal. Environ. Sci: Process. Impacts 22(4), 1084-1094.

Reusser, J.E., Verel, R., Zindel, D., Frossard, E., McLaren, T.I., 2020b. Identification of lower-order inositol phosphates (IP_5 and IP_4) in soil extracts as determined by hypobromite oxidation and solution ^{31}P NMR spectroscopy. Biogeosciences 17, 5079-5095.

Reusser, J.E., Tamburini, F., Neal, A.L., Verel, R., Frossard, E., McLaren, T.I., 2022. The molecular size continuum of soil organic phosphorus and its chemical associations. Geoderma 412, 115716.

Reverey, F., Ganzert, L., Lischeid, G., Ulrich, A., Premke, K., Grossart, H.-P., 2018. Dry-wet cycles of kettle hole sediments leave a microbial and biogeochemical legacy. Sci. Total Environ. 627. 985–996. https://doi.org/10.1016/j.scitotenv.2018.01.220.

Reverey, F., Grossart, H.-P., Premke, K., Lischeid, G., 2016 Carbon and nutrient cycling in kettle hole sediments depending on hydrological dynamics: a review. Hydrobiologia

775, 1–20. https://doi.org/10.1007/s10750-016-2715-9.
Richardson, A.E., Hocking, P.J., Simpson, R.J., George, T.S., 2009. Plant mechanisms to optimise access to soil phosphorus. Crop and Pasture Science 60(2), 124-143.
Schmieder, F., Bergström, L., Riddle, M., Gustafsson, J.-P., Klysubun, W., Zehetner, F., Condron, L., Kirchmann, H., 2018. Phosphorus speciation in a long-term manure-amended soil profile - evidence from wet chemical extaction, ^{31}P-NMR and P *K*-edge XANES spectroscopy. Geoderma 322, 19-27.
Schmieder, F., Gustafsson, J.P., Klysubun, W., Zehetner, F., Riddle, M., Kirchmann, H., Bergström, L., 2020. Phosphorus speciation in cultivated organic soils revealed by P *K*-edge XANES spectroscopy. J. Plant Nutr. Soil Sci. 183, 367-381.
Schönbrunner, I.M., Preiner, S., Hein, T., 2012. Impact of drying and re-flooding of sediment on phosphorus dynamics of river-floodplain systems. Sci. Total Environ. 432, 329–337. https://doi.org/10.1016/j.scitotenv.2012.06.025.
Schrumpf, M., Kaiser, K., Guggenberger, G., Persson, T., Kögel-Knabner, I., Schulze, E.D., 2013. Storage and stability of organic carbon in soils als related to depth, occlusion within aggregates, and attachment to minerals. Biogeosciences 10, 1675-1691.
Serrano, L., Reina, M., Quintana, X.D., Romo, S., Olmo, C., Soria, J.M., Blanco, S., Fernández-Aláez, C., Fernández-Aláez, M., Caria, M.C., Bagella, S., Kalettka, T., Pätzig, M., 2017. A new tool for the assessment of severe anthropogenic eutrophication in small shallow water bodies. Ecol. Indic. 76, 324-334.
Sims, J.T., Pierzynski, G.M., 2005. Chemistry of phosphorus in soils, in: Tabatabai, M.A., Sparks, D.L., (Eds.), Chemical Processes in Soils. SSSA, Madison, WI, USA, pp. 151-192.
Søndergaard, M., Jensen, J.P., Jeppesen, E., 2003. Role of sediment and internal loading of phosphorus in shallow lakes. Hydrobiologia 506–509, 135–145. https://doi.org/10.1023/B:HYDR.0000008611.12704.dd.
Suzumura, M., Kamatani, A., 1993. Isolation and determination of inositol hexaphosphate in sediments from Tokyo Bay. Geochim. Cosmochim. Acta 57, 2197-2202.
Spain, A.V., Tibbett, M., Ridd, M., McLaren, T.I., 2018. Phosphorus dynamics in a tropical forest soil restored after strip mining. Plant Soil 427, 105–123.
Tiessen, H., Moir, J.O., 1993. Characterization of available P by sequential extraction, in: Carter, M.R. (Ed.), Soil sampling and methods of analysis. Lewis Publishers, Boca Raton, Florida, USA, pp. 75-86.
Turner, B.L., Mahieu, N., Condron, L.M., 2003a. Phosphorus-31 nuclear magnetic resonance spectral assignments of phosphorus compounds in soil NaOH-EDTA extracts. Soil Sci. Soc. Am. J., 67, 497–510.
Turner, B.L., Cade-Menun, B.J., Westerman, D.T., 2003b. Organic phosphorus composition and potential bioavailability in semi-arid arable soils of the western united states. Soil Sci. Soc. Am. J. 67, 1168-1179.
Turner, B.L., Cade-Menun, B.J., Condron, L.M., Newman, S., 2005. Extraction of soil organic phosphorus. Talanta 66, 294-306.
Turner, B.L., 2008. Soil organic phosphorus in tropical forests: an assessment of the NaOH-EDTA extraction procedure for quantitative analysis by solution ^{31}P NMR spectroscopy. Eur. J. Soil Sci. 59, 453-466.
Vasić, F., Paul, C., Strauss, V., Helming, K., 2020. Ecosystem services of kettle holes in agricultural landscapes. Agronomy 10, 1326.
Vestergren, J., Vincent, A.G., Jansson, M., Persson, P., Ilstedt, U., Gröbner, G., Giesler, R., Schleucher, J., 2012. High-resolution characterization of organic phosphorus in soil extracts using 2D ^{1}H–^{31}P NMR correlation spectroscopy. Environ. Sci. Technol. 46, 3950–3956.
Vincent, A.G., Vestergren, J., Gröbner, G., Persson, P., Schleucher, J., Giesler, R., 2013. Soil organic phosphorus transformations in a boreal forest chronosequence. Plant Soil 367, 149–162.
Vold, R.L., Waugh, J.S., Klein, M.P., Phelps, D.E., 1968. Measurement of spin relaxation in complex systems. J. Chem. Phys. 48, 3831–3832.
Walker, T.W., Syers, J.K., 1976. The fate of phosphorus during pedogenesis. Geoderma 15, 1–19. https://doi.org/10.1016/0016-7061(76)90066-5.
Wang, L., Amelung, W., Willbold, S., 2021. 18O isotope labeling combined with 31P nuclear magnetic resonance spectroscopy for accurate quantification of hydrolyzable phosphorus species in environmental samples. Analytical Chemistry 93, 2018-2025.
Watson, S.J., Cade-Menun, B.J., Needoba, J.A., Peterson, T.D., 2018. Phosphorus forms in

sediments of a river-dominated estuary. Front. Mar. Sci. 5, 302.
Watson, F.T., Smernik, R.J., Doolette, A.L., Mosley, L.M., 2019. Phosphorus speciation and dynamics in river sediments, floodplain soils and leaf litter from the lower Murray river region. Mar. Freshw. Res. 70(11), 1522-1532.
Williams, P., Whitfield, M., Biggs, J., Bray, S., Fox, G., Nicolet, P., Sear, D., 2003. Comparative biodiversity of rivers, streams, ditches and ponds in an agricultural landscape in Southern England. Biol. Conserv. 115, 329-341.
Wu, Y.H., Prietzel, J., Zhou, J., Bing, H., Luo, J., Yu, D., Sun, S., Liang, J., Sun, H., 2014. Soil phosphorus bioavailability assessed by XANES and Hedley sequential fractionation technique in a glacier foreland chronosequence in Gongga Mountain, Southwestern China. Sci. China Earth Sci. 57, 1860–1868. https://doi.org/10.1007/s11430-013-4741-z.
Zak, D., Gelbrecht, J., Steinberg, C.E.W., 2004. Phosphorus retention at the redox interface of peatlands adjacent to surface waters in Northeast Germany. Biogeochemistry 70, 357–368. https://doi.org/10.1007/s10533-003-0895-7.
Zhang, W., Shan, B., Zhang, H., Tang, W., 2013. Assessment of preparation methods of organic phosphorus analysis in phosphorus-polluted Fe/Al-rich Haihe river sediments using solution ^{31}P-NMR. PLOS ONE 8(10), e76525.
Zhang, R., Chen, J., Wang, L., Wu, F., 2017. Characteristics of phosphorus components in surface sediments from a chinese shallo eutrophic lake (lake Taihu): new insights from chemical extraction and ^{31}P NMR spectroscopy. Environ. Sci. Pollut. Res. 24, 23518-23527.

4 Characterization of phosphate compounds along a catena from arable and wetland soil to sediments in a Baltic Sea lagoon

Julia Prüter[1], Rhena Schumann[2], Wantana Klysubun[3], Peter Leinweber[1]

[1]*University of Rostock, Soil Science, Justus-von-Liebig Weg 6, 18051 Rostock, Germany*

[2]*University of Rostock, Department of Applied Ecology, Albert-Einstein-Straße 3, 18051 Rostock, Germany*

[3]*Synchrotron Light Research Institute, Muang District, 111 Moo 6 University Avenue, Nakhon Ratchasima 3000, Thailand*

Submitted to

Soil Systems

4.1. Abstract

Phosphorus (P) is an indispensable nutrient for arable crops but at the same time contributes to excessive eutrophication in aquatic ecosystems. Knowledge about P is essential to assess possible risks of P transport towards vulnerable aquatic ecosystems. Our objective was to characterize P along a catena from arable and wetland soils towards aquatic sediments of a shallow lagoon of the Baltic Sea. Characterization of P in soil and sediment samples included a modified sequential P fractionation and P *K*-edge X-ray absorption near edge structure (XANES) spectroscopy. Concentrations of total P ranged from 390 to 430 mg kg^{-1} in the arable soils, from 728 to 2258 mg kg^{-1} in wetland soils and from 132 to 602 mg kg^{-1} in lagoon sediments. Generally, two sinks for P were revealed along the catena. The wetland soil trapped especially moderately stable P, Al-P and molybdate-unreactive P (MUP), most likely organically bound phosphates. Sediments at the deepest position of the catena acted as sink for, especially, MUP compounds among the lagoon sediments. Thus, wetlands formed by reed belts can help to prevent direct transfer of P from arable soils to adjacent waters and deeper basins, and help to avoid excessive eutrophication in shallow aquatic ecosystems.

Keywords: phosphorus; gradient; sequential fractionation; XANES spectroscopy

4.2. Introduction

Coastal wetlands, as open systems, link terrestrial and aquatic ecosystems and play an important role in the environment as habitats for fish and birds, for erosion protection and especially nutrient regulation and biogeochemical cycling of nutrients in nearby coastal sites or adjacent land (Andreu et al. 2016; Perillo et al. 2009; Reddy et al. 1999). Phosphorus (P) is an essential element for all living organisms, in coastal wetlands as well as in terrestrial ecosystems, as it contributes in arable farming to crop yields, but at the same time it has been identified as one of the major factors responsible for eutrophication in wetlands and aquatic ecosystems (Reddy et al. 1999; Correll 1998). Eutrophication causes various negative environmental impacts such as excessive algal blooms, water oxygen depletion and the release of hazardous toxins (Corell 1998; Bonsdorff et al. 1997). Since P from agricultural fertilization is primarily conserved in soils and can be transported from terrestrial to aquatic ecosystems, it is important to develop sustainable agricultural practices and similarly ensure the protection of the environment (Sims and Pierzynski 2005).

The German coast of the Baltic Sea is characterized by large coastal wetlands adjoining arable soils on the one side and aquatic lagoon systems on the other side (Karstens et al. 2015). Thus, there is a high probability of nutrients and especially P from fertilized arable soils to be transported into the adjacent wetland soils, water bodies and sediments, but these expected transfer processes have not been disclosed in detail. Generally, the speciation of P affects the risk of P transportation to surface waters (Weyers et al. 2016) as well as P availability for plant uptake. Thus, knowledge about the P speciation in soils and transformation processes towards

the coast are essential to assess possible risks of P transport into aquatic ecosystems and to develop measures preventing excessive P inputs to vulnerable water bodies.

Many previous studies have investigated chemical P composition in agricultural soils (e.g. Koch et al. 2018; Schmieder et al. 2020; Turner 2008) sediments (e.g. Frankowski et al. 2002; Kraal and Slomp 2014; Łukawska-Matuszewska and Bolałek 2008]) and P in the water column (e.g. Gunnars and Blomqvist 1997; Xie et al. 2003; Zwolsman 1994). Nonetheless, in-depth knowledge about P speciation and its transport from soils to sediments is scarce (Iglesias et al. 2011). Furthermore, few studies investigated the P speciation of samples at the fluent boundaries between terrestrial soils and sediments in aquatic environments along sequences. For instance, there were reported accumulations of organic P (P_o) in muck soils and fractions of inorganic P (P_i) in adjacent river/lake sediments in Ontario, Canada (Audette et al. 2018). Another investigation of a transect from arable soils in northern Germany towards sediments of the central Baltic Sea revealed a similar distribution of P_i and P_o fractions in the soils and sediments (Prüter et al. 2020). Furthermore, an increase in the proportion of stable P fractions (i.e., H_2SO_4-P and residual-P) compared to iron-associated P was reported in the same study with increasing distance from the coastline along a transect of Baltic Sea sediments with a length of about 600.000 m (Prüter et al. 2020). However, it is unknown if similar, or generally which P transformation processes occur at a smaller scale from coastal arable and wetland soils to adjacent sediments from a shallow Bodden of the Baltic Sea with a transect length of about 700 m.

The aim of this study was to characterize the P compounds along a sequence from arable and wetland soils towards aquatic sediments from a shallow lagoon of the Baltic Sea to fill in the knowledge the gap in the course of this mid-scale spatial expansion. We want to confirm or question the already disclosed transition of labile Al- and Fe-associated P species in terrestrial soils to more stable and Ca-bound P in aquatic sediments for this specific geomorphological setting.

4.3. Material and Methods

4.3.1. Sampling area, soil and sediment collection

Sampling of the soils and sediments took place in summer 2018 near the village Dabitz in Mecklenburg-Western Pomerania in the area of Darss-Zingst Bodden Chain, a lagoon system at the Southern Baltic Sea in Germany. The transect expands from N54°22'08.00" E12°48'08.00" to N54°22'09.31" E12°48'33.50". The study site includes an arable field cropped with barley, an adjoining coastal wetland covered by *Phragmites australis* and a shallow water body with a mean water depth of 2 m. For more details, such as a description of vegetation, water and sediment characteristics of the wetland see an earlier investigation (Karstens et al. 2016).

The soil samples and sediment cores were taken each at two depths along a transect from an arable field (A1, A2) continued to the directly bordering wetland (W1, W2) and the adjacent Bodden sediments at three different water depths (S1, S2; S3, S4; and S5, S6). The sample

description and labeling is compiled in Table 1, and Figure 1 shows a schematic drawing of the sampling strategy. The total distance between the first and terminal sample of the transect is about 700 m. Two to three single subsamples were taken at an area of approximately one m^2 and merged to one mixed sample for each soil and sediment sample location and depth. Afterwards, we merged samples with similar results for basic parameters such as water content, pH, and C, N and S contents and thus, we reduced effects of small-scale heterogeneity. Furthermore, in a recent study, examining sample pretreatments of soils and sediments, we concluded that an identical pretreatment of the soils and sediments resulted in no fundamental changes of their P speciation (Prüter et al. 2022). For this reason, all soil and sediment samples of the present investigation were dried at 40°C, sieved < 2 mm and finely ground in a mortar mill prior to further analyses.

The soil texture of the cropland at the study site was characterized as loamy sand (Karstens et al. 2016) and the sediment textures of the adjacent Bodden sediments were fine to medium sands (Bitschofsky et al. 2015).

Table 4-1 Label, sample type, origin, sampling depth and coordinates of the collected soil and sediment samples.

Label	Sample type	Origin	Samling depth in cm	Coordinates
A1	soil	arable field	0 - 30	N 54° 22' 08.00"
A2	soil	arable field	30 - 60	E 12° 48' 08.00"
W1	soil	wetland	0 - 10	N 54° 22' 08.30"
W2	soil	wetland	30 - 50	E 12° 48' 12.60"
S1	sediment	water depth 52 cm	0 - 5	N 54° 22' 09.00"
S2	sediment	water depth 52 cm	5 - 10	E 12° 48' 17.60"
S3	sediment	water depth 63 cm	0 - 5	N 54° 22' 09.20"
S4	sediment	water depth 63 cm	5 - 10	E 12° 48' 20.00"
S5	sediment	water depth 230 cm	0 - 5	N 54° 22' 09.31"
S6	sediment	water depth 230 cm	5 - 10	E 12° 48' 33.50"

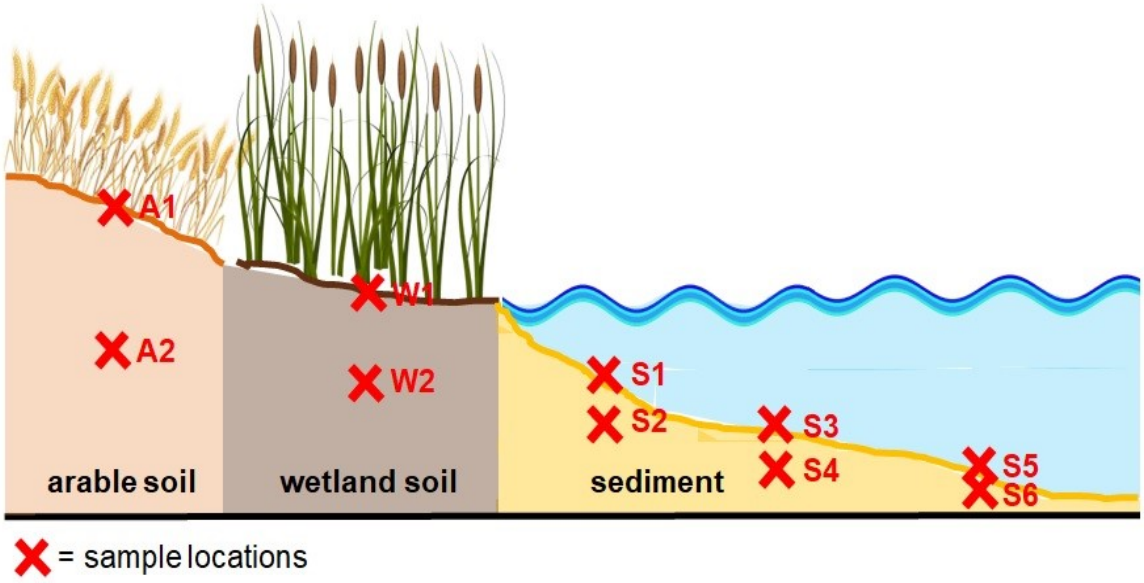

Figure 4-1 Schematic illustration of the soil and sediment sampling spots at the study site in Dabitz.

4.3.2. Determination of water content and the total concentrations of C, N, S, $CaCO_3$, P, Ca, Mg, Al, Fe

Water contents were determined by sample weighing before and after drying at 105°C. The contents of total carbon (C), nitrogen (N) and sulphur (S) were obtained by dry combustion of finely ground soil and sediment material using an elemental analyzer (VARIO EL, Elementar Analysensysteme GmbH, Hanau, Germany). Percentages of soil and sediment calcium carbonate ($CaCO_3$) were determined using a Scheibler calcimeter by calculating the carbon dioxide (CO_2) volume resulting from the reaction of hydrochloric acid (HCl) with sample $CaCO_3$. Elemental concentrations of total P (P_t), calcium (Ca), magnesium (Mg), aluminum (Al), iron (Fe) and zinc (Zn) were determined by microwave-assisted digestion (Mars Xpress CEM GmbH Kamp-Linfort, Germany) of ≤ 50 mg soil or sediment with *aqua regia* consisting of 2 mL nitric acid (HNO_3) and 6 mL HCl (ISO standard 11466). Element concentrations in digests were determined with an inductively coupled plasma-optical emission spectrometer (ICP-OES) at wavelengths of 214,914 nm for P, 317.933 nm for Ca, 258,213 nm for Mg, 396,153 nm for Al and 238.204 nm for Fe.

4.3.3. Sequential P fractionation

A slightly modified sequential P-fractionation method was used to extract different P fractions from soil and sediment (Hedley et al. 1982; Tiessen and Moir 1993). About 0.42 g finely-ground soil or sediment was weighed into 50 mL centrifuge tubes. Samples were shaken for 18 h at room temperature followed by centrifugation at 4.000 *g* for 20 min, and decanted. Chemical P fractionation included the following extraction steps: (1) H_2O, (2) anion resin strips (55164 2S, BDH Laboratory Supplies, Poole, England), (3) 0.5 M $NaHCO_3$, (4) 0.1 M NaOH and (5) 1 M H_2SO_4. In the 2nd extraction step, P was removed from the resin using 1 M HCl. The P fractions

were interpreted as follows: water (H_2O-P) and resin P (resin-P) representing the easily exchangeable and mobile P, molybdate-reactive ($NaHCO_3$-P_{mr}) and molybdate-unreactive ($NaHCO_3$-P_{mu}) bicarbonate P representing labile P_{mr} and P_{mu} weakly adsorbed to mineral surfaces as well as microbial P, molybdate-reactive (NaOH-P_{mr}) and molybdate-unreactive (NaOH-P_{mu}) sodium hydroxide P representing moderately labile P_{mr} and P_{mu} adsorbed to Al- and Fe-oxide minerals and P in humic substances. The H_2SO_4-P fraction represents insoluble P associated with Ca and Mg minerals and apatite [24]. P_t in the different extracts was measured in the decanted supernatants using an ICP-OES while the remaining sediment pellet was used for the next extraction step. Molybdate-reactive P (P_{mr}) concentrations in the extracts were determined colorimetrically with the molybdate blue method (Murphy and Riley 1962). The concentration of molybdate-unreactive P (P_{mu}) was estimated by subtracting P_{mr} from P_t. The concentration of non-extracted P (Residual-P) was calculated as the difference between the sum of the P fractions and the P_t concentration determined after digestion with *aqua regia*.

The application of the fractionation scheme, which originally has been developed for estimating the plant availability of P in amended soils, to sediments is a challenge, since different fractionation schemes have been developed and applied for sediments (e.g. Psenner 1988). In the sediment method, samples are sequentially extracted with NH_4Cl, dithionite-bicarbonate, NaOH and HCl. It is similar to the soil fractionation in starting with mild extractant to remove loosely sorbed P (NH_4Cl vs. H_2O and anion exchange resin), P bound in humic substances (NaOH) and finalizing with the removal of relatively stable Ca-bound P by strong mineral acid (concentrated HCl or H_2SO_4). The major difference is the reduction of Fe-oxides by dithionite-citrate-bicarbonate in the sediment fractionation which is not involved in the soil fractionation. Thus, the latter fractionation does not allow estimating the amount of Fe-bound P, which, however, can be derived from P *K*-edge XANES in a multimethod approach. Thus, in summary, the P fractionation schemes for soils and sediments are expected to yield similar results for the proportions of the most labile and most stable P fractions, and may be replaced by each other in this respect.

4.3.4.P K-*edge XANES analysis*

The P *K*-edge XANES spectra were recorded at the Synchrotron Light Research Institute (SLRI) in Nakhon 65 Ratchasima, Thailand on the beamline 8 (BL8) of the electron storage ring with a covering photon energy from 1.25 to 10 KeV, electron energy operated at 1.2 GeV and a beam current of 80-150 mA (Klysubun et al. 2012). The XANES data were collected from dry and finely-ground samples thinly spread on P-free kapton tape (Lanmar Inc. Northbrook, IL, USA) attached to a plastic sample holder. Data collection was operated in standard conditions with energy calibration by standard elemental P and allocating the reference energy (E_0) at 2145.5 eV using the maximum peak of the first derivative spectrum. All spectra were recorded at photon energies between 2045.5 and 2495.5 eV in step sizes of 5 eV (2045.5 to 2105.5 eV and 2245.5 to 2495.5 eV), 1 eV (2105.5 to 2135.5 eV and 2195.5 to 2245.5 eV) and 0.25 eV (2135.5 to 2195.5 eV) with a 13-channel germanium detector in fluorescence mode. Two to four scans were collected and averaged for each sample.

All P *K*-edge XANES spectra were normalized, and the replicates were merged. Linear combination fitting (LCF) was performed using the ATHENA software package (Ravel and Newville 2005) in the energy range between -20 eV and +30 eV of E_0. The XANES spectral data were baseline corrected in the pre-edge region between 2115 and 2145 eV and normalized in the post-edge region of 2190-2215 eV. The same ranges were used for the reference P *K*-edge XANES spectra to achieve consistency in the following fitting analysis (Prietzel et al. 2016). To achieve the best compatible set of references with each specified sample spectrum, LCF analysis was performed using the combinatorics function of ATHENA software to attain all possible binary to quaternary combinations between all 19 P reference spectra in which the share of each compound was ≥ 10%. The following set of reference P *K*-edge XANES spectra, all recorded in SLRI under the same adjustments (Prietzel et al. 2016; Werner and Prietzel 2015), were used for fitting and calculations: Ca, Al and Fe phytate, noncrystalline and crystalline $AlPO_4$, noncrystalline and crystalline $FePO_4 \cdot 2H_2O$, Ca 5-hydroxyapatite ($Ca_5(OH)(PO_4)_3$), inositol hexakisphosphate/phytate (IHP), ferrihydrite–IHP, montmorillonite–Al–IHP, soil organic matter (OM) Al–IHP (SOM–Al–IHP), ferrihydrite–orthophosphate, montmorillonite–Al–orthophosphate, SOM–Al–orthophosphate, boehmite–IHP, boehmite–10 orthophosphate, $CaHPO_4$, $Ca(H_2PO_4)_2$ and $MgHPO_4$. The *R*-factor values were used as goodness-of-fit criteria and significant differences between fits were evaluated using the Hamilton test ($p < 0.05$) (Calvin 2013) with the number of independent data points calculated by ATHENA, estimated as data range divided by core-hole lifetime broadening. The best fits of P reference compound combinations were considered as the most probable P species in the material. If *R* factors of fits with the same number of reference compounds were not significantly different from each other according to the Hamilton test, fit proportions were averaged. For this reason, averaged proportions of some reference compounds can be ≤ 10%.

4.3.5. Statistical analysis

Data analysis was performed using open-source statistical software R (version 3.6.3). Data of elemental concentrations and sequential P fractionation were tested for significant differences by the Student *t* test (**P* <0.05, ***P* < 0.01, ****P* < 0.001).

4.4. Results

4.4.1. Soil and sediment characteristics

The water contents of the arable and wetland soils and of the sediments differed greatly. The arable soil samples A1 and A2 contained less than 10% (*w/w*) water while the wetland soils W1 and W2 contained up to 62% (*w/w*) water. The sediments S1 to S4 had about 20% (*w/w*) water and maximum water contents of up to 75% were measured in the sediments S5 and S6 (Table 2). $CaCO_3$ has been found in the arable soil samples A1 (6%) and A2 (14%). The wetland soil and the sediments did not contain measurable amounts of $CaCO_3$.

Concentrations of total C ranged from 14 500 to 136 900 mg kg^{-1} in the soil and from 2 500 to 67 000 mg kg^{-1} in the sediment samples (Table 2). Whereas the C contents were extremely low

in the sediments S1 to S4, they were much higher contents in the sediments S5 and S6 from a water depth of 230 cm. Average C percentages were more than two times higher in the arable and wetland soils compared to the sediments. Maximum N concentrations were determined in the soil W1 (12 500 mg kg^{-1}) and in the sediments S5 (7 500 mg kg^{-1}) and S6 (6 200 mg kg^{-1}). Average N concentrations again were about two times higher in the soils compared to the sediments. Highest S concentrations were present in the sediments S5 (15 600 mg kg^{-1}) and S6 (14 700 mg kg^{-1}) while all other sediment and soil samples had < 4 000 mg kg^{-1} S.

The order of concentrations of P agreed with C and N concentrations of the soils and sediments (Table 2). The soil W1 had the maximum concentration of 2258 mg P kg^{-1}. Minimum concentrations of 130 to 140 mg P kg^{-1} were present in the sediments S1 to S4 with no significant differences, whereas sediments S5 and S6 again had higher P concentrations of 602 and 551 mg kg^{-1}. On the average, P concentrations were more than three times higher in the arable and wetland soils than in the sediments. The highest Ca concentration was present in the soil A2 and, overall, the average Ca concentrations were about 14 times higher in the soils compared to the sediments. For the concentrations of the elements Mg, Al and Fe there were also differences between the soils and sediments but not as clear as for Ca. The arable and wetland soils contained averagely about 1.8 to 3.3 times more Mg, Al and Fe than the sediments.

Table 4-2 Average proportions of water in % and elemental concentrations of carbon (C), nitrogen (N) and sulphur (S); *n* = 2 and of phosphorus (P), calcium (Ca), magnesium (Mg), aluminum (Al), and iron (Fe) in mg kg^{-1} and their ratios (C/P, P/Ca, P/Mg, P/Al, P/Fe) determined by ICP-OES; *n* = 3 in the upper and lower soil and sediment samples. Significant differences at 5% probability level between samples are designated by different letters (a, b, c, d, e, f).

Sample	Water content	$CaCO_3$	C	N	S	P	Ca	P/Ca	Mg	P/Mg	Al	P/Al	Fe	P/Fe
	%	%	mg kg^{-1}				mg kg^{-1}		mg kg^{-1}		mg kg^{-1}		mg kg^{-1}	
A1	5	6	14583	842	375	430^{e}	27835^{b}	0.02	2974^{c}	0.14	10982^{b}	0.04	13738^{e}	0.03
A2	9	14	24400	272	327	390^{e}	72935^{a}	0.01	4134^{b}	0.09	10768^{bc}	0.04	13603^{e}	0.03
W1	62	0	136917	12580	3648	2258^{a}	6944^{c}	0.33	4869^{a}	0.46	18380^{a}	0.12	34382^{a}	0.07
W2	46	0	48683	4578	1963	728^{b}	3589^{d}	0.20	3002^{c}	0.24	11344^{b}	0.06	15056^{d}	0.05
S1	20	0	2600	345	525	140^{f}	909^{e}	0.15	325^{d}	0.43	737^{d}	0.19	861^{f}	0.16
S2	20	0	2900	375	560	137^{f}	1173^{e}	0.12	404^{d}	0.34	913^{d}	0.15	1104^{f}	0.12
S3	21	0	2550	340	475	132^{f}	639^{e}	0.21	289^{d}	0.46	681^{d}	0.19	847^{f}	0.16
S4	20	0	2450	315	450	135^{f}	445^{e}	0.30	285^{d}	0.47	750^{d}	0.18	1018^{f}	0.13
S5	65	0	67050	7475	15650	602^{c}	4839^{d}	0.12	4830^{a}	0.12	9940^{c}	0.06	17637^{c}	0.03
S6	75	0	59550	6190	14740	551^{d}	3652^{d}	0.15	4751^{a}	0.12	10489^{bc}	0.05	18452^{b}	0.03

4.4.2. Sequentially extracted P fractions

The sequential chemical fractionation extracted on average 89% of P_t across all samples (Table 3). With the exception of W1, H_2SO_4-P_{mr} was generally the largest fraction, ranging from 25% to 67% of P_t in the soil and sediment samples. The maximum amount of P in the wetland soil W1 was present in the fraction of residual-P. In most sequentially extracted fractions, proportions of P_{mr} were higher than P_{mu} except for the sediments S5 and S6 in the fractions of $NaHCO_3$ and NaOH, and for the soil W2 in the fraction of NaOH, where P_{mu} was predominant. Furthermore, it is noticeable that although the absolute concentrations of P in the easily exchangeable and plant-available fractions of H_2O-P and resin-P were rather low in the sediments S1 to S4, their relative amounts of 7% to 24% of P_t were higher than in the soils and deeper sediments. There were no significant differences among the concentrations of $NaHCO_3$-P_{mr} among the soils and sediments except for W1, in which the maximum concentration of 275 mg P kg^{-1} was determined. In the fraction of NaOH-P_{mr} there were also few significant differences between the samples. Exclusively the upper and lower wetland soil samples W1 and W2 contained significantly more NaOH-P_{mr} than the other soils and sediments.

Table 4-3 Concentrations (mg kg^{-1}) and percentages (%) of the sequentially extracted molybdate-reactive (P_{mr}) and molybdate-unreactive (P_{mu}) P fractions H_2O-P, resin-P, $NaHCO_3$-P, NaOH-P, H_2SO_4-P, and residual-P, of total P (P_t) and the sums of P_{mr} and P_{mu} determined in the soil and sediment samples. Significant differences at 5% probability level between samples are designated by different letters (a, b, c, d, e, f), *n* = 3.

Sample	H_2O-P_{mr}		H_2O-P_{mu}		Resin-P_{mr}		Resin-P_{mu}		$NaHCO_3$-P_{mr}		$NaHCO_3$-P_{mu}		NaOH-P_{mr}		NaOH-P_{mu}		H_2SO_4-P_{mr}		H_2SO_4-P_{mu}		Residual-P	
	mg kg^{-1}	(%)	mg kg^{-1}	(%)	mg kg^{-1}	(%)	mg kg^{-1}	(%)	mg kg^{-1}	(%)	mg kg^{-1}	(%)	mg kg^{-1}	(%)	mg kg^{-1}	(%)	mg kg^{-1}	(%)	mg kg^{-1}	(%)	mg kg^{-1}	(%)
A1	13^{c}	(3)	2^{c}	(0)	18^{de}	(4)	1^{a}	(0)	15^{b}	(3)	13^{de}	(3)	12^{c}	(3)	14^{b}	(3)	222^{b}	(52)	37^{ab}	(9)	83^{bcd}	(19)
A2	9^{c}	(2)	0^{c}	(0)	11^{e}	(3)	0^{a}	(0)	47^{b}	(12)	2^{e}	(1)	9^{c}	(2)	0^{b}	(0)	261^{b}	(67)	29^{ab}	(7)	22^{cd}	(6)
W1	26^{a}	(1)	23^{a}	(1)	143^{a}	(6)	6^{a}	(0)	275^{a}	(12)	162^{a}	(7)	443^{a}	(20)	156^{a}	(7)	401^{a}	(18)	116^{a}	(5)	505^{a}	(22)
W2	26^{a}	(4)	8^{bc}	(1)	40^{bcd}	(5)	0^{a}	(0)	50^{b}	(7)	51^{b}	(7)	75^{b}	(10)	92^{ab}	(13)	183^{bc}	(25)	55^{ab}	(8)	149^{b}	(20)
S1	14^{c}	(10)	7^{bc}	(5)	26^{cde}	(18)	6^{a}	(4)	20^{b}	(14)	1^{e}	(1)	9^{c}	(6)	0^{b}	(0)	49^{cd}	(35)	14^{b}	(10)	0^{d}	(0)
S2	13^{c}	(9)	10^{bc}	(7)	33^{cde}	(24)	4^{a}	(3)	15^{b}	(11)	1^{e}	(1)	9^{c}	(6)	0^{b}	(0)	53^{cd}	(39)	15^{b}	(11)	0^{d}	(0)
S3	27^{a}	(21)	16^{ab}	(12)	18^{de}	(14)	0^{a}	(0)	7^{b}	(5)	1^{e}	(1)	9^{c}	(7)	0^{b}	(0)	44^{d}	(34)	10^{b}	(8)	0^{d}	(0)
S4	19^{b}	(14)	10^{bc}	(7)	17^{de}	(13)	0^{a}	(0)	15^{b}	(11)	1^{e}	(1)	11^{c}	(8)	0^{b}	(0)	60^{cd}	(45)	11^{b}	(8)	0^{d}	(0)
S5	20^{b}	(3)	15^{ab}	(2)	57^{b}	(9)	4^{a}	(1)	8^{b}	(1)	42^{bc}	(7)	18^{c}	(3)	57^{ab}	(9)	265^{b}	(44)	0^{b}	(0)	115^{bc}	(19)
S6	20^{b}	(4)	17^{ab}	(3)	47^{bc}	(9)	3^{a}	(1)	3^{b}	(1)	27^{cd}	(5)	12^{c}	(2)	35^{b}	(6)	199^{b}	(36)	77^{ab}	(14)	111^{bcd}	(20)

Sample	P_t	Sum P_{mr}		Sum P_{mu}	
	mg kg^{-1}	mg kg^{-1}	(%)	mg kg^{-1}	(%)
A1	430^{e}	280	(65)	67	(16)
A2	390^{e}	337	(86)	31	(8)
W1	2258^{a}	1288	(57)	464	(21)
W2	728^{b}	374	(51)	206	(28)
S1	140^{f}	118	(81)	28	(19)
S2	137^{f}	122	(81)	29	(19)
S3	132^{f}	105	(79)	28	(21)
S4	135^{f}	123	(85)	22	(15)
S5	602^{c}	368	(61)	119	(20)
S6	551^{d}	282	(51)	158	(29)

4.4.3. Bulk P K-edge XANES spectra

All XANES spectra were characterized by an intense white line peak at around 2152 eV and varying pre- and post-edge features. The *R* factors from LCF were 0.0033 to 0.0161 for the soil samples and 0.0022 to 0.0095 for the sediment samples (all *R* factors are compiled in Table A1 of supplementary data). The P speciations of all samples based on XANES spectra and LCF are displayed in Figure 2 (corresponding XANES spectra in Figure A1 of supplementary data). Proportions of single Fe-, Al- and Ca-P compounds were summed to compound groups of Fe-P, Al-P, Ca-P, Mg-P and P_o. Average proportions of summed Ca-P compounds were lower in the arable and wetland soils (38%) compared to the sediments (89%). All arable soil and sediment samples were dominated by Ca-associated P compounds. In the upper wetland soil W1 exclusively Al-P compounds were assigned by XANES spectroscopy and in the corresponding subsoil sample W2, Al-, Fe-P and P_o compounds were predominant. Proportions of P_o compounds were exclusively present in A1, W2 and S5 in considerable amounts.

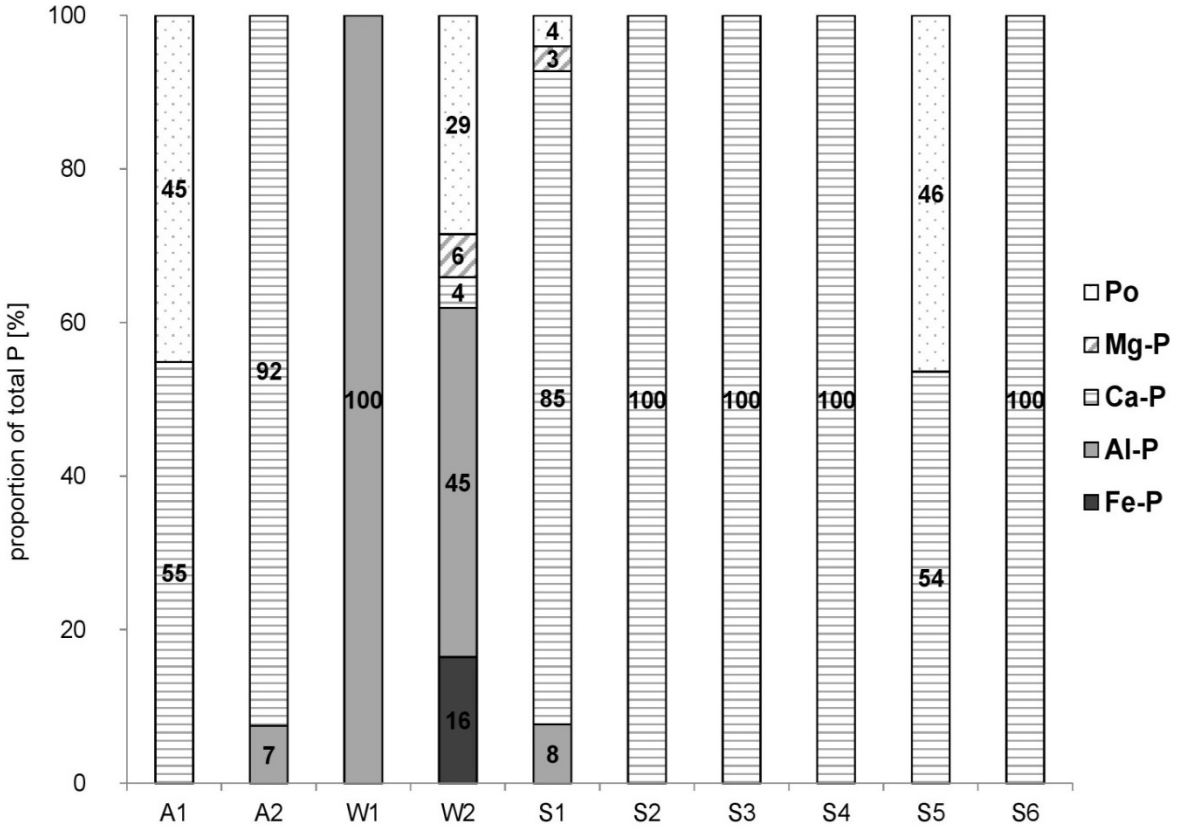

Figure 4-2 Proportions of P compounds as obtained by linear combination fitting (LCF) on P *K*-edge XANES spectra of upper and lower arable soil (A), wetland soil (W) and sediment samples (S).

4.5. Discussion

4.5.1. Elemental characteristics

The wetland is located near the ground- and surface water, whereas the arable soil is situated at higher altitude, further away from these water sources, and simultaneously located on a slope, that is affected by runoff at surface, erosion and subsurface drainage (Figure 1). Furthermore, sampling took place in early summer after a long dry period so that the arable soil had not received any precipitation for several weeks. The origin of the 6% $CaCO_3$ in A1 and 14% in A2 most likely originates from the underlying parent material glacial till at the arable field, which partially may have been incorporated into soil profile by tillage. As the arable field has a relatively high elevation and a sloping relief towards the coast (Figure 1), erosion during rain fall events can transport solid matter into the wetland (Karstens et al. 2016). Thus, topsoil material may have been transported away from the slope by erosion and, thus, the $CaCO_3$-containing underlying parent material may have been incorporated into the remaining topsoil by agricultural tillage. This explains the higher proportion of $CaCO_3$ at a depth of 30-60 cm compared to 0-30 cm of the arable soil (Table 2), although regular liming may have been added some $CaCO_3$ to the tilled soil layer.

Except for Ca, the hypothesized effect of erosion is reflected by concentrations of all elements determined. We measured higher concentrations of P, Mg, Al and Fe in W1, the upper sample of wetland soil, than in the arable soil samples A1 and A2 (Table 2). The amount of Ca is significantly higher in the arable soil compared to the wetland soil because of the entry of $CaCO_3$ from the underlying parent material into the tilled soil as already mentioned above.

The concentrations of P_t, significantly higher in the topsoil of the wetland (2258 mg kg^{-1}) compared to the topsoil at the arable site (430 mg kg^{-1}) (Table 2), indicate an accumulation of P compounds in the wetland. While P can be consumed by crops on the agricultural soil and transported away from the location by harvested crops and by erosion due to the sloping relief, there is no cultivation with harvest and less sloping at the wetland soil, and restricted organic matter oxidation. These factors together facilitate an accumulation of organic matter as peat and of P stored in that substrate. The arable field was used for farming since about 1945 (Karstens et al. 2016). Nowadays, the field crops oil seed rape, wheat and barley with high fertilizer demands are cultivated (Karstens et al. 2016). Thus, it is likely that especially fertilizer P is present in the arable soil and transported towards the wetland soil, although since 2000 only cow manure was applied instead of mineral P fertilizers (Karstens et al. 2016). This fertilizer P seems not to be transported beyond the wetland soil into the directly adjacent Bodden sediments, because P concentrations in S1 to S4 were in a very low range from 132 to 140 mg kg^{-1} (Table 2). Thus, most nutrients and especially P were transported from the arable soil towards the wetland soil and seem to be accumulated there for a longer time period. Similar relationships between the samples have been observed for the sediments S1 to S6. The amounts of P, Ca, Mg, Al and Fe were significantly higher in the sediments S5 and S6 from a greater water depth compared to most sediments from more shallow areas (S1 to S4) (Table 2).

4.5.2. Sequential chemical P fractionation

Concentrations of P_t in the soils and sediments were in a similar range of P_t contents in sediments from shallow lakes in the Yangtze River area in China (Wang et al. 2006) and except from W1 and W2 below P_t contents from 740 to 1230 mg P kg^{-1} in bottom sediments of eutrophic lakes in central and western Poland (Bryl and Sobczyński 2019). Mean concentrations of P_t were higher in the investigated soils compared to the adjacent sediments agreeing with a study of transitional agricultural ecotones, where concentrations of P_t of the site average also were significantly higher than in corresponding streambed sediment (Neidhardt et al. 2019). As summed amounts of P_{mu} were clearly higher in W1 and W2 compared to A1 and A2 (Table 2), this accumulation of especially P_{mu} in the wetland soil can be attributed to an uptake of mainly P_{mr} by the *Phragmites* plants, transformation to P_{mu}, likely mostly bound in organic matter, and its disposal in the wetland peat (Negassa at al. 2020). Furthermore, some P_{mu} can have been transported from the arable site into the wetland, accumulating there. Although organic soils are known to have lower capacities for retaining excess P from fertilization and thus pose an increased risk of P loss to aquatic environments (Daly et al. 2001; Gonzáles Jiménez et al. 2019), amounts of P were not particularly high in the directly adjacent sediments S1 to S4 (Table 3). This can be due to high concentrations of stable fractions of H_2SO_4-P and residual-P in the wetland, restricting processes of P mobilization at this site. Furthermore, a dilution of transported P within the Bodden water and/or sediments is possible or transferred P can have been mobilized immediately and accumulated by aquatic plant and animal organisms.

The proportions of H_2O-P and resin-P, characterized as labile P in soils (Tiessen and Moir 1993) and P immediately available for uptake by phytoplankton (Zhu et al. 2013a), were lower in the arable and wetland soils (0 – 4%) compared to the sediments (0 - 24%) (Table 3). This pool of loosely bound P is known to be seasonally variable in sediments, affected by enhanced sedimentation and intensive degradation of OM during high summer temperatures (Wang et al. 2006; Kisand 2005). Therefore, the comparably large proportions in sediments are not implausible. The fraction of NH_4Cl-P, also characterized as mobile, exchangeable P but determined with a sediment P fractionation method (Psenner 1988) included 1 to 20% of P_t in different sediments from eutrophic lakes in Poland [34] and thereby this fraction was in a similar range as the proportions of H_2O-P and resin-P fractions of the present study.

Within the soil P fractionation scheme, P extracted by NaOH is interpreted as predominantly associated with Al and Fe oxide minerals, eventually combined with humic substances [24,25] whereas Fe-P compounds are separately estimated in the sediment-P-methods (Psenner 1988). Especially in the fractions of NaOH-P_{mr} and NaOH-P_{mu}, higher P concentrations were measured in the wetland soil W1 and W2 than in the arable soil A1 and A2, and in the sediments S5 and S6 than in the other sediments from the Bodden (Table 3). Thus, the wetland soil and the sediments at the end of the transect at a water depth of 230 cm seem to be sinks especially for metal bound P and P in humic substances, which likely are combined with each other (Gerke 2015).

Acid extractable P_{mr} accounted for the greatest proportion of P_t in the sediments (up to 45%) in agreement with an investigation of lake sediments from (Zhu et al. 2013a). This P fraction is known as stable, Ca-bound P (Tiessen and Moir 1993), not readily available to phytoplankton (Zhu et al. 2013b). An investigation of sediments from several eutrophic lakes in Poland also resulted in up to 45% acid extractable P (HCl-P) of P_t (Bryl and Sobczyński 2019) and in surface sediments of the Mediterranean Sea 37% P of P_t were determined in the fraction of Ca-bound P (Akçay and Yücel 2023) with sediment fractionation methods (Psenner 1988). Relative proportions of H_2SO_4-P were also very high in the arable soil compared to the wetland soil (Table 3). The available amounts of $CaCO_3$ in A1 and A2 (Table 2) can facilitate the formation of Ca-bound P at the location of the eroded arable slope compared to the wetland soil.

The statement that residual-P can constitute a significant proportion of P_t from P fractionation in soils (Condron and Newman 2011) is supported by the present study as up to 22% of P_t in the soil samples was residual-P (Table 3). However, in the sediments, no residual-P was determined in S1 to S4 and about 20% in the last two sediments S5 and S6. Phosphorus in the residual fraction was characterized as stable complexes with metal ions, pedogenic oxides or organic materials such as lignin (Gonzáles Jiménez et al. 2019; Schlichting et al. 2002). Sediments from more shallow areas contained more labile P and sediments from a water depth of 230 cm at the end of the transect under study contained higher amounts of stable P associated with Ca instead of metal ions, pedogenic oxides or complex organic materials (Table 3). In contrast to labile P fractions such as resin-P and $NaHCO_3$-P, the very stable P compounds within the fraction of residual-P pose a lower risk of P loss to the aquatic environment (Negassa and Leinweber 2009). Thus, P can accumulate and be conserved in deep sediments at the end of the investigated transect.

4.5.3.P XANES spectroscopy

Most results of P XANES spectroscopy agree with the determined sequential P fractions. Especially both arable soils A1 and A2 and the sediments S1 to S4 were clearly dominated by Ca-P compounds according to XANES spectroscopy (Figure 2). In compliance with that, in these samples H_2SO_4-P_{mr} accounted for the greatest proportion of P_t in sequential fractionation and this P fraction earlier has been characterized as stable, Ca-bound P (Tiessen and Moir 1993). The dominant occurrence of Ca-P in sediments from the Baltic Sea (Prüter et al. 2020) or nearshore sediments (Noll et al. 2009) is not uncommon. Percentages of Ca-P compounds in agricultural soils with different fertilization treatments ranged from 0% to 21% (Koch et al. 2018), but due to the elevated amounts of $CaCO_3$ in A1 and A2 (Table 2) most likely from liming and the underlying glacial till, the formation of Ca-bound P in these soils can have been promoted, reaching proportions up to 92% (Figure 2).

Organic P compounds were assigned in A1, W2 and S5 in significant proportions by XANES spectroscopy (Figure 2). Summed proportions of P_{mu} from sequential fractionation were also high in A1 and W2 among the soil samples and thereby agreed with the results of XANES spectroscopy (Table 3 and Figure 2). Recently, the importance of P_o compounds for sustainable

agriculture has been emphasized (Sulieman and Mühling 2021). Absolute P_{mu} concentrations were highest in S5 and S6 among the sediments determined with sequential fractionation (Table 3), but this could be confirmed only for S5 by XANES spectroscopy because it ascertained 46% P_o compounds in S5 and 0% P_o in S6. An underestimation of P_o compounds by XANES spectroscopy is likely because XANES spectra of phytic acid are known to lack strong and distinguishing features (Ajiboye et al. 2008).

The wetland soils act as sinks for P compounds, especially Al- and Fe-P and P_o compounds (Figure 2) in the first part of the transect including the arable and wetland soils. In agreement with an earlier study about P forms along a continuum from agricultural fields to lake sediments which reported significant P losses from field soils but only small amounts of P in the nearshore lake sediment (Noll et al. 2009), the samples S5 and S6 at the end of the investigated transect at a water depth of 230 cm can also accomplish a sink function for especially P_o compounds (Figure 2 and Table 3) among the Bodden sediments. This also agrees with an earlier study, where lost P from agriculture has either become available to biota or was deposited in deeper portions of a lake system (Noll et al. 2009).

Thus, both, the wetland soil as well as the sediments S5 and S6 at the end of the transect, can act as sinks for P with a lower probability of P mobilization into the above water column. Generally, the investigated transect of soils and sediments can be divided into two separated systems. The first system consists of arable soils followed by wetland soil. Phosphorus compounds are transported from agricultural fields into the wetland by processes such as runoff and soil erosion, accumulate and can be conserved in the latter. The second system comprises the Bodden sediments with a similar sink function for P compounds in deeper sediments at the end of the investigated transect. Results from sequential P fractionation and XANES spectroscopy suggest no great transfer processes of P species from the first system towards the second.

4.6. Conclusions

In a sample set along a transect from arable and wetland soils to aquatic sediments, the methods sequential P fractionation and P XANES spectroscopy similarly determined a dominance of Ca associated P at the arable soils and Bodden sediments, and high proportions of P_{mu}/P_o at the surface arable soil (A1) and subsurface wetland soil (W2). Thus, both methods complemented each other in delivering comprehensive results concerning the P speciation and sink functions of sample locations along this transect.

The investigation revealed two sinks along the transect from arable land to adjacent aquatic lagoon sediments. As the wetland soil performs as a semiterrestrial trap for especially moderately stable P, Al-P and P_{mu}/P_o compounds, it can help to prevent direct transfer of P, e.g., by leaching or runoff during erosion events from agricultural field to the adjacent Bodden. An intact *Phragmites* wetland therefore can protect the aquatic ecosystem from further eutrophication. Consequently, it is reasonable to preserve existing buffer strips such as *Phragmites* stands along water bodies or to potentially create new ones in areas where they are

not yet abundant. Among the aquatic sediments, we detected also especially P_{mu}/P_o compounds and stable P fractions accumulating at the deepest sample location compared to sediments from more shallow positions close to the coast. Thus, it is likely that deeper basins in the investigated Bodden system act as sinks for especially stable P forms which are not directly consumed by aquatic organisms. If this concept can also be applied to aquatic ecosystems different from coastal lagoons in the Baltic Sea, it has to be investigated, if measures such as deepening of shallow aquatic areas can help to reduce pollution and eutrophication by trapping P in the sediment of deeper basins.

4.7. Acknowledgments

The authors thank Elena Heilmann and Britta Balz (Soil Science, University of Rostock) for analytical help concerning P fractionation and ICP measurement. Furthermore, we would like to thank Volker Reiff (Applied Ecology and Phycology, University of Rostock), who was a great support during the sampling process of sediments. Finally, we are grateful to Prof. Jörg Prietzel (Department of Soil Science, Technical University of Munich) for providing the P XANES reference spectra and to the technical staff at BL8 of the SLRI, Thailand for their support during XANES research.
This research was funded by the Leibniz Association within the scope of the Leibniz ScienceCampus “Phosphorus Research Rostock”.

4.8. Funding

This research was funded by the Leibniz Association within the scope of the Leibniz ScienceCampus “Phosphorus Research Rostock”.

4.9. Conflicts of Interest

The authors declare no conflict of interest.

4.10. References

Ajiboye, B., Akinremi, O. O., Hu, Y., & Jürgensen, A. (2008). XANES speciation of phosphorus in organically amended and fertilized vertisol and mollisol. *Soil Science Society of America Journal*, 72, 1256.

Akçay, İ., Yücel, M. (2023). Distinct patterns of sedimentary phosphorus fractionation and mobilization in the seafloor of the Black Sea, Marmar Sea and Mediterranean Sea. *Science of the Total Environment*, 160936.

Andreu, V., Gimeno-García, E., Pascual, J. A., Vazquez-Roig, P., & Picó, Y. (2016). Presence of pharmaceuticals and heavy metals in the waters of a Mediterranean coastal wetland: potential interactions and the influence of the environment. *Science of the Total Environment*, 540, 278-286.

Audette, Y., O'Halloran, I. P., Nowell, P. M., Dyer, R., Kelly, R., & Voroney, R.P. (2018). Speciation of phosphorus from agricultural muck soils to stream and lake sediments. *Journal of Environmental Quality*, 47. 884-892.

Bitschofsky, F., Forster, S., Powillait, M., & Gebhardt, C. (2015). Role of macrofrauna for the exchange processes between sediment and water column in an inner coastal water of southern Baltic Sea (Darss-Zingst Bodden Chain, Grabow). *Rostocker*

Meeresbiologische Beiträge, 25.
Bonsdorff, E., Blomqvist, E. M., Mattila, J., & Norkko, A. (1997). Coastal eutrophication: causes, consequences and perspectives in the archipelago areas of the Northern Baltic Sea. *Estuarine, Coastal and Shelf Science*, 44, 63-72.
Bryl, Ł., Sobczyński, T. (2019). Phosphorus and its fractionation in bottom sediments of selected lakes of Wielkopolskie Lakeland in Central and Western Poland. *Middle pomeranian scientific society of the environment protection*, 21, 1515-1532.
Calivn, S. (2013). XAFS for everyone. CRC Press, p. 427.
Condron, L. M., & Newman, S. (2011). Revisiting the fundamentals of phosphorus fractionation of sediments and soils. *Journal of Soils and Sediments*, 11(5), 830-840.
Correll, D. L. (1998). Role of phosphorus in the eutrophication of receiving waters: a review. *Journal of Environmental Quality*, 27, 261-267.
Daly, K., Jeffrey, D., & Tunney, H. (2001). The effect of soil type on phosphorus sorption capacity and desorption dynamics in Irish grassland soils. *Soil Use and Management*, 17, 12-20.
Frankowski, L., Bolałek, J., & Szostek, A. (2002). Phosphorus in bottom sediments of Pomeranian Bay (Southern Baltic - Poland). *Estuarine, Coastal and Shelf Science*, 54, 1027-1038.
Gerke, J. (2015). The acquisition of phosphate by higher plants: effect of carboxylate release by the roots. A critical review. *Journal of Plant Nutrition and Soil Science*, 178, 351-364.
González Jiménez, J. L., Healy, M. G., & Daly, K. (2019). Effects of fertiliser on phosphorus pools in soils with contrasting organic matter content: a fractionation and path analysis study. *Geoderma*, 338, 128-135.
Gunnars, A., & Blomqvist, S. (1997). Phosphate exchange across the sediment-water interface when shifting from anoxic to oxic conditions - An experimental comparison of freshwater and brackish-marine systems. *Biogeochemistry*, 37, 203–226.
Hedley, M. J., Stewart, J. W. B., & Chauhan, B. S. (1982). Changes in Inorganic and Organic Soil Phosphorus Fractions Induced by Cultivation Practices and by Laboratory Incubations. *Soil Science Society of America Journal*, 46, 970.
Iglesias, M. L., Devesa-Rey, R., Pérez-Moreira, R., Díaz-Fierros, F., Barrai, M. T. (2011). Phosphorus transfer across boundaries: from basin soils to river bed sediments. *Journal of Soils and Sediments,* 11, 1125-1134.
Karstens, S., Buczko, U., & Glatzel, S. (2015). Phosphorus storage and mobilization in coastal Phragmites wetlands: influence of local-scale hydrodynamics. *Estuarine, Coastatl and Shelf Science*, 164, 124-133.
Karstens, S., Buczko, U., Jurasinski, G., Peticzka, R., & Glatzel, S. (2016). Impact of adjacent land use on coastal wetland sediments. *Science of the Total Environment* 550, 337-348.
Kisand, A. (2005). Distribution of sediment phosphorus fractions in hypertrophic strongly straified Lake Verevi. *Hydrobiology*, 547, 33-39.
Klysubun, W., Sombunchoo, P., Deenan, W., Kongmark, C. (2012). Performance and status of beamline BL8 at SLRI for X-ray absorption spectroscopy. *Journal of Synchrotron Radiation*, 19, 930-936.
Koch, M., Kruse, J., Eichler-Löbermann, B., Zimmer, D., Wilbold, S., Leinweber, P., & Siebers, N. (2018). Phosphorus stocks and speciation in soil profiles of a long-term fertilizer experiment: Evidence from sequential fractionation, P *K*-edge XANES, and 31P NMR spectroscopy. *Geoderma*, 316, 115–126.
Kraal, P., & Slomp, C. P. (2014). Rapid and extensive alteration of phosphorus speciation during oxic storage of wet sediment samples. *PLOS One,* 9, 1-6.
Łukawska-Matuszewska, K., & Bolałek, J. (2008). Spatial distribution of phosphorus forms in seduments in the Gulf of Gdańsk (southern Baltic Sea). *Continental Shelf Research*, 28, 977-990.
Murphy, J., Riley, J. P. (1962). A modified single solution method for the determination of phosphate in natural waters. *Analytica Chimica Acta*, 27, 31-36.
Neidhardt, H., Achten, F., Kern, S., Schwientek, M., & Oelmann, Y. (2019). Phosphorus pool composition in soils and sediments of transitional ecotones under the influence of agriculture. *Journal of Environmental Quality*, 48, 1325-1335.
Negassa, W., & Leinweber, P. (2009). How does the Hedley sequential phsophorus fractionation reflect impacts of land use and management on soil phosphorus: a review. *Journal of Plant Nutrition and Soil Science*, 172, 305-325.
Negassa, W., Michalik, D., Klysubun, W., Leinweber, P. (2020). Phosphorus speciation in long-term drained and rewetted peatlands of Northern Germany. *Soil Systems*, 4(1), 11.

Noll, M. R., Szatkowski, A. E., & Magee, E. A. (2009). Phosphorus fractionation in soil and sediments along a continuum from agricultural fields to nearshore lake sediments: potential ecologial impacts. *Journal of Great Lakes Research*, 35, 56-63.

Perillo, G. M. E., Wolanski, E., Cahoon, D., & Brinson, M. (2009). *Coastal Wetlands: an integrated ecosystem approach*. Elsevier.

Prietzel, J., Harrington, G., Häusler, W., Heister, K., Werner, F., & Klysubun, W. (2016). Reference spectra of important adsorbed organic and inorganic phosphate binding forms for soil P speciation using synchrotron-based *K*-edge XANES spectroscopy. *Journal of Synchrotron Radiation*, 23, 532-544.

Prüter, J., Leipe, T., Michalik, D., Klysubun, W., & Leinweber, P. (2020). Phosphorus speciation in sediments from the Baltic Sea, evaluated by a multi-method approach. *Journal of Soils and Sediments*, 20, 1676-1691.

Prüter, J., Hu, Y., & Leinweber, P. (2022). Influence of sample pretreatment on P speciation in sediments evaluated with sequential fractionation and P *K*-edge XANES spectroscopy. *Communications in Soil Science and Plant Analysis*, 53(14), 1712-1730.

Psenner, R. (1988). Fractionation of phosphorus in suspended matter and sediment. *Ergeb. Limnol.,* 30, 98–113.

Ravel, B., & Newville, M. (2005). ATHENA, ARTEMIS, HEPHAESTUS: Data analysis for X-ray absorption spectroscopy using IFEFFIT. *Journal of Synchrotron Radiation*, 12, 537–541.

Reddy, K. R., Kadlec, R. H., Flaig, E., & Gale, P. M. (1999). Phosphorus retention in streams and wetlands: a review. Critical Reviews in Environmental Science and Technology, 29(1), 83-146.

Schlichting, A., Leinweber, P., Meer, R., & Alterman, M. (2002). Sequentially extracted phosphorus fractions in peat-derived soils. *Journal of Plant Nutrition and Soil Science*, 165(3), 290-298.

Schmieder, F., Gustafsson, J. P., Klysubun, W., Zehetner, F., Riddle, M., Kirchmann, H., & Bergström, L. (2020). Phosphorus speciation in cultivated organic soils revealed by P *K*-edge XANES spectroscopy. *Journal of Plant Nutrition and Soil Science*, 183, 367-381.

Sims, J. T., Pierzynski, G. M. (2005). Chemistry of phosphorus in soils. In M.A. Tabatabai, D. L. Sparks (Eds.), *Chemical processes in soils,* SSSA Book Series.

Sulieman, S., & Mühling, K.H. (2021). Utilization of soil organic phosphorus as a strategic approach for sustainable agriculture. *Journal of Plant Nutrition and Soil Science*, 184, 311-319.

Turner, B. L. (2008). Soil organic phosphorus in tropical forests: an assessment of the NaOH-EDTA extraction procedure for quantitative analysis by solution ^{31}P NMR spectroscopy. *European Journal of Soil Science*, 59, 453-466.

Tiessen, H., & Moir, J.O. (1993). Characterization of available P by sequential extraction. In M. R. Carter (Ed.), *Soil sampling and methods of analysis* (pp. 75-86). Lewis Publishers, Boca Raton.

Wang, S., Jin, X., Zhao, H., & Wu, F. (2006). Phosphorus fractions and ist release in the sediments from the shallow lakes in the middle and lower reaches of Yangtze River area in China. *Colloids and Surfaces A: Physicochemical and Engineering Aspects*, 273, 109–116.

Werner, F., Prietzel, J. (2015). Standard protocol and quality assessment of soil phosphorus speciation by P *K*-edge XANES spectroscopy. *Environmental Science and Technology*, 49, 10521-10528.

Weyers, E., Strawn, D. G., Peak, D., Moore, A. D., Baker, L. L., Cade-Menun, B. (2016). Phosphorus speciation in calcareous soils following annual dairy manure amendments. *Soil Science of America Journal*, 80, 1531-1542.

Xie, L. Q. , Xie, P., & Tang, H. J. (2003). Enhancement of dissolved phosphorus release from sediment to lake water by Microcystis blooms - An enclosure experiment in a hyper-eutrophic, subtropical Chinese lake. *Environmental Pollution*, 122, 391–399.

Zhu, Y., Wu, F., He, Z., Guo, J., Qu, X., Xie, F., Giesy, J. P., Liao, H., & Guo, F. (2013a) Characterization of organic phosphorus in lake sediments by sequential fractionation and enzymatic hydrolysis. *Environmental Science and Technology*, 47(14), 7679-7687.

Zhu, Y., Zhang, R., Wu, F., Qu, X., Xie, F., & Fu, Z. (2013b). Phosphorus fractions and bioavailability in relation to particle size characteristics in sediments from Lake Hongfeng, Southwest China. *Environmental Earth Sciences*, 68(4), 1041-1052.

Zwolsman, J. J. G. (1994). Seasonal variability and biogeochemistry of Phosphorus in the Scheldt Estuary, South-west Netherlands. *Estuarine, Coastal and Shelf Science*, 39, 227-248.

5 Phosphorus speciation in sediments from the Baltic Sea, evaluated by a multi-method approach

Julia Prüter[1], Thomas Leipe[2], Dirk Michalik[3], Wantana Klysubun[4], Peter Leinweber[1]

[1]University of Rostock, Soil Science, Justus-von-Liebig Weg 6, 18051 Rostock, Germany

[2]Leibniz Institute for Baltic Research, Seestraße 15, 18119 Rostock Warnemünde, Germany

[3]Leibniz Institute for Catalysis, A.-Einstein-Str. 29a, 18059 Rostock, Germany

[4]Synchrotron Light Research Institute, Muang District, 111 University Avenue, Nakhon Ratchasima 3000, Thailand

Published in

Journal of Soils and Sediments (2020), 20, 1676-1691

5.1. Abstract

Purpose Phosphorus (P) is a crucial element for living organisms at both land and sea, but simultaneously, it can cause environmental problems especially in marine ecosystems. The pathway of P from soils through riverine and coastal systems to sea sediments has not been clarified to date. Thus, the main aim of this study was to characterize P species in sediments along a gradient from the coast of Northern Germany to the Baltic Proper.

Materials and methods Six sediment samples along a transect from river outlets into the Baltic Sea in northeastern Germany to the deep basins at the Baltic Proper were analyzed. Four complementary methods were applied to explore the different sedimentary P compounds: (i) the sequential P fractionation to extract P from sediment pools of different solubility; (ii) P *K*-edge X-ray absorption near edge structure (XANES) spectroscopy as an element-specific method for speciation analyses of complex environmental samples; (iii) ^{31}P nuclear magnetic resonance (^{31}P NMR) spectroscopy as a capable technique distinguishing especially different organic P compounds based on their characteristic resonance frequencies and (iv) scanning electron microscopy (SEM) combined with energy-dispersive X-ray microanalyses (EDX) to identify certain solid particles and their elemental composition.

Results and discussion Sequential P fractionation revealed a decrease in labile P pools (resin-P; $NaHCO_3$-P) along with an increase in more stable P fractions (H_2SO_4-P; residual-P) from near-coastal sediments towards the Baltic Proper with increasing water depths of sediment deposits. In comparison, XANES analysis indicated a decline of Fe-associated P compounds in favor of Ca-bound P with increasing distance of sediments from the coastline into the Baltic Sea. Results of ^{31}P NMR spectroscopy showed that the variety of different mono- and diester P compounds decreased with increasing distance from the coast and that high proportions of orthophosphate (ortho-P) were present especially in greater water depths. The SEM-EDX analysis supported most of these results by retriving Fe phosphate particles especially in the sediments near the coast.

Conclusions The integration of several P-specific methods enabled improved insights into P speciation. A trend towards more stable Ca-P compounds towards the Gotland basin was found with sequential fractionation and P-XANES. In the future, different types of sediments will be analyzed with respect to their interactions with adjacent soils to find out a common principle of P-transformations and derive approaches for capturing P before entering susceptible marine systems.

Keywords: ^{31}P NMR • Electron microscopy • Sediment • Sequential fractionation • XANES

5.2. Introduction

Phosphorus (P), as a crucial element for organism growth, is identified as one of the major factors responsible for eutrophication of freshwater and marine ecosystems. Eutrophication leads to several negative environmental impacts, for instance excessive algae blooming, release of toxins hazardous to livestock and humans, reduced water transparency, oxygen

depletion and a deterioration of drinking water and the general water quality (Bonsdorff et al. 1997; Meissner and Leinweber 2004). The two major pathways of P entering aquatic ecosystems are external inputs and P release from sediments (Bai et al. 2009). Since the first Helsinki Convention (HELCOM) in 1974, the adjacent countries agreed to reduce their nitrogen (N) and P inputs to the Baltic Sea. Although the original target of reducing loads by 50% was never met, progress has been made in the reduction of external P input from municipal and industrial wastewater treatment plants since the early 1970s, for instance in the Finnish and Swedish archipelago in the Northern Baltic Sea (Bonsdorff et al. 1997; Walve et al. 2018). Thus, after reducing external P inputs, P released by sediments remains as a major source of a general water quality deterioration, especially in shallow eutrophic lakes (Xie et al. 2003). The potential release of sediment-based P to the water column can reach rates comparable to external inputs (Bai et al. 2009). Sedimentary P exchange depends on speciation and abundance of the distinct P forms and the actual environmental conditions such as redox and pH (Ahlgren et al. 2005; Hupfer and Lewandowski 2008; Shinohara et al. 2012). A large number of investigations about P compounds and their speciation in the water column (e.g. Zwolsman 1994; Gunnars and Blomqvist 1997; Xie et al. 2003) and in sediments from the Baltic Sea (e.g. Jensen et al. 1995; Kleeberg and Dudel 1997; Aigars 2001, Murphy et al. 2001; Frankowski et al. 2002; Łukawska-Matuszewska and Bolałek 2008; Kraal and Slomp 2014) addressed distinct topics, such as seasonal variations in P species, connections between specific P species and physical and chemical properties of the environment and processes related to diagenesis. Information about P transport pathways from soils to sediments is scarce (Iglesias et al. 2011). In the Baltic Sea basins like Arkona, Bornholm and Gdańsk are depositional areas for material transport (Leipe et al. 2000; Emeis et al. 2002). A lot of material deposited in Baltic Sea basins comes from lateral transport, controlled by wind and bottom topography (Leipe et al. 2000; Emeis et al. 2002). To the best of our knowledge, no publications about the alteration and composition of P compounds along a gradient from coastal sediments to sediments of the deep Baltic Proper determined with a multi-method approach are available.

Sequential P fractionation is a commonly applied method of distribution and mobility analysis of diverse P forms in soils and sediments (e.g., Hupfer et al. 1995; Zhang et al. 2008; Kruse et al. 2010; Koch et al. 2018). A differentiation of labile, increasingly stable and stable organic and inorganic P fractions in soils has been introduced by Hedley et al. (1982). The different extractants remove either parts or combinations of P species (Shober et al. 2006a), so the sequentially extracted fractions do not exactly match chemically defined compounds (Kar et al. 2011). Thus, to get a comprehensive view of the various P forms and their distribution, additional spectroscopic techniques are applied. The P *K*-edge X-ray absorption near edge structure (XANES) spectroscopy, as an element-specific method for speciation analyses of complex environmental samples such as soils, animal wastes, organic amendments or sediments (Hesterberg et al. 1999a; Beauchemin et al. 2003; Sato et al. 2005; Ajiboye et al. 2008a; Kar et al. 2011) has the ability to identify primarily inorganic P compounds more directly (Ajiboye et al. 2008a; Kruse et al. 2015). One drawback of XANES analysis is the limited ability in differentiating between several types of organic P compounds (Peak et al. 2002), whereas

the possibility of direct sample usage without further extraction or destruction for analyses is advantageous. ^{31}P nuclear magnetic resonance (^{31}P NMR) spectroscopy is a technique capable of distinguishing especially different organic P compounds such as orthophosphate monoesters and diesters based on their characteristic resonance frequencies in environmental samples, and so, it can be used as a complementary method together with the chemical fractionation and XANES analysis (Ahlgren et al. 2005; Turner et al. 2005; Reitzel et al. 2007). ^{31}P NMR spectroscopy enables direct molecular and structural characterization of organic and inorganic P in alkaline solution.

Scanning electron microscopy (SEM) and energy-dispersive X-ray microanalyses (EDX) inspection of solid particles is usually applied on water samples for investigation of the mineralogical and geochemical composition of suspended particulate matter (Leipe et al. 2000). In some studies, SEM-EDX was already used to characterize especially P-bearing particles in water samples from different regions (e.g. Ernstberger et al. 2004; Nausch et al. 2017). SEM-EDX enables direct visual evaluation and thereby gives a representative overview about the morphologies of single particles in the samples (Dellwig et al. 2010) combined with elemental analyses and, thus, a speciation at the single particle level. To the best of our knowledge, the methods SEM-EDX, sequential fractionation, XANES spectroscopy, and ^{31}P NMR spectroscopy never have been applied in this combination to sediment samples on a transect towards the Baltic Proper.

The aim of this study is (i) to characterize occurring P species in sediments from the Baltic Sea along a gradient from river estuaries into central parts of the Baltic Sea, and (ii) to observe changes in the composition of the sediments along their transport pathway from the coast of northern Germany to the Gotland Basin in the Baltic Proper.

5.3. Material and methods

5.3.1. Sampling area and sediment collection

Six sediment samples were selected from the stock of Leibniz Institute for Baltic Research Warnemünde (IOW). The samples were collected in the years 1982, 2013 and 2016 at different locations from the coastal land of northern Germany to the deep Baltic Proper at the River Recknitz (RE), Saaler Bodden (SB), Mecklenburg Bight (MB), Arkona Basin (AB1, AB2) and Gotland Basin (GB) as shown in Figure 1 (coordinates in Table 1). The samples RE and SB were taken manually with an UWITEC tube, MB and A2 with a Van Veen grab and AB1 and GB with a multi-corer, equipped with polycarbonate tubes. After collection, samples were dried and homogenized by grinding. These pretreatments possibly do not reflect the P speciation *in situ* (e.g. Condron and Newman 2011 and references therein) but all samples archivated for subsequent special analyses had been pretreated in this way. Along the transect from land to sea, the water depths at which the sediments were taken, increase from 2 m to 247 m in the order RE<SB<MB<AB1<AB2<GB. According to literature, the sediment samples RE and SB from 2 m depth may contain a few cm of oxic conditions in uppermost layers (Karstens et al.

2015) whereas the others from greater depth can be considered to derive from hypoxic and anoxic zones (Mort et al. 2010). The sampling depths in the sediments range from 0 to 30 cm, with exception of the sample AB1, where sediment was exclusively available in a depth of 18 to 21 cm.

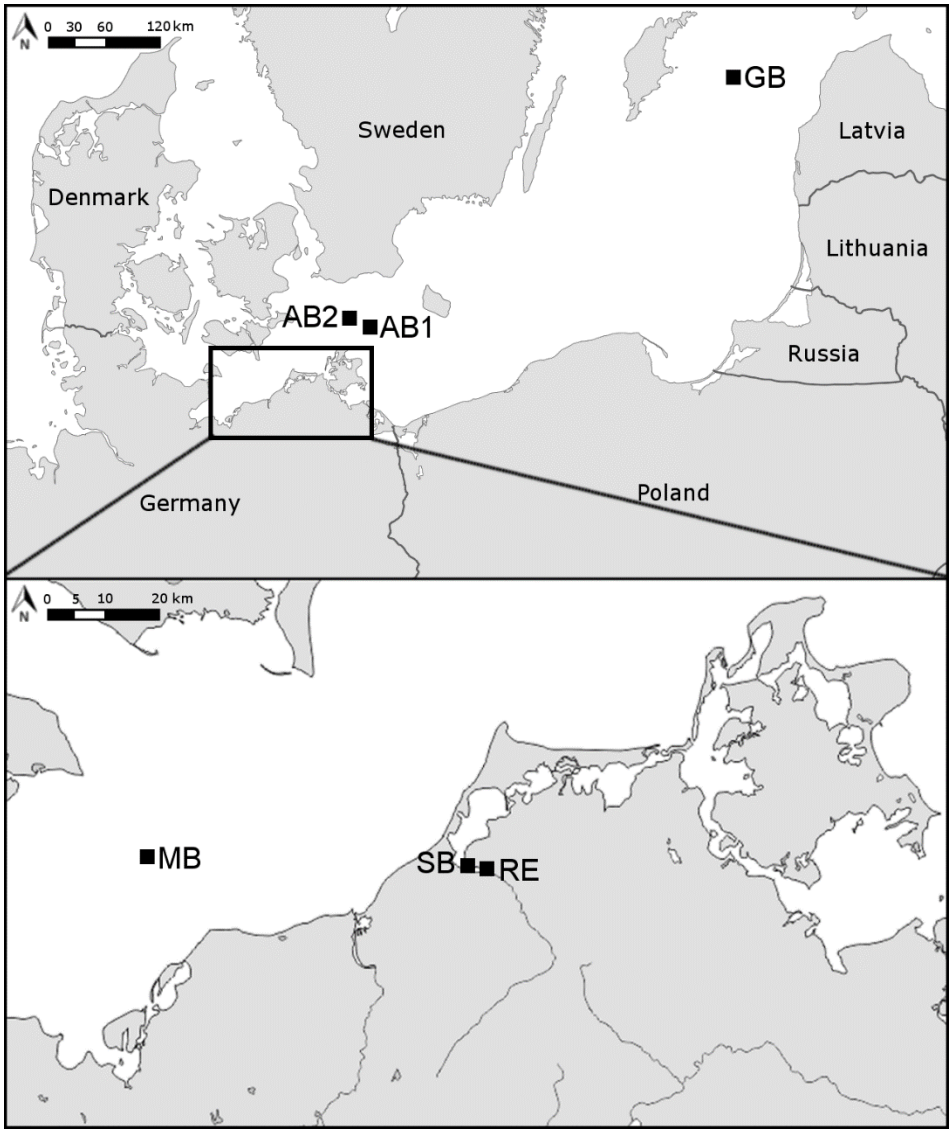

Figure 5-1 Location map of the six sampling sites at the coast of Mecklenburg-Western Pomerania and the Baltic Sea.

5.3.2. Determination of total P, Ca, Mg, Al, Fe and water content

Elemental concentrations of total P (P_t), calcium (Ca), magnesium (Mg), aluminium (Al) and iron (Fe) were determined with an inductively coupled plasma-optical emission spectrometer (ICP-OES) after microwave-assisted digestion of ≤ 50 mg sediment with aqua regia consisting of 2 mL nitric acid (HNO_3) and 6 mL hydrochloric acid (HCl) and are displayed in Table 2. Absolute water contents of the samples were obtained from IOW (Table 1).

Table 5-1 Sample codes, origins, coordinates, sampling years and methods, water and sediment depths and water content of the sediment samples.

Sample code	Origin	Coordinates	Year of sampling	Sampling method	Water depth (m)	Sediment depth (cm)	Water content (%)
RE	River Recknitz	54° 14.85 N; 12° 28.02 E	2016	UWITEC tube	2	0-10	85.2
SB	Saaler Bodden	54° 15.18 N; 12° 25.24 E	2016	UWITEC tube	2	0-6	87.8
MB	Mecklenburg Bight	54° 14.40 N; 11° 29.40 E	1982	Van Veen grab	24	0-30	66.8
AB1	Arkona Basin	54° 55.30 N; 13° 44.10 E	2013	multi-corer	46	18-21	73.2
AB2	Arkona Basin	54° 55.50 N; 13° 30.00 E	1982	Van Veen grab	48	0-30	70.3
GB	Gotland Basin	57° 19.20 N; 20° 03.00 E	2013	multi-corer	247	0-20	84.8

5.3.3. Sequential P fractionation

A sequential fractionation method according to Hedley et al. (1982), modified by Tiessen and Moir (1993) was used to extract different P fractions from sediment. About 0.42 g finely ground sediment was weighed into 50-mL centrifuge tubes. Samples were shaken for 18 h followed by centrifugation at 4000*g* for 20 min, and decanted. Chemical P fractionation included the following extraction steps: (1) resin strips, (2) 0.5 M $NaHCO_3$, (3) 0.1 M NaOH and (4) 1 M H_2SO_4, which were all conducted under ambient air temperature. In the fraction of anion exchange resin, P was removed from the resin using 1 M HCl. The P fractions were interpreted as suggested by Hedley et al. (1982): resin P (resin-P) representing the easily exchangeable and mobile P; inorganic ($NaHCO_3$-P_i) and organic ($NaHCO_3$-P_o) bicarbonate P representing labile inorganic and organic P weakly adsorbed to mineral surfaces as well as microbial P; inorganic (NaOH-P_i) and organic (NaOH-P_o) hydroxide P representing moderately labile inorganic and organic P adsorbed to aluminium- and iron oxide minerals and P in humic and fulvic acids. The H_2SO_4-P fraction represents insoluble P associated with Ca and Mg minerals and apatite (Walker and Syers 1976; Hedley et al. 1982; Tiessen and Moir 1993; Guo et al. 2000; Wu et al. 2014; Koch et al. 2018; Morshedizad et al. 2018). H_2SO_4 was used instead of HCl (Hedley et al. 1982) because Tiessen et al. (1983) criticized hot HCl as proposed by Hedley et al. (1982) for organic P losses. Total P (P_t) in the different extraction fractions was measured in the supernatants using an ICP-OES while the remaining sediment pellet was used for the next extraction step. The inorganic P (P_i) concentrations in the extracts were determined colorimetrically with the molybdate-blue method as described by Murphy and Riley (1962). The concentration of P_o was estimated by subtracting P_i from P_t. The concentration of not extractable P (Residual-P_c) was calculated as the difference between the sum of the P fractions and the P_t concentration determined after digestion with aqua regia. To compare these calculated Residual-P_c concentrations with the actual residual P in the samples, the solid

sample residue of each sample was also digested with aqua regia after completion of the sequential P fractionation and the concentration of Residual-P_m was measured in these extracts.

5.3.4.P K-*edge XANES analysis*

The P *K*-edge XANES spectra for characterizing P species in the sediment samples were recorded at the Synchrotron Light Research Institute (SLRI) in Nakhon 65 Ratchasima, Thailand on the beamline 8 (BL8). The electron storage ring covered photon energy from 1.25 to 10 keV, operated at 1.2 GeV electron energy, and the beam current was 80–150 mA (Klysubun et al. 2012). The XANES data were collected from dry and fine-ground sediment samples thinly spread on P-free kapton tape (Lanmar Inc. Northbrook, IL, USA) attached to a plastic sample holder. Samples AB1 and RE were diluted to P concentrations < 2 mg P kg^{-1} with SiO_2 powder (to eliminate self-absorption effects; Prietzel et al. 2013) and again ground and homogenized in a mini mill (Pulverisette 23, Fritsch GmbH Milling and Sizing, 55743 Idar-Oberstein, Germany). Data collection was operated in standard conditions with energy calibration by standard pure elemental P and allocating the reference energy (E_0) at 2145.5 eV using the maximum peak of the first derivative spectrum. All spectra were recorded at photon energies between 2045.5 and 2495.5 eV in step sizes of 5 eV (2045.5 to 2105.5 eV and 2245.5 to 2495.5 eV), 1 eV (2105.5 to 2135.5 eV and 2195.5 to 2245.5 eV) and 0.25 eV (2135.5 to 2195.5 eV) with a 13-channel germanium detector in fluorescence mode. The fluorescence mode is used because of its high sensitivity (Klysubun et al. 2012) and because the standard set of P-compounds was already measured in fluorescence mode. Three scans were collected and averaged for each sample.
All P *K*-edge XANES spectra were normalized, and the replicates were merged. Linear combination fitting (LCF) was performed using the ATHENA software package (Ravel and Newville 2005) in the energy range between -20 eV and +30 eV of E_0. The XANES spectral data were baseline corrected in the pre-edge region between 2115 and 2145 eV and normalized in the post-edge region of 2190-2215 eV. The same ranges were used for the reference P *K*-edge XANES spectra to achieve consistency in the following fitting analysis (Prietzel et al. 2016). To achieve the best compatible set of references with each specified sample spectrum, LCF analysis was performed using the combinatorics function of ATHENA software to attain all possible binary to quaternary combinations between all 19 P reference spectra in which the share of each compound was ≥ 10%. The following set of reference P *K*-edge XANES spectra, all recorded in SLRI in fluorescence mode under the same adjustments by Werner and Prietzel (2015) and Prietzel et al. (2016), were used for fitting and calculations; Ca, Al and Fe phytate, noncrystalline and crystalline $AlPO_4$, noncrystalline and crystalline $FePO_4 \cdot 2H_2O$, Ca 5 hydroxyapatite ($Ca_5(OH)(PO_4)_3$), inositol hexakisphosphate (IHP), ferrihydrite–IHP, montmorillonite–Al–IHP, soil organic matter Al–IHP (SOM–Al–IHP), ferrihydrite–orthophosphate, montmorillonite–Al–orthophosphate, SOM–Al–orthophosphate, boehmite–IHP, boehmite–10 orthophosphate, $CaHPO_4$, $Ca(H_2PO_4)_2$ and $MgHPO_4$. The *R*-factor values were used as goodness-of-fit criteria and significant differences between fits were evaluated using the Hamilton test ($p < 0.05$) (Calvin 2013) with the number of independent data

points calculated by ATHENA, estimated as data range divided by core-hole lifetime broadening. The best fits of P reference compound combinations were considered as the most probable P species in the material. If *R* factors of fits with the same number of reference compounds were not significantly different from each other according to the Hamilton test, fit proportions were averaged.

5.3.5. Solution ^{31}P NMR spectroscopy

Phosphorus was extracted for solution ^{31}P NMR analysis using a commonly applied procedure (Doolette et al. 2009; Doolette and Smernik 2011; Vestergren et al. 2012; Vincent et al. 2013). Although there is a risk of sample alteration caused by strongly alkaline conditions and thus an overestimation of the orthophosphate pool may occur, the most commonly used extraction protocol includes shaking the sample for 16 h with a mixture of NaOH and Na_2EDTA and a subsequent lyophilization (Kruse et al. 2015). Furthermore, line broadening in ^{31}P NMR spectra induced by paramagnetic Fe and Mn co-extracted by NaOH and EDTA mixtures remains a challenging issue (Cade-Menun 2005). The sulfide precipitation as a possible post-extraction treatment to reduce line broadening caused by high contents of metal ions and to improve the resolution of spectra was introduced by Vestergren et al. (2012). After lyophilization, Na_2S creating reductive conditions by large sulfide excess is added to the NaOH/Na_2EDTA extracts and as a consequence Fe^{3+} is reduced to Fe^{2+} with a lower affinity for phosphate groups, and thus, less P is eliminated from the solution (Vestergren et al. 2012).

About 1.5 g dry and milled sediment was shaken at ambient temperature for 16 h in 30 mL of extraction solution containing 0.25 M NaOH and 0.05 M Na_2EDTA (soil-to-solution-mass-ratio 1:20). Then the samples were centrifuged for 30 min at 9900*g*. The supernatants were filtered through P-free filters, and 2 mL of the extracts were taken to measure P_t in these EDTA extracts using an ICP-OES. The remaining supernatants were frozen at -80 °C and subsequently lyophilized, yielding in approximately 0.7 to 0.9 g solid material, respectively. After lyophilization, a Na_2S treatment was implemented to remove paramagnetic ions from NaOH/Na_2EDTA sediment extracts (Vestergren et al. 2012; Wang et al. 2017). About 0.1 g of lyophilized material was dissolved in 0.6 mL of a mixture of 0.1 mL 30% NaOD and 7.4 mL D_2O in an Eppendorf vial. To this solution, 0.5 g of $Na_2S \cdot 9H_2O$ powder was added and samples were mixed by vortex briefly. After shaking for 16 h at a horizontal mixer at ambient temperature, the samples were centrifuged at 20,160*g* at 4 °C for 45 min and 0.4 mL of the supernatant was transferred to a 5-mm-diameter NMR tube and 0.013 mL MDPA (methylenediphosphonic acid sodium salt) were added as an internal standard. This Na_2S treatment uncovered some peaks which were not present after the analysis using the single extraction with NaOH/Na_2EDTA of the sediment samples. The differences between these two sample preparations are shown in Fig S1 (Electronic Supplementary Material – ESM). In the sulfide-treated spectra peaks at the monoester and diester region become visible which were not present before.

The solution ^{31}P NMR spectra were recorded using an inverse gated decoupled (IG) pulse sequence on a Bruker Avance 500 spectrometer with a pulse width of 30° (3.3 µs), 0.41 s

aquisition time, 5.0 s pulse delay, 10,000 scans and a temperature of 300 K. Spectra were processed using standard Bruker software (TopSpin 3.5pl7) and plotted with a line-broadening of 1 Hz. The chemical shift scale was referenced to the resonance of the dominant orthophosphate peak at 6.0 ppm. To confirm the assignment of peaks in ^{31}P NMR spectra, spiking was performed on all other P compounds (compounds and chemical shifts in all samples can be found in Table S1 and Table S2 - ESM). Considering an adjustment of the chemical shift of orthophosphate to 6.0 ppm, the peak library of P compounds in ^{31}P NMR spectroscopy by Cade-Menun (2015) could be used as a rough indication for peak identification. P compounds generally appeared close to the resonances given by Cade-Menun (2015) and own spiking experiments have been conducted, confirming the correct allocation of P compounds. The P compound at 5.24 ppm could not be identified. D-Glucose-6-phosphate sodium salt, phytic acid sodium salt hydrate and D-myo-inositol-1,4,5-trisphosphate trisodium salt were spiked to match this unknown compound to one of these standards, but there was no agreement, so they could be excluded. β-Glycerophosphate and AMP appeared as one peak due to their close positions at 4.529 ppm and 4.405 ppm according to Cade-Menun (2015). Thus, their concentrations are given as a sum.

The spectra were integrated and signal intensities were expressed as portion of the sum of area integrals. The contents of the single P compounds were indicated converting their proportions into mg P kg^{-1} sediment from the measured EDTA extracts.

5.3.6. Scanning electron microscopy (SEM) and energy dispersive X-ray micro analysis (EDX)

Particle analysis was done by SEM (Zeiss Merlin Compact) and EDX (Oxford Instruments; Aztec and Inca software). Suspended particulate matter (SPM) preparation was conducted by filtration of the sample onto poly-carbonate nucleopore filters (0.4 µm HTTP), rinsed with distilled water, and dried at room temperature. Later, the samples were covered (vacuum sputter) with elemental carbon for electric conductivity. This preparation prevents carbon analysis of the sample material, but it is the best compromise for analyzing all other elements. A thin coverage of particles on the filter surface is necessary to avoid overlapping of particles for point EDX analysis. The used automated particle analysis procedure allowed the investigation of about 1500 single particles for each sample. This high number ensures the quantification of the found composition by identification of minerals and particle groups. Each single particle was analyzed for standard list of major elements (O, Na, Mg, Al, Si, P, S, Cl, K, Ca, Ti, Mn, Fe, Ba). The chemical composition of the particles is the base for a mineral/particle identification program (INCA feature 5:04, Oxford Instruments) which allows assigning the particle to minerals and particle groups.

EDX in general is a major element analysis method. Modern detectors allow reliable determination of element concentrations down to 1%. Lower values (<0.5%) are critical and detection limit normally is reached at 0.1%, especially if the element peak disappears in the background noise of the spectra. However, this method is favored for findings of element enrichments or binding in minerals and particle groups on single particle level in micrometer

scale. Photographs and control spectra of particles of special interest were taken immediately after the automated particle analysis. The coordinates (*x, y, z*) of all analyzed particles were stored and can be followed back as long as the samples stay in the SEM desk position.
The identification of common minerals or particle groups parallel to the automated particle analyses is based on threshold values of characteristic elements. These threshold values were defined by analyses of standard minerals specifically used in the development of the SEM-EDX method and modified by analyses of samples with known mineral compositions (Leipe et al. 1999). However, besides the additional information about the abundant minerals or particle groups, the whole dataset for each sample can be reworked by statistic software (xls; DataDesk) to check the found clusters of particles in the multi element "space".

5.3.7. Statistical analysis

Data analysis was performed using open-source statistical software R (version 3.4.3). R package *agricolae* was used for Tukey's HSD (honest significant difference) test, which enables multiple comparisons. The significance level was 0.05 (https://cran.r-project.org/web/packages/agricolae/index.html). The Tukey's HSD test was used to find differences in the elemental concentrations between the sediments from various sampling sites. Differences between the P concentrations measured with sequential P fractionation and ^{31}P NMR spectroscopy were tested for significance (*P < 0.05, **P < 0.01, ***P < 0.001) by the Student t test.
Calculation of correlations and regression functions for P contents of the NaOH/Na_2EDTA extracts and different sums of sequential P fractionation was conducted with the help of linear models from the R package *vegan*. Residuals were distributed normally, and thus, prerequisites for regressions were met.
Data of the sediment samples and, additionally, of a set of four soil samples from a study of Koch et al. (2018) were analyzed by nonmetric multidimensional scaling (NMDS). The results of sequential P fractionation, XANES and ^{31}P NMR spectroscopy are presented in the NMDS to give an overview of possible relationships. NMDS was calculated using a function from the *vegan* package in R. Results of the different methods were converted into relative proportions and used as input for calculating NMDS. The shown NMDS analysis was performed using Euclidean distance measure. The stress value is 0.06 and thereby indicates a reliable test performance.

5.4. Results and discussion

5.4.1. Sediment characteristics

Sediment characteristics and elemental concentrations are shown in Tables 1 and 2. Sample RE had the highest P_t contents (3973 mg kg^{-1}) followed by AB1 (3531 mg kg^{-1}) (Table 2). Among all samples, MB had the lowest P_t content (775 mg kg^{-1}). The P_t contents of SB, AB2 and GB ranged between 912 mg kg^{-1} and 1000 mg kg^{-1} and thereby were between the highest and lowest contents of P_t (Table 2).

Amounts of P_t were higher than in offshore sediments from the southeast coast of India and in estuary sediments from US Pacific northwest coast, but the general magnitude is comparable. Mohanty et al. (2018) found P_t contents of 470 to 1220 mg kg^{-1} in sediments from the Bay of Bengal and Watson et al. (2018) P_t contents of 601 to 1366 mg kg^{-1} in sediments from the Columbia River (both determined P by ignition followed by extraction with H_2SO_4), whereas the present sediments had between 775 and 3973 mg P_t kg^{-1} (Table 2).

Relatively high Ca contents indicated by low P/Ca ratios characterized SB (0.01), GB (0.07) and RE (0.08), comparably lower Ca contents and higher P/Ca ratios were found in MB, AB2 and AB1 (Table 2). The highest contents of Mg and Al, also with regard to their ratios of P/Mg and P/Al, were present in GB. Samples AB1, AB2 and MB also contained high Mg (> 8000 mg kg^{-1}) and Al contents (> 16000 mg kg^{-1}), but the ratios of P/Mg and P/Al for AB1 did not reflect this due to the high P_t contents. The samples RE and SB had the lowest contents of Mg and Al compared to the other samples. The highest concentrations of Fe were present in RE (49,608 mg kg^{-1}), whereas the smallest P/Fe ratio was analyzed for GB. The samples RE, AB1 and GB with the largest P_t contents simultaneously had the third highest contents of Fe. Considering the P/Fe ratio, the samples GB, AB2, and MB had the highest Fe amounts in relation to their P_t contents. The smallest amount of Fe was present in SB with the lowest average sediment depth, and AB1 with the greatest sediment depth had the second-highest content of Fe. For Al, samples SB and RE contained the smallest concentration with no significant difference. The Ca amount of our samples decreased with sediment depth in the order SB > RE > GB > MB > AB2 > AB1 (Table 2).

Table 5-2 Elemental concentrations of total P (P_t) Ca, Mg, Al and Fe in mg kg^{-1} and their ratios (P/Ca, P/Mg, P/Al, P/Fe). Significant differences at 5% probability level between samples are designated by different letters (a, b, c, d, e), *n* = 3.

Sample	P_t	Ca	P/Ca	Mg	P/Mg	Al	P/Al	Fe	P/Fe
	mg kg^{-1}	mg kg^{-1}		mg kg^{-1}		mg kg^{-1}		mg kg^{-1}	
RE	3973^{a}	49185^{b}	0.08	3127^{e}	1.27	6321^{d}	0.63	49608^{a}	0.08
SB	912^{c}	93568^{a}	0.01	6139^{d}	0.15	7220^{d}	0.13	21495^{e}	0.04
MB	775^{d}	6783^{d}	0.11	8185^{c}	0.09	16897^{c}	0.05	29311^{d}	0.03
AB1	3531^{b}	5959^{c}	0.59	10453^{b}	0.34	19208^{bc}	0.18	42555^{b}	0.08
AB2	930^{c}	6378^{c}	0.15	9971^{b}	0.09	21665^{ab}	0.04	33687^{c}	0.03
GB	1000^{c}	13476^{c}	0.07	11749^{a}	0.09	25877^{a}	0.04	41886^{b}	0.02

Sediment depth is considered as one important reason for changing elemental concentrations of sediments in many studies (e.g. Jensen and Thamdrup 1993; Leipe et al. 2000; Lukkari et al. 2008; Lukkari et al. 2009). Conditions of oxygen depletion, sediment accumulation rates, pH, and particle sizes vary among different sediment depths and thereby influence the presence of elements and especially P (Lukkari et al. 2008; Lukkari et al. 2009). If the present sediments are arranged vertically from low to high depths, it results in the order SB < RE < GB < MB < AB2 < AB1 whereas SB has an average sediment depth of 3 cm and AB1 of 19.5 cm (Table 1).

Lukkari et al. (2009) completely digested sediment samples and determined elemental compositions by inductively coupled plasma-atomic emission spectroscopy (ICP-AES). They observed mainly an increase of Fe, Al and Ca and a decrease of P_t with rising depths in sediments from the Gulf of Finland in the northeastern Baltic Sea. The decrease in P_t with depth has been explained by P release from sediment based on the patchy bottom topography and limitations in mixing of water in the Baltic Sea in this area (Lukkari et al. 2009). Such a trend is not that clear in our samples, but goes in a similar direction (Table 2). The Ca contents in the present investigation (Table 2) showed a reversed order compared to Lukkari et al. (2009). However, these samples were taken along the Northern Gulf of Finland characterized by a low mean water depth of 37 m and low salinity (Alenius et al. 1998). In contrast, the present sediments originate from different topographic backgrounds with inhomogeneous depths and salinities. The sample span ranges from a lowland river and a shallow brackish water estuary with water depths of 2 m to Baltic Sea sediments with a maximum of 247 m water depth. Different studies emphasized the importance of seafloor water oxygen conditions for nutrient concentrations in the water column (Hille et al. 2005) and, especially, on P release from sediments (Walve et al. 2018). Lukkari et al. (2009) suggest that an accumulation of organic matter and P_o and related intensified oxygen reduction in coastal basins increases the potential for P release from sediment and thereby causes low P contents in sediments from these areas. This indication agrees with the result of the present samples, where MB, SB and AB2 had the lowest P_t contents (Table 2).

Another reason for the wide variation of the P_t contents of the sediments may be the different sampling years of the sediments. The oxygen ventilation of the Baltic Sea is closely connected with the inflow of saltwater from the North Sea (Schinke and Matthäus 1998). Time spans with major inflows and periods of stagnation without inflows of large volumes can have very different lengths (Hille et al. 2005). For example, there was a low inflow activity to the Baltic Sea in the time between the mid-1970s and 2003 (Hille et al. 2005). Due to different inflow activities over the years and, thereby, varying oxygen conditions, the comparability of the P_t contents of the sediment samples remains questionable. Another possible explanation for the heterogeneity of the P_t contents in the sediments could be the fact that in fine sediments there is more P than in coarser ones (Łukawska-Matuszewska and Bolałek 2008).

Although there is no clear increase or decrease of P_t with increasing distance from the coast in all samples, there is a possible ranking of MB < AB2 < GB from lower to higher P_t contents. If the samples RE and SB are excluded due to their riverine and inland water origin and AB1 because of its different sediment depth, the samples MB, AB2 and GB represent a gradient of sediment-P_t in the Baltic Sea with an increasing distance from the coast. Due to an intensive sea floor transport, the absence of oxygen and the limited mixing of bottom water, the conditions for organic matter and P accumulation are favorable in deep basins of the Baltic Sea (Łukawska-Matuszewska and Bolałek 2008). This ranking agrees with an investigation of Łukawska-Matuszewska and Bolałek (2008) where maximum P concentrations were found in clays and silts from deep-water, stratified parts of the Gulf of Gdańsk and lower P concentrations in sediments from the coastal zone.

5.4.2. Merging of results from all P-methods

The NMDS in Fig. 2 merges the results of the P-specific methods sequential P fractionation, P-XANES and ^{31}P NMR spectroscopy. NMDS is a qualified ordination method for ecological data because it does not require normal distribution or linear relationships between variables (McCune et al. 2002). Thus, this NMDS analysis enables a quick overview of the sediments analyzed by the different methods and indicates relationships, which subsequently can be investigated more precisely by two-dimensional comparisons. Additional primary data of P fractionation, XANES and ^{31}P NMR spectroscopy of four soil samples from an agricultural long-term experiment at the University of Rostock were taken from Koch et al. (2018) and integrated in this statistical evaluation to expand the terrestrial-aquatic gradient towards the land. The closer together objects are located in this NMDS the more accordance they show in their results from the three different methods and inversely.

The soils are closely located to each other in the NMDS and distant from the sediments, illustrating more similarities in P speciation among the soils than between soils and sediments. The sediment RE from the River Recknitz at the coast of Northern Germany is close to the soils and, thereby, shows the greatest similarity with the soils. From the P-methods, proportions of resin-P, $NaHCO_3$-P_i and NaOH-P_i from sequential P fractionation and monoester-P from ^{31}P NMR spectroscopy cluster with the soils and the sediment RE. Apart from that, GB and AB2 from the Gotland and Arkona Basin in the central Baltic Sea are situated closer to the H_2SO_4-P fraction in the NMDS. Moreover, GB and AB2 seem to contain higher amounts of the inorganic ortho-P determined with ^{31}P NMR spectroscopy in comparison to the other sediments and soils. Inorganic pyro-P and organic diester P compounds obtained from ^{31}P NMR spectroscopy are located further away in the lower center of NMDS figure indicating little influence on differences within the whole sample set. Results from XANES analyses show overall a separation between the left side of the NMDS including Al-P and Fe-P compounds, clustering with the soils and RE, and the right side representing Ca-P and Mg-P compounds, somehow grouping with the other sediment samples.

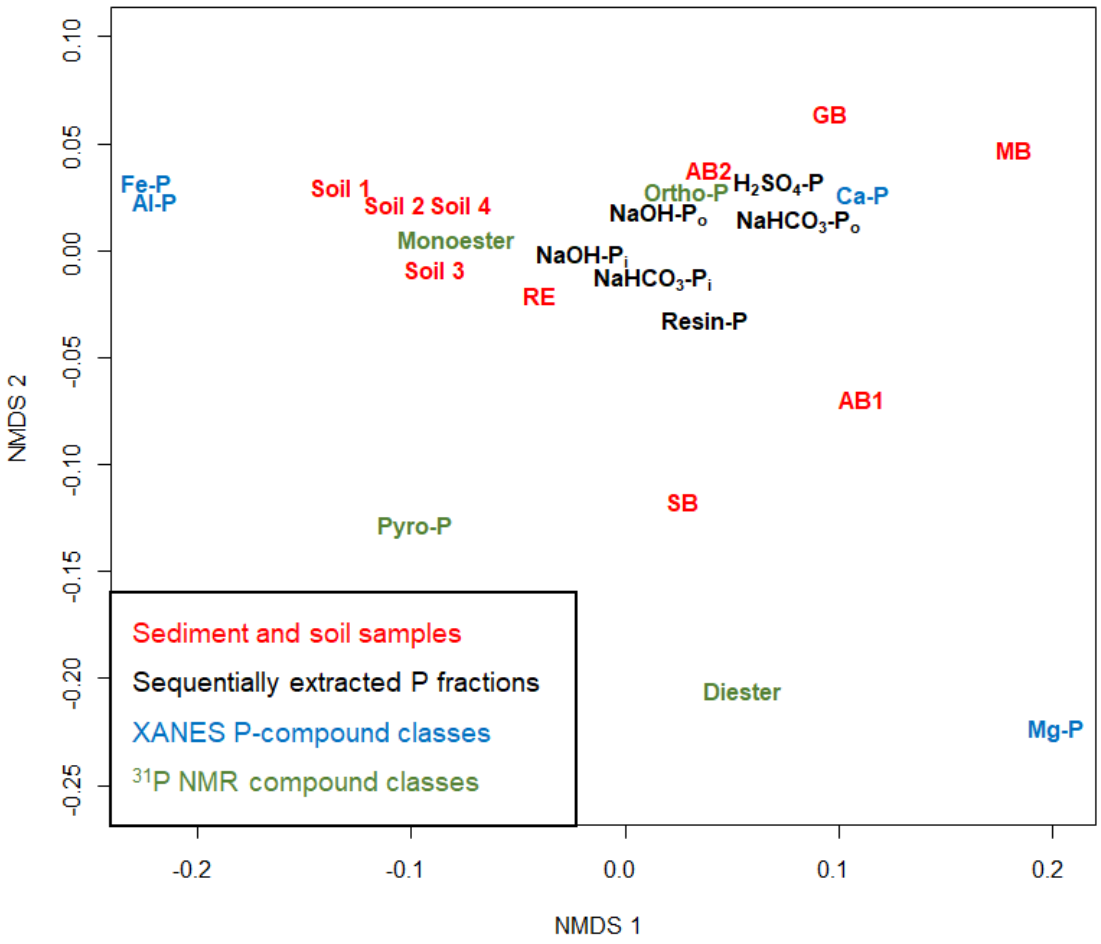

Figure 5-2 Nonmetric multidimensional scaling (NMDS) of sediments (RE, SB, MB, AB1, AB2, GB) and soil samples (from Koch et al. (2018); Soil 1= control, Soil 2 = compost, Soil 3 = TSP, Soil 4 = compost+TSP) with results of sequential P fractionation (fractions: Resin-P, $NaHCO_3$-P_i, $NaHCO_3$-P_o, NaOH-P_i, NaOH-P_o and H_2SO_4-P), XANES analysis (Fe-P, Al-P, Ca-P, Mg-P), and ^{31}P NMR spectroscopy (Monoester, Diester, Ortho-P, Pyro-P).

5.4.3. Sequentially extracted P fractions

The proportions of individual P fractions of P_t were calculated to compare samples with different P_t contents (Table 2). The average P extractability of the samples was 89% of P_t and differed in a range from 77% for GB to 97% for AB1. The proportions of labile P fractions (resin-P; $NaHCO_3$-P_i and $NaHCO_3$-P_o) in the sediment samples were ≤ 9% except for the resin-P of SB (14%) and the $NaHCO_3$-P_i fraction of AB1 (26%) (Table 3). The highest P proportions of all fractions occurred either in the moderately labile NaOH-P_i fraction for RE and AB1 or in the stable H_2SO_4-P fraction of the samples SB, MB, AB2 and GB. Proportions of calculated residual P were between 3 and 23% for all samples and their concentrations lie below the measured residual P values in the solid residues after completion of the sequential P fractionation. Generally, there was a decrease in the proportions of the labile P-fractions resin-P, $NaHCO_3$-P_i, and $NaHCO_3$-P_o with increasing distance from the coast, whereas the proportions of the stable P fractions H_2SO_4-P and residual P increased from land to sea. In the samples RE and SB, the sum of labile P fractions was 14 – 25% and declined to 7 – 17% in AB2 and GB. The summed

proportions of stable P in RE and SB made up 27 – 49% and rose to 61 – 68% in AB2 and GB. The sums of the organic and inorganic moderately labile NaOH-P fractions are 27 – 60% for RE and SB, and dropped to 23 – 25% in AB2 and GB. Opposed to the other samples, AB1 showed higher proportions of labile and moderately labile P fractions and low proportions of stable P. This difference could be explained by the fact that the sampling depth of the sediment AB1 was 18 – 21 cm, whereas all other sampling depths started at the top of the sediment. The sequential P fractionation estimates organic P in sediments as the difference between P_t and P_i determined colorimetrically with the molybdate blue method. The percentage of P_o was highest in SB (30% as sum of $NaHCO_3$-P_o and NaOH-P_o, Table 3), followed by AB2 (26%). The lowest percentages of P_o were in RE (11%) and AB1 (9%).

The decrease of labile P fractions with increasing water depth and distance from the coast can be explained by lower oxygen concentrations in the near-bottom water in deep regions of the Baltic Sea. Łukawska-Matuszewska and Bolałek (2008) found that low oxygen concentrations in deep parts of the Gulf of Gdańsk lowered the percentages of loosely bound P in sediments determined with the sequential extraction method described by Jensen and Thamdrup (1993). In contrast, a gradual increase of loosely bound P in sediments from near shore to offshore occurred on three transects at the southeast coast of India (Mohanty et al. 2018). It is explained by the assumption that high water mixing effects are more present near the coast as in offshore regions, and thus, there are more exchange processes of loosely bound P between sediment and water column (Mohanty et al. 2018). Hence, the different amounts of labile P components developed from a complex interaction of different conditions like regional and climatic characteristics. The reduced proportions of NaOH-P, representing moderately labile P adsorbed to Al- and Fe-oxide minerals, with increasing coastal distance again agree with Łukawska-Matuszewska and Bolałek (2008), who found a decline of Fe-bound P determined with sequential extraction in sediments from the Gulf of Gdańsk with increasing seaward distance from the Vistula River mouth. Coelho et al. (2004) also determined a dominance of Al- and Fe-bound P in sediments from the Mondego estuary at the Atlantic coast of Portugal with high freshwater influence and a decrease of Al-P and Fe-P with increasing salinity and coastal distance. The higher amounts of the stable P fractions H_2SO_4-P and residual P, representing insoluble P associated with Ca and Mg minerals (Hedley et al. 1982), in sediments from the Baltic Proper far away from the coast of Northern Germany agree with the observations that the $CaCO_3$-bound P fraction dominated sediments in the outer area of the Mondego estuary (Coelho et al. 2004) and the increase of Ca-P contents in sediments from near shore to offshore region at the southeast coast of India (Mohanty et al. 2018). The missing trend in the proportions of sediment P_o agrees with (Paytan et al. 2003) who described a considerable transformation from P_o to P_i in the water column and the decrease of the P_o pool with depth by microbial consumption as reviewed by Defforey and Paytan (2018). Furthermore, results of the Hedley fractionation may have been affected by the different drying/grinding pretreatments (Condron and Newman 2011).

Table 5-3 Concentrations (mg kg^{-1}) and percentages (%) of each sequentially exctracted P fraction from total P (P_t), of inorganic P (P_i) and organic P (P_o) in the different P pools Resin-P, $NaHCO_3$-P, NaOH-P, H_2SO_4-P and Residual-P (Residual-P_c = calculated P as the difference between P_t and the sum of all fractions; Residual-P_m = measured residual P in the solid residue after sequential P fractionation) in the sediment samples. Deviations from 100% are caused by rounding errors.

Sample	Resin-P		$NaHCO_3$-P_i		$NaHCO_3$-P_o		NaOH-P_i		NaOH-P_o		H_2SO_4-P		Residual-P_c		Resdiual-P_m	P_t
	mg kg^{-1}	(%)	mg kg^{-1}	(%)	mg kg^{-1}	(%)	mg kg^{-1}	(%)	mg kg^{-1}	(%)	mg kg^{-1}	(%)	mg kg^{-1}	(%)	mg kg^{-1}	mg kg^{-1}
RE	64	(2)	349	(9)	120	(3)	2049	(52)	298	(8)	881	(22)	212	(5)	334	3973
SB	126	(14)	51	(6)	50	(5)	14	(2)	228	(25)	280	(31)	163	(18)	322	912
MB	41	(5)	29	(4)	65	(8)	23	(3)	103	(13)	437	(56)	77	(10)	204	775
AB1	31	(1)	901	(26)	175	(5)	1676	(47)	146	(4)	501	(14)	101	(3)	428	3531
AB2	34	(4)	44	(5)	72	(8)	42	(5)	171	(18)	485	(52)	82	(9)	231	930
GB	4	(0)	25	(3)	42	(4)	102	(10)	150	(15)	450	(45)	227	(23)	517	1000

5.4.4.P K-*edge XANES analysis*

The XANES spectra where characterized by an intense white line peak at around 2152 eV (spectra are shown in Fig. S2 - ESM). Differences in the post-edge region and in single peak intensities were obvious between most samples. The linear combination fitting (LCF) of spectra using 19 spectra of P reference compounds indicated that the P composition of all sediment samples can be described by Ca compounds such as Ca-phytate, Ca-hydrogenphosphate ($CaHPO_4$), Ca-dihydrogenphosphate ($Ca(H_2PO_4)_2$), Ca-5-hydroxyapatite, and other inorganic and organic P compounds such as Mg-hydrogenphosphate ($MgHPO_4$), inositol-hexakisphosphate (IHP), amorphous Al-phosphate ($AlPO_4$ amorphous), and ferrihydrite–orthophosphate (ferrihydrite PO_4) (Table 4). Calcium-associated P species were summed for interpretation because quantitative XANES cannot detect one chemical species certainly in the presence of high proportions of a different species of the same element (Pickering et al. 1995). Summed Ca-associated P compounds reflect the most dominant proportion (53 to 100%) in the samples SB, MB, AB1, AB2 and GB (Table 4). In RE the proportion of Ca-associated P (34%) is between the percentages of P associated with Al (29%) and Fe (37%). Significant proportions of the P_o compound IHP were determined in SB (13%) and MB (11%). Phosphorus associated with Mg was found in SB (13%) and in AB1 (47%) (Table 4). The samples RE, SB, MB and AB1 contained P compounds associated with several elements, whereas AB2 and GB contained exclusively Ca-bound P.

Table 5-4 Proportions of Ca-phytate, Ca-hydrogenphosphate ($CaHPO_4$), Ca-dihydrogenphosphate ($Ca(H_2PO_4)_2$, Ca-hydroxyapatite, Mg-hydrogenphosphate ($MgHPO_4$), inositol hexakisphosphate (IHP), Al-phosphate ($AlPO_4$ amorphous) and ferrihydrite phosphate (ferrihydrite PO_4) in % in the samples determined with *K*-edge XANES analysis, including *R* factor as a goodness-of-fit criterion.

Sam-ple	Ca phytate	Ca HPO_4	Ca $(H_2PO_4)_2$	Ca hydroxy apatite	$MgHPO_4$	IHP	$AlPO_4$ amor-phous	Ferri-hydrit e PO_4	*R* factor
				in %					
RE	34						29	37	0.0050
SB	74				13	13			0.0020
MB	47			15		11			0.0043
AB1	24	29			47				0.0050
AB2	41	31	28						0.0072
GB	58	12		30					0.0061

Although XANES is able to divide inorganic P into distinct chemical forms (Kruse and Leinweber 2008), it cannot distinguish P adsorbed by certain minerals and by organic matter (Ajiboye et al. 2008a) because of similar energy spectra (Peak et al. 2002). Hence, the proportions of IHP found in the sediments have to be taken with caution. RE from the river Recknitz, located at the coast of Northern Germany, was the only sample containing Fe-associated P. Koch et al. (2018) derived from similar P-XANES that Fe-associated P was always the most dominant proportion in a Stagnic Cambisol soil located at Rostock, Germany (near the Baltic Sea coast). Since Fe-P

components are abundant in soils in Northern Germany, it is conceivable that such terrestrial influence explains the occurrence of Fe-bound P exclusively in the sediment RE with the shortest distance to the coast and the shallowest water depth and, thus, the most terrestrial influence. Kraal et al. (2015) discovered a continuous decrease of Fe-associated P with depth as determined by XANES in sediments from 855 to 1013 m below sea surface at the Murray Ridge in the Northern Arabian Sea. The Fe-P contents analyzed with XANES in the sediments from the Arabian Sea ranged from 63% in the shallowest sample to 0% in the deepest (Kraal et al. 2015a). Due to the fact that the sediments of the Arabian Sea come from the oxygen minimum zone, Kraal et al. (2015) explained the presence of Fe-P as a result of reductive dissolution-precipitation reactions under anoxic and non-sulfidic conditions. The content of Fe-associated P in RE is 37% and between the percentages of the sediments from the Arabian Sea. This occurrence can be attributed to an active adsorption onto precipitated Fe rather than reductive P diagenesis reactions because of the shallow sampling depth of RE and the availability of oxygen (Kraal et al. 2015a). Li et al. (2015) also detected predominantly Fe-bound P components in a terrestrial influenced region with chemical extraction, ^{31}P NMR spectroscopy, XANES and EXAFS in sediments from the Chesapeake Bay at the east coast of North America. The increase of Ca-bound P from 34% in RE to 100% in AB2 and GB with growing distance from the coast and increasing sampling depths again agreed with Kraal et al. (2015) who discovered by P-XANES increasing Ca-P contents with increasing depth in sediments from the Arabian Sea. The amount of Ca-associated P in the shallowest sediment from the Arabian Sea was 17% and in the deepest sediment 50% (Kraal et al. 2015a). These authors called this development „a transition with depth of Fe-associated P to Ca-P“. Frankowski et al. (2002) stated that a rise in Ca-P in sediments of Pomeranian Bay in the Baltic Sea went hand in hand with a decline in Fe-P and inversely; however, these results were exclusively determined by a sequential extraction scheme adapted for bottom sediments and not confirmed by other methods. In line with these outcomes, small proportions of Fe- and loosely bound P were found in deep parts of the Gulf of Gdańsk associated with lower oxygen concentrations (Łukawska-Matuszewska and Bolałek 2008). Even at locations like the Pomeranian Bay of the Baltic Sea, Ca-bound P is the dominant form of P in sediments (Frankowski et al. 2002). Less Fe-bound P compounds can also be found with increasing seaward distance from river mouths in the area of the Gulf of Gdańsk (Łukawska-Matuszewska and Bolałek 2008). The authors explain this finding by the correlation that fine sediments contain more P than coarse sediments and by the fact that P in rivers is mainly transported adsorbed onto Fe oxides and the studied river had high percentages of Fe oxides.

5.4.5. Solution ^{31}P NMR spectroscopy

The average proportion of P extracted with NaOH/Na_2EDTA was 59% P_t, and it ranged from 41% in MB to 88% in RE (Table 5). Results from ^{31}P NMR spectroscopy showed that orthophosphate was the most dominant P compound in all samples. Furthermore, the following P compounds occurred in the sediments: *α*-glycerophosphate (*α*-glycerol), *β*-glycerophosphate

(*β*-glycerol), adenosine 5‘ monophosphate (AMP), a nonassigned P compound belonging to the orthophosphate monoester region between 5.5 and 3.3 ppm, deoxyribonucleic acid (DNA) and inorganic pyrophosphate (pyro-P) (Cade-Menun 2015) (spectra given in Fig. S3 - ESM). β-Glycerophosphate and AMP were identified in all samples except for MB. DNA, which signals appear in the diester region, was present in only small proportions in RE and AB1 and a comparably high amount in SB (17%). Pyro-P appeared at -4.1 ppm in RE and SB. This resonance lies in the region of polyphosphates determined by Cade-Menun (2015). Organic P was summarized from orthophosphate monoesters and orthophosphate diesters. The percentage of P_o determined with ^{31}P NMR spectroscopy was highest in AB2 (51%, sum *β*-glycerol/AMP and unknown P compound), followed by SB (43%, sum of *α*-glycerol, *β*-glycerol/AMP and DNA). Furthermore, there were no P_o compounds detected by ^{31}P NMR spectroscopy in MB and very small portions in AB1 (6%) and GB (8%).

The predominance of ortho-P in all samples coincides with an investigation of estuary sediments from the Columbia River, USA, where ortho-P made up 71 to 84% of P_t determined with ^{31}P NMR spectroscopy (Watson et al. 2018). Orthophosphate diesters can be rapidly degraded to orthophosphate monoesters during sample preparation and extraction (Turner et al. 2003). For this reason, the absence or low proportions of diesters in the sediments can be explained, at least partly, by the extraction time of 16 h used in the present study. The compounds *α*- and *β*-glycerol, mainly present in RB and SB, are commonly known diester hydrolysis products (Cade-Menun and Liu 2014) and could originate from small quantities of diesters existing before sample extraction (Koch et al. 2018). Pyrophosphates and some orthophosphate may be also breakdown products of polyphosphates in the NaOH extract (Hupfer et al. 1995). Nevertheless, the quantities of hydrolysis products should be very small and will not have major consequences on the results (Koch et al. 2018). Pyro-P was exclusively present in RE and SB which were taken from 0 - 10 cm and 0 - 6 cm depths of sediment, agreeing with Ahlgren et al. (2005) who found pyro-P only in the upper centimeters of sediment cores from a lake in Sweden. Although MB, AB2 and GB were also taken in sediment depths starting at 0 cm, they reach up to 30 cm and so the share of the upper centimeters is small compared to RE and SB. According to Condron et al. (1985), pyrophosphates contribute to biological P cycling performed by microorganisms in surface sediments and soils. The variety of different mono- and diester P compounds decreased with increasing distance from the coast. In RE and SB, two orthophosphate monoesters and one orthophosphate diester were present, whereas in AB1 one monoester and one diester P compound, in AB2 two orthophosphate monoesters and in GB only one P monoester were found. Ahlgren et al. (2005) stated a general decrease of mono-, diester- and pyro-P with increasing sediment depth which goes along with the decline of different P compounds in our samples with increasing water and sediment depths. This could be explained by ongoing degradation processes over time (Ahlgren et al. 2005).

Table 5-5 P contents from NaOH/Na_2EDTA extracts (P_{EDTA}) in mg kg^{-1}, proportions of NaOH/Na_2EDTA extracted P of total P (% P_t) of the sediment samples and contents of the compounds orthophosphate (ortho-P), *α*-glycerophosphate (*α*-glycerol), *β*-glycerophosphate and adenosine-5'-monophosphate (*β*-glycerol/AMP), deoxyribonucleic acid (DNA), pyrophosphate (Pyro-P) and unknown compounds in mg kg^{-1} and % determined with ^{31}P nuclear magnetic resonance spectroscopy (^{31}P NMR).

Sample	P_{EDTA}	% P_t	ortho-P		*α*-glycerol		*β*-glycerol/AMP		DNA		Pyro-P		unknown	
	mg kg^{-1}	%	mg kg^{-1}	(%)	mg kg^{-1}	(%)	mg kg^{-1}	(%)	mg kg^{-1}	(%)	mg kg^{-1}	(%)	mg kg^{-1}	(%)
RE	3505	88	2753	(79)	120	(3)	176	(5)	295	(8)	160	(5)		
SB	464	51	155	(33)	40	(9)	80	(17)	78	(17)	111	(24)		
MB	314	41	314	(100)										
AB1	2937	83	2752	(94)			90	(3)	96	(3)				
AB2	399	43	194	(49)			107	(27)					97	(24)
GB	504	50	465	(92)			39	(8)						

5.4.6. Particle composition analyzed with SEM-EDX

The numbers of identified particles of each particle group in the sediments and a soil sample are shown in Table S4 (ESM). Approximately 1500 particles were analyzed in each sample. The percentage of classified particles ranged from 55% in RE to 90% in SB. The sample RE contained 215 Fe-phosphate particles and, thereby, the highest number of particles classified as Fe-phosphates among all samples. In the soil and the other sediment samples, 0 to 8 Fe-phosphate particles were found. In SB the number of calcite particles (601) was very high compared to the other samples (1 to 8 calcite particles). The particle number of Ca phosphates was comparably low in all samples and ranged from 1 in the soil sample to 7 in GB. About 12 poly-phosphate particles were detected in RE. In the other samples, this number ranged from 0 to 3 poly-PO_4 particles. Poly-P particles are organic or inorganic P compounds containing too little percentages of one distinct element beside P to allow an assignment to any other specific particle group. Most likely these poly-phosphate particles resulted from microbiological activity (Kulakova et al. 2011). In RE and SB, more poly-PO_4 particles existed than in MB, AB2 and GB; thus, the microbiological activity may be higher in sediments near the coast compared to deeper zones of the Baltic Sea. Particles assigned to the class of organic matter/chitin appeared in all sediments except AB2. The number ranged from one organic matter/chitin particle in MB to 115 particles in RE. These particles contain between 4 and 14% P and, thereby, form an important group of P containing particles in the examined sediments. Other frequently occurring particle classes in the sediments and soil were SiO_2 (opal and quartz), illite minerals, potash feldspar and albite with P contents of 0 to a maximum of 13%. Authigenic pyrite was abundant in all samples with exception of the soil and contained small P contents of 0 to 5%. Pyrite is typically formed in anoxic sediments in the Baltic Sea and can be found suspended in the water column as well (Leipe et al. 2000).

Figure 3 displays four exemplary micrographs of different particles found in the sediments. The Fe-phosphate particle from RE (Fig. 3a) had an elemental composition of 41% O, 37% Fe and 17% P (elemental proportions in Table S3 - ESM). The P content of all Fe phosphates in the sediments ranged from 5 to 18%. The displayed calcite particle from SB (Fig. 3b) is nearly P-free, but the P content of other calcite particles ranged from 0 to 19% in all samples (Table S4 - ESM), and thus, calcite can play a role for P-binding and transport by endogenous P removal from the water body via co-precipitation of P with $CaCO_3$ (Avilés et al. 2006). An organic poly-P particle from the sample RE is displayed in Fig. 3c. This polyphopsphate, as hint for microbiological activity, contains about 47% O and 30% P. The P content of poly-P particles in all sediments ranged from 20 to 30%, and thereby, this is the most P-rich particle class among all identified particles. Figure 3d shows a Ca-phosphate, more precisely a fluorapatite, from AB1 with 39% O, 34% Ca, 17% P, and 6% F. A small number of Ca-phosphates was present in each sample, and their P contents ranged from 11 to 20%, and thus, Ca-phosphate was the second most P-rich particle class. Ca-phosphates can have their origin from detritus minerals, fertilizers, and soils parent materials in Mecklenburg-West Pomerania such as glacial till (Nausch et al. 2017).

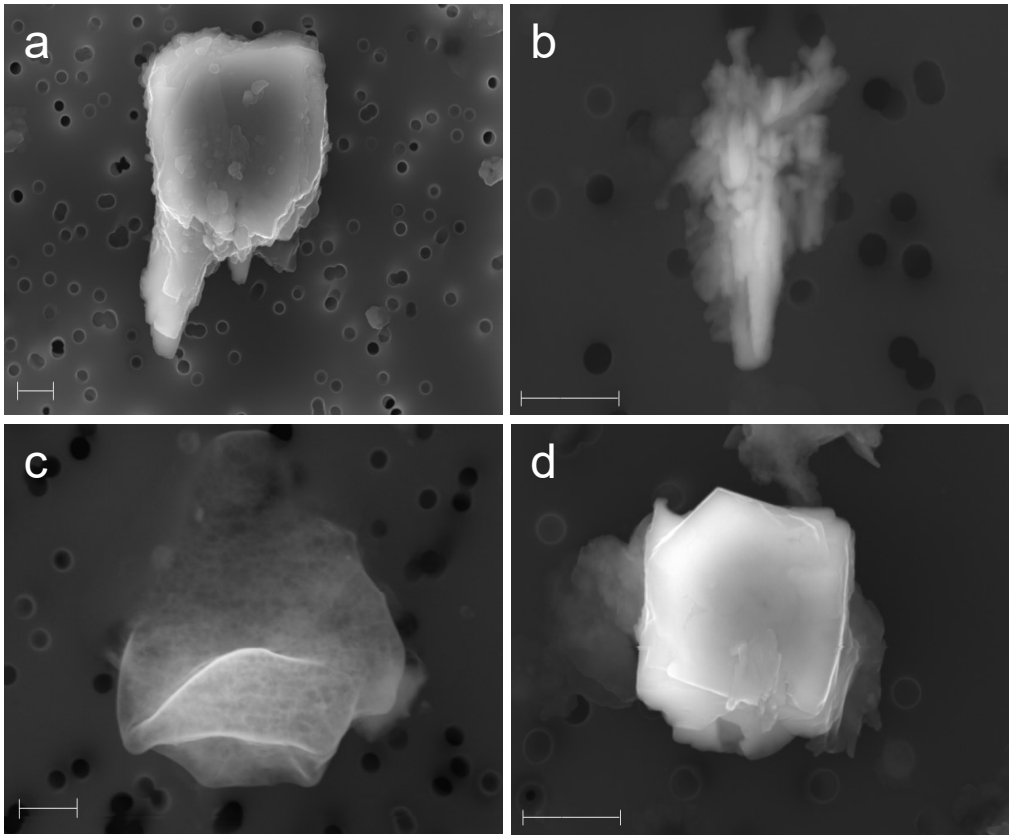

Figure 5-3 Electron micrographs of the particels Fe phosphate (a), calacite (b), poly phosphate (c) and Ca phosphate (d) determined in the sediments RE, SB, and AB1 with SEM-EDX. The given scale in each picture represents the length of 1 µm.

5.4.7. Summarizing discussion

Although the proportions of P_o from the sequential P fractionation (seq-P) (summed percentages from Table 3) can be calculated only indirectly, the P_o sums can be compared with the results of ^{31}P NMR spectroscopy (percentage data not shown), and this revealed reasonable results. Both methods showed highest P_o percentages from P_t contents for SB (seq-P_o: 30% and NMR-P_o: 43%) and AB2 (seq-P_o: 26% and NMR-P_o: 27%). The regression function for P_o contents of sequential P fractionation and ^{31}P NMR spectroscopy in mg kg^{-1} (seq-P_o = 0.41 NMR-P_o + 193.65; r^2 = 0.88**) justifies this relationship. The sequential extraction may underestimate P_o because of hydrolytic breakdowns due to the acid and alkaline extractants used during the fractionation (Golterman 1982). For MB, ^{31}P NMR spectroscopy did not detect P_o although the sequential P fractionation found some P_o even though in low contents (Table 3). The detection limit of ^{31}P NMR spectroscopy is affected by the concentration of P_t relative to the concentration of paramagnetic ions of the sample as well as by the number of scans which were collected (McDowell and Stewart 2005). The lower P_t content of MB compared to the other samples may explain the absence of P_o components determined with ^{31}P NMR spectroscopy.

There was a significant correlation between the P contents of the NaOH/Na_2EDTA extracts for ^{31}P NMR spectroscopy (NMR-P) and the sum of the fractions resin-P, $NaHCO_3$-P_i, $NaHCO_3$-P_o, NaOH-P_i, and NaOH-P_o from the sequential P fractionation, which corresponds to the extraction

power of NaOH/Na_2EDTA (seq-P = 0.89 NMR-P – 7.39; r^2 = 0.97***). A comparison of the amount of inorganic P from the NaOH/Na_2EDTA extracts for ^{31}P NMR spectroscopy (sum of ortho-P and pyro-P = NMR-P_i) and the inorganic P fractions resin-P, $NaHCO_3$-P_i, and NaOH-P_i (seq-P_i) of the sequential P fractionation showed a significant correlation with a slope close to unity (seq-P_i = 0.94 NMR-P_i – 152.57; r^2 = 0.99***). The sequential fractionation extracted on average 89% P_t (sums from Table 3) from the sediments, and this proportion was above the average extractability of 59% using the NaOH/Na_2EDTA for ^{31}P NMR (Table 5). Nonetheless, the strong correlations between results of both methods show that NaOH/Na_2EDTA was well suited as extractant for ^{31}P NMR spectroscopy. As these NMR measurements require liquid samples, the NaOH/Na_2EDTA extract has been approved to be the ideal extractant also in the majority of other studies (Cade-Menun and Liu 2014).

Results of XANES analysis and sequential P fractionation in the present study generally agreed for most samples. Sample RE showed high proportions in the fraction of NaOH-P_i (Table 3), representing inorganic P sorbed and fixed by aluminum- and iron (hydr)oxides and according to XANES analysis, $AlPO_4$ and ferrihydrite PO_4 occurred in this sample (Table 4). Looking at all sediment and soil samples, no significant correlation could be identified between Fe-P, Al-P compounds determined with XANES and the corresponding fraction of NaOH-P_i from sequential P fractionation. This could be due to the fact that Fe-P and Al-P compounds determined with XANES occurred exclusively in RE among all sediments. The high proportions of Ca-associated P determined with XANES in GB, AB2, MB, and SB correspond with the great percentages in the fractions of H_2SO_4-P and residual P in the sequential fractionation although there was no significant correlation between the percentages of Ca-P determined with XANES (Table 4) and the sum of the portions of H_2SO_4-P and residual-P_c from sequential P fractionation (r^2 = 0.47).

The application of SEM-EDX with single particles as a method complementary to sequential P fractionation, XANES and ^{31}P NMR spectroscopy of bulk or extracted samples revealed a greater diversity in P-containing mineral phases, which could not be detected by any of the other methods. For instance, *n* = 24 mineral phases contained P and were detected in at least in one of the samples (Table S4 - ESM). Even if not all elements and P compounds determined with sequential P fractionation, XANES and ^{31}P NMR spectroscopy can be discovered with SEM-EDX at the single particle level, the general increase of more stable P compounds towards the Baltic Proper is supported. The high number of Fe-P particles found with SEM-EDX in RE (Table S4 - ESM) coincides (1) with the high Fe concentration determined by microwave-assisted digestion with aqua regia in this sample (Table 2), (2) with 52% of P in the NaOH-P_i fraction (commonly interpreted as Al- and Fe-bound P) (Table 3), and (3) with XANES that showed RE as the only sample containing Fe-P (Table 4). This confirms the abundance of Fe phosphates that are transported in waterways of nearby catchments in the lowlands of northeastern Germany (Nausch et al. 2017). Thus, it seems reasonable that the highest number of Fe-P particles present in RE has a riverine origin. The maximum of Ca-P analyzed with SEM-EDX in GB corresponds with the H_2SO_4-P in sequential fraction and Ca-P in XANES, both very high in GB. The exemplary electron micrograph of the Ca phosphate (Fig. 2d) from AB1 has a

crystalline structure with sharp edges which indicates an authigenic development of these particles without long transport pathways.

The larger abundance of Fe-bound P compounds in soils and the coastal sediment RE agrees with a transect from Vistula river mouth into the Gdańsk Bay (Poland) in which the Fe concentration in suspended particulate matter in water decreased by factor 5.2 over about 70 km from shore towards the sea (Pempkowiak et al. 2000). This decrease in pedogenic Fe as binding partner for P, contrary to the Ca-P-rich sediment GB, most distant from the coast, corresponds to the finding that water saturation with respect to calcite and aragonite is highest in the Gotland Sea of the Baltic Sea (Tyrell et al. 2008) indicating favourable conditions for the precipitation of Ca-P-minerals. In this context Ready et al. (1999) reviewed that Fe-P is unstable, whereas Ca-bound P compounds are relatively stable and not readily available. Such a hypothetic transition of Fe-associated P (coastal-near, subjected to oxic/anoxic fluctuations) to Ca-associated P with rising influence of sea and simultaneously increasing water depths (constant hypoxic or anoxic conditions), agrees with a sediment investigation along a depth transect in the Arabian Sea (Kraal et al. 2015a). Thus, in general, our data set partly reflects this concept of Fe-P to Ca-P transitions although there was no perfect gradient, possibly due to the confounding effects of different sediment depths sampled, sampling years, sample pretreatments, etc. Furthermore, discussing the importance of source region, suspension/sediment transport and within-sediment processes for the P speciation would require simultaneous determination of environmental conditions such as texture, redox, salinity, and pH.

5.5. Conclusions

1. Since the sequential P fractionation and ^{31}P NMR spectroscopy agreed in the proportions of P_o and P_i, and sequential P fractionation and XANES spectroscopy yielded similar proportions of Al-P, Fe-P and Ca-P in some samples and the latter was confirmed by SEM-EDX at the single-particle level, overall, these methods are considered as complementary, even though they assessed different physical and chemical sample properties. Therefore, this approach appears straightforward in environmental P research.
2. Each method indicated differences among samples in their P species that might point to transformations from relatively labile towards more stable P compounds with an increasing aquatic influence from the coast of Northern Germany to the open Baltic Sea. Although P speciation in sediments results from initial P speciation at the source region and P dynamics during transport and at the given location, we draw the preliminary cautious conclusion that redox cycles and changes in ion concentrations, e.g., due to the impact of saltwater, are important factors in the fate of P at terrestrial-aquatic boundaries.
3. To establish the importance of redox conditions and ion concentrations in forming stable P compounds, additional sediments from diverse aquatic systems and sample transects from soil over coastal areas to sediments need to be investigated by complementary P-speciation methods along with the pertinent environmental conditions. If the reductive loss

of Fe-P in favor of Ca-P with increasing aquatic influence is a common principle, eventually technical solutions can be developed to capture P along its transport pathways from land to sea to reduce P inputs to the Baltic Sea according to the HELCOM agreement.

5.6. Acknowledgements

The authors thank Constantin Recknagel (Leibniz Institute for Baltic Research Warnemünde) for his permission to use the samples. Furthermore, we would like to thank Elena Heilmann, Britta Balz and Christoph Jahnke (Soil Science, University of Rostock) for analytical help during P fractionation and ICP measurement. We also wish to thank Heike Borgwaldt (Institute for Chemistry, University of Rostock) who helped with the analytical work of ^{31}P NMR spectroscopy, Kai-Uwe Eckhardt (Soil Science, University of Rostock) for his support in statistical questions and Sascha Plewe (Leibniz Institute for Baltic Research Warnemünde) for his help with the SEM-EDX analyses. Finally, we are grateful to Prof. Jörg Prietzel (Department of Soil Science, Technical University of Munich) for providing the P XANES reference spectra and to the technical staff at beamline 8 of SLRI for their friendly support.

5.7. Funding

This research was funded by the Leibniz Association within the scope of the Leibniz ScienceCampus Phosphorus Research Rostock (www.sciencecampus-rostock.de).

5.8. Conflict of Interest

The authors declare that they have no conflict of interest.

5.9. References

Ahlgren J, Tranvik L, Gogoll A, et al (2005) Sediment depth attenuation of biogenic phosphorus compounds measured by 31P NMR. Environ Sci Technol 39:867–872. doi: 10.1021/es049590h

Aigars J (2001) Seasonal variations in phosphorus species in the surface sediments of the Gulf of Riga, Baltic Sea. Chemosphere 45:827–834. doi: 10.1016/S0045-6535(01)00121-7

Ajiboye B, Akinremi OO, Hu Y, Jürgensen A (2008) XANES speciation of phosphorus in organically amended and fertilized vertisol and mollisol. Soil Sci Soc Am J 72:1256. doi: 10.2136/sssaj2007.0078

Alenius P, Myrberg K, Nekrasov A (1998) The physical oceanography of the Gulf of Finland: A review. Boreal Environ Res 3:97–125

Avilés A, Rodero J, Amores V, et al (2006) Factors controlling phosphorus speciation in a Mediterranean basin (River Guadalfeo, Spain). J Hydrol 331:396–408. doi: 10.1016/j.jhydrol.2006.05.024

Bai X, Ding S, Fan C, et al (2009) Organic phosphorus species in surface sediments of a large, shallow, eutrophic lake, Lake Taihu, China. Environ Pollut 157:2507–2513. doi: 10.1016/j.envpol.2009.03.018

Beauchemin S, Hesterberg D, Chou J, et al (2003) Speciation of phosphorus in phosphorus-enriched agricultural soils using X-ray absorption near-edge structure spectroscopy and chemical fractionation. J Environ Qual 32:1809. doi: 10.2134/jeq2003.1809

Bonsdorff E, Blomqvist EM, Mattila J, Norkko A (1997) Coastal eutrophication: Causes, consequences and perspectives in the archipelago areas of the Northern Baltic Sea. Estuar Coast Shelf Sci 44:63–72. doi: 10.1016/S0272-7714(97)80008-X

Cade-Menun B, Liu CW (2014) Solution phosphorus-31 nuclear magnetic resonance spectroscopy of soils from 2005 to 2013: A review of sample rreparation and experimental parameters. Soil Sci Soc Am J 78:19. doi: 10.2136/sssaj2013.05.0187dgs

Cade-Menun BJ (2005) Characterizing phosphorus in environmental and agricultural samples by 31P nuclear magnetic resonance spectroscopy. Talanta 66:359–371. doi: 10.1016/j.talanta.2004.12.024

Cade-Menun BJ (2015) Improved peak identification in 31P-NMR spectra of environmental samples with a standardized method and peak library. Geoderma 257–258:102–114. doi: 10.1016/j.geoderma.2014.12.016

Calvin S (2013) XAFS for everyone. CRC Press p 427

Coelho JP, Flindt MR, Jensen HS, et al (2004) Phosphorus speciation and availability in intertidal sediments of a temperate estuary: Relation to eutrophication and annual P-fluxes. Estuar Coast Shelf Sci 61:583–590. doi: 10.1016/j.ecss.2004.07.001

Condron LM, Goh KM, Newman RH (1985) Nature and distribution of soil phosphorus as revealed by a sequential extraction method followed by 31P nuclear magnetic resonance analysis. J Soil Sci 36:199–207. doi: 10.1111/j.1365-2389.1985.tb00324.x

Condron LM, Newman S (2011) Revisiting the fundamentals of phosphorus fractionation of sediments and soils. J Soils Sediments 11:830-840. doi: 10.1007/s11368-011-0363-2

Defforey D, Paytan A (2017) Phosphorus cycling in marine sediments: Advances and challenges. Chem Geol. doi: 10.1016/j.chemgeo.2017.12.002

Dellwig O, Leipe T, März C, et al (2010) A new particulate Mn-Fe-P-shuttle at the redoxcline of anoxic basins. Geochim Cosmochim Acta 74:7100–7115. doi: 10.1016/j.gca.2010.09.017

Doolette AL, Smernik RJ, Dougherty WJ (2009) Spiking improved solution phosphorus-31 nuclear magnetic resonance identification of soil phosphorus compounds. Soil Sci Soc Am J 73:919. doi: 10.2136/sssaj2008.0192

Emeis K, Christiansen C, Edelvang K, Jähmlich S, Kozuch J, Laima M, Leipe T, Löffler A, Lund-Hansen LC, Miltner A, Pazdro K, Pempkowiak J, Pollehne F, Shimmield T, Voss M, Witt G (2002) Material transport from the near shore to the basinal environment in the southern Baltic Sea, II: Synthesis of data on origin and properties of material. J Marine Syst 35:151-168

Ernstberger H, Edwards AC, Balls PW (2004) The distribution of phosphorus between soluble and particulate phases for seven Scottish East Coast rivers. Biogeochemistry 67:93–111. doi: 10.1023/B:BIOG.0000015319.82299.83

Frankowski L, Bolałek J, Szostek A (2002) Phosphorus in bottom sediments of Pomeranian Bay (Southern Baltic - Poland). Estuar Coast Shelf Sci 54:1027–1038. doi: 10.1006/ecss.2001.0874

Golterman HL (1982) Differential extraction of sediment phosphates with NTA solutions. Hydrobiologia 91–92:683–687. doi: 10.1007/BF00000067

Gunnars A, Blomqvist S (1997) Phosphate exchange across the sediment-water interface when shifting from anoxic to oxic conditions - An experimental comparison of freshwater and brackish-marine systems. Biogeochemistry 37:203–226. doi: 10.1023/A:1005744610602

Guo F, Yost RS, Hue NV, et al (2000) Changes in phosphorus fractions in soils under intensive plant growth. Soil Sci Soc Am J 64:1681. doi: 10.2136/sssaj2000.6451681x

Hedley MJ, Stewart JWB, Chauhan BS (1982) Changes in inorganic and organic soil phosphorus fractions induced by cultivation practices and by laboratory incubations. Soil Sci Soc Am J 46:970. doi: 10.2136/sssaj1982.03615995004600050017x

Hupfer M, Lewandowski J (2008) Oxygen controls the phosphorus release from lake sediments - a long-lasting paradigm in limnology. Internat Rev Hydrobiol 93:415-432. doi:10.1002/iroh.200711054

Hesterberg D, Zhou W, Hutchison KJ, et al (1999) XAFS study of adsorbed and mineral forms of phosphate. J Synchrotron Radiat 6:636–638. doi: 10.1107/S0909049599000370

Hille S, Nausch G, Leipe T (2005) Sedimentary deposition and reflux of phosphorus (P) in the Eastern Gotland Basin and their coupling with P concentrations in the water column. Oceanologia 47:663–679

Hupfer M, Gächter R, Giovanoli R (1995) Transformation of phosphorus species in settling seston and during early sediment diagenesis. Aquat Sci 57:305–324. doi: 10.1007/BF00878395

Iglesias ML, Devesa-Rey R, Pérez-Moreira R, et al (2011) Phosphorus transfer across boundaries: From basin soils to river bed sediments. J Soils Sediments 11:1125–1134. doi: 10.1007/s11368-011-0399-3

Jensen HS, Mortensen PB, Andersen F 0., et al (1995) Phosphorus cycling in a coastal marine

sediment, Aarhus Bay, Denmark. Limnol Oceanogr 40:908–917. doi: 10.4319/lo.1995.40.5.0908

Jensen HS, Thamdrup B (1993) Iron-bound phosphorus in marine sediments as measured by bicarbonate-dithionite extraction. Hydrobiologia 253:47–59. doi: 10.1007/BF00050721

Kar G, Hundal LS, Schoenau JJ, Peak D (2011) Direct chemical speciation of P in sequential chemical extraction residues using P *K*-edge X-ray absorption near-edge structure spectroscopy. Soil Sci 176:589–595. doi: 10.1097/SS.0b013e31823939a3

Kleeberg A, Dudel GE (1997) Changes in extent of phosphorus release in a shallow lake (Lake Großer Müggelsee; Germany, Berlin) due to climatic factors and load. Mar Geol 139:61–75

Klysubun W, Sombunchoo P, Deenan W, Kongmark C (2012) Performance and status of beamline BL8 at SLRI for X-ray absorption spectroscopy. J Synchrotron Radiat 19:930–936. doi: 10.1107/S0909049512040381

Koch M, Kruse J, Eichler-Löbermann B, et al (2018) Phosphorus stocks and speciation in soil profiles of a long-term fertilizer experiment: Evidence from sequential fractionation, P *K*-edge XANES, and31P NMR spectroscopy. Geoderma 316:115–126. doi: 10.1016/j.geoderma.2017.12.003

Kraal P, Bostick BC, Behrends T, et al (2015) Characterization of phosphorus species in sediments from the Arabian Sea oxygen minimum zone: Combining sequential extractions and X-ray spectroscopy. Mar Chem 168:1–8. doi: 10.1016/j.marchem.2014.10.009

Kraal P, Slomp CP (2014) Rapid and extensive alteration of phosphorus speciation during oxic storage of wet sediment samples. PLoS One 9:1–6. doi: 10.1371/journal.pone.0096859

Kruse J, Abraham M, Amelung W, et al (2015) Innovative methods in soil phosphorus research: A review. J Plant Nutr Soil Sci 178:43–88. doi: 10.1002/jpln.201400327

Kruse J, Leinweber P (2008) Phosphorus in sequentially extracted fen peat soils: A *K*-edge X-ray absorption near-edge structure (XANES) spectroscopy study. J Plant Nutr Soil Sci 171:613–620. doi: 10.1002/jpln.200700237

Kruse J, Negassa W, Appathurai N, et al (2010) Phosphorus speciation in sequentially extracted agro-industrial by-products: Evidence from X-ray absorption near edge structure spectroscopy. J Environ Qual 39:2179. doi: 10.2134/jeq2010.0114

Kulakova AN, Hobbs D, Smithen M, et al (2011) Direct quantification of inorganic polyphosphate in microbial cells using 4′-6-diamidino-2-phenylindole (DAPI). Environ Sci Technol 45:7799–7803. doi: 10.1021/es201123r

Leipe T, Loeffler A, Emeis KC, et al (2000) Vertical patterns of suspended matter characteristics along a coastal-basin transect in the western Baltic Sea. Estuar Coast Shelf Sci 51:789–804. doi: 10.1006/ecss.2000.0715

Li W, Joshi SR, Hou G, et al (2015) Characterizing phosphorus speciation of Chesapeake Bay sediments using chemical extraction, ^{31}P NMR, and X-ray absorption fine structure spectroscopy. Environ Sci Technol 49:203–211. doi: 10.1021/es504648d

Łukawska-Matuszewska K, Bolałek J (2008) Spatial distribution of phosphorus forms in sediments in the Gulf of Gdańsk (southern Baltic Sea). Cont Shelf Res 28:977–990. doi: 10.1016/j.csr.2008.01.009

Lukkari K, Leivuori M, Vallius H, Kotilainen A (2009) The chemical character and burial of phosphorus in shallow coastal sediments in the northeastern Baltic Sea. Biogeochemistry 94:141–162. doi: 10.1007/s10533-009-9315-y

McCune B, Grace JB, Urban DL (2002) Analysis of ecological communities. MjM Sotware Design, Gleneden Beach, OR

McDowell RW, Stewart I (2005) An improved technique for the determination of organic phosphorus in sediments and soils by ^{31}P nuclear magnetic resonance spectroscopy. Chem Ecol 21:11–22. doi: 10.1080/02757540512331334942

Mohanty AK, Bramha SN, Satpathy KK, et al (2018) Geochemical distribution of forms of phosphorus in marine sediment of Bay Of Bengal, southeast coast of India. Indian J Geo-Marine Sci 47:1132–1141

Morshedizad M, Panten K, Klysubun W, Leinweber P (2018) Bone char effects on soil: Sequential fractionations and XANES spectroscopy. Soil 4:23–35. doi: 10.5194/soil-4-23-2018

Murphy J, Riley JP (1962) A Modified single solution method for the determination of phosphate in natural waters. Anal Chim Acta 27:31–36. doi: 10.1016/S0003-2670(00)88444-5

Murphy T, Lawson A, Kumagai M, Nalewajko C (2001) Release of phosphorus from sediments in Lake Biwa. Limnology 2:119–128. doi: 10.1007/s102010170007

Nausch M, Woelk J, Kahle P, et al (2017) Phosphorus fractions in discharges from artificially

drained lowland catchments (Warnow River, Baltic Sea). Agric Water Manag 187:77–87. doi: 10.1016/j.agwat.2017.03.006

Paytan A, Cade-Menun BJ, McLaughlin K, Faul KL (2003) Selective phosphorus regeneration of sinking marine particles : evidence from 31 P-NMR. 82:55–70. doi: 10.1016/S0304-4203(03)00052-5

Peak D, Sims JT, Sparks DL (2002) Solid-state speciation of natural and alum-amended poultry litter using XANES spectroscopy. Environ Sci Technol 36:4253–4261. doi: 10.1021/es025660d

Pickering IJ, Brown, Jr GE, Tokunaga TK (1995) Quantitative speciation of selenium in soils using X-ray absorption spectroscopy. Environ Sci Technol 29:2456–2459. doi: 10.1021/es00009a043

Prietzel J, Dümig A, Wu Y, et al (2013) Synchrotron-based P *K*-edge XANES spectroscopy reveals rapid changes of phosphorus speciation in the topsoil of two glacier foreland chronosequences. Geochim Cosmochim Acta 108:154–171. doi: 10.1016/j.gca.2013.01.029

Prietzel J, Harrington G, Häusler W, et al (2016) Reference spectra of important adsorbed organic and inorganic phosphate binding forms for soil P speciation using synchrotron-based *K*-edge XANES spectroscopy. J Synchrotron Radiat 23:532–544. doi: 10.1107/S1600577515023085

Ravel B, Newville M (2005) ATHENA, ARTEMIS, HEPHAESTUS: Data analysis for X-ray absorption spectroscopy using IFEFFIT. J Synchrotron Radiat 12:537–541. doi: 10.1107/S0909049505012719

Ready KR, Kadlec RH, Flaig E, Gale PM (1999) Phosphorus retention in streams and wetlands: A review. Crit Rev Environ Sci Technol 29:83–146. doi: 10.1080/10643389991259182

Reitzel K, Ahlgren J, DeBrabandere H, et al (2007) Degradation rates of organic phosphorus in lake sediment. Biogeochemistry 82:15–28. doi: 10.1007/s10533-006-9049-z

Sato S, Solomon D, Hyland C, et al (2005) Phosphorus speciation in manure and manure-amended soils using XANES spectroscopy. Environ Sci Technol 39:7485–7491. doi: 10.1021/es0503130

Schinke H, Matthäus W (1998) On the causes of major Baltic inflows - An analysis of long time series. Cont Shelf Res 18:67–97. doi: 10.1016/S0278-4343(97)00071-X

Shinohara R, Imai A, Kawasaki N, et al (2012) Biogenic phosphorus compounds in sediment and suspended particles in a shallow eutrophic lake: A 31P-nuclear magnetic resonance (31P NMR) Study. Environ Sci Technol 46:10572–10578. doi: 10.1021/es301887z

Shober AL, Hesterberg DL, Sims JT, Gardner S (2006) Characterization of phosphorus species in biosolids and manures using XANES spectroscopy. J Environ Qual 35:1983. doi: 10.2134/jeq2006.0100

Tiessen H, Stewart JWB, Moir JO (1983) Changes in organic and inorganic phosphorus composition of two grassland soils and their particle size fractions during 60-90 years of cultivation. J Soil Sci 34:815-523

Tiessen H, Moir JO (1993) Characterization of available P by sequential extraction. In: Carter MR (ed) Soil sampling and methods of analysis. Lewis Publ, Boca Raton, FL, pp 75-86

Turner BL, Cade-Menun BJ, Condron LM, Newman S (2005) Extraction of soil organic phosphorus. Talanta 66:294–306. doi: 10.1016/j.talanta.2004.11.012

Turner BL, Mahieu N, Condron LM (2003) Phosphorus-31 nuclear magnetic resonance spectral assignments of phosphorus compounds in soil NaOH-EDTA extracts. Soil Sci Soc Am J 67:497-510

Vestergren J, Vincent AG, Jansson M, et al (2012) High-resolution characterization of organic phosphorus in soil extracts using 2D 1H-31P NMR correlation spectroscopy. Environ Sci Technol 46:3950–3956. doi: 10.1021/es204016h

Vincent AG, Vestergren J, Gröbner G, et al (2013) Soil organic phosphorus transformations in a boreal forest chronosequence. Plant Soil 367:149–162. doi: 10.1007/s11104-013-1731-z

Walker TW, Syers JK (1976) The fate of phosphorus during pedogenesis. Geoderma 15:1–19. doi: 10.1016/0016-7061(76)90066-5

Walve J, Sandberg M, Larsson U, Lännergren C (2018) A Baltic Sea estuary as a phosphorus source and sink after drastic load reduction: Seasonal and long-term mass balances for the Stockholm inner archipelago for 1968-2015. Biogeosciences 15:3003–3025. doi: 10.5194/bg-15-3003-2018

Wang L, Amelung W, Willbold S (2017) Diffusion-ordered nuclear magnetic resonance spectroscopy (DOSY-NMR): A novel tool for identification of phosphorus compounds in soil extracts. Environ Sci Technol 51:13256–13264. doi: 10.1021/acs.est.7b03322

Watson SJ, Cade-Menun BJ, Needoba JA, Peterson TD (2018) Phosphorus forms in sediments of a river-dominated estuary. Front Mar Sci 5:1–11. doi: 10.3389/fmars.2018.00302

Werner F, Prietzel J (2015) Standard protocol and quality assessment of soil phosphorus speciation by P *K*-Edge XANES spectroscopy. Environ Sci Technol 49:10521–10528. doi: 10.1021/acs.est.5b03096

Wu YH, Prietzel J, Zhou J, et al (2014) Soil phosphorus bioavailability assessed by XANES and Hedley sequential fractionation technique in a glacier foreland chronosequence in Gongga Mountain, Southwestern China. Sci China Earth Sci 57:1860–1868. doi: 10.1007/s11430-013-4741-z

Xie LQ, Xie P, Tang HJ (2003) Enhancement of dissolved phosphorus release from sediment to lake water by microcystis blooms - An enclosure experiment in a hyper-eutrophic, subtropical Chinese lake. Environ Pollut 122:391–399. doi: 10.1016/S0269-7491(02)00305-6

Zhang R, Wu F, Liu C, et al (2008) Characteristics of organic phosphorus fractions in different trophic sediments of lakes from the middle and lower reaches of Yangtze River region and Southwestern Plateau, China. Environ Pollut 152:366–372. doi: 10.1016/j.envpol.2007.06.024

Zwolsman JJG (1994) Seasonal variability and biogeochemistry of phosphorus in the Scheldt Estuary, South-west Netherlands. Estuar Coast Shelf S 39:227-248

6 Organic matter composition and phosphorus speciation of solid waste from an African Catfish Recirculating Aquaculture System

Julia Prüter[1], Sebastian Marcus Strauch[2], Lisa Wenzel[2], Wantana Klysubun[3], Harry Wilhelm Palm[2], Peter Leinweber[1]

[1]*University of Rostock, Soil Science, Justus-von-Liebig Weg 6, 18051 Rostock, Germany*

[2]*University of Rostock, Department of Aquaculture and Sea-Ranching, Justus-von-Liebig Weg 6, 18051 Rostock, Germany*

[3]*Synchrotron Light Research Institute, Muang District, 111 Moo 6 University Avenue, Nakhon Ratchasima 3000, Thailand*

Published in

Agriculture (2020), 10 (10), 466

6.1. Abstract

Recycling of phosphorus (P) from feed input in aquaculture systems gains increasing importance, especially relating to sustainable agriculture and food production. In order to find possible areas of application of African catfish solid waste, the purpose of this study was to characterize the elemental and organic matter composition and P speciation in the aquaculture fish waste. Pyrolysis-field ionization mass spectrometry (Py-FIMS) was used to investigate the composition of organic matter and P *K*-edge X-ray absorption near edge structure (XANES) spectroscopy to describe the occurring P-containing compounds in African catfish solid waste from an intensive recirculation aquaculture system (RAS). The solid fish waste was mainly composed of sterols, free fatty acids and alkylaromatics, as it is common for digestive systems of animals. Ingredients such as the phytosterol beta-sitosterin confirm plant-based feed ingredients and some recalcitrance against digestion in the African catfish gut. The P in the solid fish waste was exclusively bound as calcium-phosphates. These calcium-phosphate minerals as major constituents of African catfish waste may have beneficial effects when applied to soils, suggesting the use of this waste as possible soil amendment in the future.

Keywords: African catfish • RAS • Py-FIMS • XANES spectroscopy • aquaculture fish waste • soil amendment

6.2. Introduction

Phosphorus (P) is one essential element for organism growth and a key factor limiting the primary production of plants in various ecosystems (Elser et al. 2007). Developing circular flows of P in agriculture can enhance the environmental sustainability of P use (Leinweber et al. 2018; Withers et al. 2018). Recycling P from biological waste materials contributes to a sustainable P management (Schröder 2005; Le Corre et al. 2009). Intensive recirculation aquaculture systems (RAS) have the potential to become one of the most sustainable animal protein production systems (Martins et al. 2010). Nevertheless, up to 80% of carbon (C), 76% of nitrogen (N) and 82% of P from total feed input in aquaculture can be lost to the environment (Hall et al. 1992; Holby and Hall 1991). Thus, to assess possible environmental impacts and to enable nutrient reuse, it is highly relevant to identify the composition of aquaculture fish waste (Galasso et al. 2017).

The characteristics of traditional agricultural waste, such as compost (Gómez-Brandón et al. 2016), farmyard manure from animal production systems for pigs, poultry and cattle (Case et al. 2017), slurry (Köster et al. 2015), sewage sludge (Adani and Tambone 2005) and digestates from biogas plants (Hupfauf et al. 2016) have been intensively researched, and these materials are widely used as organic amendments and P fertilizers in arable soils. Solid waste from modern aquaculture systems, especially intensive African catfish RAS, has scarcely been investigated to date. A recent investigation demonstrated that the reuse of nutrients from commercial African catfish RAS in aquaponics can reduce the demand for mineral fertilizer in

plant production because it contains substantial amounts of P and organic matter (Strauch et al. 2018). However, the chemical composition of that organic matter is completely unknown. Pyrolysis-field ionization mass spectrometry (Py-FIMS) has been used to characterize the composition of organic matter in complex matrices, such as fertilized soils (Eshetu et al. 2012), municipal solid waste leachates (Franke et al. 2006), agro-industrial byproducts (Negassa et al. 2011a), biochars (Jegajeevagan et al. 2016), pig slurry (Aust et al. 2009) or chicken manure (Kazi et al. 2011), but not yet applied to solid waste from African catfish RAS.

The P *K*-edge X-ray absorption near edge structure (XANES) spectroscopy is a promising method to describe the P speciation of different environmental materials. Several studies used this technique to disclose the P speciation, for example, in soils of different genesis (Hesterberg et al. 1999; Prietzel et al. 2013; Acksel et al. 2016; Koch et al. 2018; Morshedizad et al. 2018), fertilized and organically amended soils (Ajiboye et al. 2008), soils treated with biosolids (Kar et al. 2011), poultry litter (Peak et al. 2002), in poultry manure (Sato et al. 2005) and in sediments (Kraal et al. 2015; Li et al. 2015; Prüter et al. 2020). Fish fecal matter has not yet been investigated by this P speciation method leaving the P speciation of solid RAS waste almost unknown. Furthermore, this material can be transported over long distances and contribute to the composition of sediments at sea bottoms (Zhang and Kitazawa 2015). For the above knowledge gaps concerning P in fish fecal matter there is no indication whether distinct P compounds occurring at the bottom of aquatic environments can have their origin in fish fecal matter. Furthermore, to support the idea of closed nutrient cycles and to estimate the suitability of solid waste from African catfish RAS as possible soil amendment, data on P speciation and the specific organic matter composition are urgently needed.

Thus, the aims of this study were (1) to characterize the organic matter composition of African catfish RAS solid waste with Py-FIMS and (2) to disclose the P speciation of this waste with XANES spectroscopy.

6.3. Material and methods

6.3.1. Solid Waste Samples

Sampling was conducted on 8 May 2017 at the research facilities of the FishGlassHouse at the University of Rostock (Faculty of Agricultural and Environmental Sciences), Germany. Within the scope of sampling, settled solids from three semi-commercial African catfish (*Clarias gariepinus*) RAS were collected. The fish were fed with Skretting ME-4.5 Meerval Top, the specified feed ingredients were poultry meal, wheat, fish meal, soy extract feed from peeled seeds, corn gluten feed, poultry fat, wheat glue and fish oil resulting in 42% crude protein, 13% crude fat, 1.8% crude fibre and 8.5% ash. Combined with nitrogen (N) free substances and water (6%–8%), the feed included 2% calcium (Ca), 0.4% sodium (Na) and 1.2% P. The three RAS consisted of nine fish tanks (FT) with 1.2 m^3 water volume each, one clarifier with lamella inserts for solid separation (point of sampling), one nitrifying trickling filter for biological oxidation of ammonia to nitrite and further to nitrate and a sump with two pumps. For further

specifications see (Palm et al. 2018). The systems differed in the size of biofilters and clarifiers, resulting in total RAS water volumes for extensive aquaculture system (EAS) of 13.9 m^3, semi-intensive aquaculture system (SIAS) of 15.1 m^3, and intensive aquaculture system (IAS) of 16.9 m^3 and allowing the different stocking densities of EAS with 35 fish FT^{-1}, SIAS with 70 fish FT^{-1} and IAS with 140 fish FT^{-1}. Due to differences in stocking densities, the feed inputs also differed. Every six days during the regular maintenance, the clarifiers were temporarily set from flow through to bypass to be able to clean them by emptying the supernatant via an integrated pump while the solid wastes deposited in the lamella inserts were removed with a high-pressure cleaner and the slurry was then collected in the clarifier. Sampling took place six days after cleaning the clarifier and a total feed input of 7.28 kg in EAS, 14.59 kg in SIAS and 28.78 kg in IAS during this time period. At the time of sampling, EAS had a total fish biomass of 147 kg RAS^{-1} (13.6 kg m^{-3}), SIAS of 287 kg RAS^{-1} (26.6 kg m^{-3}) and IAS of 551 kg RAS^{-1} (51.0 kg m^{-3}).

6.3.2. Determination of elemental concentrations

To determine the concentrations of the elements N, sulphur (S), P, aluminium (Al), iron (Fe), Ca, magnesium (Mg) and potassium (K) in the deposited solids, from the slurry samples that were collected in the clarifiers the supernatants were decanted and the remaining, concentrated slurry was transferred into glass trays and oven dried at 60 °C until weight constancy, what was reached after 24 h. The dried samples were then homogenized and acid-digested with concentrated HNO_3 and $HClO_4$ as preparation for the following analyses of S, P, Al, Fe, Ca, Mg and K with an inductively coupled plasma-emission spectrometer (ICP-OES) and N by combustion in an elemental analyzer (for methodological details see Strauch et al. (2018)).

6.3.3. Pyrolysis-field ionization mass spectrometry (Py-FIMS)

About 5 mg of finely ground and homogenized samples were thermally degraded by pyrolysis in the ion source (emitter: 4.7 kV, counter electrode −5.5 kV) of a double-focusing Finnigan MAT 95 mass spectrometer. The samples were heated in a vacuum of 10^{-4} Pa from ambient temperature to 700 °C, in temperature steps of 10 K over a time period of 15 minutes. Between magnetic scans the emitter was flash heated to avoid residues of pyrolysis products. About 60 spectra were recorded for the mass range *m/z* 15 to 900 for each of the three replicates per sample. Ion intensities were referred to 1 mg of the sample. Volatile matter was calculated as mass loss in percentage of sample weight. For spectra interpretation marker signals (*m/z*) according to different studies (Hempfling et al. 1988; Schnitzer and Schulten 1992; Schulten and Leinweber 1996; Leinweber et al. 2009; Leinweber et al. 2013) were assigned to important compound classes.

6.3.4. P K-*edge X-ray absorption near edge (XANES) spectroscopy*

The P *K*-edge XANES spectra for characterizing P species in the samples were recorded at the Synchrotron Light Research Institute (SLRI) in Nakhon Ratchasima, Thailand on the beamline 8 (BL8) (Klysubun et al. 2020). The electron storage ring with a covering photon energy from 1 to 13 KeV operated at 1.2 GeV electron energy and a beam current of 80–150 mA (Klysubun et al. 2012). The XANES data were collected from dry and finely-ground samples thinly spread on P-free kapton tape (Lanmar Inc. Northbrook, IL, USA) attached to a plastic sample holder. The samples were diluted to P concentrations < 2 mgPkg^{-1} with SiO_2 powder (to eliminate self-absorption effects (Prietzel et al. 2013)) and again ground and homogenized in a mini mill (Pulverisette 23, Fritsch GmbH Milling and Sizing, 55743 Idar-Oberstein, Germany). Data collection operated in standard conditions with energy calibration by standard pure elemental P and allocating the reference energy (E_0) at 2145.5 eV using the maximum peak of the first derivative spectrum. All spectra were recorded at photon energies between 2045.5 and 2495.5 eV in step sizes of 5 eV (2045.5 to 2105.5 eV and 2245.5 to 2495.5 eV), 1 eV (2105.5 to 2135.5 eV and 2195.5 to 2245.5 eV) and 0.25 eV (2135.5 to 2195.5 eV) with a 13-channel germanium detector in fluorescence mode. Three scans were collected and averaged for each sample.

All P *K*-edge XANES spectra were normalized and the replicates were merged. Linear combination fitting (LCF) was performed using the ATHENA software package (Ravel and Newville 2005) in the energy range between −20 eV and +30 eV of E_0. The XANES spectral data were baseline corrected in the pre-edge region between 2115 and 2145 eV and normalized in the post-edge region of 2190-2215 eV. The same ranges were used for the reference P *K*-edge XANES spectra to achieve consistency in the following fitting analysis (Prietzel et al. 2016). To achieve the best compatible set of references with each specified sample spectrum, LCF analysis was performed using the combinatorics function of ATHENA software to attain all possible binary to quaternary combinations between all 19 P reference spectra in which the share of each compound was ≥ 10%. The following set of reference P *K*-edge XANES spectra, all recorded in SLRI under the same adjustments (Werner and Prietzel 2015; Prietzel et al. 2016), were used for fitting and calculations: Ca-, Al- and Fe-phytate, noncrystalline and crystalline $AlPO_4$, noncrystalline and crystalline $FePO_4 \cdot 2H_2O$, Ca-5-hydroxyapatite ($Ca_5(OH)(PO_4)_3$), inositol hexakisphosphate (IHP), ferrihydrite–IHP, montmorillonite–Al–IHP, soil organic matter Al–IHP (SOM–Al–IHP), ferrihydrite–orthophosphate, montmorillonite–Al–orthophosphate, SOM–Al–orthophosphate, boehmite–IHP, boehmite–10 orthophosphate, $CaHPO_4$, $Ca(H_2PO_4)_2$ and $MgHPO_4$. The *R*-factor values were used as goodness-of-fit criteria and significant differences between fits were evaluated using the Hamilton test ($p < 0.05$) (Calvin 2013) with the number of independent data points calculated by ATHENA, estimated as data range divided by core-hole lifetime broadening. The best fits of P reference compound combinations were considered as the most probable P species in the material. If *R*-factors of fits with the same number of reference compounds were not significantly different from each other according to the Hamilton test, fit proportions were averaged.

6.3.5. Statistical analyses

Data analysis was performed using the open-source statistical software R (version 3.4.3, R Core Team 2019, Vienna, Austria). R package *agricolae* was used and significance level was 0.05. Differences in compound classes between the stocking densities EAS, SIAS and IAS determined with Py-FIMS were tested for significance (*P < 0.05, **P < 0.01, ***P < 0.001) by the Welch's T-test. The precondition of normal distribution was proven using the Shapiro-Wilk normality test previously.

6.4. Results

6.4.1. Elemental composition

The average chemical compositions of solid fish waste from different stocking densities EAS, SIAS and IAS are presented in Table 1. The total dry matter contents (in g kg^{-1}) of the slurry samples before drying were EAS = 24.9, SIAS = 29.9 and IAS = 18.8. There are minor differences in elemental contents between the individual stocking densities. Percentages of nitrogen (N) and sulphur (S) are quite similar in EAS, SIAS and IAS. Percentages of P and calcium (Ca) were highest in SIAS (1.7% P, 4.2% Ca) and lowest in EAS (1.4% P, 3.4% Ca). The contents of aluminum (Al), iron (Fe), magnesium (Mg) and potassium (K) all were very low in a range of 0.0% to 0.5% in all stocking densities.

Table 6-1 Chemical characterization of solid African catfish waste. Nitrogen (N), sulphur (S), C:N ratio (C:N), phosphorus (P), aluminium (Al), iron (Fe), calcium (Ca), magnesium (Mg) and potassium (K) were averaged (± standard deviation) from three measurements in each of the stocking densities EAS, SIAS and IAS.

Parameter	Unit	EAS	SIAS	IAS
N	%	5.2 ± 0.2	5.4 ± 0.2	5.1 ± 0.3
S	%	0.9 ± 0.0	0.9 ± 0.0	1.0 ± 0.1
C:N	ratio	7.9 ± 0.2	7.4 ± 0.2	7.8 ± 0.2
P	%	1.4 ± 0.1	1.7 ± 0.1	1.6 ± 0.1
Al	%	0.1 ± 0.0	0.1 ± 0.0	0.0 ± 0.0
Fe	%	0.2 ± 0.0	0.3 ± 0.0	0.3 ± 0.0
Ca	%	3.4 ± 0.1	4.2 ± 0.2	3.9 ± 0.1
Mg	%	0.2 ± 0.0	0.2 ± 0.0	0.2 ± 0.0
K	%	0.2 ± 0.0	0.3 ± 0.0	0.5 ± 0.0

EAS = extensive aquaculture system, SIAS = semi-intensive aquaculture system, IAS = intensive aquaculture system

6.4.2. Pyrolysis-field ionization mass spectrometry (Py-FIMS)

Py-FI mass spectra of all three stocking densities (Figure 1) were dominated by cholesterol (*m/z* 386) and beta-sitosterin (*m/z* 414). The compound at *m/z* 426 could be the triterpenoids lupeol/taraxerol or the marine sterol gorgosterol. The fatty acid palmitic acid $C_{16}H_{32}O_2$ at *m/z* 256 occurs in EAS, SIAS and IAS together with the fatty acids *n*-$C_{18:3}$, *n*-$C_{18:2}$, *n*-$C_{18:1}$ and *n*-$C_{18:0}$ at *m/z* 278 to 284 and *n*-$C_{15:0}$ at *m/z* 254. Compounds at *m/z* 61 and *m/z* 126 represent sugars and were also present in all samples. The lignin monomer sinapylic aldehyde (*m/z* 208) was visible in EAS but not in SIAS or IAS. All samples showed low contents of elemental S at *m/z* 255.7 but the largest concentration was present in IAS.

Similar proportions of volatile matter (VM) were revealed for EAS (79%) and SIAS (77%), whereas for IAS (86%) it was significantly higher compared to EAS (**P* = 0.0288) and SIAS (**P* = 0.0169) (Table 2). Total ion intensity (TII) was larger by factor 1.5 (**P* = 0.0113) in SIAS (1468 × 10^6 counts mg^{-1}) than in EAS (959 × 10^6 counts mg^{-1}) but there was no significant difference in TII of SIAS compared to IAS (1396 × 10^6 counts mg^{-1}). Proportions of carbohydrates, phenols and lignin monomers, lipids, alkylaromatics, sterols and amino acids, peptides and amino sugars revealed no significant differences among the stocking densities EAS, SIAS and IAS but the proportions of lignin dimers were significantly different. The proportion of lignin dimers was significantly lower in EAS (0.8%) than in IAS (1.0%; ***P* = 0.0068) and it was highest in SIAS (1.2%) and thereby significantly different compared to IAS (***P* = 0.0013). The percentage of heterocyclic nitrogen (N) containing compounds was significantly lower in EAS (1.1%) compared to SIAS (1.3%) (***P* = 0.0055) and IAS (1.4%). Similar proportions of suberin were determined in SIAS and IAS (0.8%) but in EAS (0.7%) the amount was significantly lower (***P* = 0.0036). The highest amount of free fatty acids was present in EAS (12.2%) and thereby significantly different from SIAS (7.4%; ***P* = 0.0014) and IAS (7.2%; ***P* = 0.0020).

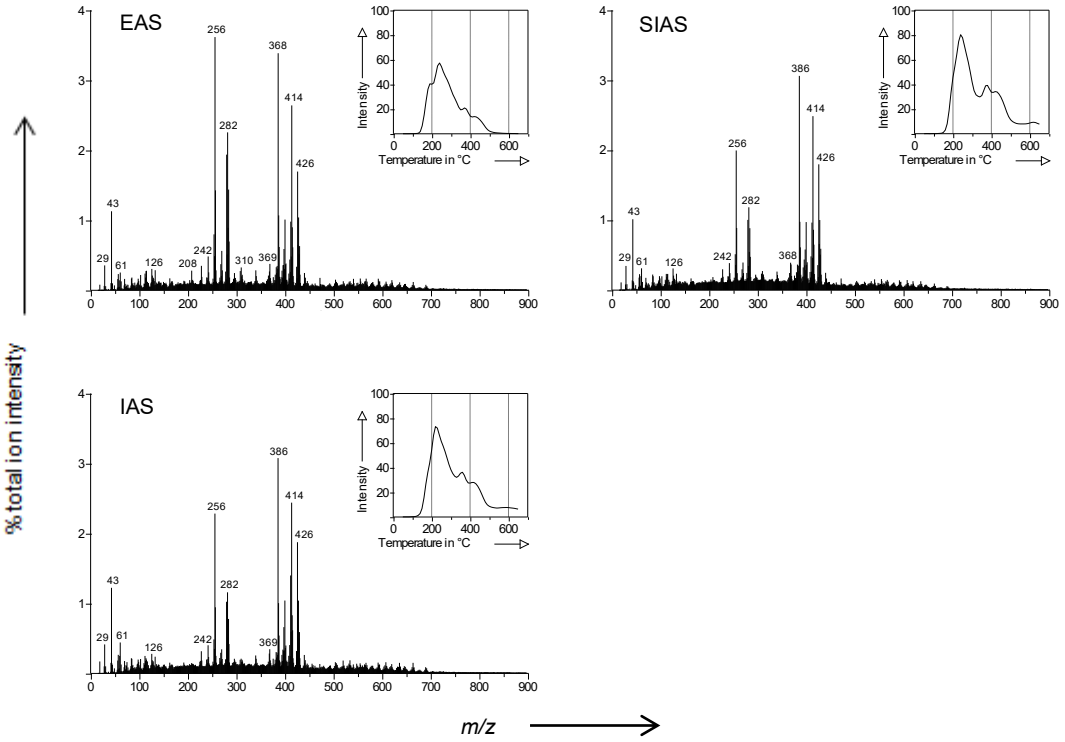

Figure 6-1 Pyrolysis-field ionization mass spectra and thermograms of the stocking densities extensive aquaculture system (EAS), semi-intensive aquaculture system (SIAS) and intensive aquaculture system (IAS).

Table 6-2 Averaged volatile matter (VM), total ion intensity and relative abundance of 10 important compound classes (% of total ion intensity (TII)) from three measurements in each of the stocking densities EAS, SIAS and IAS determined with pyrolysis-field ionization mass spectrometry (Py-FIMS). Different superscripted letters in one line represent significant differences among the stocking densities.

Sam-ple	VM	TII	%TII From Compound Classes									
	(%)	(10^6 counts mg^{-1})	CHYDR	PHLM	LDIM	LIPID	ALKYL	NCOMP	STEROL	AMID	SUBER	FATTY
EAS	78.5 ^{a}	958.5 ^{a}	2.3 ^{a}	2.3 ^{a}	0.8 ^{a}	3.6 ^{a}	6.1 ^{a}	1.1 ^{a}	14.4 ^{a}	2.6 ^{a}	0.7 ^{a}	12.2 ^{a}
SIAS	77.2 ^{a}	1467.8 ^{b}	2.5 ^{a}	2.5 ^{a}	1.2 ^{c}	3.7 ^{a}	6.2 ^{a}	1.3 ^{b}	14.1 ^{a}	2.8 ^{a}	0.8 ^{b}	7.4 ^{b}
IAS	85.8 ^{b}	1396.3 ^{b}	2.7 ^{a}	2.4 ^{a}	1.0 ^{b}	3.7 ^{a}	6.0 ^{a}	1.4 ^{b}	14.2 ^{a}	2.9 ^{a}	0.8 ^{b}	7.2 ^{b}

CHYDR = carbohydrates; PHLM = phenols and lignin monomers; LDIM = lignin dimers; LIPID = lipids; ALKYL = alkylaromatics; NCOMP = heterocyclic N containing compounds; STEROL = sterols; AMID = amino acids, peptides, amino sugars; SUBER = suberin; FATTY = free fatty acids

Thermal volatilization curves for the compound classes phenols and lignin monomers, lignin dimers, amides (amino acids, peptides, amino sugars) and free fatty acids (*n*-$C_{16:0}$ to *n*-$C_{34:0}$) of all samples are displayed in Figure 2. Graphs for the individual stocking densities show clear differences in the thermal volatilization curves. The thermogram for phenols and lignin monomers (Figure 2a) shows that EAS, SIAS and IAS contained almost similar amounts of these compounds which, however, differed in their thermal volatilization. The volatilization of phenols and lignin monomers occurred at a slightly lower temperature in EAS than in IAS and

SIAS. The thermograms for lignin dimers (Figure 2b) display the highest thermal volatilization of these compounds in EAS at the first maximum at lower temperatures and in SIAS at the second maximum at higher temperatures. Figure 2c shows a higher thermal volatilization of amides (amino acids, peptides and amino sugars) in EAS at slightly lower temperatures compared to SIAS and IAS, although the total proportion of amides was marginally higher in SIAS and IAS than in EAS (Table 2). The content of free fatty acids (*n*-$C_{16:0}$ to *n*-$C_{34:0}$) (Figure 2 d) in all samples was much larger than the proportions of the other compound classes (by factor 10). Again, the thermogram of EAS differs from SIAS and IAS (Figure 2d). The amount of free fatty acids in EAS is nearly two times higher compared to SIAS and IAS and all free fatty acids are volatilized at about 200 °C.

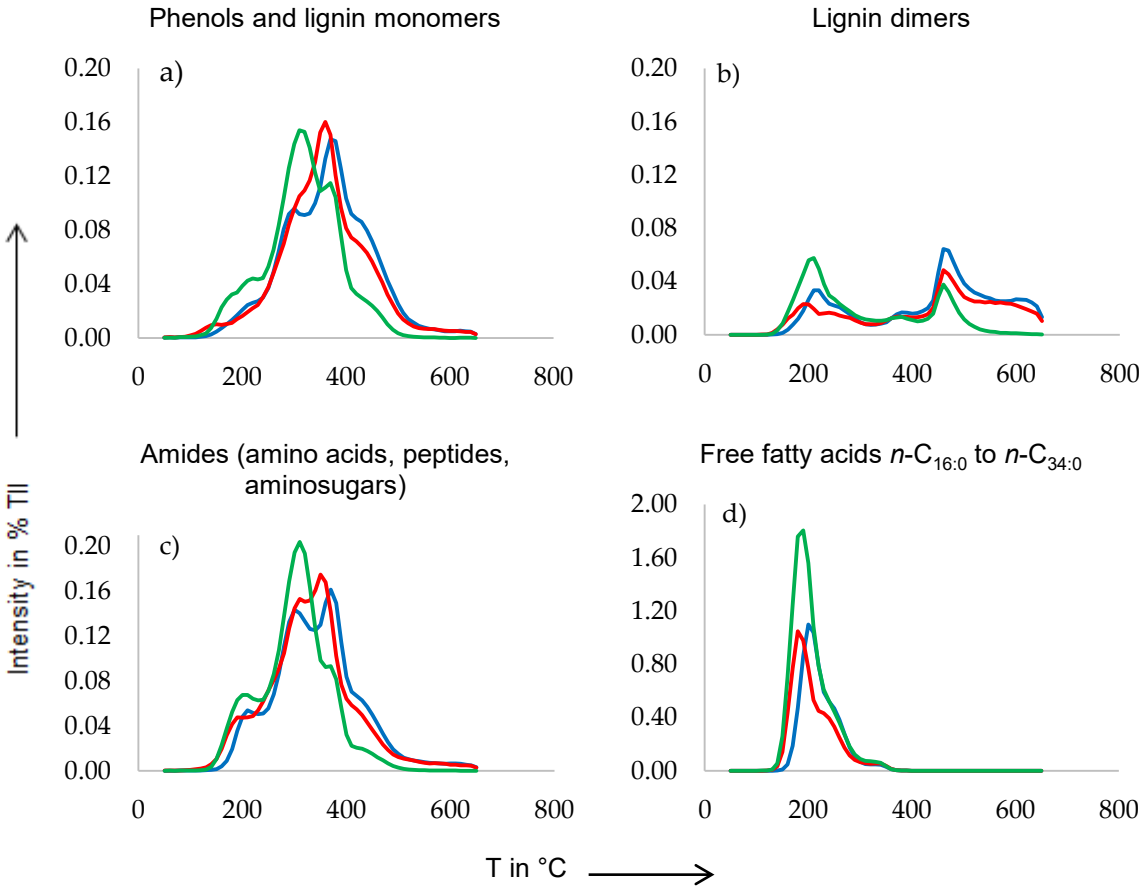

Figure 6-2 Thermograms of the substance classes **a**) phenols and lignin monomers, **b**) lignin dimers, **c**) amides (amino acids, peptides, amino sugars) and **d**) free fatty acids (*n*-$C_{16:0}$ to *n*-$C_{34:0}$) of the different stocking density samples: EAS (graph in green), SIAS (graph in blue) and IAS (graph in red). For reasons of clearness, the scale of the graph of free fatty acids is 10 times higher than the graphs of the other substance classes.

6.4.3. P K-edge X-ray absorption near edge (XANES) spectroscopy

The XANES spectra where characterized by an intense white line peak at around 2152 eV (Figure 3). The linear combination fitting (LCF) of spectra using 19 spectra of P reference compounds indicated that the P composition of all samples can be described by Ca-P-compounds like Ca-phytate, Ca-hydrogen phosphate ($CaHPO_4$) and Ca-5-hydroxyapatite (Table 3). Within these compounds Ca-phytate was most abundant in EAS (87%), whereas $CaHPO_4$ predominated in SIAS (47%). Ca-hydroxyapatite exclusively occurred in EAS and constituted 7% of all P compounds in this sample as determined by XANES spectroscopy.

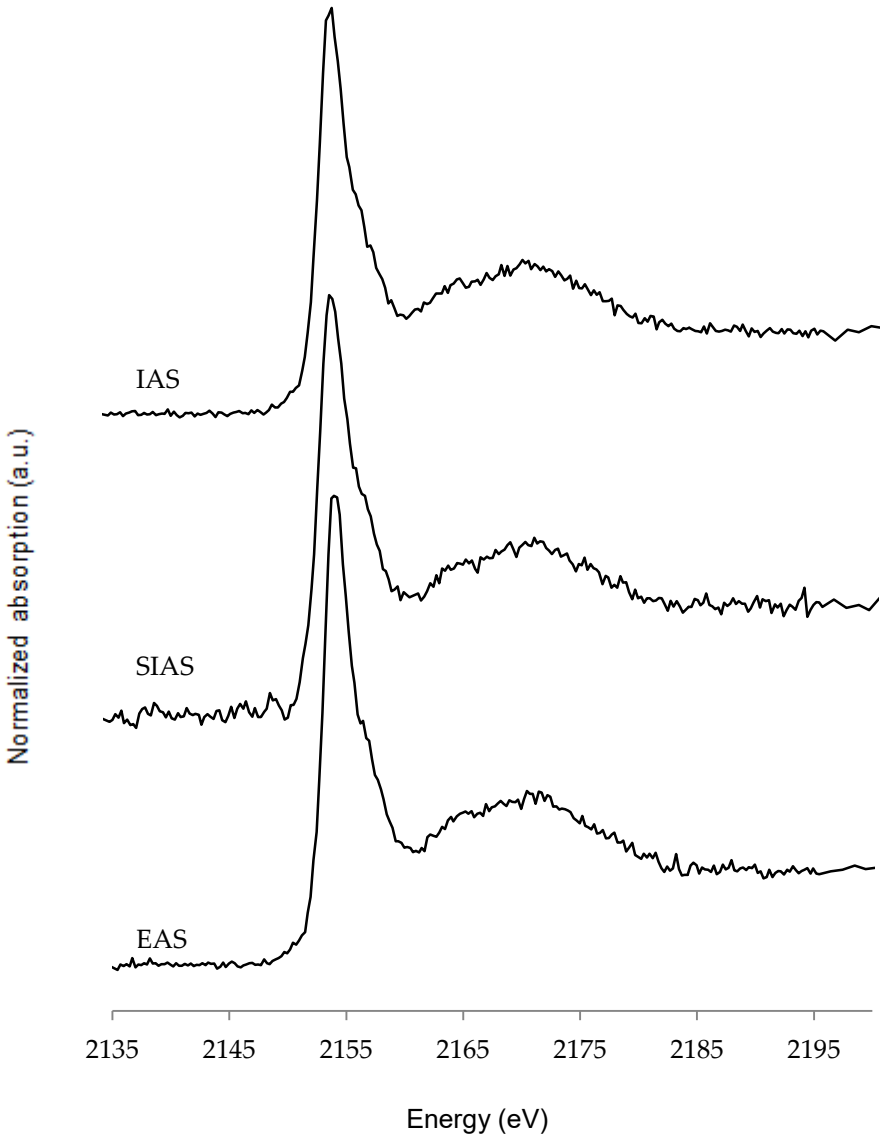

Figure 6-3 Stacked and normalized P *K*-edge X-ray absorption near edge structure (XANES) spectra of fish waste samples with the different stocking densities EAS, SIAS and IAS.

Table 6-3 Proportions of Ca phytate, Ca hydrogen phosphate ($CaHPO_4$) and Ca hydroxyapatite in % in the samples EAS, SIAS and IAS determined with *K*-edge XANES analysis, including *R*-factor as a goodness-of-fit criterion.

Sample	Ca Phytate	$CaHPO_4$	Ca Hydroxyapatite	*R*-Factor
	in %			
EAS	87	6	7	0.0094
SIAS	53	47		0.0267
IAS	76	24		0.0102

6.5. Discussion

6.5.1. Organic matter composition

Organic compounds of solid waste from African catfish RAS were mainly composed of sterols, free fatty acids and alkylaromatics (Table 2). The dominant occurrence of cholesterol (*m/z* 386) and beta-sitosterin (*m/z* 414) in the samples of all stocking densities coincided with the highest relative abundance of the compound class of sterols (14.1% to 14.4%) compared to the other compound classes of the samples (Table 2). Similarly, high proportions of sterols have been observed by Py-FIMS in samples from penguin excrement-rich gelic histosols from Antarctica and from Podzol subsoils (Leinweber et al. 2009), and in samples from pig slurry (Aust et al. 2009). Thus, high sterol proportions indicate an origin from the digestive system of animals which may be valid also for the sediment from the present RAS. Furthermore, this composition agreed with those of effluents from an Atlantic cod aquaculture facility, where sterols are also one of the major classes present in the organic matter (Both et al. 2013).

A different investigation associated high sterol proportions up to 10.2% in an arable gleyic podzol, analysed by Py-FIMS with an inhibitory effect on the mineralizability of soil organic N (Heumann et al. 2011). This effect has been as well reported in other studies (Leite et al. 2006; Negassa et al. 2011a). The phytosterol beta-sitosterin likely originates from the plant-based feed ingredients of the African catfish RAS and its occurrence in the solid waste indicates some recalcitrance against digestion in the fish gut.

A comparison of the amount of free fatty acids shows higher proportions in the solid waste from African catfish RAS than in different soils and agro-industrial byproducts (Table 2). For instance, the highest reported amounts of free fatty acids determined with Py-FIMS were 6.6% of total ion intensity in wet-processed coffee byproducts and filter cakes (Negassa et al. 2011). These proportions of fatty acids were near to those measured by Py-FIMS in SIAS (7.4%) and IAS (7.2%). In sandy arable soils, the highest proportions of free fatty acids were determined in two gleyic podzols (10.6% and 11.8% of Py-FIMS TII) (Heumann et al. 2011), which are still slightly lower than the amount of fatty acids determined in EAS (12.2%) in the present study. Next to lipids, the compound class of free fatty acids was the dominating class determined with Py-FIMS in the higher-mass range in different agro-industrial byproducts reported by Negassa et al.

(2011). Free fatty acids are one of the major compounds in effluents of an Atlantic cod aquaculture facility as well (Both et al. 2013). Furthermore, long-chain fatty acids (*n*-$C_{12:0}$ to *n*-$C_{34:0}$) were identified as abundant components of higher plant waxes (Stevenson 1994). Thus, we suppose the plant-based ingredients of the African catfish feed to be the origin of the free fatty acids in the solid waste samples, indicating that portions of the fatty acids were not digested by the fish. Free fatty acids could have positive effects on soil because evidence was found that especially *n*-$C_{21:0}$ to *n*-$C_{34:0}$ helps to stabilize aggregates in soil (Jandl et al. 2004).

The third highest amount of Py-FIMS from solid African catfish RAS waste was the compound class of alkylaromatics (Table 2). Proportions of alkylaromatics in the solid waste (6.0% to 6.2%) were in the range of those reported for different agro-industrial byproducts, e.g. 4.8% in sisal factory byproducts and 8.3% in dry-processed coffee byproducts (Negassa et al. 2011). Wheat straw had about 14% TII alkylaromatics, and this proportion decreased to a minimum of 11% TII when the straw was incubated with saprotrophic fungi for some weeks (Wiedow et al. 2007). Alkylaromatics in pig slurry accounted from 7% to 16% of TII, depending on the size of the slurry separates (Aust et al. 2009), but generally confirming that excrement can contain this compound class. By comparison, soils treated with mineral fertilizer or compost over many years showed clearly higher amounts of alkylaromatics (10.3% to 13.4%) compared to the solid fish waste (Eshetu et al. 2012). Alkylaromatic compounds in soil can have their origin in inputs from plant roots (Leue et al. 2016), they can be formed by pyrolysis of lignin (Sleutel et al. 2008) and they can originate from transformation processes by earthworms (Leue et al. 2016). In the solid fish waste, plant-derived lignin from fish feed could be the origin of alkylaromatics but a formation during digestion in the fish, or subsequently in the clarifiers and biofilters cannot be excluded. Alkylaromatic compounds were characterized as backbone of humified substances (Schulten and Schnitzer 1993; Negassa et al. 2019) and thereby play a substantial role in soil fertility and possible plant growth.

A comparison of spectral patterns (Figure 1) and proportions of compound classes (Table 2) of the three samples show that the organic matter composition slightly differed between samples from the different stocking densities. Generally, the lowest stocking density EAS differed more from SIAS and IAS than the latter among each other. The higher proportion of free fatty acids on total ion intensity in EAS (12.2%) compared to SIAS and IAS (7.4% and 7.2%) (Table 2) coincides with the visual impression from Py-FI mass spectra (Figure 1), where the palmitic acid $C_{16}H_{32}O_2$ signal at *m/z* 256 was most prominent in EAS. Furthermore the proportion of free fatty acids not only was 10 times higher than proportions of the other compound classes displayed in Figure 2, it was also nearly two times higher in EAS compared to SIAS and IAS in the thermal volatilization curves for the compound class of free fatty acids (*n*-$C_{16:0}$ to *n*-$C_{34:0}$) (Figure 2d). It seems that the lower the stocking density of African catfish RAS, the higher the proportions of fatty acids in the samples. In summary, the compound classes of sterols, free fatty acids and alkylaromatics show evidence for plant origin of several compounds in solid African catfish RAS waste. Especially the first maximum in the thermal volatilization curve of the compound class of lignin dimers (Figure 2b) confirms that the samples contain plant material, supporting previous findings on fibre analysis (Strauch et al. 2018).

It must be stated that the relatively long collection period of six days in combination with high feed input and certainly reduced oxygen availability inside the sludge layer in the clarifiers likely provided anaerobic conditions. These may have supported fermentative breakdown processes, resulting in the production of long chain fatty acids and volatile fatty acids by acid forming bacteria, explaining the observed differences in fatty acid composition (Comeau 2008). This acid production may also explain the absence of hydroxyapatite in SIAS and IAS.
A lower amount of P inside the sediments of EAS also relates to less feed input and reduced availability of dissolved P inside the process water (Strauch et al. 2018). This differs to similar proportions of N, S, Al, Fe, Mg and K, where the elementary S, also present in all samples, likely has been formed during degradation of biomass by putrefaction, other digestive processes in the fish, or by reductive decomposition processes in the clarifier.

6.5.2. P *XANES spectroscopy*

The fish waste from the stocking density SIAS contained 47% $CaHPO_4$ (Table 3) determined with XANES spectroscopy, and thereby the greatest proportion among the three stocking densities, what coincides with highest elemental percentage of Ca in SIAS (4.2%, Table 1). EAS showed the lowest amount of $CaHPO_4$ (6%) determined with XANES, again in accordance with the smallest elemental proportion of Ca (3.4%) in this sample. Additionally, EAS contained 7% of Ca hydroxyapatite but this has to be taken with caution, because XANES spectroscopy is not able to detect one chemical species certainly in the presence of great proportions of a different species of the same element (Pickering et al. 1995). Two studies reported a high correlation of XANES spectra of many P standards due to very similar spectral features (Beauchemin et al. 2003; Gustafsson et al. 2020). Furthermore, P XANES spectroscopy is capable to distinguish various chemical inorganic P forms (Kruse and Leinweber 2008) but it is limited in differentiating P adsorbed by organic matter and certain minerals (Ajiboye et al. 2008) because of very similar spectral features (Peak et al. 2002). In consequence, also the calculated proportions of organic Ca phytate in the solid African catfish RAS waste have to be considered with caution. To avoid misinterpretations of LCF results of XANES spectroscopy, some authors recommended sorting of standards into different groups such as Ca- or Fe-phosphates (Beauchemin et al. 2003; Eriksson et al. 2016). A previous study on semi-commercial African catfish RAS suggested chemical precipitation of phosphates with the binding partners Ca and Mg, resulting in lower availability of dissolved nutrients for plant production in aquaponics (Palm et al. 2018). The present study demonstrates the relatively confident occurrence of almost all P compounds in bonds with Ca in the solid fraction of African catfish RAS waste, regardless of stocking density (Table 3). This plausibly can be explained by the lower concentrations of other possible elemental P binding partners in the slurry. For instance, the elemental contents of Al, Fe, Mg and K all were very low in EAS, SIAS and IAS (< 0.1% to 0.5%, Table 1). In addition, while a related investigation reported mean pH values between 5.2 and 6.3 (Palm et al. 2018), pH of water in the current study was much lower (pH 4.5–4.9) (Strauch et al. 2018). Formation of Ca-phosphates occurs under more acidic conditions (pH ~ 5–6.5) compared with Mg-phosphates

(pH > 6.5) (Darn et al. 2006). These effects of pH on the formation of either Mg- or Ca-phosphates may therefore explain the absence of Mg-phosphates in the slurry of the present study.

We also found that the concentration of total P and Ca, largely bound as Ca-phosphates, were higher in SIAS than in EAS and IAS. It is important to note that no alkaline substances were added to the RAS to increase the pH of water. Consequently, the only input pathways for Ca were feed and tap water (Strauch et al. 2018). As a consequence of maintenance works on the RAS before the start of this study, SIAS experienced the highest and EAS the lowest water exchange over the run of the experiment (EAS = 1.6 m³, SIAS = 3.5 m³, IAS = 2.5 m³). This additional water input of freshwater in SIAS increased the input of Ca that obviously directly combines with dissolved P resulting from fish feed and possibly increasing the Ca-phosphate abundance in the slurry recovered from SIAS when compared with EAS and IAS.

Freshwater aquaculture systems that utilize groundwater sources with hard water conditions therefore might release significant amounts of Ca-phosphates to the environment. Ca-phosphates were also the most abundant P form determined in bottom sediments from the Baltic Sea (Frankowski et al. 2002). In sediments from the Arabian Sea, increasing amounts of Ca-associated P with depth were investigated (Kraal et al. 2015). It was confirmed that fecal matter from fish cultured in sea cages can contribute up to 80% to particulate organic waste in the direct aquatic environment (Zhang and Kitazawa 2015). Since the solid African catfish RAS waste exclusively contains Ca-bound P compounds, it seems reasonable to assume that such waste can also contribute to high amounts of Ca-associated P in marine sediments. However, African catfish live in freshwater and the chemical composition of solid waste especially with regard to P speciation originating from mariculture systems or fish species naturally occurring in marine environments yet have to be examined.

Similar to the results in Table 3, Ca-bound P was detected as the dominant form of P in potential alternative P fertilizers such as biochar from wetland reed and animal bone chips with XANES spectroscopy (Robinson et al. 2018). XANES spectroscopy of dairy manures, poultry litters and biosolids revealed up to 71% of total P as hydroxyapatite (Shober et al. 2006). In another study, CaO has been added to poultry waste to improve pathogenic characteristics and to avoid P losses via runoff (Maguire et al. 2006). The CaO addition increased the proportion of hydroxyapatite in the manure to a maximum of 86% (determined with XANES spectroscopy), contributing to a reduced water solubility of P (Maguire et al. 2006). Thus, Ca-phosphate minerals play a substantial and advantageous role in P fertilizers. Next to traditional organic fertilizers, such as green waste compost, solid African catfish RAS waste, especially those from intensive RAS systems with the absence of hydroxyapatite, can be considered as potential P fertilizer in agriculture based on its Ca-bound dominated P speciation.

6.6. Conclusions

1. The methodological approach of using Py-FIMS and XANES spectroscopy as methods to determine organic matter composition and P speciation of solid African catfish RAS

waste samples was appropriate. It revealed insight into the distribution of organic matter compound classes in solid waste of three different fish stocking densities and provided evidence for the occurrence of exclusively Ca-bound P compounds in African catfish RAS waste.

2. The high amounts of sterols, fatty acids and alkylaromatics in the solid waste of all three stocking densities of African catfish RAS determined by Py-FIMS reflect the plant-based feed of the fish. To assess the suitability of African catfish RAS solid waste as organic soil amendment and to prevent possible negative effects of sterols on the N-cycle in soil, further research is needed, especially on soils that have been amended by solid waste from African catfish RAS. Alternatively to direct land application of this waste, some pretreatments such as anaerobic digestion for biogas production or vermifiltration, should be tested.
3. The stocking density had an influence on feed input, water exchange rates and total oxygen concentrations in the tested African catfish RAS systems. These three factors, alone and in combination, alter solid waste composition, and its applicability as soil amendment if originating from extensive or (semi)intensive catfish aquaculture.
4. XANES spectroscopy detected exclusively Ca-associated P compounds in solid African catfish RAS waste of three different fish stocking densities. Ca-phosphate minerals as a major constituent of many bio-waste material P fertilizers have beneficial properties when applied on soils. Thus, solid African catfish RAS waste can be considered as possible addition to traditional organic P fertilizers. However, this first investigation of African catfish RAS waste with P XANES spectroscopy would benefit from the application of more different complementary techniques, such as solution ^{31}P nuclear magnetic resonance (NMR) spectroscopy and sequential P fractionation to get a more comprehensive view on P speciation.

6.7. Acknowledgments

The authors wish to thank Kai-Uwe Eckhardt (Soil Science, University of Rostock) for his support with Py-FIMS analyses and evaluation. Furthermore, we are grateful to Jörg Prietzel (Department of Soil Science, Technical University of Munich) for providing the P XANES reference spectra and to the technical staff at beamline 8 of SLRI for their friendly support.

6.8. Funding

This research was funded by the Leibniz Association within the scope of the Leibniz ScienceCampus Phosphorus Research Rostock (www.sciencecampus-rostock.de). We acknowledge financial support by Deutsche Forschungsgemeinschaft and Universität Rostock within the funding programme Open Access Publishing.

6.9. Conflicts of Interest

The authors declare no conflicts of interest. The funders had no role in the design of the study; in the collection, analyses, or interpretation of data; in the writing of the manuscript, or in the decision to publish the results.

6.10. References

Acksel A, Amelung W, Kühn P, et al (2016) Soil organic matter characteristics as indicator of Chernozem genesis in the Baltic Sea region. Geoderma Reg 7:187–200. https://doi.org/10.1016/j.geodrs.2016.04.001

Adani F, Tambone F (2005) Long-term effect of sewage sludge application on soil humic acids. Chemosphere 60:1214–1221. https://doi.org/10.1016/j.chemosphere.2005.02.031

Ajiboye B, Akinremi OO, Hu Y, Jürgensen A (2008) XANES Speciation of Phosphorus in Organically Amended and Fertilized Vertisol and Mollisol. Soil Sci Soc Am J 72:1256. https://doi.org/10.2136/sssaj2007.0078

Aust MO, Thiele-Bruhn S, Eckhardt KU, Leinweber P (2009) Composition of organic matter in particle size fractionated pig slurry. Bioresour Technol 100:5736–5743. https://doi.org/10.1016/ j.biortech.2009.06.065

Beauchemin S, Hesterberg D, Chou J, et al (2003) Speciation of Phosphorus in Phosphorus-Enriched Agricultural Soils Using X-Ray Absorption Near-Edge Structure Spectroscopy and Chemical Fractionation. J Environ Qual 32:1809. https://doi.org/10.2134/jeq2003.1809

Both A, Parrish CC, Penney RW, Thompson RJ (2013) Physical and biochemical properties of effluent leaving an onshore Atlantic cod (Gadus morhua, Linnaeus 1758; Gadiformes: Gadidae) aquaculture facility and potential use in integrated multi-trophic aquaculture. Aquac Res 44:1940–1951. https://doi.org/10.1111/j.1365-2109.2012.03199.x

Calvin S (2013) XAFS for Everyone. CRC Press: Boca Raton, FL, USA, p 427

Case SDC, Oelofse M, Hou Y, et al (2017) Farmer perceptions and use of organic waste products as fertilisers – A survey study of potential benefits and barriers. Agric Syst 151:84–95. https://doi.org/10.1016/j.agsy.2016.11.012

Comeau Y (2008) Microbial Metabolism. In: Henze M, van Loosdrecht MCM, Ekama GA, Brdjanovic D (eds) Biological Wastewater Treatment: Principles, Modelling and Design, 1st edn. IWA Publishing, London, UK, pp 16–17

Darn SM, Sodi R, Ranganath LR, et al (2006) Experimental and computer modelling speciation studies of the effect of pH and phosphate on the precipitation of calcium and magnesium salts in urine. Clin Chem Lab Med 44:185–191. https://doi.org/10.1515/CCLM.2006.034

Elser JJ, Bracken MES, Cleland EE, et al (2007) Global analysis of nitrogen and phosphorus limitation of primary producers in freshwater, marine and terrestrial ecosystems. Ecol Lett 10:1135–1142. https://doi.org/10.1111/j.1461-0248.2007.01113.x

Eriksson AK, Hillier S, Hesterberg D, et al (2016) Evolution of phosphorus speciation with depth in an agricultural soil profile. Geoderma 280:29–37. https://doi.org/10.1016/j.geoderma.2016.06.004

Eshetu B, Jandl G, Leinweber P (2012) Compost changed soil organic matter molecular composition: A py-gc/ms and py-fims study. Compost Sci Util 20:230–238. https://doi.org/ 10.1080/1065657X.2012.10737053

Franke M, Jandl G, Leinweber P (2006) Organic compounds in re-circulated leachates of aerobic biological treated municipal solid waste. Biodegradation 17:473–485. https://doi.org/ 10.1007/s10532-005-9019-5

Frankowski L, Bolałek J, Szostek A (2002) Phosphorus in bottom sediments of Pomeranian Bay (Southern Baltic - Poland). Estuar Coast Shelf Sci 54:1027–1038. https://doi.org/10.1006/ ecss.2001.0874

Galasso HL, Callier MD, Bastianelli D, et al (2017) The potential of near infrared spectroscopy (NIRS) to measure the chemical composition of aquaculture solid waste. Aquaculture 476:134–140. https://doi.org/10.1016/j.aquaculture.2017.02.035

Gómez-Brandón M, Juárez MFD, Zangerle M, Insam H (2016) Effects of digestate on soil chemical and microbiological properties: A comparative study with compost and vermicompost. J Hazard Mater 302:267–274.

https://doi.org/10.1016/j.jhazmat.2015.09.067
Gustafsson JP, Braun S, Tuyishime JRM, et al (2020) A Probabilistic Approach to Phosphorus Speciation of Soils Using P *K*-edge XANES Spectroscopy with Linear Combination Fitting. Soil Syst 4:26. https://doi.org/10.3390/soilsystems4020026
Hall OJ (1992) Chemical flux and mass balances in a marine fish cage farm. IV. Nitrogen. Mar Ecol Prog Ser 89:81–91
Hempfling R, Zech W, Schulten HR (1988) Chemical composition of the organic matter in forest soils: 2. Moder profile. Soil Sci. 146:262–276
Hesterberg D, Zhou W, Hutchison KJ, et al (1999) XAFS study of adsorbed and mineral forms of phosphate. J Synchrotron Radiat 6:636–638. https://doi.org/10.1107/S0909049599000370
Heumann S, Schlichting A, Böttcher J, Leinweber P (2011) Sterols in soil organic matter in relation to nitrogen mineralization in sandy arable soils. J Plant Nutr Soil Sci 174:576–586. https://doi.org/10.1002/jpln.200900273
Holby O, Hall P (1991) Chemical fluxes and mass balances in a marine fish cage farm. II Phosphorus. Mar Ecol Prog Ser 70:263–272. https://doi.org/10.3354/meps070263
Hupfauf S, Bachmann S, Fernández-Delgado Juárez M, et al (2016) Biogas digestates affect crop P uptake and soil microbial community composition. Sci Total Environ 542:1144–1154. https://doi.org/10.1016/j.scitotenv.2015.09.025
Jandl G, Leinweber P, Schulten HR, Eusterhues K (2004) The concentrations of fatty acids in organo-mineral particle-size fractions of a Chernozem. Eur J Soil Sci 55:459–470. https://doi.org/ 10.1111/j.1365-2389.2004.00623.x
Jegajeevagan K, Mabilde L, Gebremikael MT, et al (2016) Artisanal and controlled pyrolysis-based biochars differ in biochemical composition, thermal recalcitrance, and biodegradability in soil. Biomass and Bioenergy 84:1–11. https://doi.org/10.1016/j.biombioe.2015.10.025
Kar G, Hundal LS, Schoenau JJ, Peak D (2011) Direct chemical speciation of P in sequential chemical extraction residues using P *K*-edge X-ray absorption near-edge structure spectroscopy. Soil Sci 176:589–595. https://doi.org/10.1097/SS.0b013e31823939a3
Kazi ZH, Schnitzer MI, Monreal C, Mayer P (2011) Separation and identification of heterocyclic nitrogen compounds in biooil derived by fast pyrolysis of chicken manure. J Environ Sci Heal - Part B Pestic Food Contam Agric Wastes 46:51–61. https://doi.org/10.1080/03601234. 2010.515506
Klysubun W, Sombunchoo P, Deenan W, Kongmark C (2012) Performance and status of beamline BL8 at SLRI for X-ray absorption spectroscopy. J Synchrotron Radiat 19:930–936. https://doi.org/10.1107/S0909049512040381
Klysubun W, Tarawarakarn P, Thamsanong N, et al (2020) Upgrade of SLRI BL8 beamline for XAFS spectroscopy in a photon energy range of 1–13 keV. Radiat Phys Chem 175:108145. https://doi.org/10.1016/j.radphyschem.2019.02.004
Koch M, Kruse J, Eichler-Löbermann B, et al (2018) Phosphorus stocks and speciation in soil profiles of a long-term fertilizer experiment: Evidence from sequential fractionation, P *K*-edge XANES, and 31P NMR spectroscopy. Geoderma 316:115–126. https://doi.org/10.1016/j.geoderma. 2017.12.003
Köster JR, Cárdenas LM, Bol R, et al (2015) Anaerobic digestates lower N2O emissions compared to cattle slurry by affecting rate and product stoichiometry of denitrification - An N2O isotopomer case study. Soil Biol Biochem 84:65–74. https://doi.org/10.1016/j.soilbio.2015.01.021
Kraal P, Bostick BC, Behrends T, et al (2015) Characterization of phosphorus species in sediments from the Arabian Sea oxygen minimum zone: Combining sequential extractions and X-ray spectroscopy. Mar Chem 168:1–8. https://doi.org/10.1016/j.marchem.2014.10.009
Kruse J, Leinweber P (2008) Phosphorus in sequentially extracted fen peat soils: A *K*-edge X-ray absorption near-edge structure (XANES) spectroscopy study. J Plant Nutr Soil Sci 171:613–620. https://doi.org/10.1002/jpln.200700237
Le Corre KS, Valsami-Jones E, Hobbs P, Parsons SA (2009) Phosphorus recovery from wastewater by struvite crystallization: A review. Crit Rev Env Sci Tec 39:433-477
Leinweber P, Bathmann U, Buczko U, et al (2018) Handling the phosphorus paradox in agriculture and natural ecosystems: Scarcity, necessity, and burden of P. Ambio 47:3–19. https://doi.org/10.1007/s13280-017-0968-9
Leinweber P, Jandl G, Eckhardt K-U, Schulten H-R, Schlichting A, Hoffman D (2009) Analytical pyrolysis and soft-ionization mass spectrometry. In: Senesi N, Xing B, Huang PM (eds)

Biophysico-Chemical Processes Involving Natural Nonliving Organic Matter in Environmental Systems, 1st edn. Wiley-Interscience, Hoboken, NJ, USA, pp 539–588
Leinweber P, Kruse J, Baum C, et al (2013) Advances in Understanding Organic Nitrogen Chemistry in Soils Using State-of-the-art Analytical Techniques. Adv Agron 119:83-151
Leite SP, Vieira JRC, De Medeiros PL, et al (2006) Antimicrobial activity of Indigofera suffruticosa. Evidence-based Complement Altern Med 3:261–265. https://doi.org/10.1093/ecam/nel010
Leue M, Eckhardt KU, Ellerbrock RH, et al (2016) Analyzing organic matter composition at intact biopore and crack surfaces by combining DRIFT spectroscopy and Pyrolysis-Field Ionization Mass Spectrometry. J Plant Nutr Soil Sci 179:5–17. https://doi.org/10.1002/jpln.201400620
Li W, Joshi SR, Hou G, et al (2015) Characterizing phosphorus speciation of Chesapeake Bay sediments using chemical extraction, ^{31}P NMR, and X-ray absorption fine structure spectroscopy. Environ Sci Technol 49:203–211. https://doi.org/10.1021/es504648d
Maguire RO, Hesterberg D, Gernat A, et al (2006) Liming Poultry Manures to Decrease Soluble Phosphorus and Suppress the Bacteria Population. J Environ Qual 35:849–857. https://doi.org/10.2134/jeq2005.0339
Martins CIM, Eding EH, Verdegem MCJ, et al (2010) New developments in recirculating aquaculture systems in Europe: A perspective on environmental sustainability. Aquac Eng 43:83–93. https://doi.org/10.1016/j.aquaeng.2010.09.002
Morshedizad M, Panten K, Klysubun W, Leinweber P (2018) Bone char effects on soil: Sequential fractionations and XANES spectroscopy. Soil 4:23–35. https://doi.org/10.5194/soil-4-23-2018
Negassa W, Acksel A, Eckhardt KU, et al (2019) Soil organic matter characteristics in drained and rewetted peatlands of northern Germany: Chemical and spectroscopic analyses. Geoderma 353:468–481. https://doi.org/10.1016/j.geoderma.2019.07.002
Negassa W, Baum C, Leinweber P (2011) Soil amendment with agro-industrial byproducts: Molecular-chemical compositions and effects on soil biochemical activities and phosphorus fractions. J Plant Nutr Soil Sci 174:113–120. https://doi.org/10.1002/jpln.201000034
Palm HW, Knaus U, Wasenitz B, et al (2018) Proportional up scaling of African catfish (Clarias gariepinus Burchell, 1822) commercial recirculating aquaculture systems disproportionally affects nutrient dynamics. Aquaculture 491:155–168. https://doi.org/10.1016/j.aquaculture.2018.03.021
Peak D, Sims JT, Sparks DL (2002) Solid-state speciation of natural and alum-amended poultry litter using XANES spectroscopy. Environ Sci Technol 36:4253–4261. https://doi.org/10.1021/ es025660d
Pickering IJ, Brown, Jr GE, Tokunaga TK (1995) Quantitative speciation of selenium in soils using X-ray absorption spectroscopy. Environ Sci Technol 29:2456–2459. https://doi.org/10.1021/ es00009a043
Prietzel J, Dümig A, Wu Y, et al (2013) Synchrotron-based P *K*-edge XANES spectroscopy reveals rapid changes of phosphorus speciation in the topsoil of two glacier foreland chronosequences. Geochim Cosmochim Acta 108:154–171. https://doi.org/10.1016/j.gca.2013.01.029
Prietzel J, Harrington G, Häusler W, et al (2016) Reference spectra of important adsorbed organic and inorganic phosphate binding forms for soil P speciation using synchrotron-based *K*-edge XANES spectroscopy. J Synchrotron Radiat 23:532–544. https://doi.org/10.1107/S1600577515023085
Prüter J, Leipe T, Michalik D, et al (2020) Phosphorus speciation in sediments from the Baltic Sea, evaluated by a multi-method approach. J Soils Sediments 20:1676–1691. https://doi.org/ 10.1007/s11368-019-02518-w
Ravel B, Newville M (2005a) ATHENA, ARTEMIS, HEPHAESTUS: Data analysis for X-ray absorption spectroscopy using IFEFFIT. J Synchrotron Radiat 12:537–541. https://doi.org/10.1107/ S0909049505012719
Robinson JS, Baumann K, Hu Y, et al (2018) Phosphorus transformations in plant-based and bio-waste materials induced by pyrolysis. Ambio 47:73–82. https://doi.org/10.1007/s13280-017-0990-y
Sato S, Solomon D, Hyland C, et al (2005) Phosphorus speciation in manure and manure-amended soils using XANES spectroscopy. Environ Sci Technol 39:7485–7491. https://doi.org/10.1021/ es0503130
Schnitzer M, Schulten HR (1992) The Analysis of Soil Organic Matter by Pyrolysis-Field

Ionization Mass Spectrometry. Soil Sci Soc Am J 56:1811–1817. https://doi.org/10.2136/sssaj1992. 03615995005600060027x

Schröder J (2005) Revisiting the agronomic benefits of manure: A correct assessment and exploitation of its fertilizer value spares the environment. Bioresour Technol 96:253–261. https://doi.org/ 10.1016/j.biortech.2004.05.015

Schulten HR, Leinweber P (1996) Characterization of humic and soil particles by analytical pyrolysis and computer modeling. J Anal Appl Pyrolysis 38:1–53. https://doi.org/10.1016/S0165-2370(96)00954-0

Schulten HR, Schnitzer M (1993) A state of the art structural concept for humic substances. Naturwissenschaften 80:29–30. https://doi.org/10.1007/BF01139754

Shober AL, Hesterberg DL, Sims JT, Gardner S (2006) Characterization of Phosphorus Species in Biosolids and Manures Using XANES Spectroscopy. J Environ Qual 35:1983. https://doi.org/10.2134/jeq2006.0100

Sleutel S, Leinweber P, Begum SA, et al (2008) Composition of organic matter in sandy relict and cultivated heathlands as examined by pyrolysis-field ionization MS. Biogeochemistry 89:253–271. https://doi.org/10.1007/s10533-008-9217-4

Stevenson FJ (1994) Humus Chemistry: Genesis, Composition and Reactions, 2nd edn, John Wiley & Sons, New York, USA, pp 166–187

Strauch SM, Wenzel LC, Bischoff A, et al (2018) Commercial African Catfish (Clarias gariepinus) recirculating aquaculture systems: Assessment of element and energy pathways with special focus on the phosphorus cycle. Sustain 10:1805. https://doi.org/10.3390/su10061805

Werner F, Prietzel J (2015) Standard Protocol and Quality Assessment of Soil Phosphorus Speciation by P *K*-Edge XANES Spectroscopy. Environ Sci Technol 49:10521–10528. https://doi.org/ 10.1021/acs.est.5b03096

Wiedow D, Baum C, Leinweber P (2007) Inoculation with Trichoderma saturnisporum accelerates wheat straw decomposition on soil. Arch Agron Soil Sci 53:1–12. https://doi.org/10.1080/ 03650340601054213

Withers PJA, Doody DG, Sylvester-Bradley R (2018) Achieving sustainable phosphorus use in food systems through circularisation. Sustain 10:1–17. https://doi.org/10.3390/su10061804

Zhang J, Kitazawa D (2015) Numerical analysis of particulate organic waste diffusion in an aquaculture area of Gokasho Bay, Japan. Mar Pollut Bull 93:130–143. https://doi.org/ 10.1016/j.marpolbul.2015.02.007

7 Summarizing discussion, conclusions and outlook

7.1. Introduction

This thesis aimed at revealing the P speciation and detecting functional interactions between single chemical P compounds and transformation processes of P along transport pathways in test areas of different size including transects from terrestrial and wetland soils to aquatic sediments. For this purpose, the soil and sediment samples were analyzed by the complementary methodologies of sequential P fractionation, XANES spectroscopy, liquid ^{31}P NMR spectroscopy and SEM-EDX analysis. In this chapter, the findings of Chapters 2 to 6 are combined and previous discussions are joined in order to derive conclusions for future research. The term “soil” is used for terrestrial, agricultural used Cambisols and Luvisols, “wetland” for semiterrestrial gley soils and “sediment” for inundated, aquatic sediments in the following discussion.

7.2. Phosphorus species along different sequences from terrestrial soils to aquatic sediments

A fundamental basis to enable comparisons of the P speciation in soil and sediment samples is, next to the application of the same P research methods, a similar way of sample pretreatment. The common pretreatment procedures of soil samples includes drying, sieving and in some cases grinding prior to various chemical P laboratory analyses. Although sediments can be especially vulnerable to chemical changes due to drying and other pretreaments, we did not detect fundamental changes in the P speciation (Chapter 2). Effects of sample pretreament were much lower compared to the influence of sample origin. Thus, we carried out the following investigations on this basis and applied the same pretreatments on all samples prior to analyses with sequential P fractionation, XANES spectroscopy, liquid ^{31}P NMR spectroscopy and SEM-EDX.

Our general findings confirmed previous research results that agricultural soils were dominated by labile and moderatly labile P fractions such as resin-P, $NaHCO_3$-P and NaOH-P, whereas most aquatic sediments contained more stable fractions such as H_2SO_4-P and residual-P determined by sequential P fractionation. As shown in Chapter 3, terrestrial, arable soils from the direct surrounding area of a kettle hole contained about 127 mg kg^{-1} NaOH-P_o and 114 mg kg^{-1} $NaHCO_3$-P_i. Sediments from the kettle hole were clearly dominated by residual-P (maximum of 1729 mg kg^{-1}). Soils from the coast of northern Germany from an experimental

site at the University of Rostock contained up to 137 mg kg^{-1} NaOH-P_i, while sediments from the Baltic Sea had concentrations of about 500 mg kg^{-1} H_2SO_4-P (Chapter 5). Different from that, terrestrial soils from an agricultural site near a shallow lagoon (Bodden) of the Baltic Sea were dominated by the fraction of H_2SO_4-P (261 mg kg^{-1}) similarly as the corresponding sediments from the Bodden with a maximum of 265 mg kg^{-1} H_2SO_4-P (Chapter 4). This was the only exception of high concentrations of stable P fractions in terrestrial soils within our investigations. It can be explained by the elevated location and sloping relief of the arable field. Topsoil material was transported away from the slope by erosion and, thus, $CaCO_3$-containing underlying parent material entered the remaining topsoil by agricultural tillage. The direct comparison of P concentrations between terrestrial/semiterrestrial soils and aquatic sediments was enabled by a similar sample pretreatment of the soils and sediments including drying, sieving and grinding (Chapter 2). Although water contents of aquatic sediments are naturally different from terrestrial soils (e.g. Chapter 4; water content arable soils: 5 to 9%, water content aquatic sediments: 20 to 75%) and thereby the soils and sediments also differ in density, P concentrations were reffered to dried samples and thus comparable at a standardized scale.

Results from XANES spectroscopy were similar for most soils but different from the sediments. We determined about 61 to 100% Fe-P and Al-P in terrestrial soils around a kettle hole. The aquatic sediments from the kettle hole still contained maxima of 74% Fe-P but also up to 43% Ca-P (Chapter 3). Terrestrial soils from an experimental site in Rostock were dominated by maxima of 92% Fe-P and Al-P, whereas up to 100% of Ca-P was present in aquatic sediments from the Baltic Sea (Chapter 5). In arable soils from an agricultural site near a shallow lagoon of the Baltic Sea we determined a maximum of 92% Ca-P and in the corresponding aquatic sediments 54 to 100% Ca-P (Chapter 4). The high proportions of Ca-P in the soil can be explained by elevated concentrations of $CaCO_3$ in the terrestrial soil from the underlying parent material, promoting the formation of Ca-associated P compounds, whereas the dominance of Ca-P species in the aquatic lagoon sediments agreed with the results from other aquatic environments of the present investigations.

The results of sequential P fractionation and XANES spectroscopy were generally consistent among the three different scales of investigations of a kettle hole environment, soils and sediments around a shallow lagoon of the Baltic Sea and the total Baltic Sea. Although these investigated microscale, mesoscale and macroscale ecosystems differed not only in size but

also in their biogeochemical basic conditions such as influence of agricultural land use, climate and weather or local flora and fauna, these factors did not fundamentally affect their P speciation. The general trend of transitions from labile and moderatly labile P fractions and Fe and Al associated P species in terrestrial soils towards more stable P fractions and higher proportions of Ca-P in aquatic sediments was approved along different sequences for the first time. This transition appeared for the microscale kettle hole environment, as well as for the mesoscale Bodden test area with some exceptions within the soils due to erosion and the macroscale Baltic Sea investigation. Since we recorded data of P fractionation and XANES spectroscopy from all terrestrial/semiterrestrial soils and aquatic sediments from these three different test areas, a principle component analysis (PCA, Figure 7-1) visualizes the similarities and differences among the samples. The distribution of samples was mainly influenced by Fe-P, Al-P and Ca-P compounds from XANES spectroscopy and the H_2SO_4-P fraction from sequential fractionation. All remaining P compound groups from XANES spectroscopy and P fractionation accumulated in the middle of the PCA and thereby represent minor influence on the differentiation of the soils and sediments from various environments. A rough split of Fe and Al associated P on the one side and Ca-P and H_2SO_4-P on the other side appeared along the axis of principle component 1 (PC1), explaining 66% of variance. The occurrence of Ca-P and H_2SO_4-P on one side of the PCA confirmed the common assignment of P fractionation that acid extractable P is mainly associated with Ca-P species (Hedley et al., 1982) by analyses of soils and sediments from three different test areas. Most kettle hole samples were located on the side of Fe-P and Al-P species, many Baltic Sea lagoon soils, wetland soils and sediments on the opposite side of Ca-P and H_2SO_4-P, while samples from the total Baltic Sea were distributed on both sides. Thus, we confirm that the P speciation of kettle hole sediments was more similar to terrestrial, arable soils, whereas sediments from a Bodden and the Baltic Sea had greater agreements with P species reflecting aquatic influences. The Baltic Sea lagoon soil sample at the left bottom of the PCA is the topsoil of a wetland covered by *Phragmites australis* (W1, Chapter 4). In this sample, XANES spectroscopy determined considerably more Al-P species than in all other samples and for this reason it was separated from all other samples in the PCA.

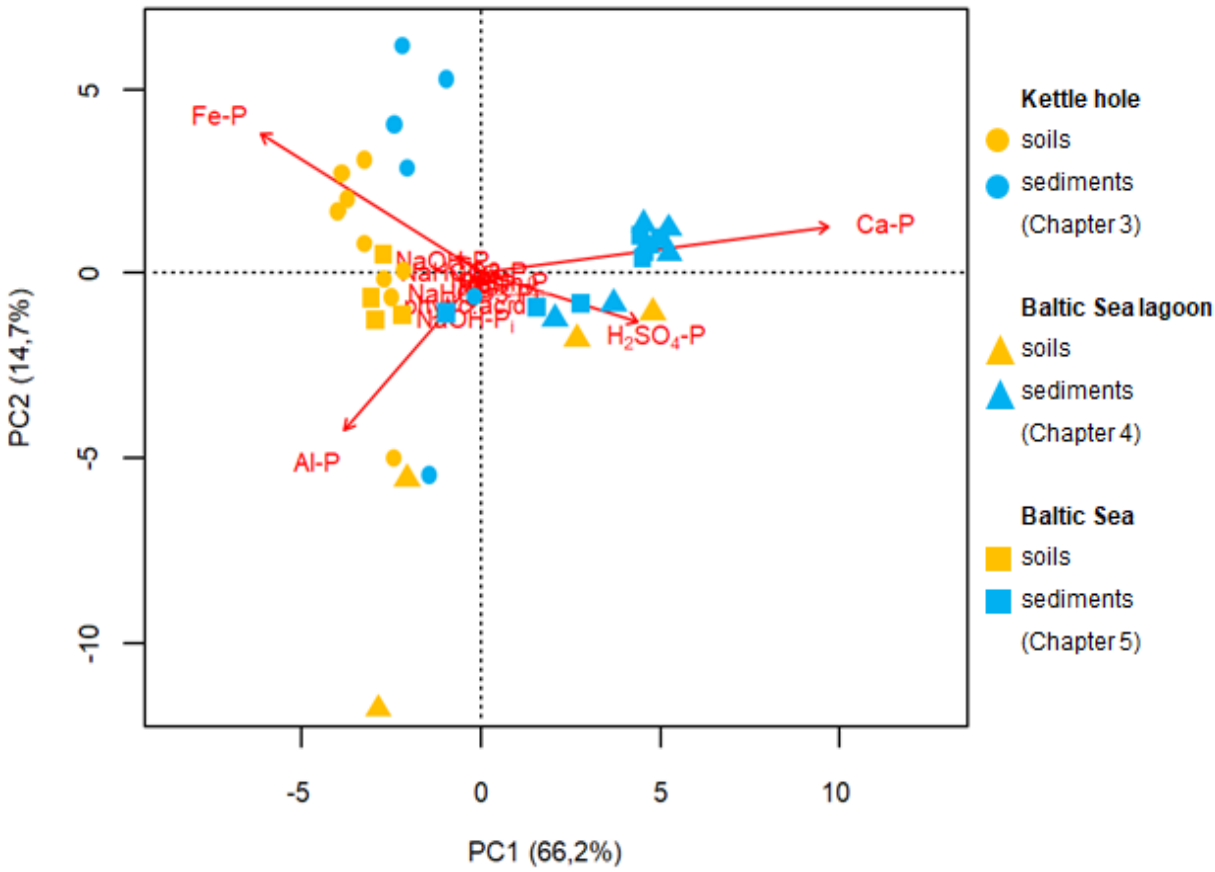

Figure 7-1 Principal component analysis (PCA) of sediment and soil samples from the investigations of the Chapters 3, 4, and 5. Results of sequential P fractionation (fractions: Resin-P, $NaHCO_3$-P_i, $NaHCO_3$-P_o, NaOH-P_i, NaOH-P_o, and H_2SO_4-P) and P XANES analysis (Fe-P, Al-P, Ca-P, Mg-P, and phytic acid) are presented and were calculated as percentages.

In addition to the results from sequential P fractionation and XANES spectroscopy, kettle hole soils and sediments and the Baltic Sea soils and sediments were analyzed with the method of ^{31}P NMR spectroscopy and the Baltic Sea sediments with SEM-EDX (Chapters 3 and 5). The analysis of Baltic Sea sediments with SEM-EDX resulted in high numbers of Fe-phosphate particles near the coast and thereby supported the findings of sequential fractionation and XANES spectroscopy on the single-particle level. ^{31}P NMR spectroscopy determined a decrease of the variety of mono- and diester P compounds and an increase of ortho-P with growing distance from the coast in the Baltic Sea sample set. Also in the kettle hole sediments, a lower variety of P_o species was found compared to the surrounding soils, particularly in the phosphomonoester region. Similarly as in the Baltic Sea samples, ortho-P was the most abundant P compound in the NaOH-EDTA extracts of the kettle hole soils and sediments. In short, results of solution ^{31}P NMR spectroscopy also confirmed an alteration of especially P_o species from terrestrial soils to aquatic sediments in different test areas.

In addition to P transformation on its transport pathways from land to sea, our investigations detected accumulations of stable Ca-P species and complex forms of P_o in kettle hole sediments compared to surrounding soils and especially moderately stable P, Al-P and P_o compounds in wetland soils between agricultural soils and natural aquatic sediments. Thus, kettle hole sediments as well as wetland soils act as sinks for P-containing particles and thereby can help to prevent direct transfer of various P species, e.g., by leaching or runoff during erosion events from agricultural soils to adjacent freshwater and/or marine resources protecting vulnerable aquatic ecosystems from further eutrophication.

Origins of P compounds in aquatic sediments can be diverse, depending on several factors such as evolution, geographical location and geological history of the respective water system. Phosphorus in river sediments frequently originates from urban runoff, municipal sewage or agricultural fertilization (Huanxin et al., 1997). Phosphorus in sediments off the coast of Northwest Africa was derived from erosion of phosphatic rocks during Pleistocene (Summerhayes et al., 1972) and possible sources of sedimentary P in the central Pacific Ocean were identified to be eolian atmospheric inputs of terrestrial particles entering the ocean by heavy events of rainfall (Ni et al., 2015). To discover, if P in sediments can also originate from aquatic organisms such as fish naturally occurring in fresh- and saltwater ecosystems, we investigated the P speciation of fish fecal matter. The solid waste from African Catfish in a recirculation aquaculture system (RAS) exclusively contained Ca-bound P compounds as determined by XANES spectroscopy (Chapter 6). Thus, this waste can contribute to high amounts of Ca-associated P in aquatic sediments. Zhang and Kitazawa (2015) confirmed that fecal matter from fish cultured in cages can contribute as much as 80% to particulate organic waste in the direct aquatic environment. Furthermore, the deposition of this waste near the sea bottom occurs not only beneath the fish cages but they can also be transported towards the sea coastlines depending on current conditions during different seasons (Zhang and Kitazawa, 2015). The contribution of fish fecal matter can be an additional influencing factor on the Ca dominated and stable P species in aquatic sediments of the present investigations, even if further research about naturally occurring fish is needed next to studies about fish cultured in cages and from RAS.

7.3. Summarizing discussion

A visual summary of determined P species and transformation processes in the different investigated environments is displayed in Figure 7-2.

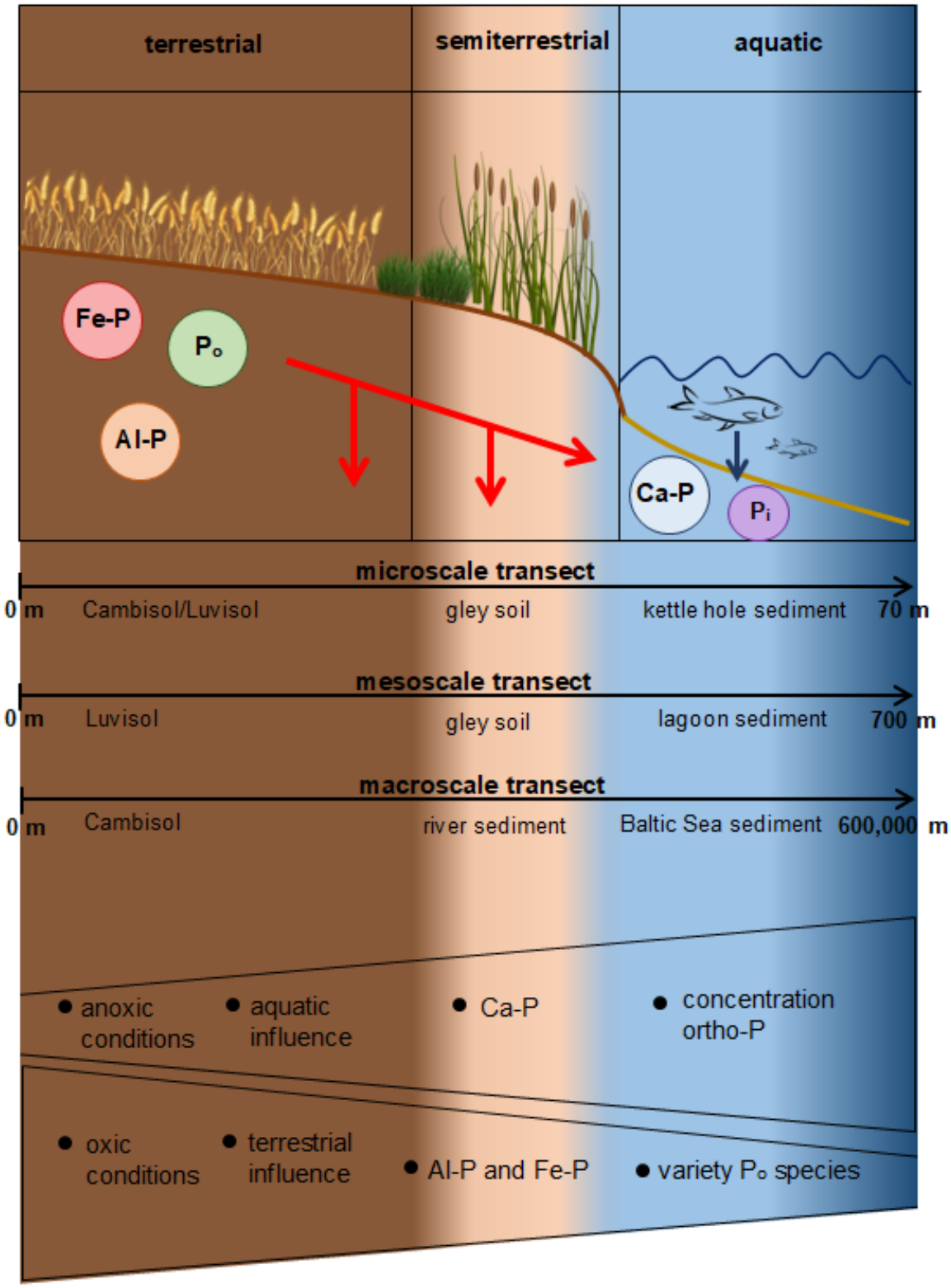

Figure 7-2 Summarizing scheme of determined P species and transformation processes from the investigations of Chapters 3 to 6.

The general transition from moderately labile Fe- and Al- associated P and the great variety of P_o in terrestrial soils over peripheral semiterrestrial areas with sink and buffer functions towards more stable and Ca dominated P species in aquatic sediments is illustrated by the red arrows in the upper part of the figure. The investigated micro-, meso- and macroscale transects of terrestrial and semiterrestrial soils and aquatic sediments are displayed below and at the bottom of Figure 7-2, the changing environmental conditions and consequences are summarized. The elevated concentrations of stable P fractions in terrestrial soils from an agricultural site near a shallow lagoon of the Baltic Sea (Chapter 4) were not included in the figure because they were considered to be an exception of the investigated environments (see dicussion above).

Movement of P can occur in dissolved or particulate forms and it already has been identified a long time ago that 75 to 90% of P in agricultural land is transported by soil erosion (Sharpley et al., 1993). The present investigation confirmed transport pathways of P from arable soils to kettle hole sediments, Baltic Sea lagoon sediments and Baltic Sea sediments. Although the general P speciation changed from soil to sediment in all investigated test areas, specific P compounds within the sediments suggested their terrestrial origin. The P_o compound of IP_6 has been indentified abundantly in terrestrial soils because it is known to act as P storage compound in plants, especially in developing seeds and has strong sorption properties to clays and soil OM (e.g. Turner et al., 2002; Negassa et al., 2010; Noack et al., 2014; Alewell et al., 2020). In aquatic sediments, IPs have been detected in substantial quantities, although only few aquatic organisms are able to synthesize them (Turner et al., 2002). Thus, most of the IPs present in aquatic sediments are suggested to be derived from terrestrial environments. We were able to determine *scyllo*-IP_6, *myo*-IP_6 and *neo*-IP_6 in arable soils as well as in adjacent kettle hole sediments (Chapter 3) confirming transport processes of IP_6 from terrestrial soil to aquatic sediments. Furthermore, the entry of soil aggregates to fluvial systems was also confirmed earlier by differentiating parameters such as density, porosity and settling velocity between soil aggregates and fluvial sediments (Droppo et al., 2004).

Phosphorus compounds entering aquatic evironments are either released to the water column and consumed by aquatic organisms such as algae and macrophytes or accumulated within the sediment. Soil particles, containing high concentrations of Fe-associated P, can be transported towards aquatic ecosystems with sediments under anaerobic reducing conditions. The lack of oxygen in sediments results in a reduction of ferric (Fe^{3+}) to ferrous (Fe^{2+}) phosphates of which

the latter are more soluble in water (Thomas, 1970). Our investigation of kettle hole sediments and adjacent soils (Chapter 3) and Baltic Sea lagoon sediments (Chapter 4) confirmed that especially stable P fractions such as H_2SO_4-P and P associated with Ca and/or Mg can be accumulated and conserved in deeper sediments lowering the probability of P mobilization into the above water column. The input of P from agriculture to adjacent waters can also be significantly reduced by wetland soils along shore areas. We identified accumulations of especially moderately stable P, Al-P and P_o compounds in *Phragmites* wetland soils (Chapter 4) saving adjacent aquatic ecosystems from direct inputs of these P species. Thus, it is one of the most important tasks of the future to create new, or to preserve and maintain existing buffer strips and coastal wetlands by removing P with harvests of the plant cover such as reeds or to find ways to regain P from the terrestrial as well as aquatic sinks to enable nutrient recycling. This is the only way we can slow down the progressive eutrophication of waterbodies around the world including associated problems such as biodiversity losses, ecosystem degradation, harmful algae blooms and oxygen deficiency (Oliveira and Machado, 2013). At the same time we can contribute to P recycling in agricultural areas in order to be able to use the limited reserves of rock phosphate more economically and environmentally friendly to answer global food necessities.

7.4. Conclusions and future research directions

The metholodogical combination of sequential P fractionation, P *K*-edge XANES spectroscopy and ^{31}P NMR spectroscopy was complementary and suitable for creating a comprehensive picture of inorganic and organic P species in transects including terrestrial/semiterrestrial soils and aquatic sediments.

The transition from labile and moderately labile Fe- and Al- associated P and great variety of P_o species in terrestrial soils over peripheral semiterrestrial areas with sink and buffer functions towards more stable Ca- and Mg-P and less differrent P_o species in aquatic sediments has been demonstrated for three different micro-, meso- and macroscaled evrionmental transects.

Kettle hole sediments, coastal wetland soils and Baltic Sea lagoon sediments acted as sinks for especially acid-extractable, Ca-associated and complex organically bound P species protecting adjacent environments from excess P inputs from agriculture.

The discovery of *scyllo*-IP_6, *myo*-IP_6 and *neo*-IP_6 not only in arable soils but as well in adjacent aquatic sediments supported the assumption of a terrestrial origin and thereby transport processes of these P species from soil to sediment.

Fish fecal matter can contribute to high amounts of stable P species in aquatic sediments because waste from an African Catfish RAS contained exclusively P compounds of Ca-phytate, Ca-hydrogen phosphate and Ca-5-hydroxyapatite.

Forthcoming investigations for the protection of aquatic ecosystems from excess P should either focus on possibilities and measures to avoid P emissions from arable areas or have to focus on how to regain P from terrestrial as well as aquatic sinks to recycle it and enable a closing of nutrient element circles in agriculture.

7.5. Literature of Chapter 1 and Chapter 7

Ajiboye, B, Akinremi, OO, Hu, Y, Flaten DN, 2007. Phosphorus speciation of sequential extracts of organic amendments using nuclear magnetic resonance and X-ray absorption near-edge structure spectroscopies. J. Environ. Qual. 36, 1563-1576

Alewell, C, Huang, J-W, McLaren, TI, Huber, L, Bünemann, EK, 2020. Phosphorus retention in constructed wetlands enhanced by zeolite- and clinopyroxene-dominated lava sand. Hydrol. Process. 35, e14040

Audette, Y, O'Halloran, IP, Nowell, PM, Dyer, R, Kelly, R, Voroney, RP, 2018. Speciation of Phosphorus from agriultural muck soils to stream and lake sediments. J. Environ. Qual. 47, 884-892

Baumann, K, Glaser, Mutz, J-E, Karsten, U, MacLennan, A, Hu, Y, Michalik, D, Kruse, J, Eckhardt, K-U, Schall, P, Leinweber, P, 2017. Biological soil crusts of temperate forests: Their role in P cycling. Soil Biology & Biochemistry 109, 156-166

Bonsdorff, E, Blomqvist EM, Mattila, J, Norkko, A, 1997. Coastal eutrophication: causes, consequences and perspectives in the archipleago areas of the Northern Baltic Sea. Estuar. Coast Shelf Sci. 44, 63-72

Cade-Menun, BJ, 2005. Characterizing phosphorus in environmental and agricultural samples by 31P nuclear magnetic resonance spectroscopy. Talanta 66, 359-371

Cade-Menun, BJ, Duhamel, S, Dodd, RJ, Lønborg, C, Parsons, CT, Taylor WD, 2019. Editorial: phosphorus along the soil-freshwater-ocean continuum. Front. Mar. Sci. 6, 28

Chen, A, Arai Y, 2020. Current uncertainties in assessing the colloidal phosphorus loss from soil. Adv. Agron. 163, 117-151

Droppo, IG, Nackaerts, K, Walling DE, Williams N, 2004. Can flocs and water stable soil aggregates be differentiatied within fluvial systems? Catena 60, 1-18

Frankowski, L, Bolałek, J, Szostek, A, 2002. Phosphorus in bottom sediments of Pomeranian Bay (Southern Baltic - Poland). Estuar. Coast. Shelf Sci. 54, 1027-1038

Gypser, S, Schütze, E, Freese, D, 2021. Single and binary Fe- and Al-hydroxides affect potential phosphorus mobilization and transfer from pools of different availability. Soil Systems 5, 33

Hedley, MJ, Stewart, JWB, Chauhan, BS, 1982. Changes in inorganic and organic soil phosphorus fractions induced by cultivation practices and by laboratory incubations. Soil Science Society of America Journal 46, 970-976

Huanxin, W, Preslex, BJ, Velinsky, DJ, 1997. Distribution and sources of phosphorus in tidal river sediments in the Washington, DC, area. Environmental Geology 30, 224-230

Kerr, JG, Burford, MA, Olley, JM, Bunn, SE, Udy, J, 2011. Examining the link between terrestrial and aquatic phosphorus speciation in a subtropical catchment: the role of selective erosion and transport of fine sediments during storm events. Water Research 45, 3331-3340

Koch, M, Kruse, J, Eichler-Löbermann, B, Zimmer, D, Wilbold, S, Leinweber, P, Siebers, N, 2018. Phosphorus stocks and speciation in soil profiles of a long-term fertilizer experiment: evidence from sequential fractionation, P *K*-edge XANES, and 31P NMR spectroscopy. Geoderma 316, 115–126. https://doi.org/10.1016/j.geoderma.2017.12.003

Kraal, P, Slomp, CP, 2014. Rapid and extensive alteration of phosphorus speciation during oxic storage of wet sediment samples. PLoS One 9, 1-6

Kruse, J, Abraham, M, Amelung, W, Baum, C, Bol, R, Kühn, O, Lewandowski, H, Niederberger, J, Oelmann, Y, Rüger, C, Santner, J, Siebers, M, Siebers, N, Spohn, M, Vestergren, J, Vogts, A, Leinweber, P, 2015. Innovative methods in soil phosphorus research: a review. J. Plant Nutr. Soil Sci. 178, 43-88

Lewis, WM, Wurtsbaugh, WA, Paerl, HW, 2011. Rationale for control of anthropogenic nitrogen and phosphorus to reduce eutrophication of inland waters. Environ. Sci. Technol. 45, 10300-10305

Łukawska-Matuszewska, K, Bolałek, J, 2008. Spatial distribution of phosphorus forms in seduments in the Gulf of Gdańsk (southern Baltic Sea). Cont. Shelf Res. 28, 977-990

McLaren, TI, Smernik, RJ, McLaughlin, MJ, Doolette, AL, Richardson, AE, Frossard, E, 2020. The chemcial nature of soil organic phosphorus: a critical review and global comilation of quantitative data. Adv. Agron. 160, 51-124

McLaren, TI, Verel, R, Frossard, E, 2021. Soil phosphomonoesters in large molecular weight material comprise of multiple components. Soil Sci. Soc. Am. J. 86, 345-357

Negassa, W, Kruse, J, Michalik, D, Appathurai, N, Zuin, L, Leinweber, P, 2010. Phosphorus speciation in agro-industrial byproducts: sequential fractionation, solution ^{31}P NMR, and P *K*- and $L_{2,3}$-edge XANES spectroscopy. Einviron. Sci. Technol. 44, 2092-2097

Ni, J, Lin, P, Zhen, Y, Yao, X, Guo, L, 2015. Distribution, source and chemical speciation of phosphorus in surface sediments of the central Pacific Ocea. Deep-Sea Research I 105, 74-82

Noack, SR, McLaughlin, MJ, Smernik, RJ, McBeath, TM, Armstrong, RD, 2014. Phosphorus speciation in mature wheat and canola plants as affected by phosphorus supply. Plant Soil 378, 125-137

Oliveira, M, Machado, AV, 2013. The role of phosphorus on eutrophication: a historical review and future perspectives. Environ. Technol. Rev. http://dx.doi.org/10.1080/21622515.2013.861877

Patrick, WH, Khalid, RA, 1974. Phosphate release and sorption by soils and sediments: effect of aerobic and anaerobic conditions. Science 186(4158), 53-55

Reusser, JE, Verel, R, Frossard, E, McLaren, TI, 2020. Quantitative measures of myo-IP6 in soil using solution 31P NMR spectroscopy and spectral deconvolution fitting inclusing a broad signal. Environ. Sci.: Processes Impacts 22, 1084

Schmieder, F, Gustafsson, JP, Klysubun, W, Zehetner, F, Riddle, M, Kirchmann, H, Bergström, L, 2020. Phosphorus speciation in cultivated organic soils revealed by P *K*-edge XANES spectroscopy. J. Plant Nutr. Soil Sci. 183, 367-381

Sharpley, AN, Daniel, TC, Edwards, DR, 1993. Phosphorus movement in the landscape. J. Prod. Agric. 6(4), 492-500

Sims, JT, Pierzynski, GM, 2005. Chemistry of phosphorus in soils. In Chemical Processes in Soils, ed. M. A. Tabatabai and D. L. Sparks, 151-192. 8th ed. Madison: SSSA Book Series

Summerhayes, CP, Nutter, AH, Tooms, JS, 1972. The ditribution and origin of phosphate in sediments off Northwest Africa. Sediment. Geol. 8, 3-28

Thomas, GW, 1970. Soil and climatic factor which affect nutrient mobility. Soil Science Society of America Special Publication No. 4, 1-20

Turner, BL, Papházy, MJ, Haygarth PM, Mckelvie, ID, 2002, Inositol phosphates in the environment. Phil. Trans. R. Soc. Land. B 357, 449-469

Turner, BL, 2008. Soil organic phosphorus in tropical forests: an assessment of the NaOH-EDTA extraction procedure for quantitative analysis by solution ^{31}P NMR spectroscopy. Eur. J. Soil Sci. 59, 453-466

Withers, PJA, Neal, C, Jarvie, HP, Doody, DG, 2014. Agriculture and eutrophication: where do we go from here? Sustainability 6, 5853-5875

Zhang, J, Kitazawa, D, 2015. Numerical analysis of particulate organic waste diffusion in an aquaculture area of Gokasho Bay, Japan. Mar. Pollut. Bull. 93, 130-143

8 Appendix

8.1. Supplemental material of the manuscript: Influence of sample pretreatment on P speciation in sediments evaluated with sequential fractionation and P *K*-edge XANES spectroscopy (Chapter 2)

Journal: Communications in Soil Science and Plant Analysis

Authors: Julia Prüter[1], Yongfeng Hu[2], Peter Leinweber[1]

[1]*University of Rostock, Soil Science, Justus-von-Liebig Weg 6, 18051 Rostock, Germany*

[2]*Canadian Light Source, Inc., University of Saskatchewan, 44 Innovation Boulevard, Saskatoon, Saskatchewan S7N 2V3, Canada*

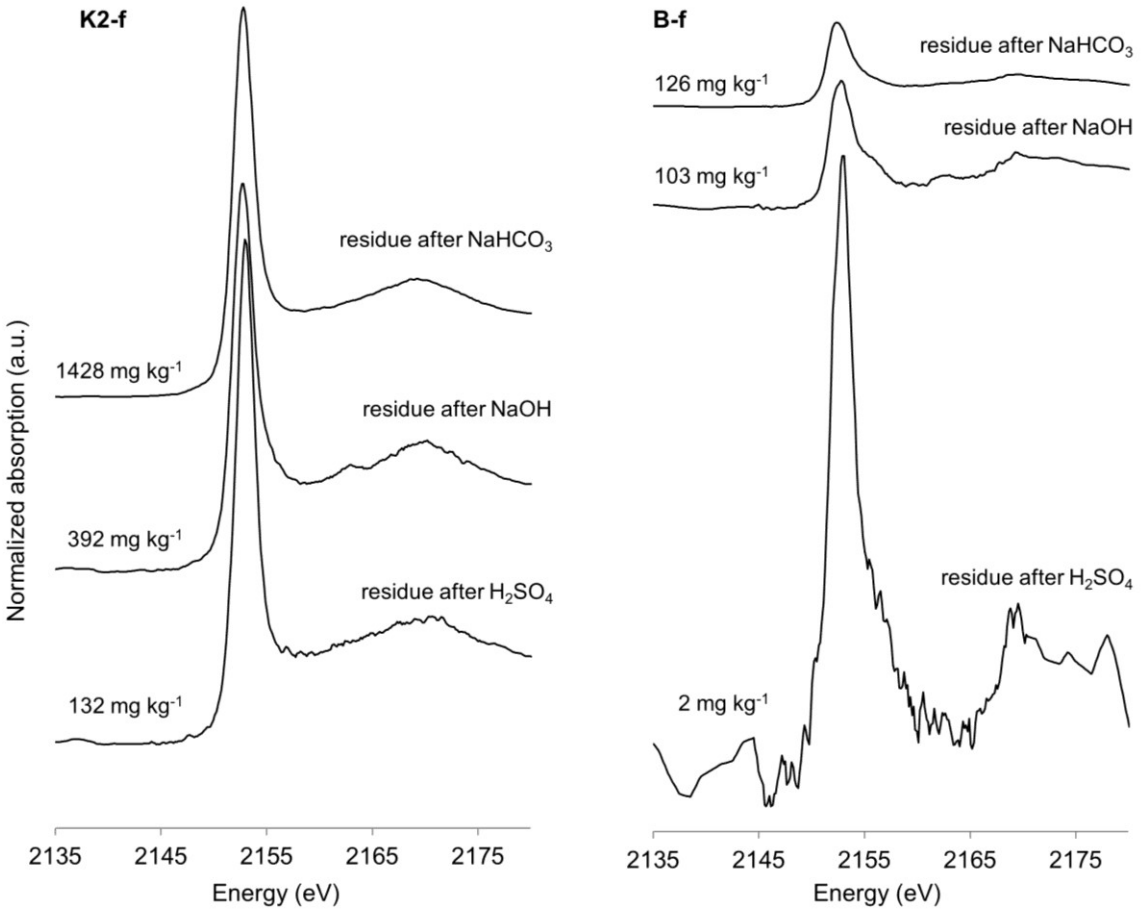

Figure 8-1-1 Stacked P *K*-edge XANES spectra of fresh kettle hole (K2-f) and Bodden (B-f) sediment solid extraction residues after the extractions steps with resin and $NaHCO_3$, NaOH, and H_2SO_4. Concentrations of P (mg kg^{-1}) were calculated as the sum of fractions from sequential P fractionation.

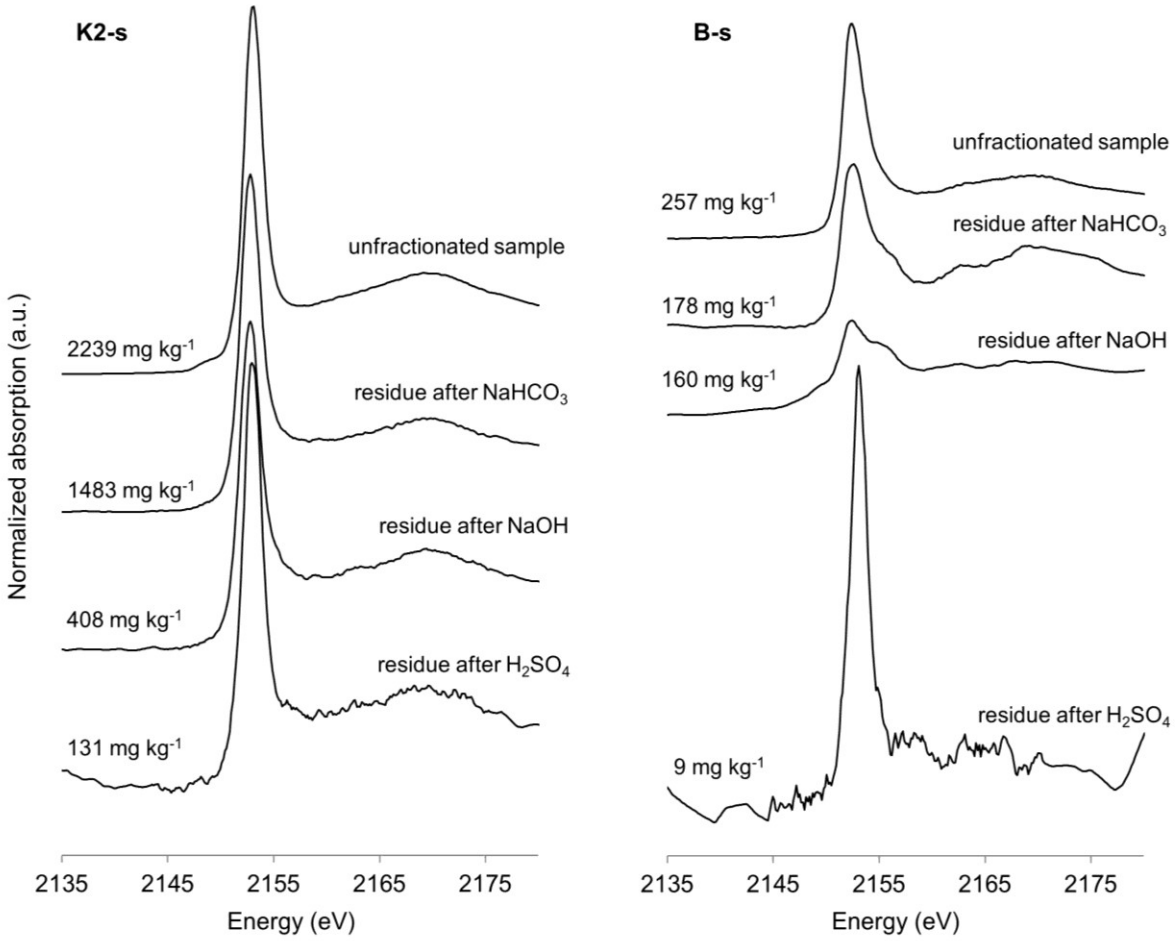

Figure 8-1-2 Stacked P *K*-edge XANES spectra of unfractionated, sieved kettle hole (K2-s) and Bodden (B-s) sediment and the respective solid extraction residues after the extractions steps with resin and $NaHCO_3$, NaOH, and H_2SO_4. Concentrations of P (mg kg^{-1}) were calculated as the sum of fractions from sequential P fractionation.

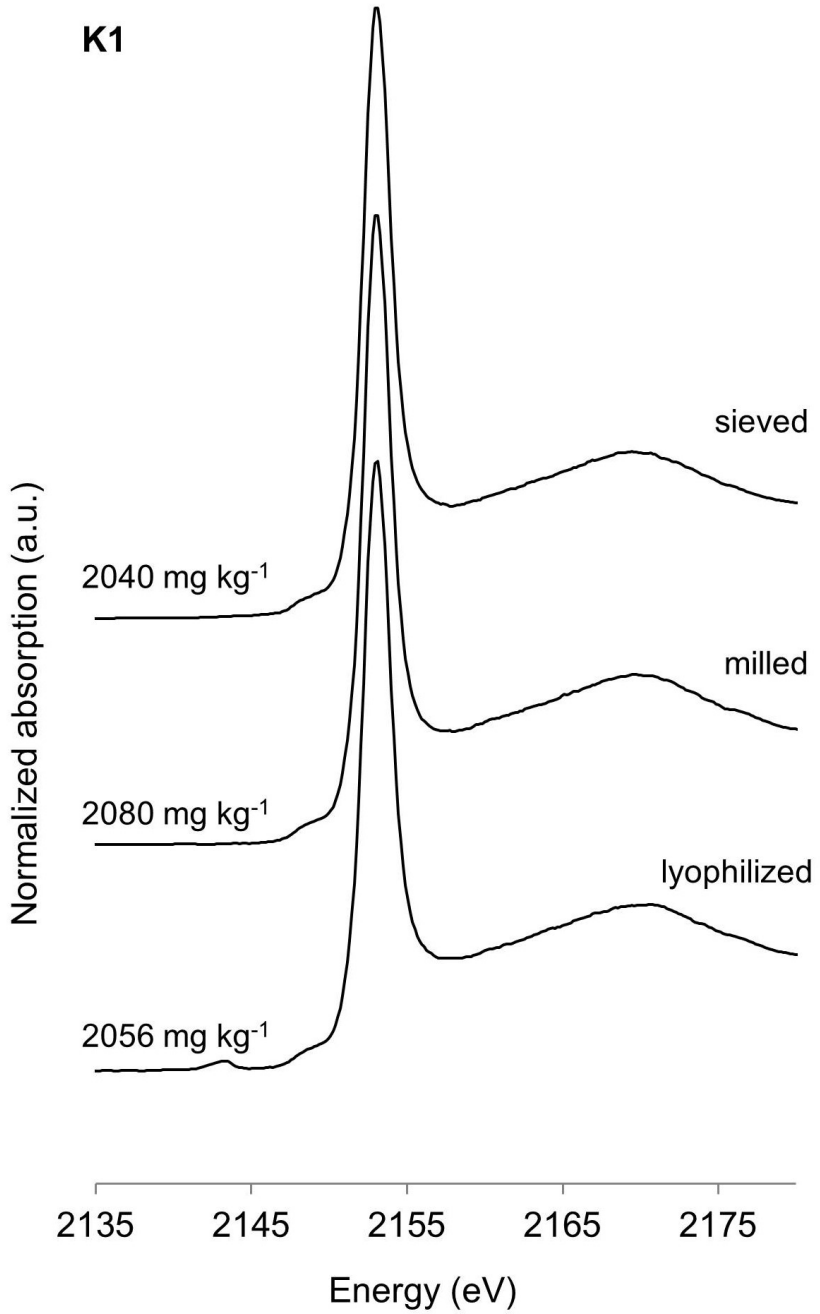

Figure 8-1-3 Stacked P *K*-edge XANES spectra of unfractionated kettle hole sediment (0-10 cm depth) of three different pretreatments sieved, milled, and lyophilized. Concentrations of P (mg kg^{-1}) were determined by ICP-OES.

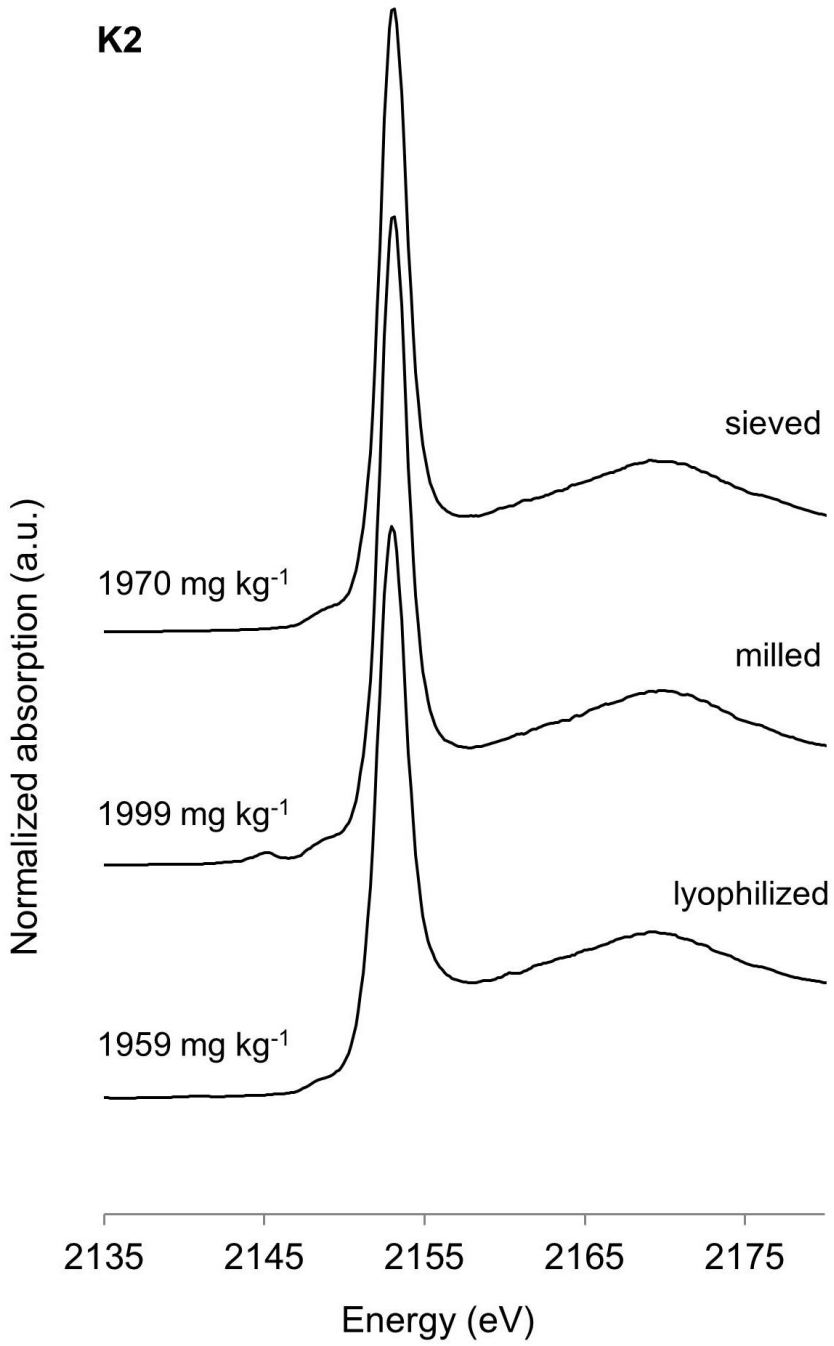

Figure 8-1-4 Stacked P *K*-edge XANES spectra of unfractionated kettle hole sediment (10-20 cm depth) of three different pretreatments sieved, milled, and lyophilized. Concentrations of P (mg kg^{-1}) were determined by ICP-OES.

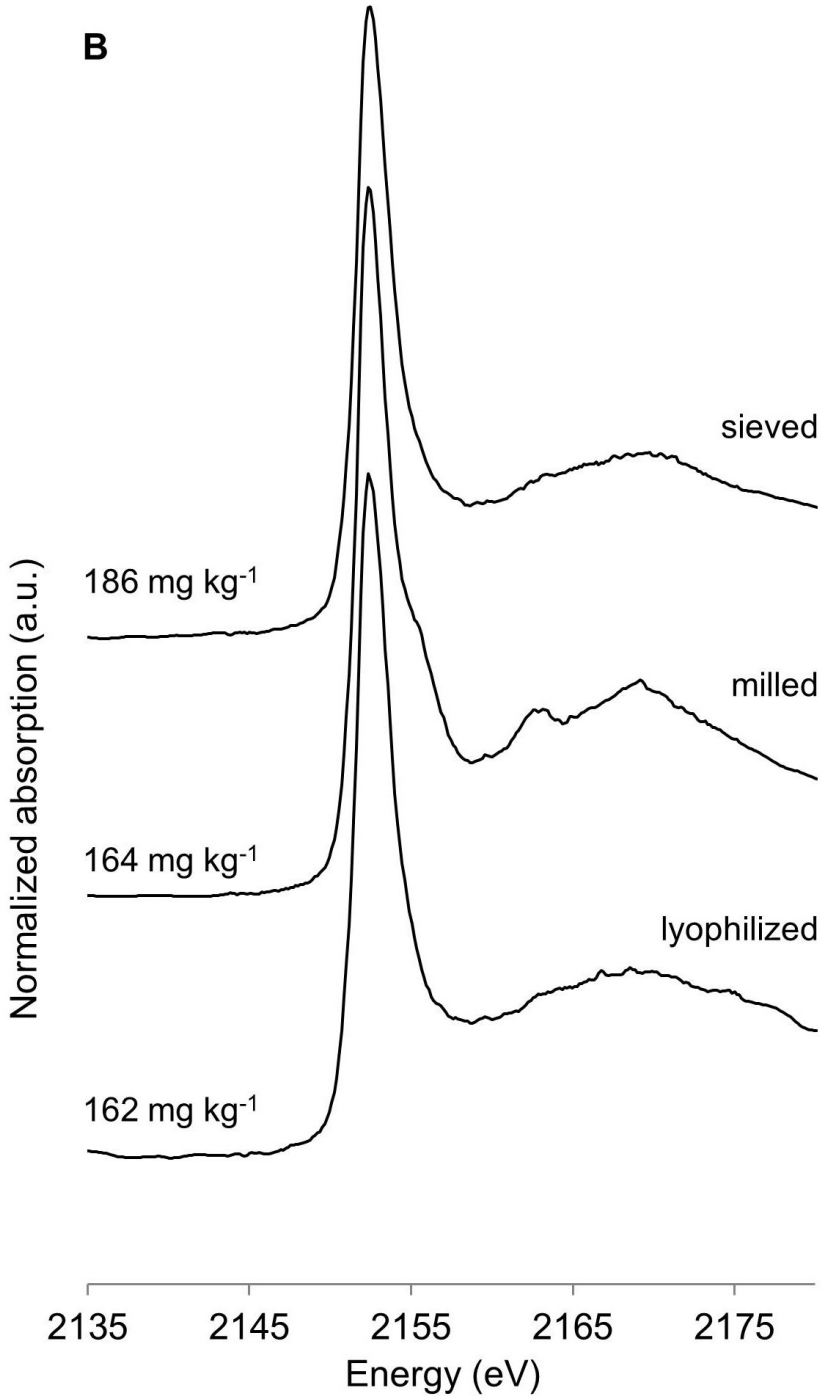

Figure 8-1-5 Stacked P *K*-edge XANES spectra of unfractionated Bodden sediment of three different pretreatments sieved, milled, and lyophilized. Concentrations of P (mg kg^{-1}) were determined by ICP-OES.

8.2. Supplemental material of the manuscript: Phosphorus speciation along a soil to kettle hole transect: sequential P fractionation, P XANES, and ^{31}P NMR spectrsocopy (Chapter 3)

Journal: Geoderma

Authors: Julia Prüter[1], Timothy I. McLaren[2], Marlene Pätzig[3], Yongfeng Hu[4], Peter Leinweber[1]

[1]*University of Rostock, Soil Science, Justus-von-Liebig Weg 6, 18051 Rostock, Germany*

[2]*University of Queensland, School of Agriculture and Food Sciences, St Lucia, Queensland 4072, Australia*

[3]*Leibniz Centre for Agricultural Landscape Research, Eberswalder Straße 84, 15373 Müncheberg, Germany*

[4]*Canadian Light Source, Inc., University of Saskatchewan, 44 Innovation Boulevard, Saskatoon, Saskatchewan S7N 2V3, Canada*

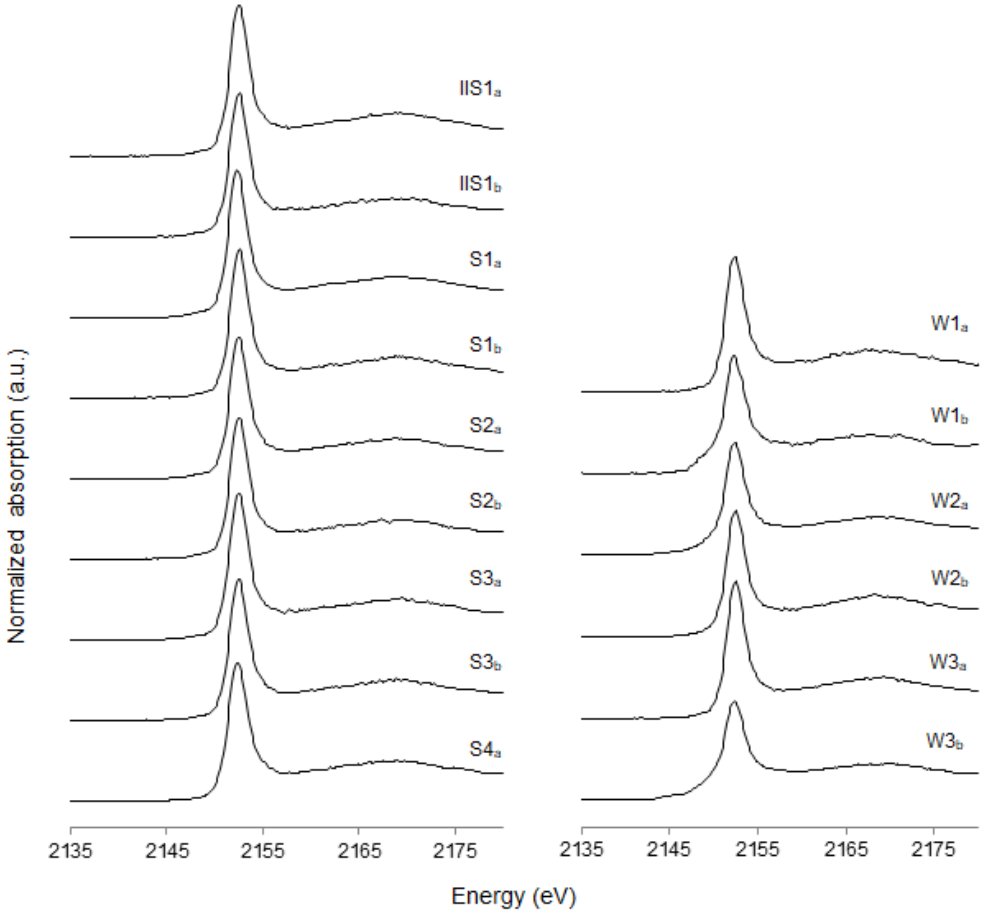

Figure 8-2-1 P *K*-edge XANES spectra of soil (S) and sediment (W) samples.

Table 8-2-1 *R* factors of the results of linear combination fitting from P *K*-edge XANES analyses of soil (S) and sediment (W) samples. If fits were averaged, the best *R* factor is given.

Sample	*R* factor
$IIS1_a$	0.0013
$IIS1_b$	0.0025
$S1_a$	0.0012
$S1_b$	0.0021
$S2_a$	0.0028
$S2_b$	0.0015
$S3_a$	0.0022
$S3_b$	0.0019
$S4_a$	0.0030
$W1_a$	0.0030
$W1_b$	0.0312
$W2_a$	0.0324
$W2_b$	0.0060
$W3_a$	0.0019
$W3_b$	0.1101

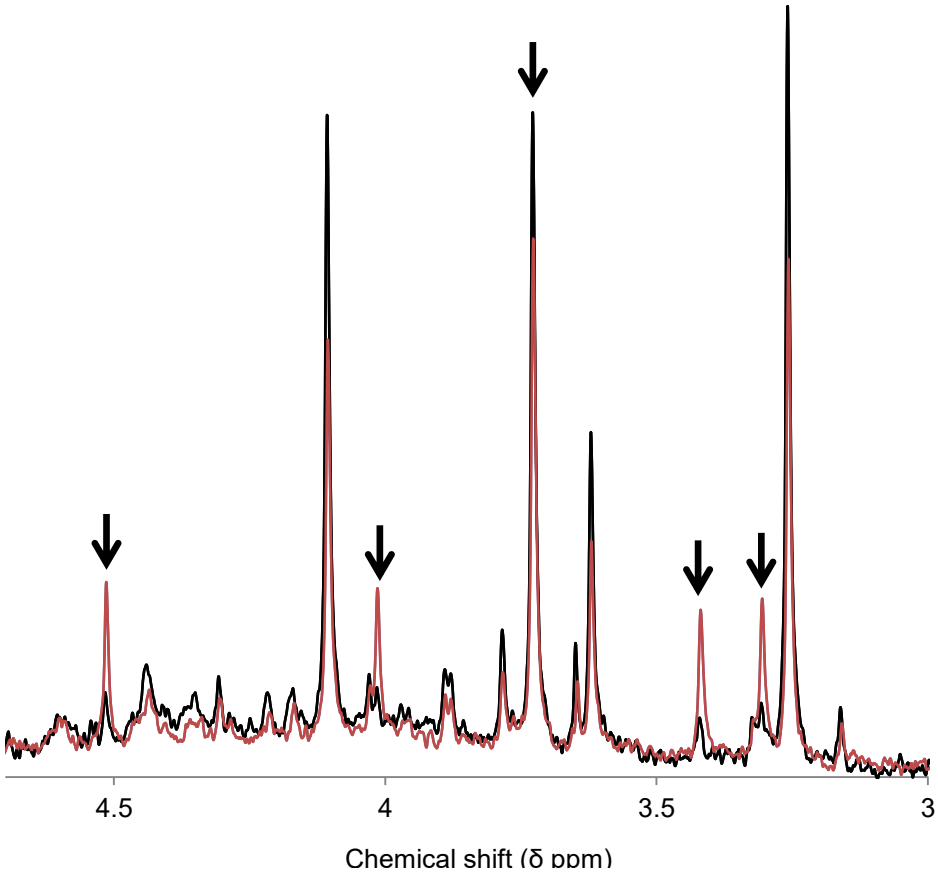

Figure 8-2-2 Solution ^{31}P NMR spectra of NaOH-EDTA soil extract $S1_b$ (black) and the same sample after spiking with an authentic standard of 10 µl of 2 mg/L of *myo*-IP_5 in D_2O (red). Presence of the (1,2,4,5,6) enantiomer of *myo*-IP_5 in the soil extract was confirmed at chemical shifts of δ 4.51 ppm, 4.01 ppm, 3.73 ppm, 3.42 ppm and 3.31 ppm (arrows).

8.3. Supplemental material of the manuscript: Characterization of phosphate compounds along a catena from arable and wetland soil to sediments in a Baltic Sea lagoon (Chapter 4)

Journal: Soil Systems

Authors: Julia Prüter[1], Rhena Schumann[2], Wantana Klysubun[3], Peter Leinweber[1]

[1]*University of Rostock, Soil Science, Justus-von-Liebig Weg 6, 18051 Rostock, Germany*

[2]*University of Rostock, Department of Applied Ecology, Albert-Einstein-Straße 3, 18059 Rostock, Germany*

[3]*Synchrotron Light Research Institute, Muang District, 111 University Avenue, Nakhon Ratchasima 3000, Thailand*

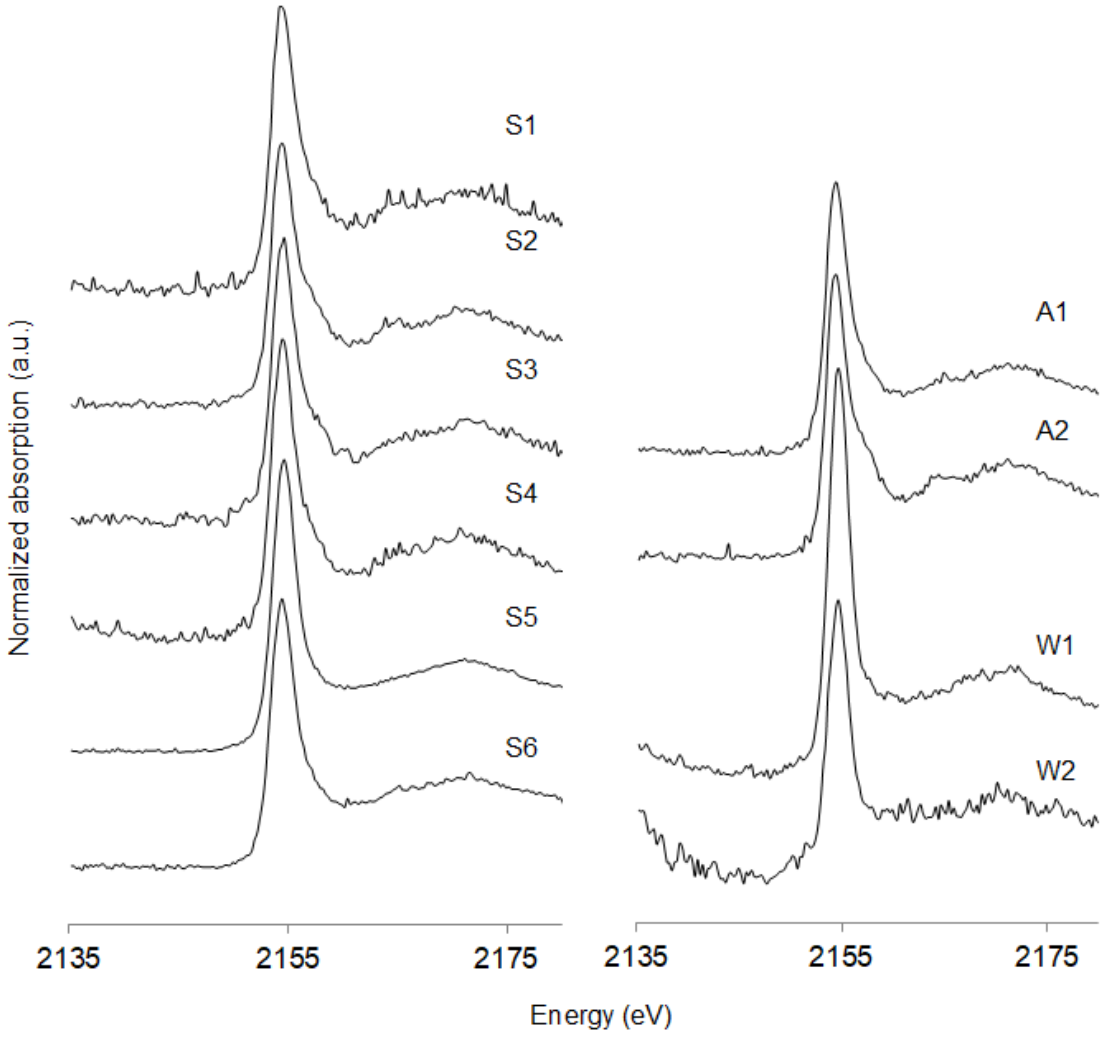

Figure 8-3-1 P *K*-edge XANES spectra of soil (A, W) and sediment (S) samples.

Table 8-3-1 *R* factors of the results of linear combination fitting from P *K*-edge XANES analyses of soil (A, W) and sediment (S) samples. If fits were averaged, the best *R* factor is given.

Sample	*R* factor
A1	0.0033
A2	0.0033
W1	0.0073
W2	0.0161
S1	0.0095
S2	0.0059
S3	0.0090
S4	0.0070
S5	0.0022
S6	0.0066

8.4. Supplemental material of the manuscript: Phosphorus speciation in sediments from the Baltic Sea, evaluated by a mulit-method approach (Chapter 5)

Journal: Journal of Soils and Sediments

Authors: Julia Prüter[1], Thomas Leipe[2], Dirk Michalik[3], Wantana Klysubun[4], Peter Leinweber[1]

[1]*University of Rostock, Soil Science, Justus-von-Liebig Weg 6, 18051 Rostock, Germany*

[2]*Leibniz Institute for Baltic Research, Seestraße 15, 18119 Rostock Warnemünde, Germany*

[3]*Leibniz Institute for Catalysis, A.-Einstein-Str. 29a, 18059 Rostock, Germany*

[4]*Synchrotron Light Research Institute, Muang District, 111 University Avenue, Nakhon Ratchasima 3000, Thailand*

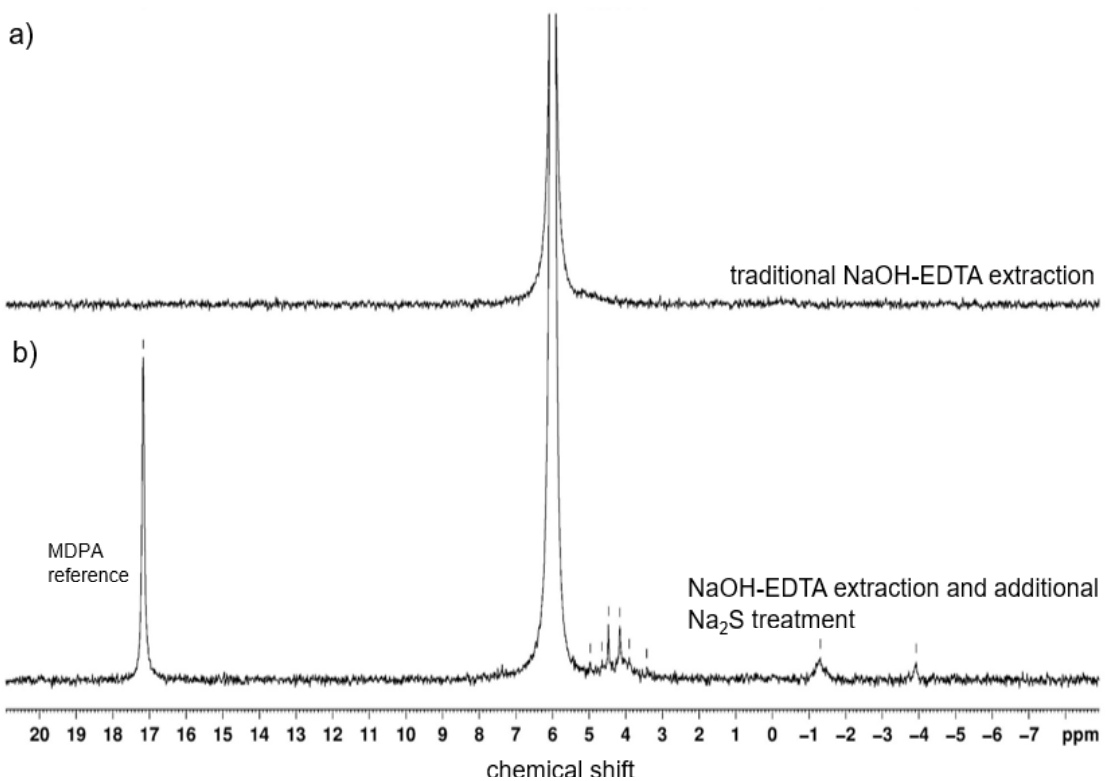

Figure 8-4-1 ^{31}P NMR spectra of sample RE. a) Traditional sample treatment with single extraction step with NaOH/Na_2EDTA and b) shows the additional sulfide treatment to remove paramagnetic ions from NaOH/Na_2EDTA sediment extracts. Note the orthophosphate peak at 6 ppm is not shown in its full height.

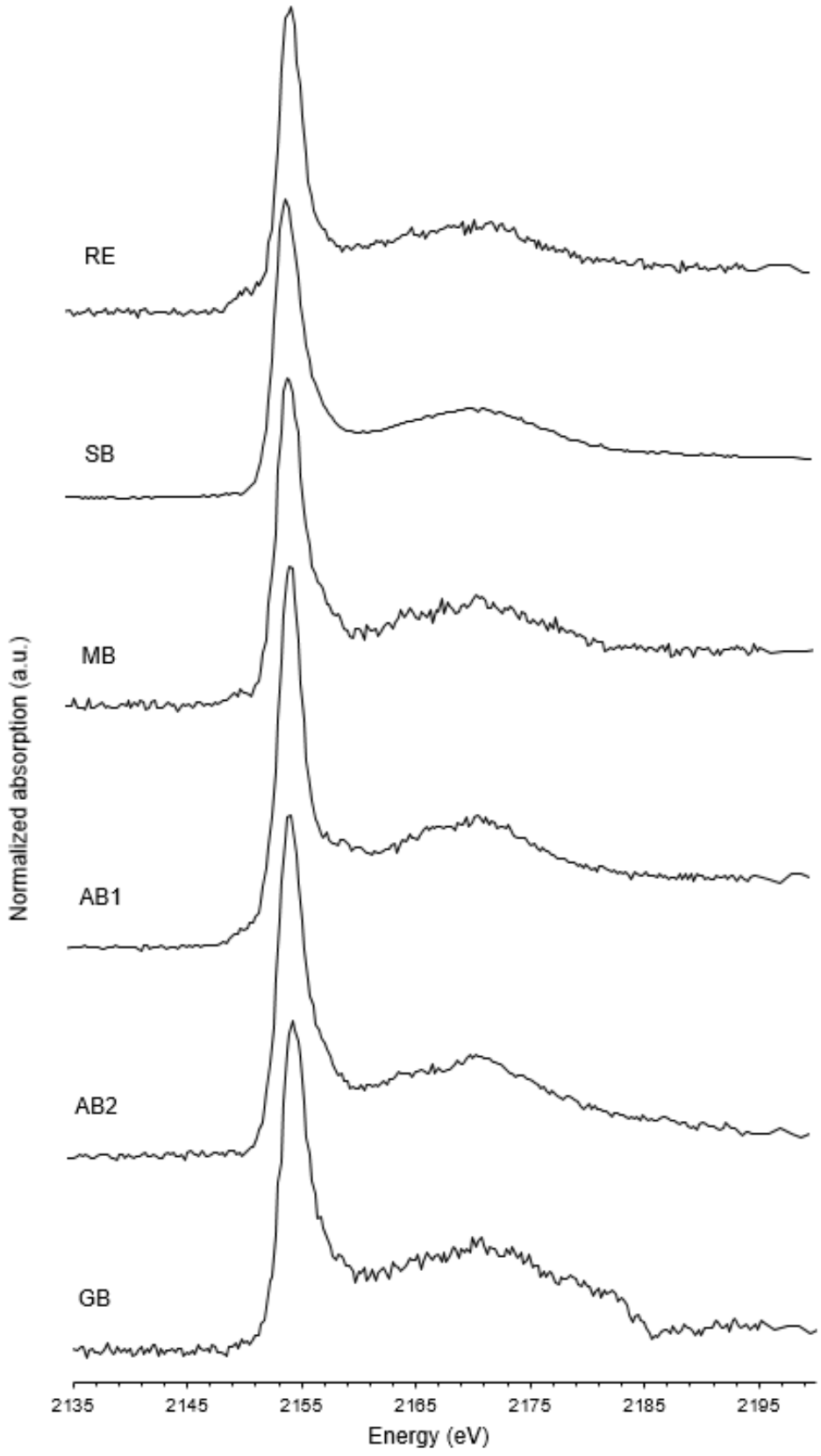

Figure 8-4-2 Stacked and normalized P *K*-edge XANES spectra of the sediments RE, SB, MB, AB1, AB2 and GB.

Table 8-4-1 List of all compounds used for spiking and associated sigma numbers in ^{31}P nuclear magnetic resonance spectroscopy (^{31}P NMR).

Full name of spiking compound	Sigma-Aldrich catalogue number
Phytic acid sodium salt hydrate	P8810
D-myo-Inositol 1,4,5 trisphosphate	I9766
D-Glucose 6-phosphate sodium salt	G7879
DL-α-Glycerol 6-phosphate magnesium salt hydrate	17766
β-Glycerophosphate disodium salt hydrate	G5422
Adenosine 5' monophosphate disodium salt	01930
Deoxyribonucleic acid sodium salt (salmon testes)	D1626
Calcium pyrophosphate	401552

Table 8-4-2 Occurring P compounds (orthophosphate (ortho-P), α-glycerophosphate (α-glycerol), β-glycerophosphate and adenosine 5‘ monophosphate (β-glycerol/AMP), deoxyribonucleic acid (DNA), pyrophosphate (Pyro-P) and unknown compound) in the sediments with their chemical shifts in ppm in each sample (ortho-P was set to 6.00 ppm) and their amounts in mg kg^{-1} determined with ^{31}P nuclear magnetic resonance spectroscopy (^{31}P NMR).

P compound	RE		SB		MB		AB1		AB2		GB	
	chemical shift [ppm]	P [mg kg^{-1}]	chemical shift [ppm]	P [mg kg^{-1}]	chemical shift [ppm]	P [mg kg^{-1}]	chemical shift [ppm]	P [mg kg^{-1}]	chemical shift [ppm]	P [mg kg^{-1}]	chemical shift [ppm]	P [mg kg^{-1}]
ortho-P	6.00	2753	6.00	155	6.00	314	6.00	2752	6.00	194	6.00	465
unknown									5.24	97		
***α*-glycerol**	4.70	120	4.70	40								
***β*-glycerol/AMP**	4.35	176	4.34	80			4.35	90	4.36	107	4.39	39
D N A	-1.00	295	-1.00	78			-1.00	96				
pyro-P	-4.08	160	-4.09	111								

Table 8-4-3 Elemental composition and size of the displayed particles in Figure 2 determined with scanning electron microscopy (SEM) and energy dispersive X-ray microanalyses (EDX) in the sediments RE, SB and AB1.

particle	sample	figure	width [µm]	length [µm]	perimeter [µm]	O [%]	F [%]	Na [%]	Al [%]	Si [%]	P [%]	Ca [%]	Fe [%]
Fe PO_4	RE	3 a)	5.4	9.1	35.3	40.9		3.0		1.2	17.3	1.0	36.6
calcite	SB	3 b)	1.9	3.3	13.6	30.1					2.5	67.3	
poly-P	RE	3 c)	4.7	5.5	47.8	46.8		23.2			30.0		
Ca PO_4	AB1	3 d)	2.8	3.5	12.7	39.0	6.1	1.2	1.3	1.8	17.0	33.6	

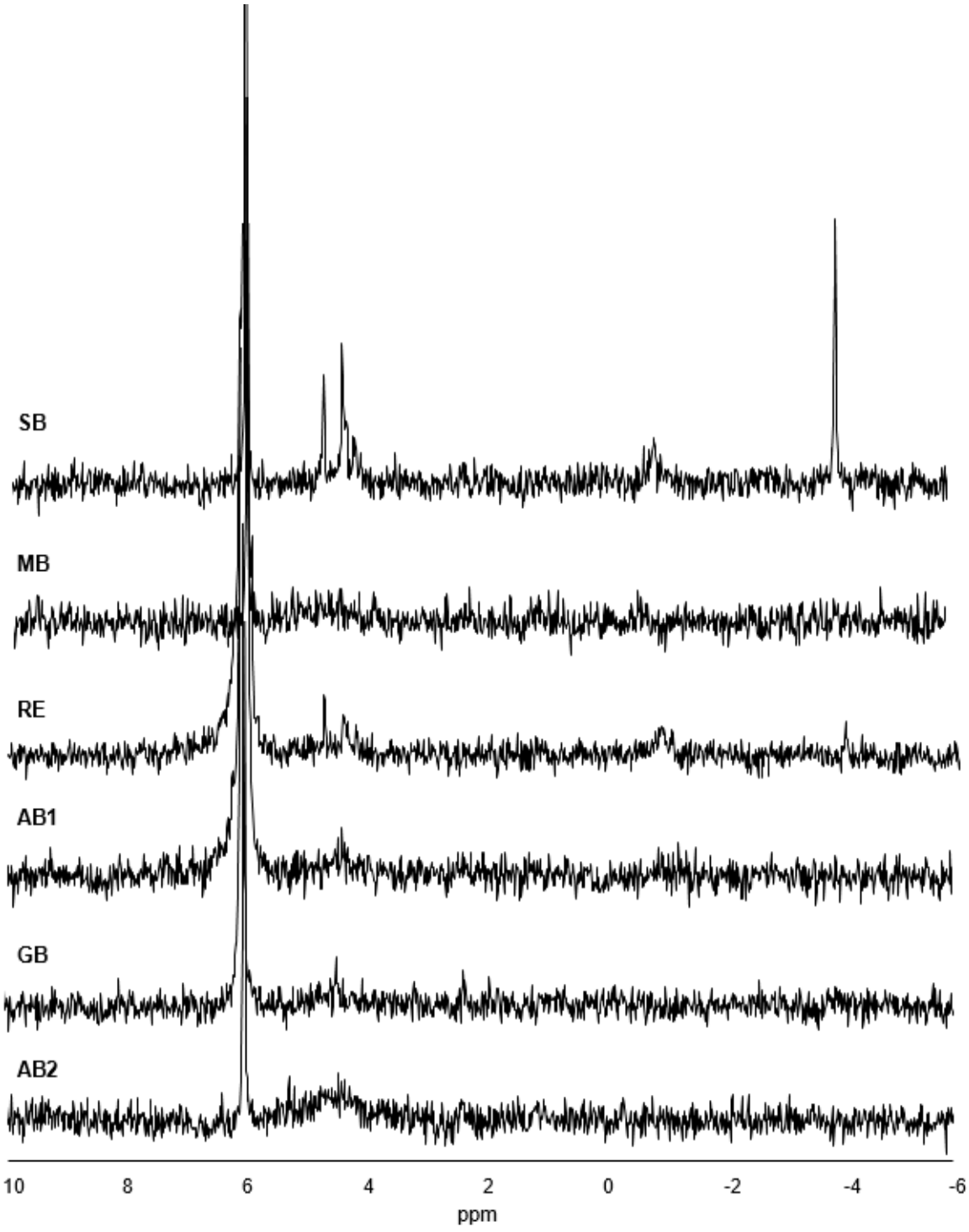

Figure 8-4-3 ^{31}P nuclear magnetic resonance spectra of the sediments SB, MB, RE, AB1, GB and AB2 in the region of 10 to -6 ppm. Note the orthophosphate peak at 6 ppm is not shown in its full height.

Table 8-4-4 Number of particles determined and assigned to different particle groups with scanning electron microscopy (SEM) and energy dispersive X-ray microanalyses (EDX) and range of P content of the individual particles of each group (in %) in the sediments RE, SB, MB, AB1, AB2, GB and one soil sample (Soil from Koch et al. 2018).

	RE	P content [%]	SB	P content [%]	MB	P content [%]	AB1	P content [%]	AB 2	P content [%]	GB	P content [%]	Soil	P content [%]
biogenic phases														
SiO_2 (opal)	44	0 - 6	58	0 - 6	237	0 - 5	153	0 - 9	199	0 - 3	261	0 - 3	256	0 - 3
calcite	2	0 - 2	601	0 - 11	3	0 - 1	2	3 - 19	8	0 - 3	1	1	3	0
organik matter/chitin	115	4 - 14	3	4 - 6	1	10	10	4 - 12	0	0	6	4 - 5	0	0
Ca PO_4	4	14 - 20	4	11 - 18	2	14 - 17	5	14 - 18	2	18 - 19	7	14 - 18	1	14
poly-PO_4	12	20 - 30	3	28 - 29	0	0	2	21 - 22	0	0	1	20	0	0
redox-sensitive phases														
Fe oxides	8	0 - 5	4	0 - 4	0	0	1	2	1	0	2	0	6	0 - 3
Mn oxides	0	0	0	0	0	0	0	0	1	0	17	1 - 3	0	0
Fe PO_4	215	5 - 18	3	5 - 6	0	0	8	9 - 16	1	6	0	0	0	0
Fe/Mn mixed PO_4	1	8	0	0	0	0	0	0	0	0	0	0	1	0
pyrite	139	0 - 5	259	0 - 3	113	0 - 1	120	0 - 4	41	0 - 1	64	0 - 2	1	0
sulphur	2	0	10	0	0	0	0	0	4	0 - 5	0	0	0	0
clay minerals														
chlorite	10	0 - 4	9	0 - 4	31	0 - 2	31	0 - 9	46	0 - 2	40	0 - 1	32	0 - 2
kaolinite	1	0	14	0 - 5	4	0 - 1	14	0 - 8	9	0 - 1	23	0 - 1	10	0
illite	6	0 - 4	30	0 - 6	83	0 - 2	114	0 - 13	93	0 - 2	85	0 - 2	65	0 - 1
illite-mixed layer	47	0 - 9	40	0 - 5	602	0 - 3	244	0 - 12	681	0 - 4	393	0 - 3	398	0 - 4
smectite	0	0	0	0	5	0 - 1	0	0	0	0	3	0	1	0
saponite	1	0	3	0	5	0 - 1	8	0 - 3	6	0	12	0 - 1	3	0
feldspar minerals/ tectosilicates														
potash feldspar	23	0 - 5	23	0 - 3	52	0 - 1	113	0 - 11	52	0 - 1	148	0 - 1	108	0 - 1
albite	40	0 - 10	54	0 - 7	57	0 - 1	86	0 - 11	58	0 - 1	169	0 - 2	58	0 - 1
plagioclase	3	0 - 6	13	0 - 4	17	0 - 4	11	0 - 7	21	0 - 3	26	0 - 7	21	0 - 3
pyroxene	0	0	2	0	3	0	2	0 - 5	0	0	2	0	2	0
other minerals														
SiO_2 (quartz)	143	0 - 10	197	0 - 8	62	0 - 2	147	0 - 10	30	0 - 2	6	0 - 1	27	0 - 1
bauxite	0	0	0	0	0	0	0	0	2	0 - 2	0	0	0	0
dolomite	1	0	1	0	5	0 - 1	1	2	9	0 - 3	0	0	0	0
titanium minerals	5	0 - 16	18	0 - 4	7	0 - 1	10	1 - 5	15	0 - 1	10	0 - 1	16	0 - 1
not classified	664	0 - 44	157	0 - 19	219	0 - 3	377	0 - 20	229	0 - 12	232	0 - 13	441	0 - 5
sum classified	822		1349		1289		1082		1279		1276		1009	
sum all	1486		1506		1508		1459		1508		1508		1450	

9 Acknowledgements

An dieser Stelle möchte ich allen beteiligten Personen meinen größten Dank aussprechen, ohne die ich die Anfertigung meiner Dissertation nicht hätte bewältigen können. Mein besonderer Dank gilt meinem Doktorvater Prof. Peter Leinweber für die enorme Unterstützung bei der Durchführung zahlreicher Experimente, über das Schreiben der einzelnen Veröffentlichungen bis hin zur Fertigstellung der Dissertation. Ihr Engagement, Ihre kreativen Ideen und Bereitschaft meine Entwürfe quasi zu jeder Tages- und Nachtzeit mit Geduld zu lesen und mir Verbesserungsvorschläge zu unterbreiten haben maßgeblich zum Gelingen dieser Arbeit beigetragen. An dieser Stelle möchte ich auch meinem Zweitbetreuer Dr. Dirk Michalik danken, der mich mit Anregungen und produktiven Gesprächen bei der Anfertigung meiner Dissertation unterstützt hat.

Außerdem möchte ich mich bei den vielen aktuellen oder ehemaligen Mitgliedern der Professur für Bodenkunde bedanken. Ich danke Britta Balz für die uneingeschränkte Unterstützung im Labor, Elena Heilmann für die Probenanalyse und die vielen deutschen als auch russischen Gespräche sowie Kai-Uwe Eckhardt, Dr. Gerald Jandl und Dr. Karen Baumann, die als erfahrene Ansprechpartner stets ein offenes Ohr für meine Fragen hatten. Mein weiterer Dank gilt Dr. Andre Acksel, der mir als ehemaliger Büronachbar in vielen Situationen Beistand geleistet hat und als gutes Vorbild in der Promotion vorangegangen ist, sowie Prof. Christel Baum, Anika Zacher und Nora Vitow, ohne die die ein oder andere Dienstreise sicher nur halb so erfolgreich verlaufen wäre. Karin Eckelt möchte ich für die Hilfe in allen bürokratischen und organisatiorischen Fragen danken.

Darüber hinaus möchte ich einen großen Dank gegenüber dem Leibniz-WissenschaftsCampus Phosphorforschung Rostock aussprechen. Diese Arbeit wurde durch die Leibniz-Gemeinschaft im Rahmen des P-Campus finanziert. Mein besonderer Dank gilt Dr. Dana Zimmer, die sich als Koordinatorin des P-Campus für die Vernetzung der Doktoranden im Projekt eingesetzt und mir viele Zusatzqualifikationen während der Promotion ermöglicht hat. Danken möchte ich

außerdem Sandra Kammannn als wichtige Ansprechpartnerin und Gefährtin auf dem Weg der Promotion und auch allen anderen Doktoranden aus dem Netzwerk des P-Campus.

Acht Monate der Promotionszeit wurden durch ein Stipendium der Landesgraduiertenförderung des Landes Mecklenburg-Vorpommern gefördert. Für diese finanzielle Unterstützung danke ich der Vergabekommision und allen beteiligten Personen.

Meiner Familie und meinen Freunden sowohl in, als auch außerhalb der Turnhalle möchte ich für ihre guten Zusprüche und kreativen Ideen während der Arbeit an dieser Dissertation meinen herzlichen Dank aussprechen. Ebenso sei allen denen ein Dankeschön ausgesprochen, die zum Gelingen dieser Arbeit beigetragen haben, aber nicht namentlich erwähnt sind.

10 Proof of individual contribution

Manuskript included in the thesis	Author (J. Prüter)	Co-authors
Prüter, J., Hu, Y., Leinweber, P.: *Influence of sample pretreatment on P speciation in sediments evaluated with sequential fractionation and P* K-*edge XANES spectroscopy.* **Communications in Soil Science and Plant Analysis** (2022) 53(14), 1712-1230. **Chapter 2**	Generating research idea, generating and evaluating data, writing the manuscript.	**Y. Hu** (assistance during XANES analyses), **P. Leinweber** (generating research idea, correcting the manuscript)
Prüter, J., McLaren, T.I., Pätzig, M., Hu, Y., Leinweber, P.: *Phosphorus speciation along a soil to kettle hole transect: sequential P fractionation, P XANES, and ^{31}P NMR spectroscopy.* **Geoderma** 429 (2023) 116215 **Chapter 3**	Generating research idea, generating and evaluating data, writing the manuscript.	**T.I. McLaren** (generating research idea, assistance during NMR analyses, correcting the manuscript), **M. Pätzig** (correcting the manuscript), **Y. Hu** (assistance during XANES analyses), **P. Leinweber** (generating research idea and data, correcting the manuscript)
Prüter, J., Schumann, R., Klysubun, W., Leinweber, P.: *Characterization of phosphate compunds along a catena from arable and wetland soil to sediments in a Baltic Sea lagoon.* **Soil Systems,** submitted **Chapter 4**	Generating research idea, generating and evaluating data, writing the manuscript.	**R. Schumann** (generating data, correcting the manuscript), **W. Klysubun** (assistance during XANES analyses), **P. Leinweber** (generating research idea and correcting the manuscript)

Manuskript included in the thesis	Author (J. Prüter)	Co-authors
Prüter, J., Leipe, T., Michalik, D., Klysubun, W., Leinweber, P.: *Phosphorus speciation in sediments from the Baltic Sea, evaluated by a multi-method approach.* **Journal of Soils and Sediments** (2020) 20, 1676-1691. **Chapter 5**	Generating and evaluating data, writing the manuscript.	**T.Leipe** (generating research idea and data, SEM-EDX analyses), **D. Michalik** (^{31}P NMR analyses), **W. Klysubun** (assistance during XANES analyses), **P. Leinweber** (generating research idea and correcting the manuscript)
Prüter, J., Strauch, S. M., Wenzel, L., Klysubun, W., Palm, H.W., Leinweber, P.: *Organic matter composition and phosphorus speciation of soild waste from an African Catfish Recirculating Aquaculture System.* **Agriculture** (2020) 10 (10), 466. **Chapter 6**	Generating research idea, generating and evaluating data, writing the manuscript.	**S.M. Strauch** (sample taking, writing the manuscript), **L. Wenzel** (sample taking, writing the manuscript), **W. Klysubun** (assistance during XANES analyses), **H.W. Palm** (generating research idea), **P. Leinweber** (generating research idea and correcting the manuscript)

11 Theses

Phosphorus speciation in soil and sediment indicating tranformation processes from terrestrial to aquatic ecosystems

presented by Julia Prüter

I Motivation and objectives of the research

Phosphorus is indispensable in agricultural production and a scarce, non-renewable resource but simultaneously it can cause severe problems entering aquatic environments by runoff or leaching from arable soils. Therefore, exemplary pathways of P from terrestrial soils towards aquatic sediments have to be verified including analyses of soil and sediment samples along transects.

Since the chemical speciation of P is one of the major factors influencing the risk of P transfer from arable soils to aquatic environments it is necessary to characterize the P speciation in agricultural soils and adjacent aquatic sediments and to reveal major differences between them.

Phosphorus concentrations in the environment are often close to the limit of detection of analytical methods. To overcome the resulting methodological limitations and to enable a justified characterization of P speciation in different environmental samples, a reasonable selection of established as well as innovative P research methods is required.

It needs to be examined if P sinks in the environment also occur within transects of P transport pathways from terrestrial soils towards aquatic sediments to uncover accumulations of P and possibly enable P recycling.

Since fish fecal matter can contribute to particulate organic waste in the aquatic environment, it needs to be investigated which P species occur in fish waste to assess the probability of contributions of P from fish fecal matter to the P speciation of sediments at the bottom of waterbodies.

II Main research results

The application of traditional soil sample pretreatments such as drying, sieving and grinding did not fundamentally change the occurrence and distribution of P species in sediment samples from different environments. Thus, similar pretreatment procedures of soils and sediments were possible in subsequent investigations.

The common assignment of P species to operationally defined P pools of sequential fractionation has been confirmed for sediments from different ecosystems with the help of P *K*-edge XANES spectroscopy, which detected even very low P concentrations in extraction residues of sequential P fractionation.

The complementary results of sequential P fractionation, P *K*-edge XANES spectroscopy and ^{31}P NMR spectroscopy revealed a transition from labile and moderately labile Fe- and Al-associated P and great variety of organic P species in terrestrial soils towards more stable Ca- and Mg-P and less differrent organic P species in aquatic sediments along transects from land to sea.

Kettle hole sediments, coastal wetland soils and Baltic Sea lagoon sediments acted as sinks for especially acid-extractable, Ca-associated and complex organically bound P species with the chance to preserve adjacent environments by a protection from further P inputs.

The detection of some organic P species with terrestrial origin in arable soils as well as in adjacent sediments confirmed transport of these P species from soil to sediment.

The method of P *K*-edge XANES spectroscopy especially detected Ca-P species in solid waste of African catfish from an intensive recirculation aquaculture system indicating a possible contribution of P from fish fecal matter to high amounts of Ca-P species in aquatic sediments.

III Conclusions and outlook

The results obtained by the complementary methods of sequential P fractionation, P *K*-edge XANES spectroscopy and ^{31}P NMR spectroscopy compiled in the present work confirmed transport of P from terrestrial towards aquatic ecosystems.

The transition from labile and moderately labile P in terrestrial soils towards more stable P species in aquatic sediments were in general agreement and independent of transect length in the investigated micro-, meso- and macroscale ecosystems.

Future challenges are the preservation and maintenance or the construction of new kettle holes, coastal wetland buffer strips and deeper areas in shallow Baltic Sea lagoons to create P sinks and thereby protect more vulnerable environments from excess P inputs.

Forthcoming studies have to focus on possibilities how to regain and recycle P from terrestrial as well as aquatic sinks to contribute to the closure of P cycles in agricultural systems.

12 Declaration of primary authorship

I declare, that I have written the present thesis for doctorate and without help of others. Other than the presented references were not used and quoted results were always marked with the relevant reference. The present thesis was never either abroad or in Germany submitted for examination in the present or a similar version.

Eidesstattliche Erklärung

Hiermit erkläre ich durch eigenhändige Unterschrift, die vorliegende Dissertation selbstständig verfasst und keine anderen als die von mir angegebenen Quellen und Hilfsmittel verwendet zu haben. Die aus den Quellen direkt oder indirekt übernommenen Gedanken sind als solche kenntlich gemacht. Die Dissertation ist in dieser Form noch keiner anderen Prüfungsbehörde vorgelegt worden.

Rostock, 25.01.2023